KHIRTANA RAVEENDRAN MASTER OF SCIENCE 2025

FORMULATION AND OPTIMIZATION VIA RESPONSE SURFACE METHODOLOGY AND GREENNESS EVALUATION OF CREATINE-FUNCTIONALIZED MAGNETIC ADSORBENTS AS A MICRO-SCALE EXTRACTION TOOL FOR ANTIDEPRESSANT DRUG ANALYSIS

KHIRTANA RAVEENDRAN

MASTER OF SCIENCE
UNIVERSITI MALAYSIA TERENGGANU

2025

FORMULATION AND OPTIMIZATION VIA RESPONSE SURFACE METHODOLOGY AND GREENNESS EVALUATION OF CREATINE-FUNCTIONALIZED MAGNETIC ADSORBENTS AS A MICRO-SCALE EXTRACTION TOOL FOR ANTIDEPRESSANT DRUG ANALYSIS

KHIRTANA RAVEENDRAN

Thesis Submitted in Fulfilment of the Requirement for the Master of Science in the Faculty of Science and Marine Environment
Universiti Malaysia Terengganu

DECEMBER 2025

Pusat Pembangunan Pengurusan Akademik (PPPA)
@
Pusat Pengurusan Siswazah (PPS)

Borang Pengesahan Penyerahan Tesis / Disertasi/ Laporan Kertas Projek
Declaration Form for Submission of Theses/ Dissertation / Project Paper

Tajuk / *Title :* Formulation and optimization via response surface methodology and greenness evaluation of creatine-functionalized magnetic adsorbents as a micro-scale extraction tool for antidepressant drug analysis

Nama Pelajar / *Student's Name* : Khirtana A/P Raveendran
No. Matrik / *Matric No.*: P5700

Saya dengan ini mengaku membenarkan Tesis/Disertasi/Laporan Kertas Projek ini disimpan di Perpustakaan Sultanah Nur Zahirah, Universiti Malaysia Terengganu ("UMT") dan mengakui bahawa UMT mempunyai hak-hak seperti berikut:
I hereby declare that I have allowed this Theses/Dissertation/Project Paper to be kept by Perpustakaan Sultanah Nur Zahirah, Universiti Malaysia Terengganu ("UMT") and acknowledged that UMT reserves the rights as follows:

1. Hak cipta Tesis/Disertasi/Laporan Kertas Projek ini adalah hak milik UMT.
   The copyright of this Theses/Dissertation/Project Paper belongs to UMT.

2. UMT berhak untuk membuat salinan Tesis/Disertasi/ Laporan Kertas Projek ini untuk tujuan akademik.
   UMT shall has the right to make copies of this Theses/Dissertation/Project Paper for the academic purpose.

3. UMT berhak membuat salinan Tesis/Disertasi/Laporan Kertas Projek ini sebagai bahan pertukaran antara institusi pengajian tinggi.
   UMT shall has the right to make copies for this Theses/Dissertation/Project Paper as an exchange between higher learning institutions.

4. Hak-hak UMT yang dinyatakan dalam perkara 2 dan 3 di atas adalah tertakluk kepada kategori Tesis/Disertasi/Laporan Kertas Projek seperti yang dinyatakan di dalam ini.

The rights of UMT stated in items 2 and 3 above are subject to the category of the Thesis/Dissertation/Project Paper Report as stated herein.

Sila tanda (/) bagi pilihan kategori di bawah:
Please tick (/) from the categories below:

(/)	Tidak Terhad / *Open Access*	Tersedia untuk diakses secara terbuka *Available for open access*
( )	Terhad / *Restricted*	Mengandungi maklumat terhad yang telah ditentukan oleh organisasi/badan di mana penyelidikan ini dijalankan / *Contains restricted information as specified by the organization/body where research was done.*
( )	Sulit / *Confidential*	Mengandungi maklumat yang dikategorikan di bawah keselamatan atau kepentingan Malaysia seperti yang termaktub dalam Akta Rahsia Rasmi 1972 / *Contains information categorized under the security or interests of Malaysia as stipulated in the Official Secrets Act 1972.*
( )	Embargo / *Embargo*	Tesis ini tertakluk kepada tempoh embargo selama _____ tahun dan tidak boleh diakses oleh umum sehingga tamatnya tempoh tersebut. *This thesis is subject to an embargo of _____ years and shall not be accessible to public until the embargo period ends.*

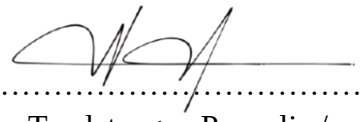

……..
Tandatangan Penyelia /
Supervisor's Signature
(Nama dan Cop Rasmi/ *Name & Official Stamp*)

Tarikh/*Date*: 27th April 2026

Catatan:
1. Jika Tesis/Disertasi/Laporan Kertas Projek ini SULIT @ TERHAD, sila lampirkan surat dari pihak berkuasa/organisasi berkenaan dengan menyatakan

sekali sebab dan tempoh Tesis/Disertasi/Laporan Kertas Projek ini perlu dikelaskan sebagai SULIT atau TERHAD.

2. Status klasifikasi Tesis/Disertasi/Laporan Kertas Projek hendaklah ditentutkan dan disahkan oleh Penyelia Tesis.
3. Tempoh embargo hendaklah tidak kurang daripada satu (1) tahun dan tidak melebihi lima (5) tahun.

Note:

1. *If this Theses/Dissertation/Project Paper is CONFIDENTIAL @ RESTRICTED, please attach the letter from the relevant authority/organization stating its reason and duration of this Theses/Dissertation/Project Paper should be classified as CONFIDENTIAL or RESTRICTED.*
2. *The classification status of the Thesis/Dissertation/Project Report shall be determined and certified by the Thesis Supervisor.*
3. *The embargo period shall be not less than one (1) year and shall not exceed five (5) years.*

DEDICATION

Dedicated this thesis to:

My all: Mr. Raveendran V. Raghavan Pillai and Mrs. Sasikala Kollanthavelu

My anchor throughout the storm & turbulence:

Miss Yashwini, Miss Khirti, Mr. Hanesh, and Miss Yadavi

I owe you guys, big time

Thanks a lot

God Almighty for His countless blessing

Abstract of thesis presented to the Senate of Universiti Malaysia Terengganu in fulfillment of the requirements for the degree of Master of Science

FORMULATION AND OPTIMIZATION VIA RESPONSE SURFACE METHODOLOGY AND GREENNESS EVALUATION OF CREATINE-FUNCTIONALIZED MAGNETIC ADSORBENTS AS A MICRO-SCALE EXTRACTION TOOL FOR ANTIDEPRESSANT DRUG ANALYSIS

KHIRTANA A/P RAVEENDRAN

DECEMBER 2025

Main Supervisor : Assoc. Prof. Wan Mohd Afiq Wan Mohd Khalik, Ph.D
Co-Supervisor : Assoc. Prof. Loh Saw Hong, Ph.D
Faculty : Faculty of Science and Marine Environment

Pharmaceutical residues in water pose growing environmental and health concerns due to their persistence, bioaccumulation, or ecological risks, demanding for efficient and sustainable sample preparation methods capable of detecting these pollutants at trace levels. This study reports the development of a green method by functionalizing creatine onto a magnetite-based adsorbent and applying magnetic dispersive micro-solid phase extraction (μ-SPE) coupled with high-performance liquid chromatography with diode-array detection for the simultaneous detection of five antidepressants: sertraline, escitalopram, paroxetine, fluvoxamine, and fluoxetine. The creatine-functionalized Fe_3O_4@SiO_2 magnetic adsorbent was synthesized via co-precipitation and characterized using Fourier transform infrared spectroscopy (functional groups), scanning electron microscopy with energy dispersive X-ray spectroscopy (surface morphology and elemental composition), transmission electron microscopy (particle size and structure), vibrating sample magnetometry (magnetic properties), X-ray diffraction (crystalline structure), thermogravimetric analysis (thermal stability), Brunauer-Emmett-Teller analysis (surface area and porosity), and zeta-potential measurement (surface charge). Seven factors influencing extraction efficiency namely sorbent weight, effervescent weight, sample volume, pH, extraction

temperature, contact time, and desorption solvent volume were examined using Plackett-Burman design and optimized by central composite design, which identified four critical factors (0.5g sorbent weight , pH 11, temperature 22 ℃, 7 min contact time) that produced the highest recovery. The optimized method demonstrated excellent performance with linearity (R^2 = 0.974-0.999), extraction recoveries of 80.0-94.9%, and detection limits from 0.012 µg/mL (escitalopram) to 0.087 µg/mL (fluoxetine). Precision studies showed inter-assay RSDs of 3.6-10.5% and intra-assay RSDs of 9.4-11.8%. The adsorbent also exhibited good reusability up to four cycles and stability with recoveries of 84.0-94.9%. Isotherm and kinetic studies revealed that adsorption followed the Freundlich isotherm and pseudo-second-order kinetic models. The greenness of the method was confirmed using analytical eco-scale (85/100), AGREE metric (0.7/1.0), green analytical procedure index (five green criteria), blue applicability grade index (67.5%), and sample preparation metric of sustainability (8/10), demonstrating its environmentally friendly profile. Overall, the dispersive magnetic µ-SPE method provides a simple, sustainable, and efficient solution for the simultaneous extraction and detection of pharmaceutical residues in environmental waters.

Abstrak tesis yang dikemukakan kepada Senat Universiti Malaysia Terengganu sebagai memenuhi keperluan untuk Ijazah Sarjana Sains

FORMULASI DAN PENGOPTIMUMAN MELALUI KAEDAH GERAK BALAS PERMUKAAN SERTA PENILAIAN HIJAU PENJERAP MAGNETIK BERFUNGSIKAN-KREATINA SEBAGAI ALAT PENGEKSTRAKAN BERSKALA MIKRO UNTUK ANALISIS UBAT ANTIDEPRESAN

KHIRTANA RAVEENDRAN

DISEMBER 2025

Penyelia Utama : Prof. Madya Wan Mohd Afiq Wan Mohd Khalik, Ph.D
Penyelia Bersama : Prof. Madya Loh Saw Hong, Ph.D
Fakulti : Fakulti Sains dan Sekitaran Marin

Residu farmaseutikal dalam air menimbulkan kebimbangan isu alam sekitar dan kesihatan yang semakin meningkat disebabkan oleh sifatnya yang kekal, bioakumulasi, serta risiko ekologi, maka menuntut kaedah penyediaan sampel yang cekap dan lestari bagi mengesan pencemar ini pada aras surih. Kajian ini melaporkan pembangunan kaedah hijau dengan memfungsikan kreatina pada penjerap berasaskan magnetit serta mengaplikasikan pengekstrakan mikro fasa pepejal sebaran magnetik (μ-SPE) yang digabungkan dengan kromatografi cecair prestasi tinggi pengesan susunan diod pengesanan serentak lima ubat antidepresan iaitu sertraline, escitalopram, paroxetine, fluvoxamine, dan fluoxetine. Penjerap Fe_3O_4@SiO_2 terfungsikan kreatina telah disintesis melalui kaedah pemendakan bersama dan dicirikan menggunakan spektroskopi inframerah transformasi Fourier (kumpulan fungsi), mikroskopi elektron imbasan bersama spektroskopi serakan tenaga sinar-X (morfologi permukaan dan komposisi unsur), mikroskopi elektron transmisi (saiz dan struktur zarah), magnetometri getaran sampel (sifat magnetik), pembelauan sinar-X (struktur hablur), analisis termogravimetri (kestabilan terma), analisis Brunauer-Emmett-Teller (luas permukaan dan porositi), serta pengukuran potensi zeta (cas permukaan). Tujuh faktor yang mempengaruhi kecekapan pengekstrakan iaitu berat

penjerap, berat prakursor buakan, isipadu sampel, pH, suhu pengekstrakan, masa buakan, dan isipadu pelarut nyahjerapan telah dikaji menggunakan reka bentuk Plackett-Burman dan dioptimumkan melalui reka bentuk komposit pusat, yang mengenal pasti empat faktor kritikal (0.5g berat penjerap, pH 11, suhu 22 °C, 7 min masa buakan) yang menghasilkan perolehan tertinggi. Kaedah optimum menunjukkan prestasi cemerlang dengan linearitiy (R^2 = 0.974-0.999), perolehan semula pengekstrakan dari 80.0-94.9%, serta had pengesanan dari 0.012 µg/mL (escitalopram) hingga 0.087 µg/mL (fluoxetine). Kajian kejituan menunjukkan RSD antara ujian adalah 3.6-10.5% dan RSD dalam ujian adalah 9.4-11.8%. Penjerap juga mempamerkan kebolehgunaan semula sehingga empat kitaran dan kestabilan dengan perolehan ialah 84.0-94.9%. Kajian isoterm dan kinetik mendedahkan bahawa penjerapan mematuhi model isoterma Freundlich dan model kinetik pseudo-tertib kedua. Kecekapan hijau kaedah ini disahkan menggunakan analisis skala-eko (85/100), metrik AGREE (0.7/1.0), indeks prosedur analisis hijau (lima kriteria hijau), indeks gred kebolehgunaan biru (67.5%), dan metrik kelestarian penyediaan sampel (8/10) yang menunjukkan profil mesra alam. Secara keseluruhan, kaedah µ-SPE sebaran magnetik ini menyediakan penyelesaian yang mudah, lestari, dan cekap untuk pengekstrakan dan pengesanan serentak residu farmaseutikal dalam air persekitaran.

ACKNOWLEDGEMENTS

First and foremost, I offer my deepest praise and thanks to God Almighty for His countless blessings and guidance, which were instrumental in the successful completion of this research. I wish to express my profound and sincere gratitude to my research supervisor, Assoc. Professor ChM Dr. Wan Mohd Afiq Wan Mohd Khalik, and my co-supervisor, Assoc. Professor ChM Dr. Loh Saw Hong, for providing me with the opportunity to conduct this research. Their invaluable guidance, unwavering encouragement, and constant motivation throughout this journey are deeply appreciated. I am incredibly grateful to my parents, Mr. Raveendran V. Raghavan Pillai and Mrs. Sasikala Kollanthavelu, for their unconditional love, prayers, care, and immense sacrifices in supporting my education. I also extend my heartfelt thanks to my siblings Miss Yashwini, Miss Khirti, Mr. Hanesh, and Miss Yadavi and my dearest friend, Mr. Kughan Anpalagan for their constant reassurance and belief in me. A special note of thanks is due to my uncles, Dr. Sattian Kollanthavelu and Mr. Saravanan Kollanthavelu, to whom I owe a great deal for standing by me in pursuing this field. Their support and trust were truly pivotal, and I thank them wholeheartedly.

I would also like to express my appreciation to the Faculty of Science and Marine Environment for their support during my research. My sincere thanks go to the science officers and staff of the Analytical and Environmental Laboratory, Universiti Malaysia Terengganu (UMT), for their invaluable assistance and genuine support. At the same time, I wish to extend my gratitude, on behalf of my research, to Hospital Bahagia, Tanjung Rambutan, and Hospital Pulau Pinang for granting me permission to carry out exploration and sampling. I would like to sincerely acknowledge the financial support under Ministry of Higher Education Malaysia provided through the research grant (FRGS/1/2023/STG04/UMT/02/3), which made this study possible. The funding enabled the acquisition of essential materials, laboratory facilities, and technical resources required to successfully conduct and complete this research.

Finally, I offer my heartfelt thanks to all individuals who have supported me, both directly and indirectly, in completing this research work.

APPROVALS

I certify that an Examination Committee has met on 22nd December 2025 to conduct the final examination of Khirtana Raveendran, on her Master of Science thesis entitled **"Formulation and optimization via response surface methodology and greenness evaluation of creatine-functionalized magnetic adsorbents as a micro-scale extraction tool for antidepressant drug analysis"** in accordance with the regulations approved by the Senate of Universiti Malaysia Terengganu. The Committee recommends that the candidate be awarded the relevant degree. The members of the Examination Committee are as follows:

Fatimah Hashim, Ph.D
Associate Professor,
Faculty of Science and Marine Environment
Universiti Malaysia Terengganu
(Chairperson)

Tuan Nurul Sabiqah Tuan Anuar, Ph.D
Associate Professor,
Faculty of Science and Marine Environment
Universiti Malaysia Terengganu
(Internal Examiner)

Wan Nazihah Wan Ibrahim, Ph.D
Associate Professor,
Faculty of Applied Sciences
Universiti Teknologi MARA
(External Examiner)

WAN MOHD KHAIRUL WAN MOHAMED ZIN, Ph.D
Professor/ Dean
Faculty of Science and Marine Environment
Universiti Malaysia Terengganu

Date

This thesis has been accepted by the Senate of Universiti Malaysia Terengganu in fulfilment of the requirement for the degree of Master of Science.

WAN MOHD KHAIRUL WAN MOHAMED ZIN,
Ph.D
Professor/ Dean
Faculty of Science and Marine Environment
Universiti Malaysia Terengganu

Date:

DECLARATION

I hereby declare that the thesis is based on my original work except for quotations and citations which have been duly acknowledged. I also declare that it has not been previously or concurrently submitted for any other degree at UMT or other institutions.

Khirtana Raveendran

Date: 27th April 2026

TABLE OF CONTENTS

LIST OF TABLES

LIST OF FIGURES

LIST OF ABBREVIATIONS

AAS	Atomic Absorption Spectroscopy
Ag	Silver
AGREE	Analytical Greenness Metric
ANOVA	One-way analysis of variance
BAGI	Blue Applicability Grade Index
BET	Brunauer–Emmett–Teller
CCD	Central Composite Design
CO_2	Carbon Dioxide
COOH	Carboxyl
D-μSPE	Dispersive Micro Solid Phase Extraction
DoE	Design of Experiments
ESC	Escitalopram
Fe_3O_4	Iron Oxide Nanoparticles
$Fe_3O_4@SiO_2$	Silica Coated Iron Oxide Nanoparticles
$Fe_3O_4@SiO_2$@CS NP	Chitosan-Functionalized $Fe_3O_4@SiO_2$ Nanoparticles
FLV	Fluvoxamine
FLX	Fluoxetine
FTIR	Fourier Transform Infrared
GAC	Green Analytical Chemistry
GAPI	Green Analytical Procedure Index
GC	Gas Chromatography
HPLC	High Performance Liquid Chromatography
HPLC- DAD	High Performance Liquid Chromatography equipped Diode Array Detector

ICP-MS	Inductively Coupled Plasma Mass Spectrometry
k_2	Rate Constant
K_F	Freundlich Constant
K_L	Langmuir Constant
LC-MS	Liquid Chromatography - Mass Spectrometry
LLE	Liquid-Liquid Extraction
LOD	Limit of Detection
LOQ	Limit of Quantitation
MAO	Monoamine Oxidase
MEPS	Microextraction by Packed Sorbent
MIP	Molecularly Imprinted Polymer
MNPs	Magnetic Nanoparticles
MOF	Molecularly Organic Frameworks
NEMI	National Environmental Methods Index
NH_2	Amine
OFAT	One-Factor-At-A-Time
PAR	Paroxetine
PBD	Plackett-Burman Design
PF	Preconcentration Factor
PFO	Pseudo First Model
PSO	Pseudo Second Model
Q_e	Equilibrium Capacity
q_{max}	Maximum Adsorption Capacity
RSD	Relative Standard Deviation
RSM	Response Surface Methodology
SBSE	Stir Bar Sorptive Extraction

SEM-EDS	Scanning Electron Microscopy- Energy Dispersive X-ray Spectroscopy
SER	Sertraline
SNRI	Serotonin-Norepinephrine Reuptake Inhibitor
SPME	Solid Phase Microextraction
SPE	Solid Phase Extraction
SPMS	Sample Preparation Metric Sustainability
SSRI	Selective Serotonin Reuptake Inhibitor
TEM	Transmission Electron Microscopy
TFME	Thin-Film Microextraction
TGA	Thermogravimetric Analysis
TCA	Tricyclic Antidepressant
VSM	Vibrating Sample Magnetometer

LIST OF FORMULAS

CHAPTER 1

INTRODUCTION

1.1 Background of the Study

Sample preparation is a critical step in analytical chemistry, serving as the bridge between raw sample collection and reliable analytical results. Its primary goals are to isolate target analytes from complex matrices, eliminate interfering substances, and transform the sample into a form compatible with analytical instrumentation (Smith & Johnson, 2020). The effectiveness of this step has a direct influence on the accuracy, sensitivity, and reproducibility of the analytical process. Common sample preparation techniques include liquid-based extraction, solid-based extraction, purification, pre-concentration, and derivatization, in which each method selected based on the sample type and the analytical requirements (Lee *et al.*, 2019). For example, biological fluids often require protein precipitation, while environmental samples typically demand extensive cleanup to mitigate matrix effects (Wang *et al.*, 2021). Well-executed sample preparation not only improves detection limits but also protects analytical instruments from contamination, thereby extending their operational lifespan.

Miniaturization represents a shift toward performing analytical processes at smaller scales, where efficiency and performance are enhanced through reduced system dimensions and resource use. The advent of miniaturization has transformed traditional sample preparation techniques by adapting them to smaller sample volumes and reagent quantities (Zhang *et al.*, 2022). This approach offers benefits such as enhanced mass transfer due to increased surface-to-volume ratios, and improved integration with modern instrumentation. Techniques such as solid-phase

microextraction (SPME) and dispersive liquid-liquid microextraction (DLLME) exemplify this trend, enabling efficient analyte isolation while significantly reducing solvent consumption (Garcia *et al.*, 2021). Miniaturized methods also promote portability, supporting on-site applications in fields like environmental monitoring and clinical diagnostics (Chen & Liu, 2023). Moreover, integration with microfluidic devices or lab-on-a-chip systems allows for seamless coupling of sample preparation and analysis, facilitate workflows or reducing of human error (Martinez *et al.*, 2020).

Miniaturization offers several analytical advantages. Firstly, it improves sensitivity by providing higher enrichment factors and lower detection limits, known critical for analyzing trace-level analytes in complex matrices such as environmental pollutants or biological metabolites (Brown *et al.*, 2022; Taylor *et al.*, 2021). Secondly, it supports green chemistry initiatives by minimizing organic solvent usage and hazardous waste generation, leading to both cost savings and environmental sustainability (Clark *et al.*, 2022). Thirdly, miniaturized techniques facilitate high-throughput analysis; faster extraction kinetics and greater automation enable rapid processing of multiple samples including manipulate magnetism properties (Adams *et al.*, 2023). Magnetic adsorbent is one of popular method to replace conventional dispersion strategies. Lastly, miniature methods are highly compatible with advanced analytical systems, thus minimizing sample loss and enhancing reproducibility. Nonetheless, challenges remain, including the need for specialized equipment and concerns over sample representativity at ultra-small volumes (Nguyen *et al.*, 2022).

1.2 Problem Statement

Pharmaceutical drugs enter the environment through multiple pathways, resulting in a complex and persistent contamination issue (Anderson *et al.*, 2021). Major sources include the improper disposal of unused medications, incomplete removal during wastewater treatment processes, and agricultural runoff from farms where veterinary pharmaceuticals are extensively applied (Kumar *et al.*, 2020). These substances continuously accumulate in water bodies and soils, where their persistence leads to widespread ecological exposure.

The emergence of pharmaceutical compounds into aquatic ecosystems can trigger declining effects across trophic levels (Davis *et al.*, 2021). These contaminants disrupt ecological balances, often contributing to population declines through various mechanisms. A particularly alarming consequence is the emergence and spread of antibiotic-resistant bacteria within microbial communities, which alters community structure and reduces biodiversity (Corcoran *et al.*, 2010; Singh *et al.*, 2022). Furthermore, pharmaceuticals active ingredients can interfere with physiological processes in both aquatic and terrestrial organisms. Documented effects include developmental abnormalities, increased mortality rates, and, notably, reproductive impairments caused by endocrine-disrupting compounds (Diaz, 2021).

These environmental impacts carry significant implications for human health through different magnitude of exposure (Miller *et al.*, 2022). For instance. the evolution of antibiotic-resistant strains in natural ecosystems threatens the efficacy of essential medical treatments. Additionally, chronic exposure to low concentrations of pharmaceutical residues poses potential long-term health risks to both wildlife and human populations, risks that remain poorly understood (Baker *et al.*, 2023). The full extent of these ecological and public health consequences continues to be explored, with main attention given to the synergistic effects of pharmaceutical mixtures and their transformation products in the environment (Harris *et al.*, 2021).

Analysing pharmaceutical residues in environmental samples presents considerable analytical challenges due to their low concentrations and the complexity of environmental matrices (Rutkowska *et al.*, 2014). These samples often contain interfering substances such as natural organic matter, inorganic salts, and co-contaminants, known it can affect the accuracy of pre-concentration and detection processes (Nguyen *et al.*, 2022). Most pharmaceuticals are found in literature studies at ultra-trace levels typically in the nanogram-per-liter (ng/L) to microgram-per-liter (µg/L) range necessitating the use of highly sensitive and selective analytical methods (Garcia *et al.*, 2023).

Accurate analysis requires techniques capable of differentiating between structurally similar pharmaceuticals and their metabolites, while effectively

minimizing the existence of matrix interferences (Clark *et al.*, 2021). Although sample pre-concentration is crucial for enhancing detection sensitivity, it introduces additional difficulties, including potential analyte loss especially for volatile or highly polar compounds (Adams *et al.*, 2022). Handling small volumes during sample preparation also requires high precision to ensure reproducibility (Wilson *et al.*, 2023), and method validation is often constrained by the limited availability of certified reference materials. Moreover, the absence of standardized protocols for emerging pharmaceutical contaminants impedes inter-laboratory consistency and complicates regulatory decision-making.

These analytical limitations hinder accurate quantification of antidepressant drugs, reported as widely detected pharmaceutical contaminants due to their extensive. Without selective and efficient extraction strategies, the occurrence and potential ecological risks of these compounds may be substantially underestimated (Smith *et al.*, 2023). In this context, the usage of creatine as a functional sorbent modifier enhanced affinity toward antidepressant molecules through specific intermolecular interactions, while magnetic adsorbents enable rapid and reliable separation of analytes from complex matrices. Together, chromatographic analysis coupled with creatine-functionalized magnetic sorbent-based microextraction provide a promising approach to overcome existing analytical challenges in trace-level detection.

1.3 Significant of the Study

This study offers new knowledge in advancing green analytical chemistry by developing an optimized magnetic dispersive micro solid phase extraction (D-μSPE) method tailored for the efficient analysis of pharmaceutical contaminants in environmental samples. The innovation of the proposed method yields substantial environmental benefits, including the minimization of hazardous waste, a significant reduction in energy and solvent consumption, and the elimination of unnecessary procedural steps. These improvements align with the overarching goals of sustainable science, where analytical effectiveness is achieved without compromising environmental and human health.

Response Surface Methodology (RSM) is a powerful statistical and mathematical tool used to evaluate the relationships between multiple experimental factors and responses, enabling the simultaneous optimization of system like extraction phase. In this study, RSM allows for the systematic investigation of main factors such as adsorbent dosage, extraction time, sample pH, and desorption conditions, while minimizing the total number of experiments required. This approach not only conserves valuable laboratory resources but also increases the reliability and reproducibility of the microextraction method. Furthermore, the adoption of RSM in methodology supports the green chemistry framework by designing method development in a resource-efficient manner, thereby reducing experimental waste and labour (Martinez & Adams, 2022). This strategy enhances the method's analytical performance and contributes to the development of more sustainable, science-driven extraction technologies.

Traditional dispersive adsorbents often require labour-intensive separation methods such as centrifugation or vacuum filtration, which demand extra time, energy, and additional consumables, thus addresses several critical limitations in previous sample preparation techniques (Wilson *et al.*, 2023). In next level of sample preparation innovation, the integration of magnetic properties into the adsorbent allows for rapid, efficient, and solvent-free separation including simple use of an external magnet. This not only systematize the workflow but also reduces mechanical stress on the analytes, preserving their stability. The fabrication of the magnetic adsorbent through this study prioritizes the use of environmentally benign materials and avoids the inclusion of toxic solvents. The composite material like creatine possesses large surface area, specific functional groups ($-NH_2$), and strong affinity for pharmaceutical compounds contribute to enhanced extraction efficiency, while its biodegradable nature and low environmental toxicity ensure compatibility with green chemistry principles (Brown *et al.,* 2021). This innovation supports the development of more sustainable and practical sample preparation approaches, making them well-suited for routine analysis of environmental contaminants.

Next, the application of quantitative greenness assessment tools provides a structured and scientifically metric assessment to evaluating the environmental impact

of the proposed analytical method. Unlike traditional qualitative descriptions of "green" practices, tools such as the Analytical Eco-Scale, Green Analytical Procedure Index (GAPI), and AGREE metrics offer numerical or visual evaluations of a method's sustainability (Alexander *et al.*, 2023). These tools consider multiple parameters, including the amount and toxicity of solvents used, energy consumption, waste generation, and method complexity. By applying five metric assessments, the study objectively demonstrates the eco-friendly nature of the D-μSPE technique and allows for direct comparison with other conventional and emerging methods.

1.4 Objectives

The research study aims to achieve the following objectives: -

1. To fabricate and characterise the physicochemical properties of the creatine-functionalized magnetic adsorbent.
2. To construct the best optimal condition for magnetic dispersive micro-solid phase extraction using the fabricated adsorbent with the aid of response surface methodology.
3. To evaluate the method performance of magnetic adsorbent through analytical figures of merit criteria for qualitative analysis.
4. To assess the green profile criteria of the developed analytical method using five quantitative greenness metric tools (AGREE, BAGI, Eco-Scale, GAPI, SPMS).

1.5 Hypothesis

This study hypothesizes that creatine-functionalized Fe_3O_4@SiO_2 nanoparticles can be effectively utilized as a magnetic adsorbent for the extraction of

five selective serotonin reuptake inhibitor (SSRI) antidepressant drugs. The presence of creatine functional groups is expected to enhance adsorption efficiency through hydrogen bonding, electrostatic interactions, and π–π interactions, while the SiO_2 coating stabilizes the Fe_3O_4 core and prevents aggregation in liquid phase. It is further proposed that this functionalized magnetic adsorbent will enable rapid, selective, and reusable extraction of SSRIs from complex matrices, thereby improving analytical performance. Thus, the developed analytical method is also expected to increase greenness criteria in the sample preparation process of the analytical method.

1.6 Overview of Thesis Structure

This thesis is structured into five well-organized chapters, designed to guide the reader through the research in a logical and easy-to-read manner. Chapter 1 introduces the study by outlining the research background, clearly stating the problem statements, defining the objectives, and explaining the significance of the work related to analytical chemistry field. Chapter 2 offers a thorough yet accessible review of the relevant literature, covering topics such as sorbent phase microextraction, different types of functionalization on magnetic adsorbents, the emergence and route of pharmaceutical residues enter into water, and description on both conventional and modern extraction techniques used to determine antidepressant drugs. It also explores adsorption models and introduces the principles of green analytical chemistry.

Chapter 3 describes the experimental methods in a detailed but easy-to-follow format, including sample preparation, formulation of adsorbent and their physical and chemical characteristics, screening and optimization of microextraction procedures, data analysis through different method validation assays includes kinetic and isotherm models. It also outlines how the environmental impact of the method was assessed using semi-quantitative tools of green analytical chemistry. Chapter 4 presents and interprets the experimental results, discussing their meaning in the context of the research questions and existing literature. Finally, Chapter 5 concludes the thesis by summarizing the main findings, highlighting the study's contributions, and offering suggestions for future work. The overview of the thesis structure is illustrated in Figure 1.1.

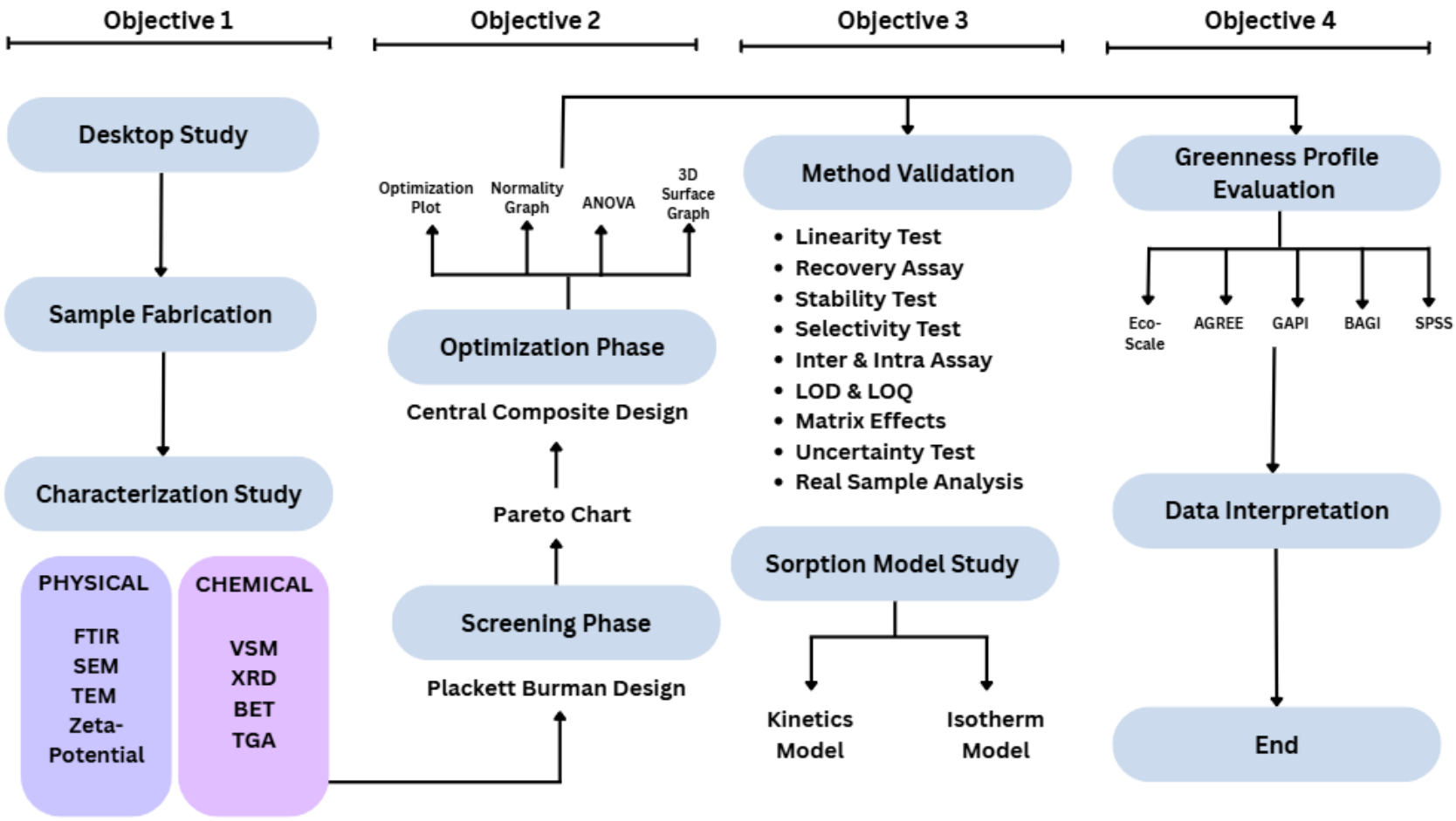

Figure 1.1. The overview of the thesis structure

CHAPTER 2

LITERATURE REVIEW

2.1 Sorbent Phase Microextraction

2.1.1 General Overview

Microextraction is a sample preparation technique that enables the efficient isolation and pre-concentration of analytes from a variety of matrices using minimal sample volume, solvent, and time. It is especially suited to modern analytical workflows due to its simplicity, eco-friendliness, and compatibility with advanced instrumentation. By enhancing analyte detection while reducing resource consumption, selection microextraction aligns with the growing demand for green and high-throughput analytical methods.

Microextraction techniques are gaining increasing relevance in pharmaceutical analysis (He & Concheiro, 2018; Seidi *et al.*, 2018). These methods provide an efficient means of isolating and concentrating target analytes from complex matrices, with broad applications ranging from drug analysis to forensic toxicology (Ahmad *et al.*, 2021; He & Concheiro, 2018). Traditional sample preparation approaches often require large volumes of solvents and are typically time-consuming and labour-intensive (Moustafa, 2022). In contrast, microextraction techniques offer several advantages, including reduced solvent consumption, lower operational costs, and improved environmental sustainability (Moein *et al.*, 2014; Moustafa, 2022). Furthermore, there is growing interest in employing these methods for analysing controlled drugs not only in biological samples but for forensic contexts, revealing

their versatility and importance across various microextraction types and applications (Ahmad *et al.*, 2021).

Figure 2.1 illustrated the classification of microextraction methods available in analytical chemistry. Among the various microextraction methods, Solid-Phase Microextraction (SPME) or also known as Micro Solid Phase Extraction (µ-SPE) remains one of the most extensively employed methods in analytical chemistry. For instance, the use of a fused-silica fibre coated with sorbent materials such as polydimethylsiloxane (PDMS), polyacrylate (PA), or divinylbenzene (DVB) to facilitate the selective extraction of analytes from complex matrices (Pawliszyn, 2012). Recent innovations in SPME have focused on enhancing extraction efficiency and selectivity through the development of novel coatings, including carbon nanotubes (CNTs), which offer increased surface area, while molecularly imprinted polymers (MIPs), which provide molecular-level selectivity for intended purpose (Piri-Moghadam *et al.*, 2016).

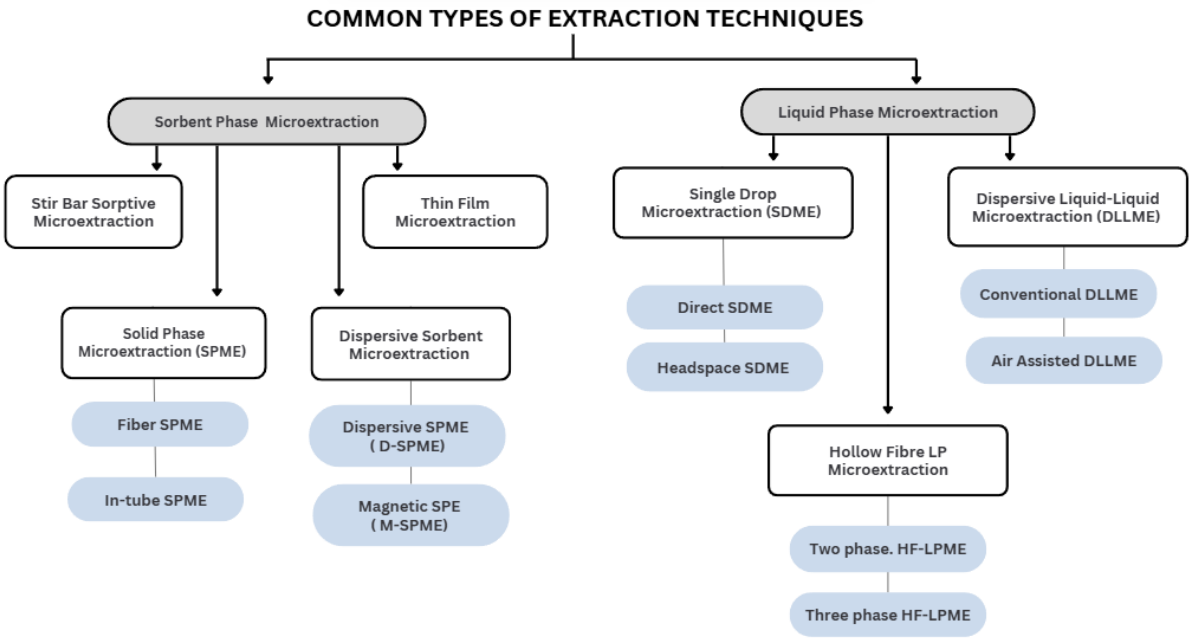

Figure 2.1. Main classification of microextraction methods in analytical chemistry

Notably, MIP-coated fibres have demonstrated high extraction performance, with reported recoveries exceeding 90% when it tested for determine presence of antibiotics in wastewater samples (Turiel *et al.*, 2007). Despite its advantages, SPME faces certain limitations, particularly the fragility of the extraction fibres and the limited commercial availability of advanced sorbent coatings. It is essential to recognize that while SPME represents a prominent form of sorbent-phase microextraction, it is not the only one. Other notable sorbent-based microextraction techniques include microextraction by packed sorbent (MEPS), stir bar sorptive extraction (SBSE), and thin film microextraction (TFME) which also offer valuable alternatives depending on the analytical context (He & Concheiro, 2018; Pereira *et al.*, 2013), summarised in Table 2.1.

Stir bar sorptive extraction (SBSE) is a sorbent-based microextraction technique that significantly enhances extraction efficiency using a polymer based-coated magnetic stir bar, which provides a substantially larger sorbent volume than conventional SPME fibres (David & Sandra, 2007). This increased phase volume contributes to higher analyte recovery, particularly suited for trace-level analysis. Technological advancements have further improved SBSE performance through the introduction of dual-phase coatings, such as ethylene glycol (EG)-silicone, which facilitate the simultaneous extraction of both polar and non-polar compounds from complex matrices (Kawaguchi *et al.*, 2013). A prominent application of SBSE is in the environmental analysis of endocrine-disrupting compounds, where coupling with gas chromatography–mass spectrometry (GC–MS) has enabled detection limits as low as 0.1 ng/L (Alvarez-Rivera *et al.*, 2020). Despite its high sensitivity and broad applicability, SBSE is constrained by its relatively long equilibration times, which can extend up to 24 hours, thereby limiting its suitability for high-throughput analytical workflows.

Table 2.1. Major classification of sorbent phase microextraction

Technique	Working Principle	Major Advancements	Applications	References
Solid-Phase Microextraction (SPME)	Fiber coated with sorbent adsorbs analytes from sample/headspace	MOFs, carbon nanotubes, MIPs for selectivity High-temperature resistant fibres	VOC analysis pesticides metabolomics	Piri-Moghadam *et al.* (2016)
Stir Bar Sorptive Extraction (SBSE)	Stir bar with sorbent extracts analytes via stirring	Dual-phase coatings (EG-Silicone) Automated TD-GC/MS coupling	Endocrine disruptors pharmaceuticals in water	David & Sandra (2007)
Microextraction by Packed Sorbent (MEPS)	Miniaturized SPE with sorbent packed in syringe	Online LC-MS for high throughput Mixed-mode sorbents	Drug monitoring bioanalysis	Abdel-Rehim (2011)
Thin-Film Microextraction (TFME)	High-surface-area sorbent film for extraction	Flexible/reusable films Blended coatings for multi-analyte extraction	Environmental water Forensics	Bojko *et al.* (2012)

Thin film microextraction (TFME) is a sorbent-based technique that utilizes sorbent-coated films or blades, such as polydimethylsiloxane (PDMS) or C_{18} coatings, to offer a high surface area for efficient and rapid analyte extraction (Bojko *et al.*, 2012). The large surface-to-volume ratio of TFME devices enhances mass transfer and extraction kinetics, making the technique particularly advantageous for time-sensitive analyses. Due to its portability, simplicity, and reusability, TFME is especially well-suited for on-site and field sampling applications. For instance, TFME sheet have been successfully employed to extract abuse drugs from blood samples with minimal matrix interference, ensuring high selectivity and reliability (Gorynski *et al.*, 2019). Recent innovations in TFME include the integration of electro spun nanofiber sorbents, which further enhance extraction performance by reducing diffusion path lengths, thereby accelerating analyte uptake and improving sensitivity (Bagheri *et al.*, 2021).

The selection of an appropriate sorbent for a designing analytical method necessitates a comprehensive and systematic approach that considers the physicochemical properties of the analyte, the characteristics of the sorbent, and the composition of the sample matrix (Moustafa, 2022). Major consideration in this process is the type of molecular interactions such as hydrophobic, π–π, hydrogen bonding, or electrostatic forces between the sorbent and the sorbate, which ultimately determine the selectivity and binding affinity of the extraction system (Ghorbani *et al.*, 2020). Therefore, choosing the right sorbent is essential to reduce matrix effects and to achieve accurate and consistent analytical results (Ridgway *et al.*, 2007). Surface modification of sorbents can also be employed to improve extraction efficiency (Ghorbani *et al.*, 2020).

While the type of extraction technique and solvent selection are important operational parameters, other influential factors must also be considered. These include the chemical and physical properties of the target compounds, as well as extraction time, temperature, pH, and the specific nature of the matrix (Ivanović *et al.*, 2020). To further mitigate matrix-related interferences, pre-extraction sample preparation strategies such as dilution, filtration, or matrix modification can be

employed to enhance method performance and improve the robustness of the microextraction procedure.

Managing the sample matrix is very important because complex samples often contain non-targeted substances that can compete with the target analytes for binding sites on the sorbent. This can lower the extraction efficiency and increase background noise. (Barros *et al.*, 2013; Vesper *et al.*, 2007). To address these challenges, strategies such as the use of protective agents, matrix-matched standards, or the standard addition method are recommended to counteract matrix-induced signal suppression or enhancement (Nanita, 2013). When conventional analytical methods fail to achieve adequate separation and quantification due to matrix interference, sample pre-treatment becomes a critical step (Slingsby & Kiser, 2001). Microextraction methods, with their low solvent and reagent requirements and compatibility with small sample volumes, are effective in reducing matrix effects and enriching target analytes (Moein *et al.*, 2014; Díaz-Montes, 2022).

2.1.2 Dispersive Micro Solid Phase Extraction

Dispersive micro solid phase extraction (D-µSPE) is a promising sample preparation technique using solid materials designed for the isolation and preconcentration of target analytes from complex matrices prior to instrumental analysis. This method synergistically combines principles from both dispersive liquid–liquid microextraction and solid-phase extraction, resulting in enhanced extraction efficiency and selectivity (Li *et al.*, 2011; Romanik *et al.*, 2006).

In a typical D-µSPE procedure, a carefully selected sorbent usually in the form of fine particles is directly dispersed into the sample solution (Yılmaz & Soylak, 2020). The sorbent, chosen based on its affinity for the target analytes, facilitates effective extraction by adsorbing the analytes from the matrix (Rutkowska *et al.*, 2018). After extraction, the sorbent particles containing the analytes are separated from the sample using centrifugation or filtration (Georgiou *et al.*, 2023). The analytes are then eluted

from the sorbent using an appropriate solvent, yielding a concentrated extract suitable for subsequent instrumental analysis (Abdelmohsen *et al.*, 2022).

The performance of D-µSPE depends on multi parameters, including the type and amount of sorbent, the choice of elution solvent, extraction time, and sample pH. The sorbent material is especially critical, as it governs both the selectivity and efficiency of the extraction (Ivanović *et al.*, 2020; Barros *et al.*, 2013). A variety of sorbents includes activated carbon, molecularly imprinted polymers, and metal organic frameworks have been successfully employed in D-µSPE, each offering distinct advantages in terms of capacity and target specificity (Ridgway *et al.*, 2007). In line, optimizing the extraction time and sample pH during mass transfer of analytes is essential to achieve high analyte recovery (Chambers *et al.*, 2007). The elution solvent must be selected to effectively desorb the analytes while minimizing the co-extraction of unwanted compounds.

D-µSPE has been widely applied across diverse fields, including environmental monitoring, food safety, and pharmaceutical analysis. Its versatility is further demonstrated by its compatibility with a broad range of analytical techniques, such as gas chromatography–mass spectrometry (GC-MS), high-performance liquid chromatography (HPLC), and capillary electrophoresis (Fanali, 2017; Díaz-Montes, 2022). This broad compatibility enables the sensitive and selective detection of analytes in complex samples.

2.1.3 Effervescence-assisted in Microextraction

Effervescence-assisted microextraction (EA-ME) is an emerging sample pre-concentration method that utilizes carbon dioxide (CO_2) gas bubbles, it's generated via a reaction between a CO_2 donor and an H^+ donor to rapidly disperse the extraction agent. This process enhances contact between the extraction agent and target analytes, thereby improving extraction efficiency and enrichment factor (Ghorbani *et al.*, 2020; Ye *et al.*, 2023). In general, EA-ME involves a chemical reaction between an acid (H^+ donor) and a carbonate or bicarbonate salt (CO_2 donor), generating gas bubbles within the aqueous sample (Lasarte-Aragonés *et al.*, 2020). These bubbles promote the

dispersion of a low-density, water-immiscible organic solvent throughout the sample. The resulting increase in interfacial contact facilitates efficient mass transfer of analytes into the organic phase. After extraction, the phases are separated, and the enriched organic layer is analysed using instrumental analysis such as gas chromatography (GC) or high-performance liquid chromatography (HPLC).

The efficiency of EA-ME depends on several parameters, including the type and ratio of acid and carbonate, extraction solvent volume, extraction time, and the presence of salts or surfactants that influence bubble formation and stability. EA-ME offers several advantages: it is simple, rapid, cost-effective, and requires minimal organic solvent (Kokosa, 2012; Psillakis & Kalogerakis, 2002). The use of gas bubbles for solvent dispersion eliminates the need for vigorous agitation, reducing the risk of analyte degradation and simplifying the workflow compared to traditional methods. The technique is adaptable to diverse sample matrices and compatible with multiple analytical platforms. Moreover, microextraction techniques like EA-ME promote environmental sustainability by minimizing reagent and solvent use and enabling the analysis of small sample volumes (He & Concheiro, 2018; Moein *et al.*, 2014).

Effervescence enhances sorbent dispersion by minimizing particle aggregation and promoting uniform distribution, become crucial needed in complex matrices where interfering substances may hinder extraction. The turbulence caused by CO_2 evolution disrupts the stagnant layer around sorbent particles, reducing diffusional resistance and improving mass transfer. In some approaches, the effervescence results from a reagent intentionally added to the sample to trigger gas generation. Among them, dispersive micro-solid phase extraction (D-µSPE), a related technique, benefits from improved sorption and elution kinetics when combined with effervescence, due to enhanced sorbent dispersion and surface contact (Bagheri *et al.*, 2015; Chisvert *et al.*, 2018; Racamonde *et al.*, 2015), then in line with green chemistry principles such as minimizing solvent use, energy consumption, and waste generation (Ivanović *et al.*, 2020; Liu *et al.*, 2019). Not limited to sorbent phase type, previous study reveals when ionic liquids used as extracting agent, it has shown potential in EA-ME due to their ability to completely disperse in aqueous media and quickly accelerate analyte migration (Li *et al.*, 2011).

2.1.4 In-syringe Type in Microextraction

In-syringe microextraction has emerged as a powerful and versatile sample preparation technique in modern analytical chemistry. It is a miniaturized method performed directly within a syringe, integrating extraction, separation, and pre-concentration into a single step (Trujillo-Rodríguez *et al*., 2020). Its simplicity, rapid rate, reduced solvent consumption, and compatibility with a wide range of analytical instruments make it especially attractive for high-throughput analysis. This technique is particularly valuable in areas such as environmental monitoring, food safety, and clinical diagnostics, where fast and reliable extraction of analytes from complex matrices is essential.

The principle of in-syringe microextraction involves partitioning target analytes between two immiscible phases inside the syringe. Typically, a small volume of extraction solvent or sorbent is drawn into the syringe, followed by the sample solution. The syringe is then agitated to facilitate mass transfer of the analytes into the solvent or sorbent (Figure 2.2). Once the extraction is complete, the phases are allowed to separate, and the final phase containing the enriched analytes is withdrawn and directly introduced into an analytical instrument for quantification analysis (Pawliszyn & Pedersen-Bjergaard, 2006). This approach not only simplifies the sample preparation process but minimizes analyte loss and contamination, thereby enhancing accuracy (Dugheri *et al.*, 2020).

Compared to traditional sample preparation methods such as liquid–liquid extraction (LLE) and solid-phase extraction (SPE), in-syringe microextraction offers several advantages. Conventional techniques are often laborious, time-consuming, and reliant on large volumes of toxic organic solvents, which raise environmental and cost-related concerns (Moustafa, 2022). In contrast, in-syringe microextraction operates with minimal solvent consumption and reduced labour, offering improved automation potential and operational efficiency (Psillakis & Kalogerakis, 2002; Chormey & Bakırdere, 2018). However, some limitations remain, such as matrix interferences and the small sample volume, which may affect sensitivity in trace-level applications. Therefore, careful optimization of extraction conditions especially solvent or sorbent selection, known is crucial to achieve high selectivity and recovery.

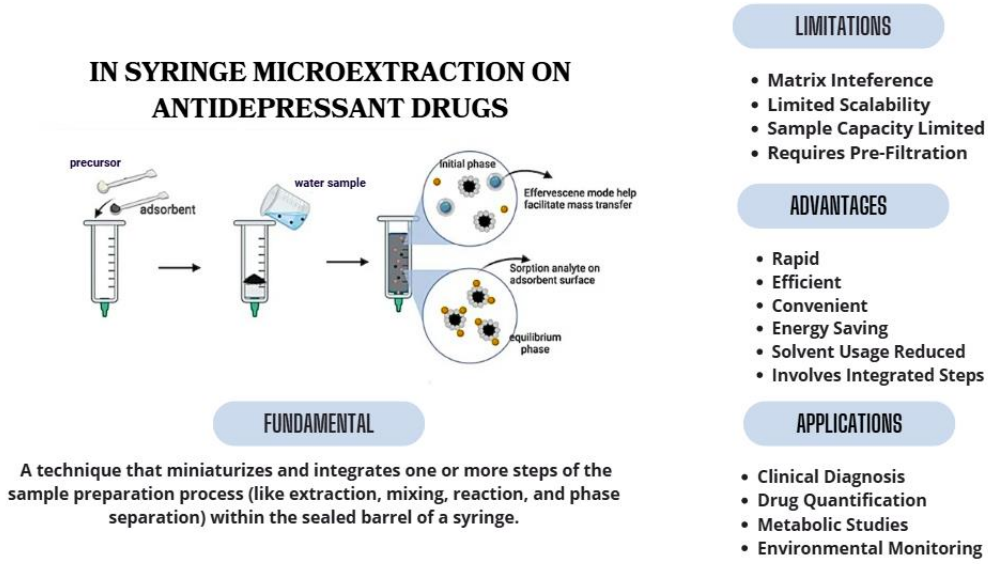

Figure 2.2. Application of in-syringe microextraction for pre-concentration of pharmaceutical drugs

To address the limitations of LLE and enhance automation, in-syringe-based methods were introduced as alternatives. Among the various miniaturized formats on in-syringe, microextraction by packed sorbent (MEPS) has gained significant attention. MEPS is carried out within a syringe containing a small amount of solid sorbent, allowing for the integration of sample extraction and injection into a single device.

For example, Rani (2011) reported a rapid and sensitive MEPS-based technique for detecting antidepressants from the same therapeutic class. The proposed method achieved good detection limits and was suitable for routine analysis of both clinical and forensic tested sample matrices. Similarly, Wietecha-Posłuszny *et al.* (2012) optimized a MEPS-LC-DAD method for six tricyclic antidepressants (amitriptyline, nortriptyline, imipramine, desipramine, doxepin, and nordoxepin) in serum samples. Their method, which involved the selection of optimal sorbent type, sample volume, and washing/elution conditions, yielded detection limits of 0.02-0.05 μg/mL with strong precision and accuracy. The use of certified reference materials confirmed the method's reliability, and its performance was comparable to conventional SPE.

Bagheri *et al.* (2016) also developed a MEPS-based method for the simultaneous determination of five antidepressants (amitriptyline, imipramine, clomipramine, mirtazapine, and citalopram) using LC-UV and GC-MS. The method demonstrated high sensitivity, with detection limits ranging from 0.088–0.284 ng/mL for GC-MS and 0.133-0.360 ng/mL for LC-UV and was validated for the analysis of plasma and urine sample.

2.2 Rationale for Adsorbent Functionalisation

2.2.1 General Overview

Adsorption is a widely adopted technique for removing pollutants from water, air and industrial effluents. Nevertheless, unmodified ("raw") adsorbents often display low selectivity and limited capacity. To overcome these drawbacks, their surface chemistry is routinely tailored, also known as functionalised with moieties such as silica, polymers or biomolecules. Functionalisation enhances the density and nature of binding sites, thereby improving capacity, affinity and selectivity toward specific contaminants (Rouquerol *et al.*, 2013). When properly engineered, a functionalised adsorbent can exhibit markedly higher affinities for heavy metals, organic dyes, or gases such as CO_2 (Kyzas & Matis, 2015). Among the available supports, magnetic nanoparticles (MNPs) are particularly attractive because their high surface-area-to-volume ratio maximises binding, while their super-paramagnetic cores enable rapid separation in an external magnetic field (Wu *et al.*, 2015). Most common functionalisation strategies for adsorbents are summarized in Table 2.2.

Table 2.2. Common functionalisation strategies for adsorbents

Method	Underlying Mechanism (Non-Exhaustive)	Representative Modifiers	Typical Target Adsorbates	References
Chemical grafting	Covalent coupling (e.g. salinization, amidation, esterification)	$–NH_2$, –COOH, –SH, $–SO_3H$	CO_2; Pb^{2+}, Cd^{2+}; dyes	Zhao *et al.*, 2022; Li *et al.*, 2020
Physical coating	Non-covalent deposition/encapsulation	Polyelectrolytes; Fe_3O_4; Ag NPs	Organic dyes; bacteria; gases	Wang *et al.*, 2019; Santhosh *et al.*, 2016
Biological functionalisation	Immobilisation of biomolecules (enzymes, DNA, proteins)	Laccase; aptamers; chitosan	Organic pollutants; pharmaceuticals	Ahmed *et al.*, 2021; Crini & Lichtfouse, 2019
Inorganic modification	Integration of MOFs, metal oxides or hybrid composites	TiO_2, ZnO, MOFs	CO_2/N_2 separation; VOCs; heavy metals	Zhao *et al.*, 2022; Rouquerol *et al.*, 2013

2.2.2 Physical Functionalization

Physical functionalization is a widely employed method to modify the surface properties of magnetic nanoparticles (MNPs), particularly those composed of iron oxide (Fe_3O_4), due to its simplicity, mild reaction conditions, and easy to tailor with other compounds. Unlike chemical grafting, which involves covalent bonding, physical functionalisation relies on non-covalent interactions such as hydrogen bonding, van der Waals forces, and electrostatic attraction to anchor functional materials onto the surface of the nanoparticles. These coatings can be achieved through simple mixing, adsorption, or precipitation processes, making this technique advantageous for applications requiring minimal solvent use, low energy input, and rapid processing time (Ahmed *et al.*, 2021).

One of the most common approaches involves the initial synthesis of Fe_3O_4 nanoparticles followed by encapsulation with a silica (SiO_2) shell. The silica layer provides three main benefits: it protects the magnetic core from oxidation, enhances colloidal stability, and offers a high density of surface silanol groups (–SiOH) for further interaction with functional materials (Reddy & Lee, 2013). Once coated with silica, the Fe_3O_4@SiO_2 nanoparticles can be further functionalised by physically adsorbing small molecules, polymers, or biomolecules onto their surface. This allows for tailoring of the adsorbent's surface properties without altering its magnetic core. Compared to bare Fe_3O_4, silica-coated nanoparticles have demonstrated improved chemical stability and ease of functionalisation, as shown by Mahmoud *et al.* (2018), who reported superior dispersibility and resistance to aggregation in aqueous phase.

In physical functionalisation, the selection of the coating material plays a critical role in determining the adsorbent's affinity and selectivity toward target contaminants. Researchers commonly used modifiers include natural polymers (e.g., chitosan, alginate), surfactants, metal nanoparticles, and small organic molecules. These materials introduce functional groups such as hydroxyl, amine, or carboxyl groups, which facilitate the binding of specific analytes through electrostatic interaction, hydrogen bonding, or π–π interactions. Additionally, such modifiers often enhance the biocompatibility, environmental friendliness, and cost-effectiveness of the

resulting adsorbents. For instance, biocompatible compounds like creatine and glutathione have been used as surface modifiers due to their ability to interact with pharmaceutical contaminants, possess different functional groups lead to strong mechanisms (Gupta *et al.*, 2016; Kyzas *et al.*, 2018).

Previous studies have demonstrated that functionalisation of Fe_3O_4@SiO_2 magnetic nanoparticles with creatine offers a promising green approach for pharmaceutical extraction, including antidepressants, due to creatine's zwitterionic nature, biocompatibility, and multimodal binding capabilities (Gupta *et al.*, 2016; Kyzas *et al.*, 2018). The silica shell enhances nanoparticle stability (Reddy & Lee, 2013), while creatine provides accessible active sites for interaction with polar and charged drug molecules, facilitating high adsorption efficiency and good magnetic recovery. This simple, non-toxic coating method, thus avoiding complex synthesis routes. Previous applications include successful extraction of heavy metals (Aladaghla, 2024), phthalic acid esters (Guo, 2014), and drug compounds like curcumin (Nguyen, 2022), all showing good to excellent recoveries. Laffafchi (2022) demonstrated that creatine-functionalised Fe_3O_4@SiO_2 sorbents achieved high recovery rates (80-92.7%) for antidepressants such as escitalopram and chlordiazepoxide in biological matrices, supporting their potential for micro solid-phase extraction (µ-SPE) of antidepressants in environmental applications.

2.2.3 Chemical Functionalization

In the growing analytical method, chemical functionalization plays a crucial role in enhancing the performance, reliability, and efficiency of processes related to the detection and extraction of target analytes from environmental samples. The primary objective of chemical modification on sorbent materials is to transfer the target analytes from complex sample matrices into a medium that is more compatible for analysis, while also considering sustainability and eco-friendliness (Augusto, 2009). Research on the fundamentals of SPME has driven the development and characterization of novel sorbents and adsorbents. The main focus in sorbent design has been the improvement of adsorptive capacity, stability, and durability to extend the lifetime of analytical devices (Augusto, 2009). Traditionally, sorbents in

microextraction included silica-based phases, C_{18}, and activated carbon. However, these have evolved into advanced nanomaterials, including bio-based options inspired by green analytical chemistry. Examples include carbon nanotubes, metal–organic frameworks (MOFs), and biopolymers, all of which possess high surface area and porosity, reducing the required sorbent amount in SPME. Functionalization of these materials further increases their versatility and broadens their applicability.

For instance, silica-coated iron oxide nanoparticles can be magnetized externally, but they must be stabilized with polymer-based materials or functionalized mesoporous silica surfaces. Silica functionalization provides a stable, biocompatible shell that protects the nanoparticles from environmental degradation, such as oxidation. To synthesize functionalized adsorbents, several preparation techniques are employed to improve adsorption efficiency. Among them, chemical grafting is the most widely used for modifying and functionalizing adsorbents, particularly magnetic nanoparticles. Acid treatments can introduce oxygen-containing groups, improving hydrophilicity (Herrera-Herrera, 2013). Functionalization can involve covalent or non-covalent binding interactions, enhancing selectivity toward specific analytes. For polymer sorbents, functionalization strategies must be carefully tailored to maintain sustainability. Functional groups on modified surfaces are often characterized using Infrared (IR) spectroscopy, while their reactivity can also be assessed indirectly by evaluating microextraction efficiency.

Previous studies demonstrate the benefit of functionalization. For example, Panella (2009) grafted aminopropyl groups onto iron oxide magnetic nanoparticles enclosed in a silica matrix through epoxy functionalization. The epoxy groups reacted with amine groups of other molecules, and successful functionalization was confirmed by Attenuated Total Reflection Infrared Spectroscopy (ATR-IR). Next, Zhang (2012) synthesized graphene sheets functionalized with sulfonic acid groups via sulfonation method. The modified graphene exhibited high precision, reproducibility, and linearity in the extraction of polycyclic aromatic hydrocarbons (PAHs) from water.

Lirio (2016) investigated polymers grafted onto activated carbon for phthalate ester extraction via SPME. Polymer embedding through heating polymerization

significantly improved adsorption efficiency, yielding recoveries between 76.2–99.3%, compared with the bare activated carbon. While Goudarzi (2022) employed chemical grafting to functionalize stainless-steel fibres for the SPME of mercury ions from biological samples. After optimization, the fibres showed high recovery rates over 30 sorption–desorption cycles compared to commercial fibres.

In another study, Kumar (2024) synthesized a chitosan–magnesium oxide nanocomposite derived from waste shrimp shells. This sustainable and biocompatible adsorbent demonstrated high potential for removing acenaphthene from wastewater. More recent advances include the use of covalent organic frameworks (COFs), as highlighted by Wang (2025). COFs material contain rich functional groups on active sites, providing excellent extraction properties in SPME for detecting wide range of polar analytes.

2.3 Pharmaceutical Residue in the Environment

2.3.1 General Overview

The global rise in pharmaceutical consumption has led to an increasing concern about their presence in natural environments. Pharmaceuticals, including commonly prescribed drugs such as antidepressants, antibiotics, and painkillers, are designed to interact with specific biological pathways in humans and animals. However, incomplete metabolism in the body and insufficient removal during conventional wastewater treatment allow these compounds to enter rivers, lakes, and coastal waters, raising both environmental and ecological disturbance (Khan *et al.*, 2021).

After ingestion, humans and animals excrete a substantial proportion of pharmaceuticals and their active metabolites, which subsequently enter sewage systems (Kasprzyk-Hordern *et al.*, 2009). Wastewater treatment plants, however, are primarily designed to remove organic matter and nutrients, not trace levels of pharmaceuticals, resulting in measurable concentrations being discharged into surface waters (Paiga *et al.*, 2017). In addition, the improper disposal of unused or expired medications, such as flushing them down toilets or discarding them with household

waste, further contributes to contamination into the environments (Daughton, 2016) as illustrated in Figure 2.3.

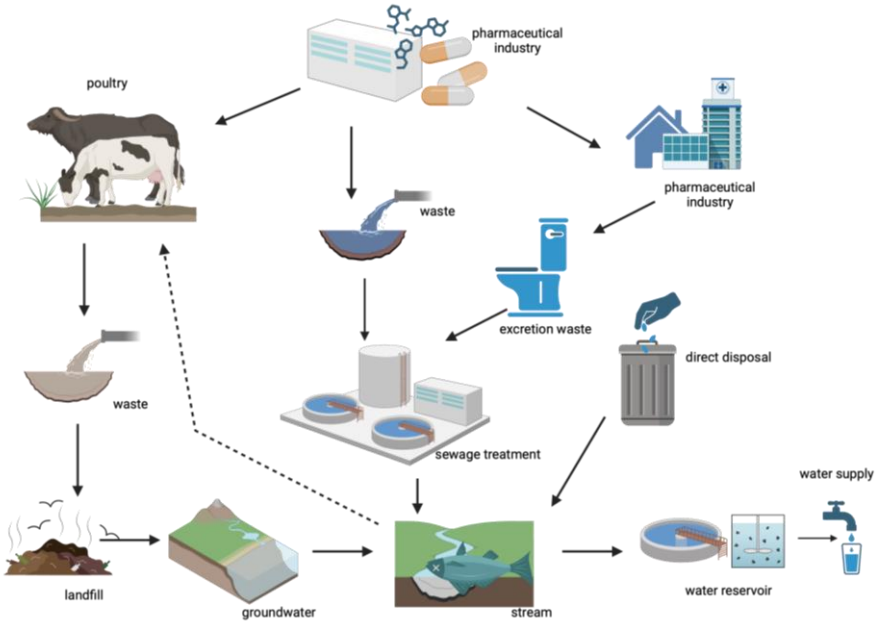

Figure 2.3. Possible routes of pharmaceutical drugs residues enter aquatic ecosystems (illustrated using biorender.com)

Pharmaceutical residues are biologically active compounds, and many targets physiological pathways that are conserved across different species. As a result, even low concentrations in aquatic environments can influence the behaviour, reproduction, and survival of aquatic organisms (Brodin *et al.*, 2014). For example, fish exposed to psychoactive drugs may display altered feeding and reproductive patterns, while invertebrates such as molluscs and crustaceans may show changes in locomotion and reproductive capacity (Weinberger & Klaper, 2014; Ford & Fong, 2016). These disruptions can cascade through food webs, ultimately threatening ecosystem stability.

Although concentrations of pharmaceuticals in surface waters are generally within the nanogram-to-microgram per liter range, their continuous release results in chronic exposure for aquatic life (Silva *et al.*, 2015). Environmental concerns are linked to the potential for bioaccumulation, as well as the fact that organisms are often exposed to complex mixtures of pharmaceuticals rather than single compounds (Aus

der Beek *et al.*, 2016). Moreover, while not all pharmaceuticals directly contribute to antimicrobial resistance, their coexistence with antibiotics and other bioactive substances in the environment may worsen emerging environmental health issues (Kümmerer *et al.*, 2018).

Addressing the environmental risks associated with pharmaceuticals requires a multifaceted strategy. Public awareness campaigns on the safe disposal of unused medicines can reduce direct contamination (Tong *et al.*, 2011). Advancements in wastewater treatment technologies such as advanced oxidation processes, membrane filtration, and activated carbon adsorption offer improved removal of pharmaceutical residues (Verlicchi *et al.*, 2012). In parallel, the development of highly sensitive and selective analytical methods is essential to detect trace levels of pharmaceuticals in complex environmental matrices, enabling low detection, details monitoring and risk assessment. Furthermore, the pharmaceutical industry can play a proactive role by developing "green pharmacy" approaches, designing drugs that are effective in clinical but less persistent in the environment (Daughton, 2016).

2.3.2 History of Antidepressants and Their Emergence in the Environment

The history of antidepressants dates to the 1950s, when two major breakthroughs transformed the treatment of depression (Figure 2.4 and Table 2.3). The first was the accidental discovery of iproniazid, an anti-tuberculosis drug later found to have mood-lifting effects due to its inhibition of monoamine oxidase (MAO) (López-Muñoz & Alamo, 2009). This led to the development of the first class of antidepressants, the monoamine oxidase inhibitors (MAOIs). Around the same time, imipramine, originally investigated as an antipsychotic, was found to alleviate depressive symptoms by blocking serotonin and norepinephrine reuptake, becoming the first tricyclic antidepressant (TCA) (Ban, 2001). Although effective, both MAOIs and TCAs had significant drawbacks. MAOIs required strict dietary restrictions to prevent hypertensive crises triggered by interactions with tyramine-rich foods (Shulman *et al.*, 2013), while TCAs caused anticholinergic side effects and carried a high risk of fatal overdose (Rudorfer & Potter, 1999).

By the 1960s and 1970s, researchers refined TCAs (e.g., amitriptyline, nortriptyline) but sought safer alternatives. This shifted the focus toward selectively targeting serotonin, culminating in the development of fluoxetine (Prozac) in 1987, the first selective serotonin reuptake inhibitor (SSRI) (Wong *et al*., 2005). SSRIs marked a major advancement in psychiatry: they produced fewer side effects, were safer in overdose, and quickly became the first-line treatment for depression (Cipriani *et al.*, 2018). Other SSRIs, including sertraline (Zoloft) and paroxetine (Paxil), were later introduced, further expanding therapeutic options.

The 1990s saw the emergence of novel mechanisms antidepressant on human bodies. Venlafaxine (Effexor), the first serotonin-norepinephrine reuptake inhibitor (SNRI), provided dual action on serotonin and norepinephrine, proving effective in both depression and chronic pain (Thase *et al.*, 2001). Mirtazapine (Remeron), classified as an atypical antidepressant, demonstrated benefits in patients with insomnia and appetite loss due to its sedative and weight-promoting properties (Anttila & Leinonen, 2001). Similarly, bupropion (Wellbutrin), a norepinephrine-dopamine reuptake inhibitor, became a preferred choice for patients with fatigue, low motivation, or those seeking aid in smoking cessation (Hurt *et al.*, 1997). To date, research continues to explore new antidepressant derivatives, particularly those with rapid and sustained therapeutic effects. Current directions emphasize precision medicine, aiming to match patients with optimal treatments based on genetic and biochemical biomarkers (Williams *et al.*, 2022).

In the 21st century, the COVID-19 pandemic triggered a significant global increase in antidepressant prescriptions across all age groups. This surge was driven by heightened psychological distress, social isolation, economic challenges, and adaptations within healthcare systems. Studies reported a 28% rise in depression cases worldwide, accompanied by an 18% increase in antidepressant use in the U.S. and a 6% increase in the UK (Santomauro *et al.*, 2021; Express Scripts, 2020; NHS Digital, 2021). Young adults (18–25 years) experienced the sharpest increase, nearly 30%, while children and adolescents showed a 5–10% rise, largely due to school closures and disrupted daily routines (Lu *et al.*, 2021; Pfefferbaum & North, 2020). Middle-aged and older adults also demonstrated elevated antidepressant use, often associated

with job losses, caregiving burdens, grief, and post-COVID neuropsychiatric symptoms (Pan *et al.*, 2021; Taquet *et al.*, 2021).

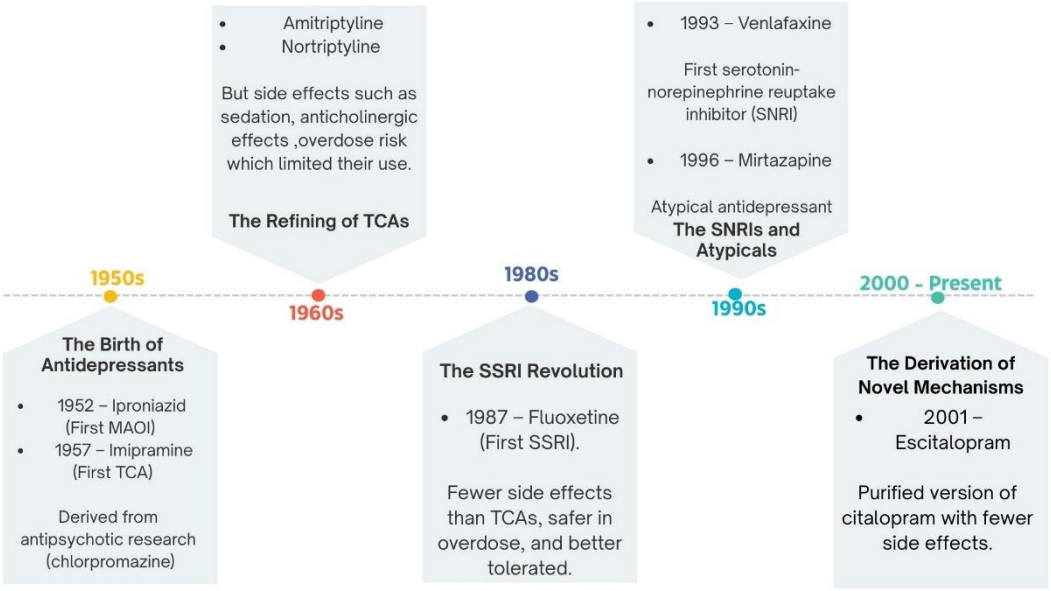

Figure 2.4. The chronology development of antidepressant drugs in pharmaceutical industry (Wong *et al.*, 2005; Thase *et al.*, 2001)

This surge in antidepressant consumption has inevitably increased the demand for psychotropic treatments, alongside rising pharmaceutical production. Consequently, a greater volume of pharmaceutical residues is released into the environment, raising long-term concerns about ecological and public health impacts. Antidepressants are excreted in significant amounts as both the parent drug and active metabolites, many of which are only partially removed by conventional wastewater treatment processes. As a result, these compounds have been consistently detected in surface waters, groundwater, and even drinking water at concentrations ranging from nanograms to micrograms per litre.

The persistence of antidepressants in aquatic systems is concerning because their mechanisms of action such as altering serotonin, dopamine, or norepinephrine pathways are conserved across many species. Fish exposed to trace levels of selective serotonin reuptake inhibitors (SSRIs) often display altered reproductive behaviours, feeding patterns, and predator avoidance, while invertebrates like crustaceans may

Table 2.3. Comparison of the three main general classes of antidepressants

Feature	TCAs	SSRIs	SNRIs	References
Mechanism	Block reuptake of 5-HT & NE; H_1, α_1 receptors	Selective 5-HT reuptake inhibition	Selective 5-HT & NE reuptake inhibition	(Stahl, 2013)
Efficacy	High (especially for severe depression, chronic pain)	Moderate (first-line for mild-moderate depression)	High (similar to TCAs but better tolerated)	(Cipriani *et al.* 2018)
Side Effects	- Anticholinergic (dry mouth) - Sedation - Cardiac toxicity	- Nausea, headache - Sexual dysfunction - Insomnia (initially)	- Nausea, sweating - Hypertension (dose-dependent) - Less sexual dysfunction than SSRIs	(Ferguson, 2001; Sansone *et al.* 2012)
Overdose Risk	High (fatal arrhythmias)	Low	Moderate (safer than TCAs)	(Rudorfer *et al.* 1999)
Key Uses	- Treatment-resistant depression - Neuropathic pain - Migraine prophylaxis	- Major depressive disorder - anxiety disorders	- MDD with fatigue - Chronic pain (fibromyalgia)	(Thase *et al.* 2001; Trivedi *et al.* 2006)
Advantages	- Effective for comorbid pain - Low cost	- Safer in overdose - Better tolerability	- Balanced efficacy for mood and energy - Pain modulation	(Bauer *et al.* 2013)
Disadvantages	- High side effect burden - Dangerous in overdose	- Delayed onset (2–4 weeks) - Sexual dysfunction	- May increase blood pressure - Withdrawal symptoms	(Zimmerman *et al.* 2004)

show impaired locomotion and reduced reproductive success. These disruptions can be triggered through food webs, ultimately threatening ecosystem balance. In addition, the continuous presence of antidepressants contributes to chronic exposure scenarios, where even low concentrations may accumulate over time, leading to long-term ecological effects.

2.3.3 Previous Studies on Antidepressant Extraction Methods

Over the years, various analytical methods have been developed to extract antidepressant analytes from different types of matrices. To achieve this, diverse materials have been functionalized into common adsorbents to improve their extraction efficiency (Table 2.4). For example, Fahimirad *et al.* (2018) synthesized an adsorbent functionalized with nitrogen-rich groups using an effervescent salt-assisted dispersive magnetic solid-phase microextraction method. The targeted analytes were amitriptyline and nortriptyline, tested in urine and pharmaceutical wastewater samples. Under optimized conditions, the extraction recovery exceeded 80%, demonstrating that the adsorbent was highly effective for microextraction applications.

Carbon-based adsorbents have also been widely explored due to their influence on microextraction efficiency. Bigdelifam *et al.* (2014) employed magnetic multiwalled carbon nanotubes in magnetic solid-phase extraction to determine fluoxetine in human urine samples. This approach achieved 95% recovery under optimized conditions, proving the high efficiency of carbon nanotube-based magnetic adsorbents. Similarly, Khoshnood *et al.* (2018) investigated the use of carbon nanotubes in SPME to detect and extract fluoxetine from hospital wastewater. Under optimized conditions, the method achieved an extraction recovery of 96%, with no observed carryover, confirming the efficiency of the adsorbent in drug retrieval.

In addition, polymer-based adsorbents have been developed for the determination and extraction of antidepressants. In previous work, Abdouss *et al.* (2012) synthesized a molecularly imprinted polymer (MIP) to detect citalopram in biological fluids such as urine and human serum. The method achieved extraction recoveries ranging from 82–86% in serum and 83–85% in urine under optimized

Table 2.4. Comparison of different analytical methods for determining antidepressant drugs

Method	Type	Target Analyte	Sample Type	Recovery (%)	Detection Limit	Reference
m-d-SPE	MOF-Carbon	Atomoxetine, Venlafaxine Duloxetine	Water, Biological Samples	90.2-96.4	0.1-0.4[b]	(Alhmaunde *et al.*, 2023)
µSPE	Carbon Nanotube	Fluoxetine, Venlafaxine, Citalopram, Sertraline	Urine	89.5	0.014 - 0.041[a]	(Bagheri *et al.*, 2018)
µSPE	Carbon Nanotube	Amitriptyline, Chlorpromazine	Water Samples	92.04-110	3.13 - 3.6[c]	(Wan Ibrahim *et al.*, 2020)
µSPE	Carbon Nanotube	Fluoxetine	Urine	95-105.5	0.06[a]	(Bigdelifam *et al.*, 2014)
µSPE	Carbon Nanotubes	Fluoxetine	Hospital Wastewater	96.7	0.0001[c]	(Khoshnood *et al.*, 2018)
µSPE	Carbon Nanotubes	Escitalopram	Human Plasma	73.06-110.27	0.1 - 0.35[b]	(Moon *et al.*, 2021)
µSPE	Graphene	Desipramine, Sertraline, Citalopram	Biological Samples	93.5-101.8	0.6 - 1.5[b]	(Aladaghlo *et al.*, 2021)
µSPE	Graphene	Paroxetine, Escitalopram, Citalopram	Hospital Wastewater	58.4-102.6	1.1 - 98.7[d]	(Kalaboka & Sakkas, 2023)
µSPE	Graphene	Fluoxetine, Citalopram	Urine, Wastewater	93.5-101.8	0.6 - 1.5[b]	(Zhao *et al.*, 2019)
m-SPE	Graphene	Napoxetine, Chlorpromazine, Citalopram	Environmental Water	99.6-102.1	3.1 - 4.6[b]	(Tabish *et al.*, 2019)
d-µSPE	MOF-Polymer	Amitriptyline, Norfluoxetine, Impramine, Sertraline	Plasma	94.9 - 102	0.03 - 0.2[a]	(Bazargan *et al.*, 2021)
µSPE	Polymer Based	Escitalopram	Environmental Water	84 - 120	2 - 22[b]	(Muñoz-bartual *et al.*, 2024)
d-µSPE	MIP	Sertraline	Biological Samples	92	0.2 - 0.5[c]	(Khalilian et al., 2017)
d-µSPE	Polypyrrole	Sertraline, Citalopram	Biological Samples	93.4 - 99	0.2 - 1.0[c]	(Asgharinezhad *et al.*, 2015)
d-µSPE	Polystyrene	Citalopram	Medical Wastewater	90 - 98	0.4-0.6[b]	(Moon et al., 2021)

µSPE	Silica Based	Fluoxetine	Environmental Water	93.8 - 97	0.53[b]	(Es'haghi *et al.*, 2015)
m-µSPE	Silica	Amitriptyline, Chlorpromazine	Biological Samples	86.1- 115.4	0.008-0.01[c]	(Kamaruzaman *et al.*, 2017)

Note: [a] µg/mL; [b] ng/mL; [c] µg/L; [d] ng/L

parameters. Demeestere *et al.* (2010) focused on the development, optimization, and validation of polymer-based adsorbents for analysing trace concentrations of psychoactive pharmaceuticals in river water. Relevant to antidepressants, the study reported recoveries of 81–104% for paroxetine, 56–86% for fluoxetine, and 59–94% for citalopram under optimized conditions. Further advancement in polymer-based functionalization was reported by Asgharinezhad *et al.* (2015), who synthesized polypyrrole-coated magnetic nanoparticles for dispersive solid-phase microextraction of citalopram and sertraline in biological samples. Optimization of extraction parameters yielded high recoveries, ranging from 93.4–99% for citalopram and 94–98.4% for sertraline, confirming the successful application of this method.

2.4 Design of Experiment

2.4.1 General Overview

Design of Experiments (DoE) is a systematic method used to plan, conduct, analyse, and interpret controlled tests to evaluate the factors that influence a response variable. It is widely applied in research, manufacturing, and process optimization to improve quality and efficiency (Montgomery, 2019). The working principles of DoE are randomization, replication, and blocking. In randomization, the random assignment of experimental units to treatment groups minimizes systematic bias and ensures that extraneous variables are evenly distributed across conditions (Box *et al.*, 2005). This principle is particularly crucial in clinical research, where random patient allocation to treatment and control groups helps mitigate selection bias and confounding effects.

Replication, or conducting multiple experimental trials under identical conditions, enables researchers to quantify random variability and enhance the reliability of their findings (Montgomery, 2019). For instance, repeating a chemical synthesis process multiple times allows for the assessment of yield consistency and process stability. Blocking, on the other hand, involves the strategic grouping of homogeneous experimental units to control for known sources of variability that could

otherwise obscure treatment effects (Anderson & Whitcomb, 2016). A classic application used in agricultural research, where field plots are blocked based on soil characteristics to isolate the true effect of different fertilizer treatments.

The common DoE techniques include factorial designs and response surface methodology (RSM). Factorial designs provide a systematic approach to investigating multiple factors and their interactions simultaneously within a single experimental framework (Box *et al.*, 2005). Full factorial designs examine all possible combinations of factor levels, while fractional factorial designs offer a more efficient alternative for screening experiments with many factors. This technique is particularly valuable for identifying synergistic or antagonistic effects between variables. Another widely used technique is response surface methodology, an advanced optimization approach that employs statistical and mathematical modelling to analyse the relationship between input variables and response outcomes (Myers *et al.*, 2016). RSM is most effective tool for process optimization, enabling researchers to determine optimal operating conditions through designs such as the central composite design and the Box–Behnken design. Additionally, Taguchi methods, developed by Genichi Taguchi, emphasize robust parameter design to minimize performance variation in the presence of noise factors (Taguchi, 1987). This approach uses orthogonal arrays to efficiently evaluate multiple parameters, with a focus on improving quality by making processes insensitive to uncontrollable environmental influences.

2.4.2 Plackett-Burman Design

Experimental design is a critical component of scientific research, ensuring efficiency, reliability, and cost-effectiveness in data collection. Among various design strategies, the Plackett–Burman Design (PBD) always preferred as screening tool that allows researchers to identify the most influential factors in a process with minimal experimental runs (Plackett & Burman, 1946). Originally developed for industrial applications, PBD has since been widely adopted in pharmaceuticals, analytical chemistry, and biotechnology studies. Plackett–Burman Design operates on several key principles that govern its proper implementation. The design follows a strict screening philosophy in which the number of factors (k) must always maintain the

relationship $k = N - 1$, with N being the number of runs (a multiple of 4) (Plackett & Burman, 1946). This orthogonal array structure provides significant advantages, allowing researchers to evaluate up to 11 factors in just 12 experimental runs, while focusing exclusively on main effects rather than interactions (Box *et al.*, 2005). The balanced assignment of high/low levels across all factors ensures that each variable receives equal consideration in the analysis.

The selection of run numbers follows specific guidelines that directly impact the design's capabilities. Researchers must choose from predetermined run numbers, with a minimum of 8 runs (suitable for screening 7 factors), while 12 runs are typically recommended for evaluating 11 factors (Montgomery, 2019). Larger factor sets may require 16, 20, or 24 runs to maintain proper experimental structure. It is important to note that the design resolution remains at Resolution III, meaning that main effects may become confounded with two-factor interactions (Anderson & Whitcomb, 2017). This characteristic necessitates careful interpretation of results, particularly when multiple factors appear significant.

The level assignment protocol in PBD requires precise implementation to ensure valid results. Each factor must be assigned exactly two levels, typically coded as –1 (low) and +1 (high), representing the practical extremes of the operating range (Myers *et al.*, 2016). Unlike more complex designs, classical PBD does not incorporate centre points, focusing instead on comparing these binary extremes. While this simplification contributes to the design's efficiency, it also limits its ability to detect nonlinear responses. The choice of levels therefore plays a critical role in the experiment's sensitivity, requiring researchers to select ranges that are both operationally feasible and sufficiently wide to capture meaningful effects (Box *et al.*, 2005).

Randomization is an absolute requirement in PBD implementation to prevent bias. Randomizing the order of runs helps avoid systematic errors that might arise from instrument drift, operator fatigue, or environmental changes during the experimental sequence (Montgomery, 2019). This principal safeguards against confounding time-dependent variables with the actual factor effects under investigation. Proper

randomization ensures that each factor-level combination has an equal chance of being influenced by external variations, thereby preserving the validity of statistical comparisons (Anderson & Whitcomb, 2017).

The PBD is widely applied in the literature for screening significant factors across various fields, and the following examples illustrate its practical applications. For instance, Funda (2015) demonstrated the use of PBD in developing a solid-phase microextraction method for the extraction of cobalt ions from food samples. Statistically significant parameters such as pH, the volume of ligand (DDTC), the volume of supramolecular solvent (1-decanol/THF), and centrifugation time were investigated using PBD. The optimum conditions identified were pH 6, 125 μL of 1-decanol, 450 μL of THF, 300 μL of DDTC (0.1%, w/v), and 8 minutes of centrifugation. Under these optimized conditions, the method achieved a relative standard deviation (RSD) of 1.51% (n = 8, recovery 94–98%), a limit of detection (LOD) of 1.89 μg/L, a limit of quantitation (LOQ) of 6.32 μg/L, and a preconcentration factor (PF) of 30.

Similarly, Ghorbani (2016) employed PBD in the optimization of a magnetic dispersive solid-phase microextraction method for the determination of zonisamide (ZNS) in human plasma. To achieve higher selectivity, sensitivity, and precision in the extraction of MRT and its metabolites with the SPME method, parameters such as pH, donor phase volume, surfactant volume (Triton X-100), extraction time, dispersing time, desorption time, desorption solvent volume, type of desorption solvent, amount of sorbent, amount of salt, and shaking rate were systematically investigated. The design involved 15 experiments, including 12 runs and three centre points, conducted in random order to eliminate uncontrolled variable effects. Each experiment was repeated three times, and the mean extraction recovery was calculated as the response. The responses were evaluated using analysis of variance (ANOVA) at a 95% confidence level, where factors with p-values <0.05 were considered statistically significant.

2.4.3 Central Composite Design

In the field of analytical chemistry and pharmaceutical research, optimizing experimental conditions is crucial for achieving high sensitivity, accuracy, and efficiency. While screening designs such as the Plackett–Burman Design (PBD) help identify significant factors, the Central Composite Design (CCD) advances the process further by enabling precise optimization of complex, nonlinear systems. Developed by Box and Wilson (1951), CCD is a promising tool of response surface methodology (RSM) and is widely applied in method development, drug formulation, and process engineering.

Unlike traditional one-factor-at-a-time (OFAT) approaches, CCD systematically investigates the entire experimental process. Its unique structure integrates factorial points that capture linear effects and interactions, axial points that explore quadratic responses, and centre points that assess system stability. This design enables researchers to uncover synergistic relationships between variables that would otherwise remain hidden in simpler designs. For example, in solid-phase microextraction (SPME) of antidepressants, CCD revealed a critical interaction between pH and temperature that improved recovery rates from 82% to 97% (Wu *et al.*, 2017). The true power of CCD lies in its integration with RSM, as it enables researchers to visualize efficiency peaks, quantify sensitivity thresholds, and identify best optimal conditions (Lehotay *et al.*, 2021). Such features are particularly valuable in complex extraction systems where multiple factors simultaneously influence outcomes.

Central Composite Design follows several fundamental rules to ensure proper implementation and validity. First, the selection of factor levels must be carefully planned. Researchers must define two extreme levels (typically coded as –1 and +1) and a centre point (0) for each factor (Box & Draper, 1987). For rotatable designs, axial points should extend beyond the factorial points ($\alpha > 1$), though face-centred CCDs with $\alpha = 1$ may be used when experimental constraints exist (Myers *et al.*, 2016). This careful level selection is critical for capturing the true response surface. The sequencing of experimental runs must follow strict randomization principles to prevent

systematic bias. Centre points should be evenly distributed throughout the experimentation process, and blocking becomes necessary when experiments are conducted in multiple batches (Anderson & Whitcomb, 2017). Proper randomization accounts for potential time-dependent variations in experimental conditions, ensuring the reliability of results. The importance of randomization cannot be overstated, as it forms the foundation for valid statistical analysis.

The determination of the alpha (α) value depends on the type of CCD being implemented. Rotatable CCDs are chosen to achieve equal prediction variance in all directions, while face-centred CCDs use $\alpha = 1$ for practical execution (Box & Wilson, 1951). Orthogonal CCDs calculate α based on design requirements to ensure independent estimation of coefficients. This choice significantly affects the design's properties and should be made carefully in alignment with the study's objectives and constraints. Centre point replication serves multiple critical functions in CCD. A minimum of three centre points is required for basic designs, while 5–6 centre points are recommended for processes with high variability, designs involving more than three factors, or when precise estimation of pure error is needed (Myers *et al.*, 2016). These replicates provide essential information about experimental error and verify the stability of the process at the centre of the design space.

Model validation in CCD follows rigorous statistical requirements. Analysis of variance (ANOVA) should yield a model F-value with $p < 0.05$, lack-of-fit $p > 0.05$, and preferably $R^2 > 0.90$ (Anderson *et al.*, 2017). Researchers must perform confirmation experiments at the predicted optimum and examine residual plots for random patterns. These steps ensure that the developed model accurately represents the true relationships between factors and responses. The inclusion and exclusion of factors in CCD must follow specific guidelines. Only factors proven significant in preliminary screening, such as through PBD, should be included, with a practical limit of 5–6 factors to maintain a manageable number of runs (Box & Draper, 1987). Insignificant terms ($p > 0.10$) should be removed through backward elimination to develop a parsimonious model. This careful factor selection preserves both the efficiency and interpretability of the design. Finally, the experimental domain must be carefully defined. The design space should be operationally feasible, avoiding

extrapolation beyond tested ranges while ensuring factor ranges cover the expected optimum (Myers *et al.*, 2016). Proper consideration of these aspects is essential before proceeding to instrumental analysis such HPLC, as they often determine the difference between successful optimization and wasted experimental effort.

2.4.4 Isotherm Models

The Langmuir isotherm model is one of the most widely used adsorption models in environmental science and material chemistry for describing the interaction between adsorbates and adsorbent surfaces. Proposed by Irving Langmuir in 1918, the model assumes that adsorption occurs on a homogeneous surface with a finite number of identical sites, each capable of holding one molecule, leading to the formation of a monolayer. It further assumes that there are no interactions between adsorbed molecules and that adsorption energy is constant across all sites. The model is mathematically expressed as a relationship between the amount of solute adsorbed per unit mass of adsorbent and its equilibrium concentration in solution, governed by parameters such as the maximum adsorption capacity (q_{max}) and the Langmuir constant (K_L), which reflects adsorption affinity. Due to its simplicity and strong theoretical basis, the Langmuir isotherm is extensively applied to evaluate adsorption efficiency, surface properties of adsorbents, and to design adsorption systems for water treatment and pollutant removal (Foo *et al.*, 2010; Zhang *et al.*, 2018).

Several studies have successfully applied the Langmuir isotherm to investigate mechanism of antidepressant on sorbent surface using SPME. For example, Zhang *et al.* (2018) investigated the adsorption of selective serotonin reuptake inhibitors (SSRIs) on adsorbents and found that the Langmuir model provided an excellent fit (R^2 >0.98), indicating monolayer adsorption of fluoxetine and sertraline. The study reported a q_{max} of 12.5 µg/g and a K_L of 0.45 L/µg, suggesting strong binding affinity. Kataoka *et al.* (2020) studied the extraction of tricyclic antidepressants (TCAs) using carbon-based SPME adsorbents and observed deviations from the Langmuir model at high concentrations, likely due to multilayer adsorption and competitive binding between analytes.

Despite its widespread use, the Langmuir model has several limitations that affect its accuracy. Firstly, it assumes that all adsorption sites on the SPME adsorbent possess identical energy and affinity, which is rarely the case in practice. Commercial SPME adsorbents such as PDMS, C_{18}, or mixed-mode coatings often exhibit surface heterogeneity due to variations in polymer crystallinity, pore distribution, or functional group availability (Zhang *et al.*, 2018). From other study, graphene-coated adsorbents used for fluvoxamine extraction display energetically heterogeneous sites, resulting in deviations from ideal Langmuir behaviour (Martínez-Pérez *et al.*, 2022).

Another limitation arises in biological and wastewater samples, where multiple antidepressants coexist varied in term of concentration levels. The Langmuir model does not inherently account for competitive adsorption, where analytes compete for the same binding sites. Kataoka *et al.* (2021) reported that paroxetine outcompeted fluoxetine due to stronger hydrogen bonding, requiring more complex isotherm models for accurate description. These limitations are particularly evident when studying creatine-coated adsorbents. The unique molecular structure of creatine, featuring both amine ($–NH_2$) and carboxyl (–COOH) functional groups in a zwitterionic configuration, offers multiple interaction sites for antidepressants (Garcia Ruiz *et al.*, 2023; Smith *et al.*, 2021). This makes creatine-coated adsorbents especially promising for SPME of SSRIs from complex matrices. However, the inherent heterogeneity of creatine-coated surfaces, resulting from variations in crystallinity, zwitterion orientation, and pore structure, suggests that the Freundlich isotherm may provide a better fit than the Langmuir model (Jones *et al.*, 2020).

The Freundlich isotherm, originally developed by Herbert Freundlich in 1906, describes adsorption processes on heterogeneous surfaces using an empirical formula (Foo *et al.*, 2010). This model is particularly valuable for SPME applications as it accommodates the complex, multi-mechanistic adsorption processes occurring on functionalized adsorbents (Thompson *et al.*, 2022). These include hydrogen bonding, electrostatic interactions, and hydrophobic effects processes that are better captured by the Freundlich model than by simpler isotherm approaches (Wilson *et al.*, 2023).

The adsorption behaviour of antidepressants on functionalized adsorbents varies considerably by targeted analytes. For instance, fluoxetine shows K_F values ranging from 4.8 to 5.5 μg/g with *n* values between 1.4 and 1.6, indicating moderately strong adsorption dominated by hydrophobic interactions (Kim *et al.*, 2023). In contrast, sertraline demonstrates higher adsorption capacity (K_F = 7.2–8.3 μg/g) but lower *n* values (1.1–1.3), reflecting strong π–π stacking interactions with the creatine coating (Lee *et al.*, 2022). Paroxetine displays unusually high *n* values (1.5–1.8), suggesting particularly favourable hydrogen bonding interactions with the zwitterionic surface (Martinez *et al.*, 2023). These compound-specific differences highlight the importance of the Freundlich model's flexibility for accurately characterizing adsorption across antidepressant classes.

Compared with traditional SPME coatings, functionalized adsorbents show several distinct advantages. Studies comparing creatine coatings with polydimethylsiloxane (PDMS) adsorbents revealed a 2.1-fold increase in K_F values for polar SSRIs (p <0.01), indicating significantly enhanced extraction efficiency (Wilson *et al.*, 2023). In biological matrices such as urine and plasma, creatine coatings reduced matrix effects by 40% compared with commercial C_{18} adsorbents (Roberts et al., 2023). Furthermore, creatine coatings demonstrated superior batch-to-batch reproducibility (12% RSD) compared to molecularly imprinted polymers (25% RSD), addressing a common limitation of many advanced adsorbent materials (Zhao *et al.*, 2023). These advantages position creatine-coated adsorbents as a highly promising alternative for routine antidepressant analysis in both environmental and clinical study.

2.4.5 Kinetic Models

The pseudo-first-order (PFO) kinetic model is one of the most widely applied models in adsorption studies, particularly for describing the initial stages of solute uptake onto adsorbent surfaces. Originally proposed by Lagergren in 1898, the model assumes that the rate of adsorption is directly proportional to the number of unoccupied sites available on the adsorbent (Ho and McKay, 1998). This makes it especially suitable for systems where physical adsorption predominates, and adsorption occurs rapidly at the beginning of the process. The PFO model is often expressed in its

linearized form, which enables the determination of main kinetic parameters such as the rate constant (k_1) and the equilibrium adsorption capacity (q_e). Its simplicity, ease of application, and good fit to experimental data in many adsorption systems have contributed to its extensive use in environmental and pharmaceutical adsorption studies. However, while the PFO model effectively explains initial adsorption behaviour (Wang *et al.*, 2022), it may not always accurately predict equilibrium capacities, especially in systems dominated by chemisorption or complex multi-layer adsorption processes.

The pseudo-first-order (PFO) kinetic model has emerged as a fundamental tool for analysing the initial adsorption rates of target analytes such pharmaceuticals onto surface of adsorbents. The theoretical basis of the PFO model is expressed through derived formula, described details in methodology section (Ho, 2006). Recent studies have revealed notable variations in PFO parameters among different antidepressant compounds. Fluoxetine, for instance, typically shows k_1 values ranging from 0.035 to 0.045 min^{-1} in aqueous matrices (Kim *et al.*, 2022), while sertraline exhibits faster adsorption kinetics (k_1 = 0.050–0.060 min^{-1}), attributed to enhanced π–π interactions with the creatine coating used as adsorbent (Lee & Park, 2023). Paroxetine, on the other hand, displays slightly lower k_1 values (0.030–0.040 min^{-1}) but achieves higher equilibrium capacities, reflecting its strong hydrogen-bonding potential (Martinez *et al.*, 2023). These compound-specific differences highlight the importance of considering molecular structure when applying the PFO model to antidepressant extraction.

Comparative studies between creatine-coated adsorbents and conventional SPME coatings provide details mechanism between adsorbent and adsorbate. Creatine-based adsorbents consistently demonstrate 1.5–2.0 times higher k_1 values than PDMS coatings for polar antidepressants (Wilson *et al.*, 2023), along with high reproducible PFO behaviour across experimental batches (RSD <15%) compared to molecularly imprinted polymers (Harris, 2023). The excellent fit of experimental data to the PFO model ($R^2 > 0.95$) during the first 60 minutes of extraction further supports its suitability for creatine-coated adsorbents (Liu & Thompson, 2023; Zhang *et al.*, 2023).

The zwitterionic nature of creatine coatings, containing both amine and carboxyl functional groups, creates unique kinetic behaviours that often follow PFO patterns during the initial adsorption phase (Wang *et al.*, 2022). Studies show that optimal k_1 values for most SSRIs occur at physiological pH (7.4), where both functional groups of creatine are ionized and available for interaction (Thompson *et al.*, 2023). Under acidic conditions (pH < 4), protonation of carboxyl groups reduces k_1 values by 20–30%, while basic conditions (pH > 9) typically decrease adsorption rates by 15–25% due to diminished hydrogen-bonding potential (Garcia-Ruiz *et al.*, 2023; Morgan *et al.*, 2022). This makes the PFO model especially suitable for studying the rapid uptake of selective serotonin reuptake inhibitors (SSRIs) and other antidepressants in both biological and environmental samples (Zhang *et al.*, 2023).

Despite its strengths, the PFO model also presents limitations when applied to functionalized adsorbents. It often underestimates equilibrium capacities (q_e) by 10–20% compared with experimental results (Taylor *et al.*, 2023), and its accuracy diminishes for thick (>100 μm) or highly porous coatings (Zhao, 2023). To overcome these shortcomings, researchers have proposed several strategies, including transitioning to pseudo-second-order models after the initial adsorption phase (Adams *et al.*, 2023) and incorporating intraparticle diffusion terms for a more comprehensive kinetic analysis (Baker *et al.*, 2023). Such hybrid approaches provide a more complete characterization of the entire extraction process.

The pseudo-second-order (PSO) kinetic model originally developed by Ho and McKay (1999), the model provides a robust framework for analyzing adsorption processes dominated by chemisorption, where electron sharing or exchange occurs between the adsorbent and adsorbate molecules (Simonin, 2016). The mathematical formulation of the PSO model provides valuable information into adsorption behaviour. Its linearized form, enables simultaneous determination of the equilibrium adsorption capacity (q_e) and the rate constant (k_2) from experimental data (Ho, 2006). Studies have shown that the PSO model often fits the entire adsorption process on material-coated adsorbents better than the pseudo-first-order model, particularly for antidepressants forming strong, specific interactions with the coating (Liu &

Thompson, 2023). Its ability to describe both the initial rapid adsorption phase and the subsequent equilibrium stage makes it highly valuable for method optimization.

Compound-specific differences performance in PSO parameters have also been observed. For fluoxetine, k_2 values typically range from 0.0021 to 0.0028 g/μg min^{-1} in aqueous matrices, reflecting moderate adsorption affinity (Zhang *et al.*, 2023). Sertraline exhibits faster kinetics, with k_2 values between 0.0032 and 0.0039 g/μg min^{-1}, largely due to enhanced π–π stacking interactions with the aromatic groups in creatine coatings (Lee & Park, 2023). Paroxetine demonstrates intermediate rate constants (0.0025–0.0031 g/μg min^{-1}) but achieves the highest equilibrium capacities among common SSRIs, likely because of its strong hydrogen bonding with the zwitterionic surface (Martinez *et al.*, 2023). These variations highlight the importance of considering molecular structure when applying the PSO model in antidepressant extraction studies.

Comparisons between coated adsorbent like creatine and conventional SPME materials reveal clear advantages of the zwitterionic coatings. Creatine-based adsorbents consistently show 1.8–2.5 times higher k_2 values than PDMS coatings for polar antidepressants, indicating significantly faster adsorption kinetics (Wilson *et al.*, 2023). Materials also display more reproducible PSO parameters across experimental batches (RSD <12%) compared with C_{18} adsorbents, suggesting superior consistency in performance (Harris, 2023). Importantly, experimental data from creatine-coated adsorbents typically exhibit excellent agreement with the PSO model (R^2 >0.99) across the entire adsorption profile, from initial uptake to equilibrium (Zhang & Chen, 2023). This strong correlation validates the use of PSO kinetics for method development and optimization.

Nevertheless, the PSO model has limitations when applied to functionalized adsorbents. Its accuracy decreases for very thin coatings (<10 μm), where boundary layer effects become more prominent (Taylor *et al.*, 2023). The model also struggles with multi-analyte systems, as its formulation does not account for competitive adsorption between coexisting compounds (Zhao, 2023). To address these challenges, researchers have developed hybrid models that integrate PSO kinetics with

intraparticle diffusion (Adams *et al.*, 2023) and machine learning algorithms that predict k_2 values from molecular descriptors (Wilson, 2023). Real-time monitoring techniques using spectroscopic methods now allow more precise determination of adsorption rates and capacities (Stevens *et al.*, 2023). At the same time, improvements in coating fabrication provide greater control over surface properties, resulting in more predictable kinetic behaviour (Wang *et al.*, 2024).

2.5 Greenness profile

2.5.1 General Overview

Green chemistry, a rapidly evolving discipline, aims to design chemical processes and products that minimize environmental impact while maximizing efficiency and sustainability. However, green chemistry metrics are not directly applicable in analytical chemistry because they refer to the mass of the product, whereas analytical determinations do not generate products with measurable mass. The evaluation of greenness profiles in analytical methods has been evolving since the 1990s, and it is crucial for promoting eco-friendly practices in various fields, particularly in pharmaceuticals (Anastas, 1998). Previous studies have introduced various metrics and methodologies to assess the environmental impact of analytical techniques, ensuring alignment with green chemistry principles. This evaluation considers factors such as solvent usage, energy consumption, and waste generation, which collectively support the development of more sustainable analytical practices.

In green analytical chemistry, twelve criteria form the basis for evaluating newly developed methods (Figure 2.5). The twelve principles of green chemistry provide a framework for designing sustainable chemical processes and products (Bystrzanowska *et al.*, 2020). First, prevention emphasizes avoiding waste generation rather than treating it afterward. Atom economy encourages maximizing the incorporation of all reactants into the final product to minimize waste. Less hazardous chemical syntheses prioritize the use and production of non-toxic substances, while designing safer chemicals ensures functionality with minimal toxicity. Safer solvents

and auxiliaries should be eliminated or replaced with benign alternatives, and energy efficiency should be optimized by favouring ambient conditions.

Renewable feedstocks are preferred over depletable resources, and reducing derivatives minimizes unnecessary steps that generate waste. Catalysis is favoured over stoichiometric reagents for improved efficiency, and design for degradation ensures chemicals break down harmlessly after use. Real-time analysis helps prevent pollution by enabling immediate monitoring, and inherently safer chemistry reduces risks of accidents such as spills or explosions. Collectively, these principles promote sustainability, safety, and environmental responsibility in chemical practices (Marcello, 2023)

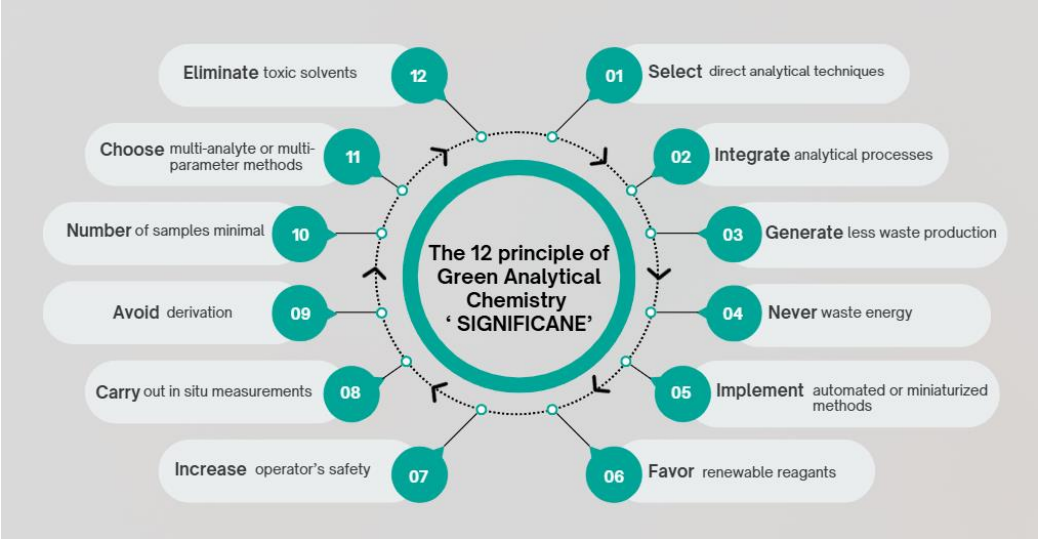

Figure 2.5. Twelve principles of green analytical chemistry (Bystrzanowska *et al.*, 2020)

2.5.2 Analytical Eco-Scale

The Eco-Scale was first introduced by Van Aken *et al.* (2006) as a penalty-based metric to evaluate the environmental impact of chemical processes, particularly in organic synthesis. This semi-quantitative approach assigns a score between 0 and 100, where 100 represents an ideal green process with no environmental penalties. The scoring system works by deducting points based on several main factors: the toxicity

and quantity of reagents used, the hazards and volume of solvents, energy requirements, waste generation, and occupational safety risks. Each of these categories carries specific penalty points, allowing researchers to quantitatively assess and compare the greenness of different methodologies (Table 2.5).

Table 2.5. The penalty criteria based on the evaluation of Analytical Eco-Scale

Category	**Penalty Points**
Hazardous reagents	1–8 per reagent
Harmful solvents	1–6 per solvent
High energy consumption	1–5 per step
Excess waste (>10 g)	1–6 per waste type
Safety risks	1–4 per hazard

A significant advantage of the Eco-Scale is its simplicity and practical applicability in laboratory settings. For example, a synthetic reaction using 1.0 g of a toxic reagent (6 penalty points), 50 mL of dichloromethane (5 points), heating at 80 °C (3 points), and generating 15 g of waste (4 points) would yield an Eco-Score of 82 (100 – 18 = 82). This score indicates a reasonably green process with room for improvement (Van Aken *et al.*, 2006). The straightforward calculation makes the Eco-Scale particularly useful for quick assessments and method optimization during early-stage research and development.

However, the Eco-Scale does have limitations. As noted by Gałuszka *et al.* (2012), the penalty system can be somewhat subjective, as hazard classifications may vary between users or regulatory frameworks. Additionally, the metric treats all penalty categories equally, without weighting, which may overlook more significant environmental impacts. The original Eco-Scale also does not account for important sustainability factors such as the renewability of feedstocks or the biodegradability of

waste products. These limitations led to the development of more comprehensive assessment tools, including the Analytical Eco-Scale.

The Analytical Eco-Scale, an adaptation by Gałuszka *et al.* (2012), modified the original concept specifically for analytical chemistry applications. This version has been widely applied to evaluate techniques such as chromatography (HPLC, GC), spectroscopy (ICP-MS, AAS), and sample preparation methods (SPE, LLE) in pharmaceutical and environmental analysis. The adaptation maintained the core penalty-based approach while tailoring it to analytical methodologies, demonstrating the flexibility and enduring utility of the Eco-Scale concept in green chemistry assessment.

2.5.3 Green Analytical Procedure Index

The Green Analytical Procedure Index (GAPI) represents a significant advancement in environmental impact assessment tools for analytical methodologies. Developed by Płotka-Wasylka (2018), this metric addresses holistic approach to evaluating the greenness of analytical procedures by considering multiple stages of the analytical process. Unlike previous metrics that focused on isolated aspects such as solvent use or energy consumption, GAPI provides a systematic framework for assessing environmental impacts across the entire analytical workflow.

GAPI builds upon foundational green chemistry principles (Anastas & Warner, 1998) while addressing specific needs in analytical chemistry. Its development was motivated by the limitations of earlier metrics such as the National Environmental Methods Index (NEMI), which relied on oversimplified binary assessments (Płotka-Wasylka *et al.*, 2017). The five-sector design reflects the analytical process lifecycle, providing a more nuanced evaluation compared to single-score systems. The integration of GAPI into the development and optimization of analytical procedures is crucial for minimizing environmental burdens and safeguarding human health throughout the entire analytical workflow (Meher & Zarouri, 2025).

In GAPI assessments, a distinct symbol consisting of five pentagons is employed to evaluate an analytical method. The colour scale, representing the ecological impact of materials at each step of the methodology, ranges from green (the most favourable) through yellow (moderate) to red (the least favourable). Each pentagon reflects a specific feature of the assessed analytical method (Figure 2.6). Areas are filled with green when conditions are met or with red when conditions are not achieved. This graphic presentation enables investigators to draw clear conclusions about different green measures. Hence, this greenness assessment tool is highly valuable for comparing methods, as it highlights the weakest points in analytical procedures. Nevertheless, GAPI does not provide numerical evaluation.

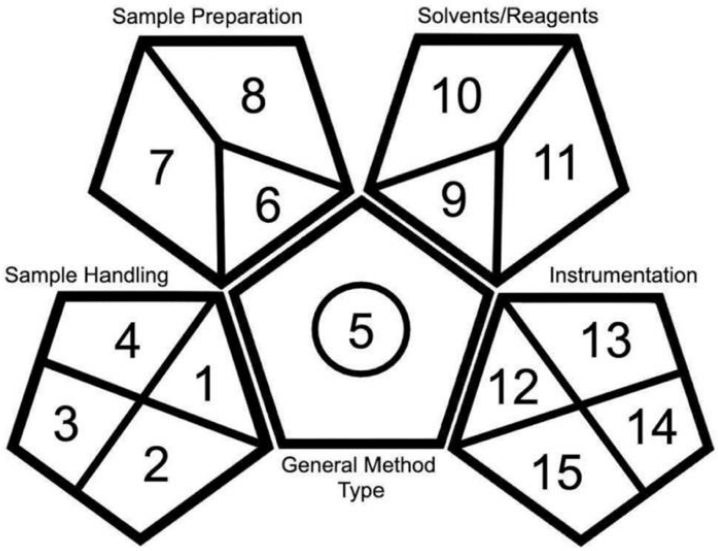

Figure 2.6. The pictogram of GAPI (Płotka-Wasylka *et al.*, 2017)

The first pentagon assesses the environmental impact of sample collection (1), preservation (2), transportation (3) and storage (4). This stage evaluates whether methods require chemical preservatives, refrigeration, or other stabilization techniques that may generate waste or consume energy. Green ratings are awarded for direct analysis or non-invasive sampling, while yellow and red ratings indicate increasing environmental burdens (Gałuszka *et al.*, 2013). For example, methods requiring no preservatives (e.g., immediate analysis of fresh wastewater) score green, whereas those requiring hazardous preservatives such as mercury compounds receive red ratings. Recent studies emphasize that proper sample handling significantly contributes to

overall method sustainability, making this pentagon crucial for life cycle assessment (Tobiszewski *et al.*, 2017).

The second pentagon examines extraction (6), and pretreatment procedures (8), focusing on solvent (7), energy requirements, and derivatization steps. This is often where analytical methods show the greatest variability in greenness. Solvent-free techniques such as SPME consistently achieve green ratings, while conventional methods like liquid–liquid extraction score poorly due to high organic solvent consumption (Pena-Pereira *et al.*, 2020). The third pentagon specifically evaluates the toxicity (10; 11), quantity (9), and renewability of chemicals used. Recent research shows that solvent selection accounts for up to 70% of a method's environmental impact, making this pentagon particularly significant (Clark *et al.*, 2016). The assessment also considers whether renewable feedstocks are used (Principle 7), with bio-based solvents increasingly improving GAPI scores in modern methods (Capello *et al.*, 2007).

The fourth pentagon assesses the energy intensity (12) and equipment requirements of the analytical process (13). Techniques such as ambient mass spectrometry score well (green), while energy-intensive methods such as LC–MS typically receive yellow or red ratings (Armenta *et al.*, 2008). This evaluation aligns with Principle 6 (Energy Efficiency), and recent advances in miniaturized instruments show promise for improved ratings (Manz *et al.*, 2021). The final pentagon examines waste management (14; 15), considering the quantity of waste per analysis, the hazard level of byproducts, and recycling or reuse potential. Microextraction techniques often score green due to minimal waste generation (<0.1 g), whereas conventional methods generating >10 g of hazardous waste receive red ratings (Płotka-Wasylka *et al.*, 2021). This assessment embodies Principle 1 (Prevention) and Principle 10 (Design for

Degradation) linked to develop biodegradable analytical materials (Bojko *et al.*, 2023).

2.5.4 Analytical Greenness Metric (AGREE)

AGREE is a recently introduced method of greenness evaluation, developed by Pena-Pereira *et al.* (2023). This method directly addresses the 12 principles of green analytical chemistry (GAC), abbreviated as SIGNIFICANCE. In calculating greenness, the AGREE tool incorporates all 12 principles of GAC, making the assessment flexible, comprehensive, and straightforward to interpret. The AGREE evaluation generates a colourful pictogram divided into 12 sections at the border (Figure 2.7). Each section represents one of the GAC principles and is assigned a score ranging from 0 to 1, where 1 indicates a fully green practice (green colour) and 0 indicates a non-green practice (red colour), with intermediate scores shown in gradient shades. At the centre of the pictogram, an overall numerical score is displayed, summarizing the greenness of the method. The AGREE tool was designed based on solid guidelines emphasizing input flexibility, inclusiveness, clarity, and simplicity, as detailed in the original work by Pena-Pereira *et al.* (2023), summarized in Table 2.6.

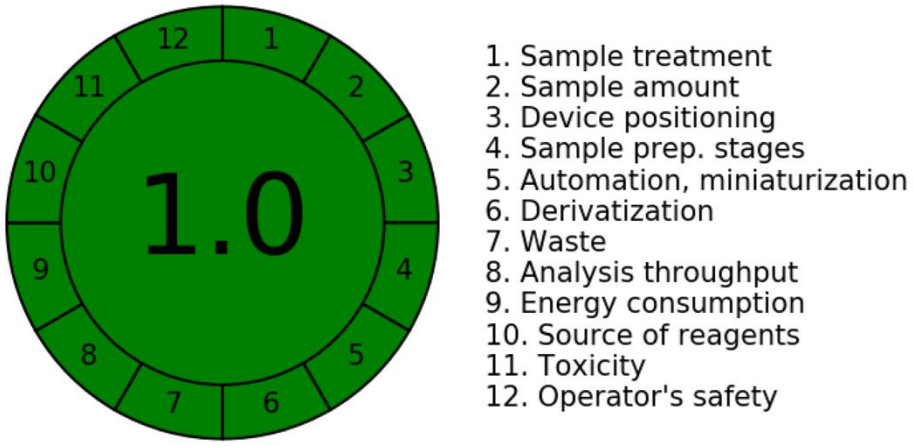

Figure 2.7. AGREE – Analytical Greenness Metric (Pena-Pereira *et al.*, 2023)

The AGREE tool has documented in previous studies. For example, Atiah (2022) applied AGREE to assess six chromatographic methods for the simultaneous analysis of five important neurotransmitters namely acetylcholine (Ach), serotonin (5-HT), dopamine (DA), gamma-aminobutyric acid (GABA), and glutamate (Glu). Among the six methods, method 1 was identified as the most suitable choice for analysts due to its favourable greenness score (0.66 according to the AGREE pictogram), broad applicability (allowing the analysis of seven components), high sensitivity (detecting as low as 2 pg for Ach, 5-HT, and Glu, and 10 pg for DA, norepinephrine, GABA, and

glycine), and rapid analysis (completion within 5 minutes). However, the AGREE assessment revealed compromises in operator safety and energy consumption across all methods. Notably, the four most heavily weighted criteria (reagent toxicity, waste generation, sample preparation, and energy consumption) strongly influenced the discrimination of greenness between methods. Similarly, Suthar (2024) applied AGREE to evaluate the analysis of cilnidipine (CLN). The developed method achieved an AGREE score of 0.80, the highest among the reported methods, and was therefore considered the greenest. In contrast, the least green method received an AGREE score of 0.60.

Table 2.6. Description of main greenness criterion in AGREE calculator

Category	**Weight (%)**	**Description**
Sample Preparation	10	Evaluates solvent use, energy, and waste in extraction
Sample Size	5	Smaller samples = lower environmental impact
Reagent Toxicity	15	Penalizes hazardous chemicals (GHS classifications)
Energy Consumption	10	High-energy methods (e.g., GC, HPLC) score lower
Waste Generation	15	Measures waste volume and disposal methods
Operator Safety	10	Assesses exposure to toxic/corrosive substances
Method Type	5	Direct analysis (e.g., sensors) scores highest
Throughput & Automation	5	High-throughput methods reduce per-sample impact
Renewable Resources	5	Use of bio-based solvents or materials
Degradability	5	Chemicals should break down into non-toxic byproducts

2.5.5 Blue Applicability Grade Index

In the evolving landscape of analytical chemistry, there is a growing need for robust metrics that assess not only the environmental impact of analytical methods but also their practical applicability in real sample analysis. The Blue Applicability Grade Index (BAGI) was introduced as a comprehensive evaluation tool to address this need by systematically measuring the implementation potential of analytical procedures (Pena-Pereira *et al.*, 2020). Unlike purely environmental assessment tools, BAGI provides a balanced evaluation of ten critical factors that determine a method's viability in routine laboratory practice.

BAGI was developed in response to the gap between method development and practical implementation in analytical laboratories (Nowak *et al.*, 2021). The index operates on a 100-point scale, where higher scores indicate greater methodological robustness and applicability. This quantitative framework complements environmental metrics such as AGREE and GAPI by emphasizing practical implementation factors rather than focusing exclusively on ecological considerations (Tobiszewski *et al.*, 2019).

The BAGI framework evaluates analytical methods according to ten principles (Figure 2.8). The first principle focuses on technical complexity, where methods requiring minimal operational steps and no specialized expertise achieve the highest scores, while complex procedures with delicate steps are penalized for their limited feasibility in routine laboratories (Armenta *et al.*, 2017). The second principle relates to equipment requirements, rewarding methods that rely on standard laboratory instrumentation and penalizing those dependent on highly specialized or costly devices (Manz *et al.*, 2020). The third principle evaluates the availability and stability of reagents, giving preference to methods that employ common and commercially accessible chemicals over those requiring exotic or unstable materials (Clark *et al.*, 2016).

The fourth principle addresses analysis time, with rapid procedures that complete analyses within 30 minutes per sample receiving optimal scores (Gałuszka

et al., 2013). The fifth principle considers economic aspects, including both consumable costs and equipment depreciation, ensuring that cost-efficient methods are recognized for their practicality (Plotka-Wasylka *et al.*, 2021). The sixth principle highlights throughput capacity, rewarding methods capable of high-throughput or parallel sample processing over strictly sequential procedures, which is increasingly important in modern laboratories (Bojko *et al.*, 2022).

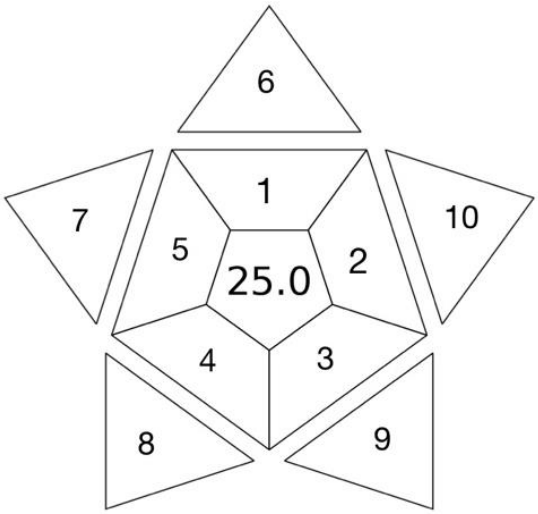

Figure 2.8. BAGI assessment metric tool (Pena-Pereira et al., 2020)

The seventh principle emphasizes robustness and reproducibility by assessing method performance across operators and laboratory conditions, with consistent results under variable settings scoring highest (Pena-Pereira *et al.*, 2022). The eighth principle focuses on matrix compatibility, recognizing methods that maintain accuracy and precision in complex matrices such as wastewater or biological fluids (Anastas & Warner, 1998). The ninth principle considers safety, rewarding methods that minimize the use of hazardous, toxic, explosive, or carcinogenic substances, thus aligning with workplace safety regulations (Tobiszewski *et al.*, 2019). Finally, the tenth principle evaluates regulatory compliance, where methods that align with established frameworks such as EPA or ICH guidelines, and require minimal modification for approval, achieve the highest applicability scores (Pena-Pereira *et al.*, 2020).

In practical applications, BAGI has been employed to evaluate the greenness profile of developed method such as solid-phase microextraction (SPME). The results showed scores ranging between 62.5 and 65, highlighting that SPME is a robust extraction approach that not only reduces solvent consumption but also enhances extraction efficiency. These findings demonstrate BAGI's utility in bridging the gap between theoretical method development and practical laboratory implementation.

2.5.6 Sample Preparation Metric of Sustainability

Sample preparation is one of the key steps in many analytical procedures and is often unavoidable when dealing with complex samples or when adequate sensitivity is required. Conventional sample preparation methods are usually considered the least green step of the analytical workflow because they involve tedious and time-consuming processes, large amounts of hazardous solvents, and high energy consumption.

Due to increasing concerns regarding the sustainability of sample preparation, remarkable progress has been achieved over the past few decades in developing greener extraction techniques (Clark *et al.*, 2016). The proposed Sample Preparation Metric of Sustainability (SPMS) is based on the evaluation of nine parameters that directly influence the performance and sustainability of most extraction approaches. These parameters were selected because they can significantly affect both the environmental and practical aspects of analytical methods. They are divided into four categories according to the type of information provided: (i) sample information (sample amount, either volume for liquid samples or weight for solid samples); (ii) extractant information (amount, nature, and reusability); (iii) sample preparation procedure information (number of steps, extraction time, need for additional steps after extraction, and sample throughput); and (iv) energy consumption and waste (Zhang *et al.*, 2021), illustrated in Figure 2.9.

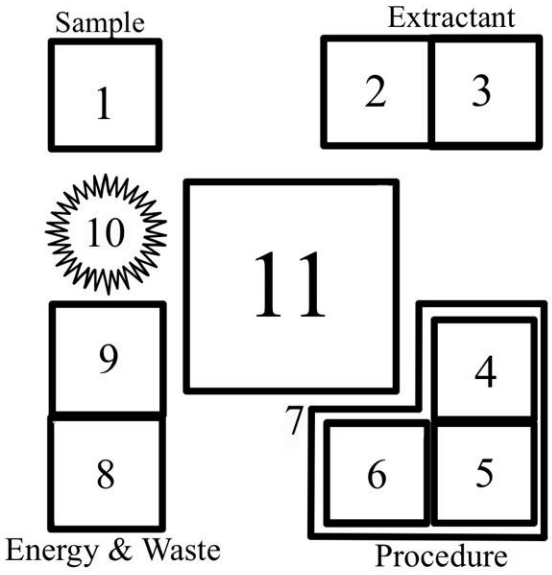

Figure 2.9. Sample Preparation Metric of Sustainability (SPMS) metric for evaluation greenness score (Zhang et al., 2021)

Table 2.7 summarizes the parameters of the SPMS, divided by category, and the possible numeric scores assigned according to parameter values. Each parameter has a different weight in the overall score of the metric depending on its relative impact on sustainability, which is then combined into a global score that reflects the greenness of the sample preparation method.

A recent study by Hedy *et al.* (2025) successfully developed, characterized, and implemented a novel magnetic activated carbon adsorbent synthesized from aloe vera leaf waste through alkaline activation. This innovative material was applied in a magnetic dispersive micro-solid phase extraction (D-μSPE) approach for the extraction and pre-concentration of selective serotonin reuptake inhibitor (SSRI) antidepressants specifically escitalopram, fluoxetine, and paroxetine from aqueous samples. The method demonstrated strong environmental sustainability, with green chemistry assessments yielding an SPMS value of 7.26. These quantitative evaluations collectively confirm the method's eco-friendly profile and alignment with sustainable analytical chemistry principles.

Table 2.5. Main metric parameters for evaluation of SPMS

Category	Segment	Metric Parameter	Unit
Sample Information	1	Sample Amount	mL
Extractant Information	2	Amount of Extractant (sorbent)	g
	3	Nature of Extractant	
Procedure Information	4	Number of Steps	
	5	Extraction Time	
	6	Additional Steps after Extraction	
Energy Consumption and Waste	7	Energy Consumption	
		Dispersion	
		Separation	
		Temperature	
	8	Total Waste	mL
Reusability Mark	9	Reusable	
Sample Throughput	10	Sample Treated at a time	
		Total Score	
	11	Global Score	

CHAPTER 3

METHODOLOGY

3.1 Overview of the Methodology

The formulation of creatine-functionalized Fe_3O_4@SiO_2 magnetic adsorbent involves a stepwise transition from basic starting materials to a stable composite. Fe_3O_4 nanoparticles are first synthesized via co-precipitation with an alkaline activator, forming the magnetic core with superparamagnetic properties. To enhance stability and prevent aggregation, the core is coated with a SiO_2 shell, which provides structural protection and a reactive surface. Creatine molecules are then immobilized onto the silica layer through amine, carboxyl, and imidazole groups, introducing multiple active binding sites. This composite integrates magnetic responsiveness, stability, and selective adsorption, making it suitable for sustainable sample preparation. Transition from starting materials to adsorbent features illustrated in Figure 3.1.

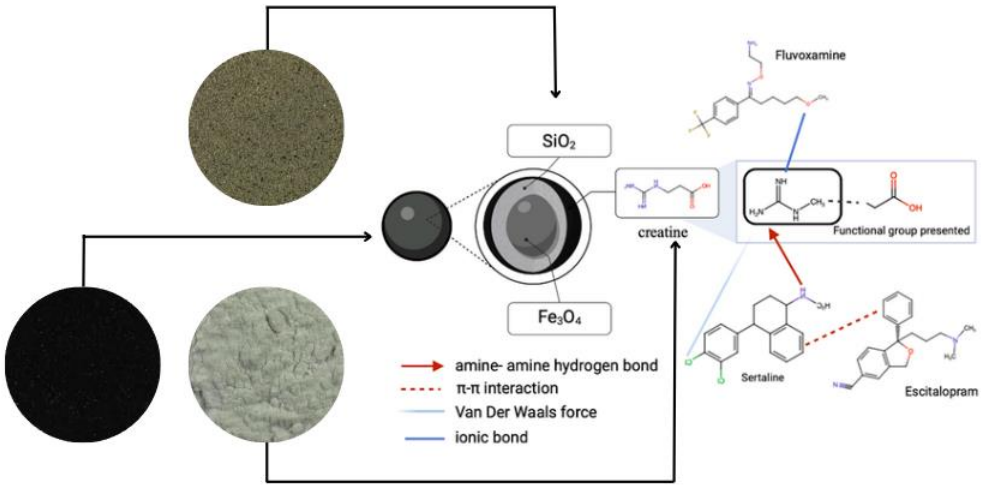

Figure 3.1. Formulation of creatine-functionalized Fe_3O_4@SiO_2 magnetic adsorbent

3.2 Reagent and Materials

Pharmaceutically active compounds (PhACs) standards, namely Sertraline Hydrochloride ($C_{17}H_{17}C_{l2}N$, CAS No. 79559-97-0), Escitalopram Oxalate ($C_{20}H_{21}FN_2O$, CAS No. 219861-08-2), Paroxetine Hydrochloride ($C_{19}H_{20}FNO_3$, CAS No. 110429-35-1), Fluvoxamine Maleate ($C_{15}H_{21}F_3N_2O_2$, CAS No. 61718-82-9), and Fluoxetine Hydrochloride ($C_{17}H_{18}F_3NO$, CAS No. 56296-78-7) were purchased from Dr. Ehrenstorfer (Augsburg, Germany) with purities ranging from 98.00% to 99.98%. (refer to Table 3.1 and Figure 3.2). The HPLC-grade acetonitrile (C_2H_3N), methanol (CH_3OH), and ethanol (C_2H_5OH) were obtained from Merck Company (Darmstadt, Germany).

Analytical-grade reagents of sodium bicarbonate powder Reagent Plus® ($NaHCO_3$, CAS No. 144-55-8), citric acid anhydrous powder EMPROVE® EXPERT ($C_6H_8O_7$), and potassium dihydrogen phosphate dihydrate EMSURE® (KH_2PO_4, CAS No. 7778-77-0) were acquired from Merck Company (Darmstadt, Germany). Creatine Monohydrate ($CNCH_2CO_2H$, CAS No. 6020-87-7), Silica Oxide, Iron (II, III) oxides (Fe_3O_4) (50-100 nm) were used as principal constituents in the characterization and preparation of magnetic adsorbent, and were obtained from Sigma-Aldrich (Steinheim, Germany). Purified deionised water was obtained from a Millipore Milli-Q reference water purification system with a resistivity of 18.2 MΩ.cm at 25 °C (Bedford, MA, USA).

3.3 Preparation of Stock and Working Solution

Based on National Report Malaysian National Essential Medicines, five pharmaceutically active compounds (SSRIs) namely escitalopram, fluoxetine, fluvoxamine, paroxetine, and sertraline, which are used as model analytes in this study.

Table 3.1. Chemical properties of the target pharmaceutically active compounds

Compound and purpose	Molecular Weight (g/mol)	Boiling Point (°C)	pKa Value	Solubility in Water (mg/mL)	Solubility in Organic Solvent (mg/mL)
Escitalopram Oxalate $C_{20}H_{21}FN_2O$ To treat depression and generalized anxiety disorder	324.43	205	9.78	14	40
Fluvoxamine Maleate $C_{15}H_{21}F_3N_2O_2$ To treat obsessive-compulsive disorder	312.39	190	8.86	1.5	10
Fluoxetine Hydrochloride $C_{17}H_{18}F_3NO$ To treat obsessive-compulsive disorder and bulimia	309.34	245	9.80	0.2	12.5
Paroxetine Hydrochloride $C_{19}H_{20}FNO_3$ To treat depression and anxiety	329.36	220	9.77	5.4	20
Sertraline Hydrochloride $C_{17}H_{17}Cl_2N$ To improve cognition in depressed patients	306.43	282	9.56	3.8	15.7

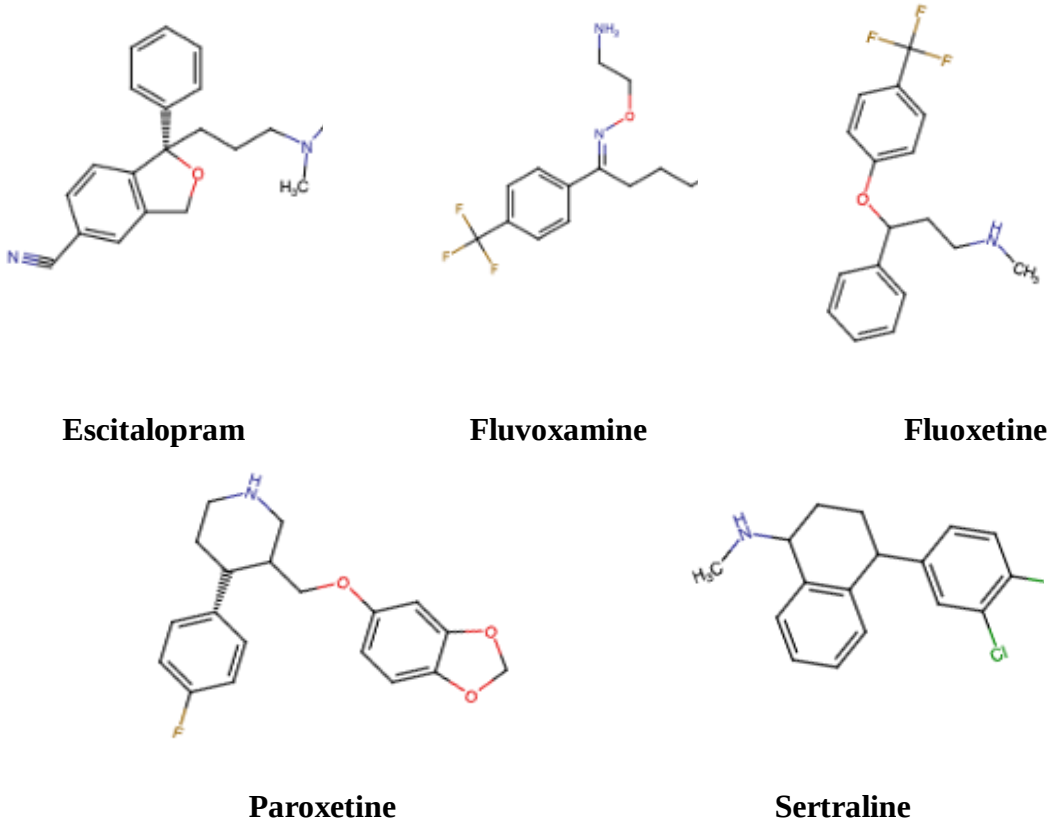

Figure 3.2. Chemical structure of the targeted pharmaceutically active compounds

Standard stock solutions of these compounds were prepared at 10 µg/mL, while working solutions were diluted to 0.5 µg/mL. Initially, 1.0 mg of each compound was dissolved in methanol in individual volumetric flasks to prepare the stock solutions. The working standard solutions, at various concentrations ranging from 0.01 µg/mL to 0.5 µg/mL, were prepared by mixing 5 mL of each stock solution and diluting the mixture with methanol, followed by homogeneous shaking. All prepared stock and working standard solutions were stored in a chiller at 4 °C for later use.

3.4 Fabrication of Creatine-Functionalized Fe_3O_4@SiO_2 Magnetic Adsorbent

To fabricate the magnetic adsorbent, the co-precipitation method was employed. First, a water bath was prepared and maintained at 90 °C. 100 mL of deionized water and 10 g of Fe_3O_4 powder were added to a 250 mL beaker, which was then placed in the water bath. The mixture was stirred intermittently for 15 minutes using a glass rod. Next, 10 g of silica oxide was added and stirred for another 15 minutes. To increase the basicity of the adsorbent and control the size and shape of the nanoparticles, two drops of 1M sodium hydroxide solution were added and stirred for an additional 15 minutes. Finally, 10 g of creatine monohydrate was incorporated and stirred intermittently for 2 hours.

After the stirring process, the mixture was rinsed with 500 mL of ethanol followed by 500 mL of deionized water to remove excess hydroxide. The resulting powder was filtered using a vacuum pump and left to air dry overnight. On the following day, the slightly damp powder was transferred to a petri dish and dried in an oven at 60 °C for 30 minutes. The final product was a fine, black, and shiny powder. This fabrication process was repeated multiple times to ensure a sufficient quantity for future use. The procedure is illustrated in Figure 3.3.

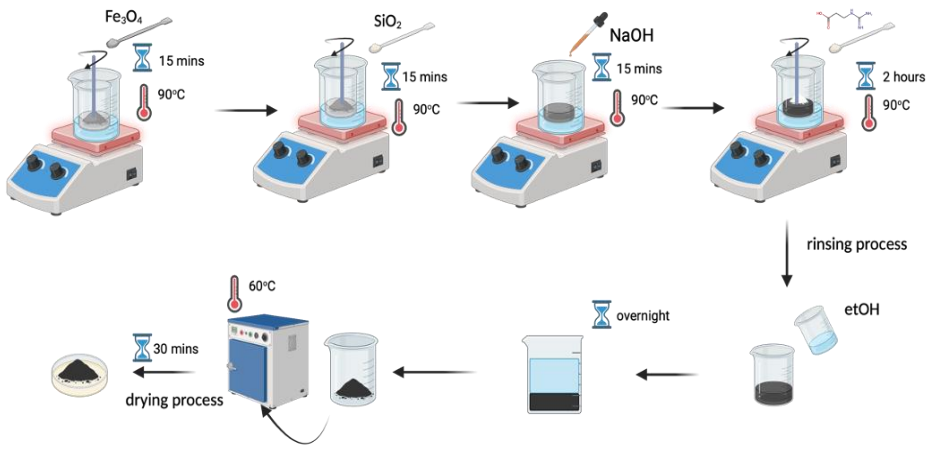

Figure 3.3. Fabrication of creatine-functionalized Fe_3O_4@SiO_2 using co-precipitation method

3.5 Characterization of Creatine-Functionalized Fe_3O_4@SiO_2 Magnetic Adsorbent

3.5.1 Scanning Electron Microscopy (SEM)

A scanning electron microscope (SEM) (Jeol JSM-6360LV, Japan) was used to analyse the morphology of the magnetic sorbent. The SEM operated at an accelerating voltage of 10 kV, with a probe current ranging from ≈1 pA to 1 µA and a resolution of 3.0 nm. Prior to the examination, approximately 0.1 to 1.0 g of fine magnetic powder was mounted onto a 10 mm × 10 mm SEM specimen aluminium stub using double-sided adhesive tape for secure attachment. Any unbound powder was carefully removed using a rubber air blower to minimize pressure on the samples. To ensure electrical conductivity, the magnetic sorbent was coated with a thin layer of gold approximately 30 µm thick, applied using a fine auto coater (Jeol JFC-1600, Japan). The coating process was conducted for 60 seconds at a beam current of 30 mA. Morphological studies were performed at various magnifications, ranging from 500× to 45,000×. The auxiliary sorbent underwent a similar SEM analysis, coupled with energy-dispersive X-ray (SEM-EDX) spectroscopy to determine its elemental composition. Additionally, the magnetic sorbent without creatine functionalization was characterized as a control for comparative purposes.

3.5.2 High-Resolution Transmission Electron Microscope (HRTEM)

The morphology of the prepared magnetic sorbent was analysed using a High-Resolution Transmission Electron Microscope (HRTEM) equipped with a Gatan Orius 11 Mpx Camera (USA). HRTEM was also used to measure the particle size of Fe_3O_4 nanoparticles incorporate in SiO_2 structural network. The microscope operated at an accelerating voltage of 200 kV with a LaB_6 source. Approximately 1.0 g of the magnetic sorbent in powder form was prepared for analysis. A small amount of the powder was added to an ethanol solution, and the mixture was sonicated for 15 to 30 minutes to ensure homogeneous dispersion of the particles in the solvent. Next, 1 to 2 drops of the prepared suspension were deposited onto a copper grid coated with an ultrathin carbon layer. The samples on the copper grid were allowed to air-dry completely before being mounted on a TEM sample holder for imaging. The magnetic sorbent was examined at various magnifications ranging from 6,000× to 25,000×. As a control, the magnetic sorbent without creatine functionalization was also characterized.

3.5.3 Fourier Transform Infrared (FTIR) Spectroscopy

Attenuated Total Reflectance-Fourier Transform Infrared (ATR-FTIR) spectroscopy (Shimadzu IRTracer-100, Japan), equipped with a temperature-controlled DLATGS detector, was used to analyse the presence of different functional groups in the samples. Approximately 1.0 mg of the magnetic sorbent in powder form was prepared for analysis. The powder was placed onto a cleaned ATR diamond crystal (Specac, United Kingdom). The spectra were recorded in transmittance mode with 40 scans at a resolution of 4 cm^{-1}, covering a wavenumber range from 4000 to 400 cm^{-1}. As a control, the magnetic sorbent without creatine functionalization, pure iron oxide, and magnetic sorbent after post-extraction were also characterized.

3.5.4 Vibrating Sample Magnetometer (VSM)

A Vibrating Sample Magnetometer (VSM) (Lakeshore VSM 7404, USA) was used to evaluate the magnetic properties of creatine-functionalized Fe_3O_4@SiO_2 magnetic adsorbent. The magnetic characteristics of the sorbent were measured under applied magnetic fields ranging from -14,000 G to 14,000 G at ambient temperature, with a maximum magnetic field strength of 1.40 Tesla. The VSM operated at a vibrational frequency of 80 Hz with a time constant of 3 seconds. For analysis, the magnetic sorbent was prepared in powder form at a minimum concentration of 0.05 mg. The powder was magnetized by subjecting it to a homogeneous magnetic field. Each analysis required approximately 10.75 minutes, and the magnetic measurements were recorded as a hysteresis curve. The results were expressed as mass magnetization, representing the magnetic moment per unit mass of the sample.

3.5.5 X-ray Diffraction (XRD)

The crystalline structure of the magnetic sorbent was investigated using a powder X-ray diffraction (XRD) machine (D8 Quest, Bruker, Germany) equipped with a LynxEye detector. The analysis was performed at room temperature (25 °C) using Cu Kα radiation (1.54060 Å) at 40 kV and 40 mA, with a scan rate of 0.04°/min. A fixed slit system with a divergence slit of 0.3° was utilized. For the analysis, approximately 1.0 g of the magnetic sorbent powder was prepared. The powder was mounted in a suitable sample holder, then placed on a goniometer at the appropriate sample stage for examination. Each analysis required 7 minutes. As a control, the magnetic sorbent without creatine functionalization was also characterized. The results were presented as intensity versus 2θ.

3.5.6 Zeta Potential Analysis

The Zetasizer (Malvern Panalytical, Version 7.12) was used for dynamic light scattering (DLS) and zeta potential measurements to characterize the particle size and

stability of the magnetic sorbent. For sample preparation, the sorbent was optimally diluted in ethanol at a concentration of 1.361 mg/mL, with a viscosity of 1.1 cP. DLS measurements were conducted at a consistent temperature of 24.9 °C for several minutes, using a detection angle of 173° to enhance sensitivity. Zeta potential measurements were performed in a folded capillary cell with an electric field strength of 24.5 V/cm and a measurement position of 2 mm. Data analysis was carried out using appropriate models, such as cumulant analysis, with repeated measurements (26 runs) to ensure reliability. In comparison, the magnetic sorbent without creatine functionalization was also characterized.

3.5.7 Brunauer-Emmett-Teller Analysis (BET)

The Brunauer-Emmett-Teller (BET) (Micromeritics, TriStar II Plus 3.03) analysis is a widely used technique for measuring the surface area and porosity of the magnetic sorbent. The process begins with weighing the sample (0.252 g, density 1 g/cm³), followed by degassing to remove moisture and impurities. The sample is then cooled to the temperature of liquid nitrogen (-196 °C), and nitrogen gas is incrementally introduced into a vacuum chamber. As the nitrogen pressure increases, the amount of gas adsorbed onto the sorbent surface is recorded. The BET equation is then applied to this adsorption data to calculate the specific surface area, typically reported in square meters per gram (m²/g). Additionally, desorption data can be analysed using the BJH (Barrett-Joyner-Halenda) method to determine the pore size distribution and total pore volume.

3.5.8 Thermogravimetric analysis (TGA)

Thermogravimetric analysis (TGA) with a TGA-50 detector is an analytical technique used to assess changes in the mass of a material as it is subjected to controlled temperature conditions, typically involving a gradual increase in temperature. For sample preparation, 14.14 mg of the magnetic sorbent is placed on a precision microbalance within a furnace and heated at 10 °C/min in a nitrogen

atmosphere with a gas flow rate of 50 mL/min. As the temperature rises, any changes in the sample's mass such as those due to evaporation, decomposition, or oxidation are recorded. This data allows for the determination of material properties such as thermal stability, degradation temperatures, and moisture content. For example, polymers often exhibit distinct mass loss steps that correlate with the breakdown of specific chemical bonds, revealing details about their thermal degradation pathways (Shukla *et al.*, 2020). TGA data is particularly useful in material characterization, quality control, and development, as well as in kinetic studies.

3.6 Screening and Optimization Design

3.6.1 HPLC-DAD Operational Settings

A Shimadzu high-performance liquid chromatography (HPLC) system (Kyoto, Japan) was utilized for the detection of target antidepressant drugs. The system was equipped with a system controller (model CBM-40), a degassing unit (model DGU-405), a solvent delivery module (model LC-40D XS), an autosampler (model SIL-40C XS), and a diode array detector (model SPD-M40). The column used was a Shim-pack GIST C18 (5 μm, 4.6 mm I.D. × 150 mm), and the column temperature was maintained at 40 °C throughout the experiments. Table 3.2 summarizes five variables studied to optimize detection target analytes in HPLC-DAD.

Table 3.2 Variables range of HPLC-DAD conditions from preliminary assessment.

Factors	Low (-1)	High (+1)
Mobile Phase*	1:4:5	5:4:1
Wavelength (nm)	200	380
Injection Volume (μL)	10	40
Temperature (^{o}C)	40	90
Flow Rate (mL/min)	0.8	1.0

*Composition; CH_3OH, ACN, H_2O with different composition, buffer KH_2PO_4

3.6.2 Plackett-Burman Screening Design

A two-level Plackett-Burman design was applied to screen the significant chromatographic response (sum of total peak areas) influenced by variables associated with the separation efficiency of multianalyte antidepressant drugs. A total of seven factors, listed in Table 3.3 were tested and the value chosen were predetermined from literature studies. The design comprised 8 randomized run orders to minimize experimental errors. Significant effects on the HPLC-DAD sensitivity were determined by analyzing ANOVA data sets. By conducting these 8 experiments and analyzing the results, we identified which of the 7 factors had a statistically significant effect on the response. Insignificant factors were excluded, allowing subsequent experiments to focus on the critical variables. Statistically significant effects were visualised using a Pareto chart, where the presence of a vertical line indicated the significance threshold. Factors were deemed statistically significant at a 95% confidence level ($p = 0.05$) if their corresponding bars extended beyond the vertical line.

Table 3.3 Range of factor studied for screening phase.

Factors	Code	Low (-1)	High (+1)
Weight of Sorbent (g)	X_1	0.5	1.0
Amount of Effervescence (g)	X_2	0.5	1.0
Extraction Temperature (^oC)	X_3	45	90
Volume of Water (mL)	X_4	15	45
pH of Water	X_5	5	9
Contact Time (min)	X_6	1	5
Volume of methanol (µL)	X_7	250	750

3.6.3 Magnetic Dispersive Micro Solid Phase Extraction (Screening Phase)

Referring to the matrix generated by the Plackett-Burman design, a water sample was prepared by transferring a specified volume of deionized water into a 100 mL beaker. The water pH was adjusted as needed using 1 N nitric acid (HNO_3) or 1 N sodium hydroxide (NaOH) solutions. To introduce a known concentration of the analyte, 1 mL of a 0.5 µg/mL standard mixture solution was added to the water, and the mixture was gently stirred with a glass rod to ensure thorough homogenization. The beaker was then placed on a heating plate, and the solution was heated to the desired temperature, as specified in the experimental conditions. Once the desired temperature was reached, the water sample was transferred into a glass syringe priorly prepared containing Fe_3O_4@SiO_2 creatine adsorbent and an effervescence powder (a mixture of citric acid and sodium bicarbonate). The dispersive micro solid phase extraction process commenced upon the observation of an acid-base reaction that generated microbubbles. A timer was started at the onset of effervescence, and the extraction was allowed to proceed for a predefined contact time.

Upon completion of the extraction, a neodymium magnet was used to separate the magnetic adsorbent from the aqueous phase. The magnet ensured the adsorbent remained attached while the water was released through the syringe's end cap. The adsorbent was then transferred to a 20 mL glass vial using a plastic spatula, followed by the addition of an appropriate amount of organic modifier, namely methanol. The 20-mL vial was vortexed to facilitate the desorption of organic compounds from the adsorbent. Finally, the methanol layer containing the extracted antidepressant drugs was collected, filtered using nylon 0.22 µm diameter 12 mm, and transferred into a 1.5 mL HPLC vial for subsequent analysis. The experimental steps and conditions are summarized in Table 3.4 and illustrated in Figure 3.4.

Table 3.4 Design matrix generated by Plackett-Burman design for screening phase

Run Order	Weight of Adsorbent (g)	Amount of Effervescence (g)	Extraction Temperature (°C)	Water Volume (mL)	pH of Water	Contact Time (min)	Volume of Methanol (µL)
1	0.5	0.5	45	45	9	5	250
2	1.0	0.5	45	15	5	5	750
3	0.5	1.0	45	15	9	1	750
4	1.0	1.0	45	45	5	1	250
5	0.5	0.5	90	45	5	1	750
6	1.0	0.5	90	15	9	1	250
7	0.5	1.0	90	15	5	5	250
8	1.0	1.0	90	45	9	5	750

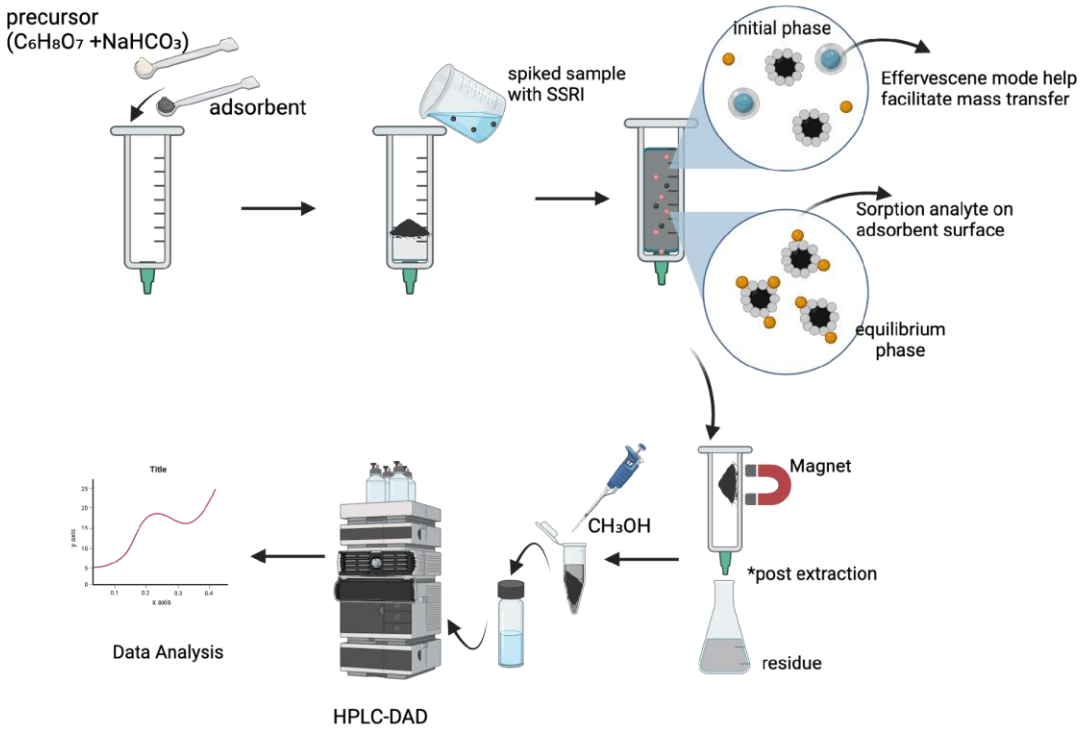

Figure 3.4 Screening method of experiment for dispersive magnetic μ-SPE using Plackett-Burman design.

3.6.4 Magnetic Dispersive Micro Solid Phase Extraction (Optimization Phase)

A Central Composite Design (CCD) was adapted in the design of the experiment for the optimization phase. The Plackett-Burman (PB) design serves as an initial screening tool to identify the most critical factors influencing a response, allowing researchers to narrow the number of variables for more focused experimentation. Once the main studied factors have been identified using the PB design, a CCD is implemented to explore these factors in greater detail by examining their linear, interaction, and quadratic effects. The CCD provides a more comprehensive understanding of how these factors impact the response, offering insights into optimal conditions and experimental conditions that may not have been evident in the PB screening phase. For the optimization phase, a water sample was prepared by transferring 15 mL of deionized water into a 100 mL beaker. The desired pH was adjusted using 1 N nitric acid (HNO_3) or 1 N sodium hydroxide (NaOH) solutions, as appropriate. To introduce a known analyte concentration, 1 mL of a 0.5

µg/mL standard mixture solution was added to the water, and the mixture was gently stirred with a glass rod to ensure thorough homogenization.

The beaker was then placed on a heating plate, and the solution temperature was adjusted according to the experimental conditions. Once the target temperature was reached, the water sample was transferred into a glass syringe containing 0.5 g of Fe_3O_4@SiO_2 creatine adsorbent and 1.0 g of effervescence powder (a mixture of 0.5 g citric acid and 0.5 g sodium bicarbonate). The extraction process commenced upon observing an acid-base reaction, which generated microbubbles. A digital timer was started at the onset of effervescence, and the extraction was allowed to proceed for the specified contact time. After the extraction phase ended, a neodymium magnet was used to separate the magnetic adsorbent from the aqueous phase, ensuring that the adsorbent remained attached to the magnet while the water was released through the syringe's end cap.

The adsorbent was transferred to a 20 mL glass vial using a plastic spatula, followed by the addition of 250 µL of methanol. The vial was vortexed to facilitate the desorption of antidepressant drugs. Finally, the methanol layer containing the extracted analytes was collected using a 3-mL syringe, filtered using nylon 0.22 µm diameter 12 mm, and transferred into a 1.5 mL HPLC vial for subsequent analysis. The analytes were then separated and analysed using high-performance liquid chromatography equipped with a diode array detector (HPLC-DAD). A summary of the experimental works is presented in Table 3.5.

Table 3.5 Design matrices generated by Central Composite design for optimization phase.

Run Order	Weight of Adsorbent (g)	Extraction Temperature (°C)	pH of Water	Contact Time (min)
1	0.5	45	5	1
2	0.5	45	5	5
3	0.5	45	9	1
4	0.5	45	9	5
5	0.5	90	5	1
6	0.5	90	5	5
7	0.5	90	9	1
8	0.5	90	9	5
9	1.0	45	5	1
10	1.0	45	5	5
11	1.0	45	9	1
12	1.0	45	9	5
13	1.0	90	5	1
14	1.0	90	5	5
15	1.0	90	9	1
16	1.0	90	9	5
17	0.3	67	7	3
18	1.3	67	7	3
19	0.8	22	7	3
20	0.8	112	7	3
21	0.8	67	3	3
22	0.8	67	11	3
23	0.8	67	7	-1
24	0.8	67	7	7

Table 3.5 Design matrices generated by Central Composite design for optimization phase (continued).

Run Order	Weight of Adsorbent (g)	Extraction Temperature (°C)	pH of Water	Contact Time (min)
25 (C)	0.8	67	7	3
26 (C)	0.8	67	7	3
27 (C)	0.8	67	7	3
28 (C)	0.8	67	7	3
29 (C)	0.8	67	7	3
30 (C)	0.8	67	7	3

Note: Value -1 for contact time equal to less than 30 seconds.

3.6.5 Feasibility study

Operational feasibility assesses ease of use and compatibility with existing laboratory workflows, while environmental feasibility focuses on minimizing solvent waste, aligning with green chemistry principles. Regulatory feasibility ensures adherence to industry standards, particularly in applications like pharmaceutical analysis (Rocha *et al.*, 2020). The feasibility study evaluated the response of the developed method under various operational settings for the magnetic dispersive µ-SPE method. The extraction procedure was performed at a concentration level of 0.5 µg/mL spiked in water samples. Operational settings include minimum, optimum, and maximum were analysed in triplicate, n = 3 (Table 3.6), with total peak areas counted as mean. The chromatographic values obtained were compared with the predicted values from the proposed models.

Table 3.6 Operational setting of minimum, optimum and maximum for feasibility study.

Factors	Minimum (-1)	Optimum	Maximum (+1)
Weight of Adsorbent (g)	0.3	0.5	1.3
Extraction Temperature (°C)	22	22	112
pH of Water	5	9	11
Contact Time (min)	-1	7	7

3.7 Analytical Figure of Merits

3.7.1 Linearity

The linearity test in HPLC method validation is an essential procedure to evaluate whether an analytical method provides results that are directly proportional to the analyte concentration across a specified range. Two calibration methods are commonly employed for this purpose namely standard addition method and external calibration method. The standard addition method involves spiking known quantities of the analyte directly into the sample matrix at varying concentrations. This method is particularly advantageous for minimizing matrix effects, as the analyte response is measured in the presence of the sample's inherent components. Conversely, the external calibration method uses standard solutions of the analyte prepared independently of the sample matrix. These solutions are analysed separately to construct a calibration curve, which is then applied to determine the analyte concentration in the sample.

In this study, the linearity of the developed analytical method was evaluated by preparing a series of working solutions at seven concentration levels (0.5, 0.3, 0.1, 0.05, 0.03, and 0.01 µg/mL) through spiking water samples with multianalyte antidepressant drugs. For standard addition method, the analytes were added directly to the water samples. For external calibration method, independently prepared

standard solutions were utilized. The spiked samples underwent extraction using optimized conditions and were analysed in triplicate using HPLC-DAD to construct the respective calibration curves.

The calibration curves were generated by plotting peak area response against analyte concentration. Statistical parameters, including the correlation coefficient (typically $r \geq 0.990$), slope, y-intercept, and residual sum of squares, were assessed to verify the method's linearity. The comparative evaluation of the standard addition and external calibration methods provided insights into the accuracy and reliability of the developed analytical method, particularly in complex sample matrices.

3.7.2 Recovery

Relative recovery is a critical parameter used to evaluate the performance of an extraction method. It is defined as the ratio of the analyte concentration measured after the extraction process to the initial known concentration spiked into the sample matrix, expressed as a percentage:

$$\text{Relative Recovery (\%)} = \left[\frac{\text{Amount Extracted}}{\text{Amount Present in the Matrix}}\right] \text{x } 100\% \qquad \text{(Eq. 3.1)}$$

In this study, the magnetic dispersive µ-SPE method was performed under optimized conditions using three analyte concentration levels: 0.5, 0.1, and 0.03 µg/mL). These concentration levels were selected to represent high, medium, and low analyte concentrations, simulating real situation in which the method might be applied. Testing across this range ensures the method's robustness, accuracy, and reliability over a wide dynamic range of analyte concentrations found in the environment. Recovery assays were conducted in triplicate for each concentration level to enhance statistical reliability. The results are reported as mean relative recovery values, providing a detail evaluation of the method's consistency and performance.

3.7.3 Matrix Effect

Matrix effect refers to the influence of other components (e.g., organic matter, co-elute pollutant, residual solvent, etc.) in the sample matrix on the analyte's extraction and detection, which can result in suppression or enhancement of the analytical signal. This study evaluated the magnetic dispersive µ-SPE method performance using different aqueous matrices namely river water, wastewater and deionized water. Each analysis consisted of triplicate samples at three different concentration levels (0.5, 0.1, and 0.03 µg/mL). To quantify the matrix effect, the following equation was applied:

$$\text{Matrix Effects (\%)} = \left[\frac{\text{Peak Areas in Matrix Sample}}{\text{Peak Areas in Deionized Water}} - 1\right] \times 100\% \qquad \text{(Eq. 3.2)}$$

The signal (herein denoted as peak areas) in the matrix corresponds to the response of the analyte in the spiked river water, while the signal in deionized water represents the response in a clean, interference-free matrix. A positive value indicates signal enhancement, while a negative value indicates signal suppression.

3.7.4 Detection and Quantification Limits

Detection Limit (DL) refers to the lowest concentration of an analyte that can be detected by the analytical method but not necessarily quantified with acceptable precision and accuracy. It serves as an indicator of the method's sensitivity and is typically defined at a signal-to-noise (S/N) ratio of 3:1. Quantification Limit (QL) represents the lowest concentration of an analyte that can be quantitatively measured with acceptable precision and accuracy. The quantification limit ensures reliable analyte measurement within the method's working range and is typically defined at a signal-to-noise ratio of 10:1.

In this study, the detection limit and quantification limit were evaluated under optimized experimental conditions to assess the sensitivity of the magnetic dispersive μ-SPE method for detecting trace levels of the target analytes. These limits were determined by analyzing samples at a concentration of 0.01 μg/mL and further diluting the samples until the required signal-to-noise ratios were achieved.

In comparison, the detection limit and quantification limit also theoretically calculated using linear regression method. Both were calculated using the following formulas based on the standard deviation of the response and the slope (*S*) of the calibration curve:

$$\text{Detection Limit (DL)} = \left[\frac{3.3\ \sigma}{\text{S}}\right] \quad \text{(Eq. 3.3)}$$

$$\text{Quantification Limit (DL)} = \left[\frac{10\ \sigma}{\text{S}}\right] \quad \text{(Eq. 3.4)}$$

Where, σ is the standard deviation of the response (e.g., peak areas) from replicate analyses of a blank or low-concentration sample. *S* is the slope of the calibration curve, which represents the sensitivity of the method.

3.7.5 Intra- and Inter-Day Precision

Intra-day precision is critical for evaluating how consistently the method performs under identical conditions within a single analysis session. It ensures that the measurement variations within a single day are minimal and that the method provides reliable results in routine analyses. The intra-day relative standard deviations (RSDs) of the magnetic dispersive μ-SPE method were determined to assess its repeatability. This evaluation was accomplished by analyzing spiked samples at three different concentration levels (0.5, 0.1, and 0.03 μg/mL), all carried out on the same day.

Inter-day precision assesses the method's reliability over time, ensuring that performance remains consistent across different analysis sessions, accounting for variations in environmental factors, equipment stability, and operator handling. This measure of reproducibility is crucial for ensuring that the method is not influenced by day-to-day fluctuations. To evaluate inter-day precision (reproducibility), the same spiked samples at the three concentration levels were analysed on two separate days.

For both intra- and inter-day assays, the RSD for each analyte was calculated using the average response obtained from triplicate analyses (n = 3) at each concentration level. The RSD is a main indicator of precision, calculated as follows

$$\text{Relative Standard Deviation (RSD \%)} = \left[\frac{\text{Standard Deviation (SD)}}{\text{Mean of response}} \times 100\%\right] \qquad \text{(Eq. 3.5)}$$

3.7.6 Stability Assay

Stability assay in method validation evaluates the analyte's stability under various conditions to ensure that the analytical method consistently provides accurate and reproducible results over time. Stability assay is a critical component of method validation as it assesses the reliability of both the analyte and the method when subjected to storage or varying environmental conditions. In this study, the short-term stability of the magnetic dispersive μ-SPE method for the extraction of multiple analytes was investigated. Triplicate extracted samples were stored and retrieved on the 1^{st}, 3^{rd}, and 5^{th} days before analysis using HPLC-DAD. This approach ensured that any potential degradation of analytes, loss of adsorptive capacity, or chemical changes in the adsorbent or analytes over time could be evaluated.

The stability was evaluated by comparing the relative recovery percentages of the analytes at each time point. A stable system would show minimal variation in these parameters over time, typically assessed using the percentage of analytes lost between two calculated recovery assays, expressed as follows:

$$\text{Stability (\%)} = \left[\frac{\text{Recovery on Final Day}}{\text{Recovery on Initial Day}} \times 100\%\right] \quad \text{(Eq. 3.6)}$$

3.7.7 Selectivity Assay

The drug selectivity assay evaluates the ability of the developed analytical method to accurately measure the target analyte in the presence of other drugs with minimal interference. Potential interferences from other compounds, includes metabolites, impurities, degradation products, or matrix components that may coexist in the sample (Sambasiva, 2024). For cases of this study, interference was investigated on aspect on competitiveness different drugs adsorb on surface of magnetic adsorbents. To validate the magnetic dispersive µ-SPE method, drugs from different classes were spiked into the sample matrix at three different concentration levels (0.5, 0.1, and 0.03 µg/mL). This was done to assess whether the method could selectively extract and detect the five main analytes without interference from the additional compounds. The inclusion of drugs from diverse classes ensures the method's robustness and reliability when applied to complex sample matrices. In our study, amlodipine and nifedipine were used model analytes for compete active bindings site on surface's adsorbent.

The method's ability to resolve the target analytes from non-target compounds was evaluated by comparing chromatograms. Peaks corresponding to the target analytes were checked for any changes in retention time, peak shape, or intensity. In addition, relative recovery of the five main analytes was measured in the presence of other drugs to confirm that their extraction efficiency remained consistent and unaffected by the added compounds.

3.7.8 Regeneration and Leaching Analysis

The regeneration potential of the magnetic adsorbent was investigated to evaluate the cost-effectiveness and sustainability of the magnetic dispersive µ-SPE method, as well as its ability to maintain extraction efficiency across multiple uses.

After completing the first batch of extractions, the magnetic adsorbent was dried in an oven at 60 °C for 1 hour and reused for subsequent extraction cycles. This process allowed for the assessment of the adsorbent's stability and performance during the microextraction procedure. A total of four extraction cycles were conducted, with the initial and final weight of the magnetic adsorbent recorded after each cycle to monitor any loss in material mass. The analyte recovery rates were evaluated in each cycle to determine if the adsorbent's efficiency remained consistent after regeneration.

To evaluate the potential release of iron ions from the magnetic adsorbent into the extraction medium, a leaching test was conducted, followed by quantitative determination using flame atomic absorption spectroscopy. Iron was measured at a wavelength of 248.3 nm using an air–acetylene flame, with typical operating conditions of lamp current 7–10 mA, spectral bandwidth 0.2–0.4 nm, and acetylene/air flow rates of approximately 2.0/13.5 L min^{-1}. External calibration was performed using aqueous iron standard solutions, and all measurements were carried out in triplicate. To simulate potential leaching conditions, post-extraction residues were treated with a diluted iron (III) chloride ($FeCl_3$) solution. The treated samples were subsequently diluted at a 1:5 ratio with deionized water to prepare them for analysis. Using AAS, the iron content in the supernatant was quantified, with specific focus on detecting any increase in iron concentration after each extraction cycle.

3.7.9 Uncertainty

In analytical methods such as magnetic dispersive micro-solid phase extraction, the quantification of measurement uncertainty is a critical step to ensure the reliability, accuracy, and comparability of results. Measurement uncertainty defines the range within which the true value of an analyte concentration is expected to lie, considering all potential sources of variability throughout the extraction and analysis processes. Several factors contribute to measurement uncertainty in the developed analytical method is taken account. Instrumental precision is a significant source, arising from variability in detector responses during analysis. Sample

preparation errors, including inaccuracies in weighing, dilution, or spiking procedures, further impact the precision and accuracy of the results (Cortada *et al.* 2011).

Extraction efficiency, which can vary due to inconsistencies in the performance of the magnetic adsorbent across different batches, is another critical factor. Moreover, matrix effects resulting from the presence of interfering components in real samples such as river water or hospital effluent may alter analyte detection and quantification. Lastly, repeatability and reproducibility, as reflected in variations during intra-day and inter-day measurements, also contribute to the overall uncertainty.

These components are quantified individually and combined to calculate the overall uncertainty of the method. Instrumental precision (u_{inst}) accounts for variability in the detector response, such as the standard deviation of replicate injections in high-performance liquid chromatography (HPLC-DAD). Recovery (u_{rec}) quantifies the variability in the recovery percentages of spiked samples (Cortada *et al.* 2011). This is calculated using the formula:

$$u_{rec} = \left[\frac{\text{Standard deviation of recovery}}{\sqrt{n}}\right] \quad \text{(Eq. 3.7)}$$

Where n is the number of replicates.

Matrix effects (u_{matrix}) are determined by comparing the analyte response in matrix-matched standards to that in pure standards. This is expressed as:

$$u_{matrix} = \left|\frac{\text{Response in matrix} - \text{Response in pure standard}}{\text{Response in pure standard}}\right| \quad \text{(Eq. 3.8)}$$

Repeatability and reproducibility (u_{rep}) reflect variations within and between analytical runs. It is calculated using the relative standard deviation (RSD) of multiple replicates, according to the equation:

$$u_{rep} = \frac{\text{Mean concentration} \times \text{RSD}}{100} \quad \text{(Eq. 3.9)}$$

The combined uncertainty (u_c) integrates these individual components using the root sum of squares method:

$$U_c = \sqrt{u_{inst}^2 + u_{rec}^2 + u_{matrix}^2 + u_{rep}^2} \quad \text{(Eq. 3.10)}$$

Finally, the expanded uncertainty (U) is calculated by multiplying the combined uncertainty by a coverage factor (k), which depends on the desired confidence level (e.g., k = 2 for 95% confidence):

$$U = k \times U_c \quad \text{(Eq. 3.11)}$$

3.7.10 Analysis of Real Samples

Analyzing real samples is a crucial step in method validation, ensuring the magnetic dispersive µ-SPE method is applicable to complex matrices beyond synthetic or spiked standards. Real samples typically contain various interfering components, such as proteins, lipids, salts, and other foreign substances, which can affect the detection and quantification of target analytes. Validation using real samples confirms the method's robustness and reliability in addressing these challenges, making it suitable for routine applications.

For this study, real samples were collected from two distinct sources: river water (freshwater) collected from Terengganu River and hospital effluent (wastewater) obtained from Penang and Perak. The samples were collected in 2.5 L high-density polyethylene bottles to minimize contamination risks. Bottle was priorly pre-cleaned with Decon-90, rinsed twice with deionised water. Immediately after collection, the samples were preserved at temperatures below 4°C to prevent degradation of analytes

and to maintain their original matrix composition. Upon arrival at the laboratory, the samples were immediately processed using the developed magnetic solid phase extraction to ensure that their integrity and analyte concentrations remained representative of the initial conditions. Final determination using HPLC-DAD analysis, followed by identification using LC-MS.

3.8 Adsorption Models

3.8.1 Isotherm Models

The Langmuir equation is one of the most widely employed adsorption isotherm models, based on the hypothesis that the number of homogeneously distributed binding sites on the adsorbent surface is finite (Langmuir, 1918; Onkal Engin *et al.*, 2012). The general equation for single-component adsorption is expressed as:

$$q_e = \frac{K_L Q_{max} C_e}{1 + K_L C_e} \quad \text{(Eq. 3.12)}$$

In this equation, q_e represents the amount of solute adsorbed per unit mass of adsorbent at equilibrium (mg/g or mol/g). The parameter Q_{max} denotes the maximum adsorption capacity (mg/g or mol/g), which corresponds to the point at which all binding sites are occupied, indicating monolayer coverage. The constant K_L (L/mg or L/mol) reflects the energy of adsorption or the affinity between the solute and the adsorbent, with higher values indicating stronger affinity. Finally, C_e is the equilibrium concentration of the solute in solution (mg/L or mol/L). To determine the parameters Q_{max} and K_L from experimental data, the equation is typically rearranged into its linearized form:

$$\frac{C_e}{q_e} = \frac{1}{K_L Q_{max}} \times \frac{1}{C_e} + \frac{1}{Q_{max}} \quad \text{(Eq. 3.13)}$$

The Freundlich isotherm is based on the hypothesis that adsorption occurs on heterogeneous surfaces with sites of varied adsorption energies, unlike the assumption of uniform sites in the Langmuir model (El Qada *et al.*, 2006; Tayebi *et al.*, 2016). The heterogeneity factor, $1/n_F$, provides the mathematical characterization of this isotherm. The nonlinear form of the Freundlich equation is expressed as:

$$q_e = K_F\, Ce^{1/nF} \qquad \text{(Eq. 3.14)}$$

In this equation, q_e denotes the equilibrium adsorption capacity (µg/g), while K_F is the Freundlich constant, expressed in ((µg/g) $(L/µg)^{1/n_F}$), which is related to the adsorption capacity. The variable C_e represents the equilibrium concentration of adsorbate in the liquid phase (µg/L). The factor n_F corresponds to the heterogeneity of the surface and the adsorption intensity. The linearized form of the Freundlich isotherm can be written as:

$$\ln q_e = K_F + 1/nF \ln Ce \qquad \text{(Eq. 3.15)}$$

The value of $1/n_F$ represents the degree of surface heterogeneity, while n_F reflects the deviation from ideal adsorption. A value of n_F=1 corresponds to linear adsorption, values of n_F >1 suggest cooperative adsorption, and values approaching zero indicate increasing surface heterogeneity (Sadeghi *et al.*, 2023). The Temkin isotherm model is also useful in describing adsorption equilibria, particularly when the adsorbent surface possesses heterogeneous binding sites. Unlike the Langmuir model, the Temkin model considers interactions between adsorbate molecules and assumes that the heat of adsorption decreases linearly with coverage. This model is often suitable for describing adsorption using solid adsorbents in organic extractions (Cortada *et al.* 2011). In this study, the Temkin model is considered appropriate since the adsorbent surface was functionalized with creatine, resulting in a non-uniform surface, as supported by scanning electron microscopy (SEM) and transmission electron microscopy (TEM) imaging. The Temkin isotherm equation is expressed as:

$$q_e = \left(\frac{RT}{b}\right) In(A_T C_e) \quad \text{(Eq. 3.16)}$$

In this equation, q_e is the equilibrium adsorption capacity (mg/g or mmol/g), while C_e is the equilibrium concentration of the solute in the aqueous phase (mg/L or mmol/L). The parameter A_T is the Temkin isotherm equilibrium binding constant (L/mg), which is related to the maximum binding energy. The constant b is associated with the heat of adsorption. The variables R and T represent the universal gas constant (8.314 J/mol·K) and the absolute temperature (K), respectively.

3.8.2 Kinetic Models

Adsorption kinetics refers to the study of the amount of adsorbate adsorbed as a function of time. By analyzing adsorption kinetics, the rate of the adsorption process can be determined. This is important for investigating the mechanism of the overall adsorption process and for evaluating the quality of the adsorbent (Wang *et al.*, 2022). A kinetic model in chemistry generally describes the rates at which chemical reactions occur as well as the mechanisms that govern these processes. These models employ mathematical expressions to relate reaction rates to variables such as concentration, and temperature.

Over the last two decades, the most widely used kinetic models have been the Pseudo-First-Order (PFO) and Pseudo-Second-Order (PSO) rate equations (Arun *et al.*, 2012). These models have been applied to a wide variety of adsorption systems, including adsorbents ranging from biomass to nanomaterials, and adsorbates ranging from heavy metals to pharmaceutical compounds. The use of these models was popularized by Ho and McKay (1999), who analysed several literature datasets using their linear forms (Revallame *et al.*, 2020).

The Pseudo-First-Order (PFO) kinetic model, also known as the Lagergren rate equation, was first reported by Lagergren and is commonly used to describe adsorption

kinetics (Pooresmaeil *et al.*, 2020). This model assumes that the adsorption rate is proportional to the difference between the equilibrium adsorption capacity (q_e) and the amount of solute adsorbed at time t (q_t) (Wang *et al.*, 2023). The linearized form of the model is expressed as:

$$ln\ (q_e - q_t)\ = ln\ q_e - k_1 t \qquad \text{(Eq. 3.17)}$$

In this equation, q_e is the equilibrium adsorption capacity, q_t is the amount adsorbed at time t, and k_1 is the pseudo-first-order rate constant. This model assumes that the rate-limiting step is diffusion-controlled, meaning that it depends solely on the concentration of the adsorbate. The overall rate of adsorption is believed to be governed by the transfer of adsorbate molecules from the bulk solution to the adsorbent surface (Simonin *et al.*, 2016). The PFO model is most often associated with physisorption, a process driven by weak intermolecular forces.

The Pseudo-Second-Order (PSO) kinetic model, also referred to as the Ho and McKay rate equation, is widely used to describe adsorption processes (Pooresmaeil *et al.*, 2020). This model assumes that the rate-limiting step involves the sharing or exchange of electrons between the adsorbent and the adsorbate, implying that chemisorption is the dominant mechanism. The model is expressed as:

$$\frac{t}{q_t} = \frac{1}{k_2 q_e^2} + \frac{t}{q_e} \qquad \text{(Eq. 3.18)}$$

Here, q_e is the equilibrium adsorption capacity, q_t is the amount adsorbed at time t, and k_2 is the pseudo-second-order rate constant. According to Simonin *et al.* (2016), the rate-determining step in the PSO model involves chemisorption, including electron sharing or exchange between adsorbate molecules and adsorbent surfaces. The model also accounts for possible interactions between adsorption sites during the rate-limiting step, although alternative interpretations have been proposed. Compared with the PFO model, the PSO model is often more suitable for describing complex

adsorption processes because it incorporates chemical interactions, while the PFO model primarily represents diffusion-controlled adsorption. Adsorption isotherm and kinetic studies were systematically performed over a temperature range of 20–45 °C and contact times of 3–11 min, under the optimized conditions established for the microextraction method, including pH, sorbent dose, and sample volume.

3.9 Greenness Profile

Greenness profiles in extraction procedures at first attempt refer to the evaluation of the environmental impact of the methods employed for extracting natural products. This evaluation considers multiple factors throughout the extraction process, with the primary goal of minimizing the ecological footprint (Chemat *et al.*, 2012). Various metrics and tools are available for assessing the greenness of extraction procedures, including life cycle assessments, environmental risk assessments, and green solvent selection guides. These approaches help quantify the environmental impact of different extraction methods. In general, such assessment systems consider criteria such as energy efficiency, water consumption, the use of sustainable materials, and overall environmental quality to determine the degree of "greenness" (Steinemann *et al.*, 2016; Marchi *et al.*, 2021). In this study, the greenness of the proposed extraction procedures is evaluated using five assessment tools, which collectively provide a comprehensive overview of their environmental performance. These tools enable the identification of strengths and weaknesses in the proposed analytical method, while also facilitating comparison with conventional approaches.

3.9.1 Analytical Eco-scale

The Analytical Eco-Scale is a framework used to evaluate the environmental impact and sustainability of activities, products, or processes. It considers several parameters, including carbon footprint, resource consumption, waste generation, and effects on biodiversity. By ranking activities on a scale from high to low environmental impact, the Analytical Eco-Scale highlights eco-friendly practices such as the use of

renewable energy and zero-waste systems, while also identifying harmful practices such as reliance on fossil fuels and excessive waste production. In the context of analytical method, penalty points (PPs) are assigned for each parameter of an analytical procedure that does not conform to the principles of green analysis. These parameters include hazards, waste generated, energy consumption, and the type of reagents used. The total score is then calculated by subtracting the penalty points from the ideal score of 100, where higher scores indicate greener analytical methods (Gałuszka *et al.*, 2012).

In this study, the Analytical Eco-Scale is integrated as first greenness assessment tools to classify the environmental profile of the magnetic dispersive µ-SPE method. The interpretation of the Analytical Eco-Scale score follows a standard classification: values greater than or equal to 75 indicate excellent green analysis, scores between 50 and 74 are considered acceptable, and values below 50 are regarded as inadequate. By calculating the total score, the sustainability of the proposed method can be quantitatively evaluated and compared against conventional approaches, thereby identifying both its strengths and areas requiring improvement in future work.

3.9.2 Greenness Analytical Procedure Index

The Green Analytical Procedure Index (GAPI) is a comprehensive tool designed to evaluate the environmental impact of analytical methods across their entire workflow. It provides a holistic greenness profile by assessing critical parameters such as sample preparation, the type and amount of reagents, instrumentation requirements, and waste management practices. GAPI uses a color-coded pentagram to visually represent the greenness of each criterion: green indicates environmentally friendly practices, yellow denotes a moderate environmental impact, and red highlights significant concern. This visual representation enables rapid identification of sustainable practices as well as areas requiring improvement.

In this study, the GAPI is integrated as second assessment tools to evaluate the sustainability of the magnetic dispersive µ-SPE method. By considering factors such as reagent toxicity, energy consumption, and waste generation, the GAPI evaluation provides a clear and practical overview of the method's environmental performance. The resulting pentagram allows for straightforward comparison with conventional methods and supports decision-making aimed at adopting greener and more sustainable analytical practices.

3.9.3 AGREE

The Analytical GREEnness (AGREE) metric is a comprehensive tool designed to evaluate the environmental sustainability of analytical procedures. Based on the 12 principles of Green Analytical Chemistry (GAC), AGREE provides a balanced and quantitative assessment of an analytical method by scoring it on a scale from 0 (least green) to 1 (most green), as proposed by Pena-Pereira *et al.*, (2023). The results are displayed in a circular diagram divided into 12 segments, each corresponding to a GAC principle, and color-coded to visually represent performance, with green indicating compliance and red signalling areas of concern. In this study, AGREE is applied as third assessment tools to assess the overall greenness of the magnetic dispersive µ-SPE method. By considering criteria such as reagent use, energy consumption, safety, waste generation, and operational simplicity, AGREE provides a holistic view of the method's sustainability. The metric not only enables straightforward comparison with conventional techniques but also guides improvements to align with environmentally responsible analytical practices. Based on value obtained from optimal conditions, input was added into tool for generate circular diagram.

3.9.4 Blue Applicability Grade Index

The Blue Applicability Grade Index (BAGI) is a recent tool in GAC that evaluates both the environmental sustainability and the practical applicability of analytical methods. Unlike some tools that focus solely on ecological aspects, BAGI

integrates environmental impact factors such as resource efficiency, reagent safety, and waste generation with analytical performance indicators like sensitivity, precision, and robustness. The outcome is expressed as a comprehensive score or grade, allowing methods to be ranked based on their balance of eco-friendliness and analytical reliability.

In this study, BAGI is utilized as fourth assessment tools to evaluate the greenness of the magnetic dispersive μ-SPE method. By addressing both environmental and performance dimensions, BAGI complements the other metrics and provides an additional layer of insight into the method's sustainability. Its dual focus ensures that greener practices are adopted without compromising analytical quality, thereby promoting practical and environmentally responsible laboratory solutions. Based on value obtained from optimal conditions, input was added into tool for generate star shape diagram with blue tone color.

3.9.5 Sample Preparation Metric of Sustainability

Sample preparation is a critical step in most analytical methods and is often regarded as the least green stage of the entire procedure. Traditional metrics developed for sample preparation have primarily focused on analytical performance parameters such as recovery, precision, selectivity, and sensitivity, while paying little attention to environmental impact. To address this gap, the Sample Preparation Metric of Sustainability (SPMS) was introduced, explicitly expanding the evaluation framework to incorporate the broader cost of achieving high analytical performance in terms of resource use and ecological burden.

The SPMS uses a weighted scoring system that assigns numeric values to different parameters based on their environmental impact, thereby providing a more comprehensive and quantitative assessment of sustainability. The evaluation results are typically presented in a clock-like diagram, offering a clear visual representation of the method's greenness profile. Unlike simple checklists, the weighted approach of

SPMS captures the varying degrees of influence that each factor such as solvent consumption, energy requirements, and waste generation has on overall sustainability.

In this study, SPMS is applied as fifth greenness assessment tools to evaluate the magnetic dispersive µ-SPE method. Its focus on both performance and environmental cost ensures a balanced evaluation, helping to identify approaches that maintain analytical reliability while minimizing ecological impact (Figure 3.5).

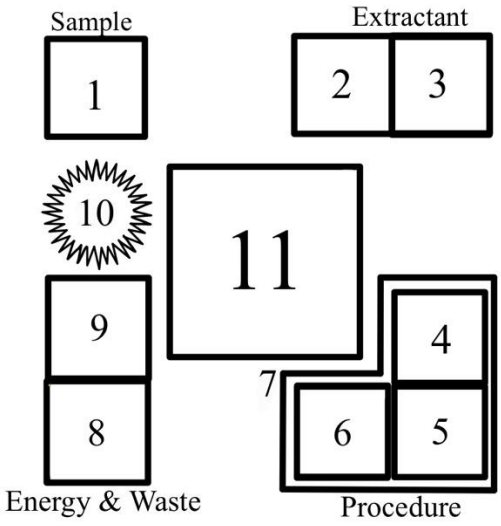

Figure 3.5. Main segments in SPMS scoring system (Zhang *et al*., 2021)

Category 1 focuses on sample information, emphasizing the amount of material required for analysis. Using smaller sample volumes is considered inherently more sustainable, as it lowers the environmental burden of collection, reduces storage and preservation needs, and minimizes the amount of discarded waste. Category 2 addresses extractant information, which is often the most critical aspect of sustainability since solvents and chemicals are the primary contributors to waste and hazards. This category evaluates the amount of extractant used, the nature of its chemical composition, and its potential for reuse, thereby encouraging solvent-free, microextraction, or reusable systems.

Category 3 evaluates the sample preparation procedure itself, with attention to workflow efficiency, complexity, and practicality. Factors such as the number of steps, total extraction time, need for post-extraction processes like evaporation or derivatization, and overall sample throughput are considered, with streamlined procedures favoured for their reduced resource demand and lower error potential. Finally, Category 4 examines energy consumption and waste generation, offering a holistic view of the method's environmental footprint. This includes measuring total energy requirements from processes such as heating, cooling, sonication, or centrifugation, alongside the amount of waste generated in both solvent and solid forms. Methods that operate under ambient conditions and generate minimal waste achieve higher sustainability scores, as this category captures the cumulative resource cost and pollution potential of the sample preparation process. Main description of metric parameters in sample preparation metric of sustainability, summarised in Table 3.7.

Table 3.7. Main description of metric parameters in sample preparation metric of sustainability

Category	Segment	Metric Parameter	Values of the Parameter and Assigned Numeric Scores			
Sample Info	1	Sample Amount (mL)	x≤10 5	10<x ≤50 3	50 <x≤100 2	x>100 1
Extractant Info	2	Amount of Extractant (sorbent) (g)	x≤0.1 20	0.1<x≤0.5 12	0.5<x≤1 6	x>1 2
	3	Nature of Extractant	Natural 20	Alternate degradable 12	Alternate persistent 6	Conventional persistent 2
Procedure Info	4	Number of Steps	x≤2 10	2<x≤4 6	4<x≤6 3	x>6 1
	5	Extraction Time	x≤5 10	5<x≤15 6	15<x≤60 3	x>60 1
	6	Additional Steps after Extraction	None 10	Dilution 6	Evaporation 3	Derivatization 1
Energy Consumption and Waste	7	Energy Consumption				
		Dispersion	Manual / Vortex 3	Ultrasounds/Peristaltic pump 2		Stirrer/ Shaker 1
		Separation	No centrifuge 2		Centrifugation 1	
		Temperature	Standard 5	Microwave 3	Heater 1	Freezer/ Cooler 1
	8	Total Waste (ml)	x≤10 10	10<x ≤50 6	50<x≤100 3	x>100 1
Reusability Mark	9	Reusable	Yes Mark		No No mark	
Sample Throughput	10	Sample Treated at a time	Multiple samples Mark		Single sample No mark	
	11	Total Score Global Score	95 (Σ Score / 95) x10 Score (1-10)			

CHAPTER 4

RESULTS AND DISCUSSION

4.1 Interaction Mechanism between Creatine and Silica-Coated Magnetite

The functionalization of Fe_3O_4@SiO_2 with creatine is controlled by the physical characteristics of each component. Materials Fe_3O_4 provides a nanosized magnetic core with superparamagnetic properties, while the SiO_2 shell stabilizes the core, prevents oxidation, and offers abundant hydroxyl groups for surface modification. Creatine, a zwitterionic molecule with amino, carboxyl, and guanidino groups, readily interacts with these hydroxyl groups through hydrogen bonding or covalent linkages (Wang *et al.* 2022). This modification introduces nitrogen-rich active sites, enhancing hydrophilicity, biocompatibility, and adsorption capability, while maintaining the core's magnetic responsiveness, thus yielding a stable multifunctional material for separation and sensing applications. Schematic image of functionalized materials is illustrated in Figure 4.1.

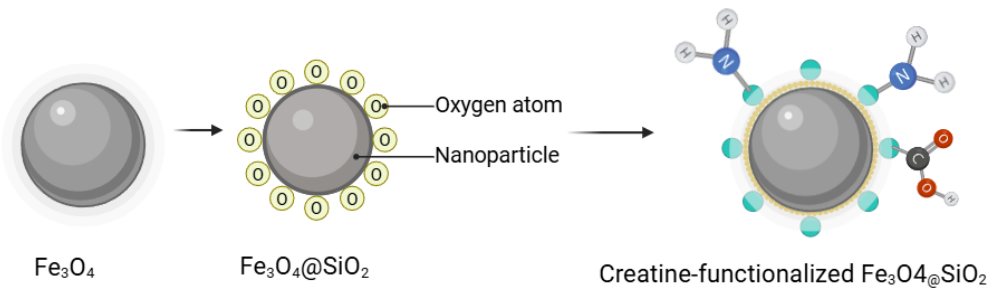

Figure 4.1. Schematic image of functionalized materials

4.1.1 Scanning Electron Microscopy Analysis

The commercial purchased iron oxide nanoparticles, characterized using Scanning Electron Microscopy (SEM), exhibited a consistent spherical morphology with particle sizes ranging from 50 to 100 nm. High-resolution scanning electron images revealed smooth surfaces, indicative of a well-controlled fabrication process (Figure 4.2). Energy Dispersive X-ray (EDS) Spectroscopy analysis confirmed the presence of iron and oxygen as the primary elements, with an atomic ratio (3:4) consistent with Fe_3O_4. The absence of impurities in the EDS spectra suggests a high level of purity, crucial especially in preparation magnetic adsorbent materials (Johnson *et al.*, 2022).

The silicon dioxide sample displayed a highly porous structure, featuring an interconnected network of particles with sizes ranging from 200 to 500 nm. The surface morphology revealed smooth, spherical particles, reflecting a well-controlled synthesis process. The observed porosity suggests a high surface area, advantageous for materials used in catalysis and adsorption study.

The creatine monohydrate sample exhibited crystalline structures with distinct, flat, plate-like features, measuring between 20 to 50 microns in length. The smooth, well-defined surfaces suggested its maintain crystallinity during fabrication process. EDS analysis confirmed the elemental composition of creatine monohydrate, showing the expected presence of carbon, nitrogen, oxygen, and hydrogen (Miller *et al.*, 2021). In spectrum (e), the elemental composition of the Fe_3O_4@SiO_2 sample revealed 20.77% oxygen, 12.22% silicon, and 67.01% iron. Spectrum (f) confirmed the presence of nitrogen atoms, attributable to the presence of creatine monohydrate, which major functional contain amino groups. The absence of foreign elements in the EDS spectra further underscores the sample's purity, aligning with previous studies on the structural characteristics of silicon dioxide (Brown *et al.*, 2021).

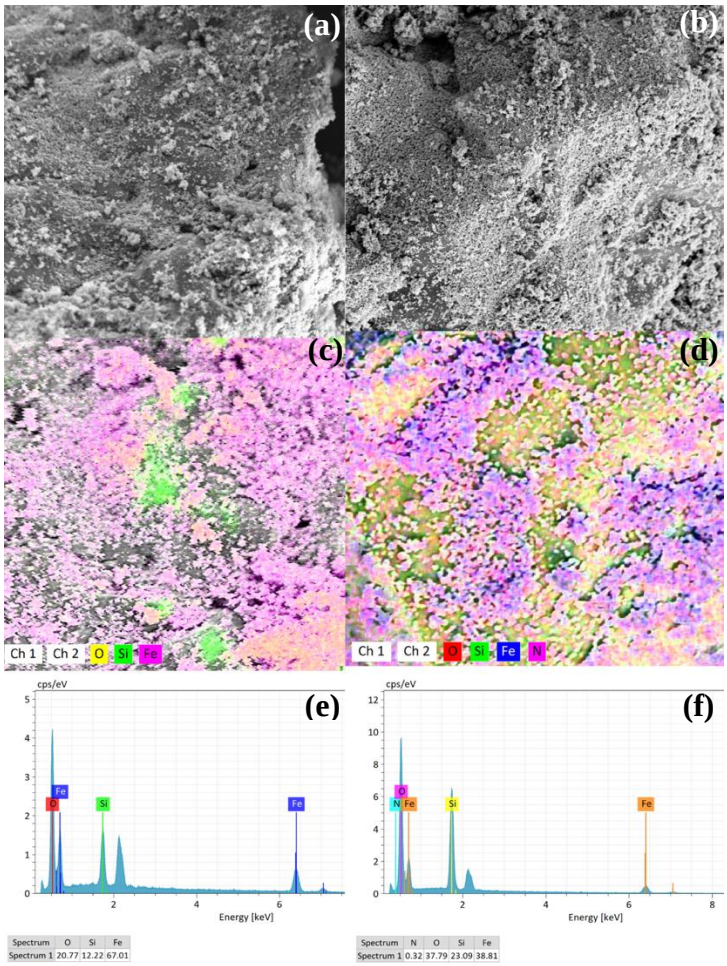

Figure 4.2 Morphology of surface of the magnetic adsorbent under 2000x magnification (a) $Fe_3O_4@SiO_2$, (b) creatine-functionalized $Fe_3O_4@SiO_2$, (c) mapping of $Fe_3O_4@SiO_2$, (d) mapping of creatine-functionalized $Fe_3O_4@SiO_2$ and (e) spectrum of percentage of elements present in $Fe_3O_4@SiO_2$, and (f) spectrum of percentage of elements present in creatine-functionalized $Fe_3O_4@SiO_2$

After functionalization, the $Fe_3O_4@SiO_2$ nanoparticles displayed a modified surface morphology, with the smooth, spherical core-shell structure of $Fe_3O_4@SiO_2$ clearly retaining its original shape while exhibiting additional surface modifications from the creatine coating. This functionalization resulted in the appearance of surface features characteristic of amino group incorporation, such as slight roughening and subtle surface irregularities (Aladaghla, 2024). At a magnification of 2000x, the SiO_2 shell was visible and appeared as layered, confirming the encapsulation phase of the

iron oxide core. EDS analysis further validated the presence of iron oxide as the primary element, along with trace amounts of silicon and creatine monohydrate, supporting the expected composition of the functionalized magnetic adsorbent.

4.1.2 Transmission Electron Microscopy Analysis

The size and morphology of creatine-functionalized Fe_3O_4@SiO_2 were further examined using high-resolution transmission electron microscopy (HRTEM). At high magnification (Figure 4.3), the Fe_3O_4@SiO_2 nanoparticles initially appeared smaller and spherical, with an average size ranging from 67.57 nm to 175 nm. In contrast, the creatine-functionalized Fe_3O_4@SiO_2 nanoparticles were measured larger, with sizes ranging increase from 102 nm to 314.23 nm. Particle size and shape were quantitatively assessed using image analysis software, which allowed for precise measurement of particle diameters from the TEM images. The size distribution data were processed using Velox software to obtain a detailed analysis of the particle population.

The increase in particle size upon functionalization is attributed to the encapsulation of the iron oxide core by the silica shell, followed by the deposition of a creatine monohydrate layer. This finding explains the crystalline structure of the Fe_3O_4 core is maintained, which is essential for preserving the magnetic properties. Its required for applications in microextraction study, when materials serve as magnetic adsorbent. Additionally, the TEM images revealed that the functionalized nanoparticles were well-dispersed, with minimal aggregation, indicating successful functionalization and stability during fabrication process.

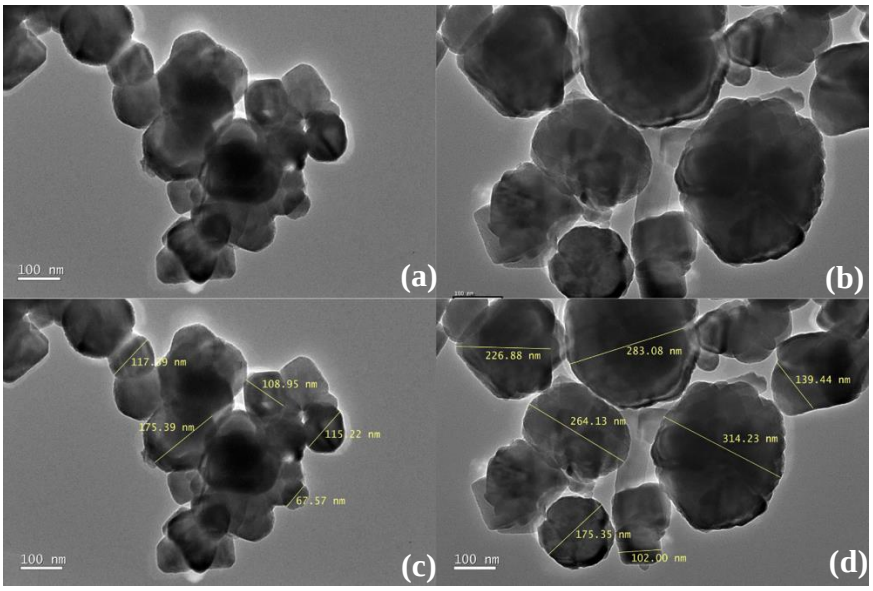

Figure 4.3 Morphology of surface of the magnetic adsorbent under 25000x magnification (a) Fe_3O_4@SiO_2, (b) creatine-functionalized Fe_3O_4@SiO_2, (c) measurements on size dispersion of Fe_3O_4@SiO_2, and (d) creatine-functionalized Fe_3O_4@SiO_2

4.1.3 Fourier Transmission Infrared Spectroscopy Analysis

The Attenuated Fourier Transform Infrared Spectroscopy (ATR-FTIR) analysis was performed to examine the functional groups present in the magnetic adsorbent formulate both with and without presence of creatine. The FTIR spectra are shown in Figure 4.4. The FTIR spectrum of Fe_3O_4 (magnetite), shown in Figure 4.4(d), reveals a strong absorption band in the range of 570–580 cm^{-1}. This band is characteristic of Fe-O stretching vibrations within the spinel crystal structure of Fe_3O_4 (Kashyap *et al.*, 2022). These vibrations are a signature of the Fe-O bond and confirm the presence of magnetite in the adsorbent materials.

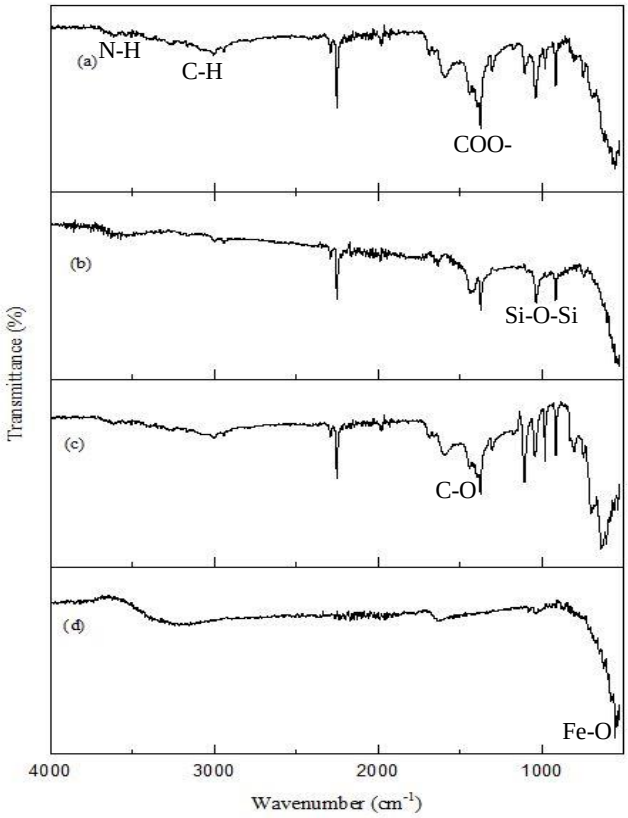

Figure 4.4 FTIR spectra of (a) creatine-functionalized Fe_3O_4 @SiO_2 (post-extraction), (b) creatine-functionalized Fe_3O_4@SiO_2 (pre-extraction), (c) pure creatine, and (d) pure Fe_3O_4

The FTIR spectrum of the SiO_2 shell, illustrated in Figure 4.4(c), displays peaks in the range of 1080–1100 cm^{-1}, which correspond to Si–O–Si asymmetric stretching vibrations. Additional peaks at 800 cm^{-1} (symmetrical stretching) and 460 cm^{-1} (Si-O-Si bending vibrations) are also observed. These vibrations are typical for silica (SiO_2), indicating the formation of a silica shell around the magnetic nanoparticles (Arévalo-Cid *et al.*, 2018). The presence of these peaks suggests that the SiO_2 shell is intact and plays an important role in the stability of the adsorbent.

When the Fe_3O_4 nanoparticles were encapsulated with SiO_2 and functionalized with creatine, distinct changes were observed in the FTIR spectra. The characteristic

Fe-O stretching vibration at 570 cm^{-1}, which is attributed to the Fe_3O_4 core, remains intact, confirming that the magnetic core is preserved. Simultaneously, the peak at 1080 cm^{-1}, associated with Si–O–Si asymmetric stretching, confirms the integrity of the silica shell surrounding the Fe_3O_4 core. These findings, seen in Figures 4.4 (a) and (b), indicate successful encapsulation and functionalization of the nanoparticles. The SiO_2 shell enhances the thermal stability of the Fe_3O_4 core, protecting it from oxidation, hence support the finding of TGA analysis which discussed in detail later.

The FTIR spectrum of creatine exhibits several distinct peaks that are indicative of its functional groups. A small peak appeared around 3200–3400 cm^{-1} corresponds to N-H stretching vibrations from both the primary amine and guanidinium groups in creatine, as well as O-H stretching vibrations, which might overlap due to the presence of water or hydrogen bonding interactions. This broad peak is indicative of intermolecular interactions, such as hydrogen bonding, which is crucial for the adsorption and stabilization of creatine on the surface of the adsorbent. Additionally, a sharp peak near 1700–1750 cm^{-1} is attributed to C=O stretching vibrations, characteristic of the carboxyl group (-COOH) in creatine, further supporting the presence of this functional group.

Peaks around 1400–1500 cm^{-1} are due to C-N stretching and bending vibrations of the amine group in creatine. The peak near 1050–1100 cm^{-1} corresponds to C-N stretching vibrations, which partially overlap with the Si-O-Si peaks from the silica shell. This overlap suggests that creatine interacts with the SiO_2 surface, likely through covalent or hydrogen bonding interactions between the functional groups of creatine and the hydroxyl groups on the silica surface (Arévalo-Cid *et al.*, 2018).

The N–H stretching vibration (3200–3400 cm^{-1}) and the C=O stretching vibration (1700–1720 cm^{-1}) provide further evidence of interaction between creatine and the SiO_2 surface, possibly through hydrogen bonding or electrostatic interactions. The Si–O–Si peaks in the 1000–1100 cm^{-1} range confirm successful bonding between the silica shell and creatine, highlighting the role of the silica shell in stabilizing the

functionalized adsorbent. The presence of the peaks in the ~1600–1720 cm^{-1} range (N–H and C=O stretching vibrations) further supports the presence of creatine and confirms its attachment to the SiO_2 surface. The broad peak in the 3200–3400 cm^{-1} range suggests that hydrogen bonding plays a significant role in the interaction between creatine and the silica shell, which may enhance the overall stability and functionality of the adsorbent (Wang *et al.*, 2022).

These FTIR observations confirm that the functionalization of Fe_3O_4 with a SiO_2 shell and subsequent attachment of creatine were successful. The FTIR data also suggest that the silica shell not only protects the magnetic core from oxidation but also facilitates the functionalization with creatine, likely through hydrogen bonding or other interactions, which may enhance the adsorbent's ability to interact with target molecules. Major of functional groups for all characterized samples are summarized in Appendix.

4.1.4 Vibrating Sample Magnetometry Analysis

The magnetism properties of adsorbent materials, containing Fe_3O_4 is characterized using vibrating sample magnetometry (VSM). This technique allows for the determination of main magnetic parameters such as saturation magnetization (M_s), remanent magnetization (M_r), and coercivity (H_c), which provide critical information related to the magnetic behaviour and potential applications of these materials. Magnetite (Fe_3O_4), also known as ferrimagnetic material, inherently exhibits high saturation magnetization, a characteristic that reflects strong magnetic interactions within the material (Gao *et al.*, 2021). However, when Fe_3O_4 nanoparticles are functionalized with non-magnetic materials like SiO_2 and creatine, the magnetic core expected becomes diluted, resulting in a reduction of the M_s value.

In this study, the magnetic properties of the adsorbent were measured in both before and after functionalization, using a sample mass of 1.74 g and controlled at room temperature (Figure 4.5) to understand the changes of superparamagnetic

properties. The Fe_3O_4 nanoparticles exhibited a maximum M_s of 63.73 emu/g, consistent with the high magnetic activity typically observed for pure Fe_3O_4, calculated at 90-100 emu/g. This reduction in M_s can be attributed to the dilution of the magnetic core by the non-magnetic SiO_2 shell and the creatine molecule's structure. Upon functionalization with creatine and SiO_2, the saturation magnetization of the post-extraction Fe_3O_4@SiO_2 (red line) measured to be decreased at 40.66 emu/g, while the remanent magnetization (M_r) was found to be 6.25 emu/g. M_s refers to the maximum magnetization a material can achieve when all its magnetic moments align in the direction of an external magnetic field and is a main indicator of the material's magnetic strength (Sharma *et al.*, 2020). For superparamagnetic materials, the M_r should be negligible or close to zero, which is confirmed in this case by the reduced value of M_r in the functionalized material.

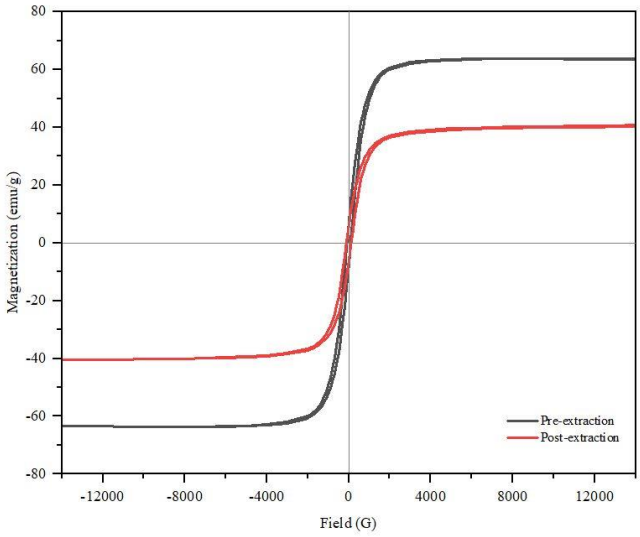

Figure 4.5 VSM graph for (red line) creatine-functionalized Fe_3O_4 (post-extraction), and (black line) creatine-functionalized Fe_3O_4 (pre-extraction)

The hysteresis loops obtained from the magnetic adsorbent displayed a characteristic S-shape, which is typical feature of superparamagnetic materials. This is good evidence that the Fe_3O_4 nanoparticles retain their superparamagnetic properties even after surface functionalization with SiO_2 and creatine. Superparamagnetic is a

desirable property for various applications include microextraction study because it enables the nanoparticles to respond to an external magnetic field without exhibiting permanent magnetization. The S-shaped curve observed in the hysteresis loops demonstrates the absence of coercivity (H_c) and the rapid response of the material to changes in the applied magnetic field, highlighting the feasibility of using these functionalized Fe_3O_4 nanoparticles (Li *et al.*, 2017; Gao *et al.*, 2021; Philips *et al.*, 2022).

4.1.5 X-ray Diffraction Analysis

The X-ray Diffraction (XRD) analysis is a powerful technique used to characterize the structural properties of materials at the atomic level. The XRD data reveals the structural characteristics of Fe_3O_4@SiO_2 nanoparticles before and after functionalization with creatine, alongside a JCPDS reference pattern for comparison (Figure 4.6). In pattern (a), diffraction peaks at 2θ values of 30.1°, 35.5°, 43.1°, 53.4°, 57.2°, and 62.7° correspond to the crystal planes (220), (311), (400), (422), (511), and (440) of Fe_3O_4 (magnetite), confirming its cubic spinel structure. The sharp, intense peaks indicate high crystallinity and well-preserved Fe_3O_4 cores, essential for maintaining the desired magnetic properties (Hedy *et al.*, 2025).

In pattern (b), the peaks remain consistent with those in (a), suggesting that the functionalization process preserved the cubic spinel structure. However, slight reductions in peak intensity and broadening indicate the presence of an amorphous layer, likely from the SiO_2 shell or creatine coating. Amorphous materials like silica typically contribute a broad hump around 20-30°, though this is less visible due to the dominance of Fe_3O_4 peaks (Hedy *et al.*, 2025). These changes further suggest successful surface modification, with the crystalline Fe_3O_4 core partially masked by the surrounding layers. The reference pattern (c) aligns well with the patterns in (a) and (b), confirming that the crystalline structure of Fe_3O_4 is maintained throughout the synthesis, coating, and functionalization processes.

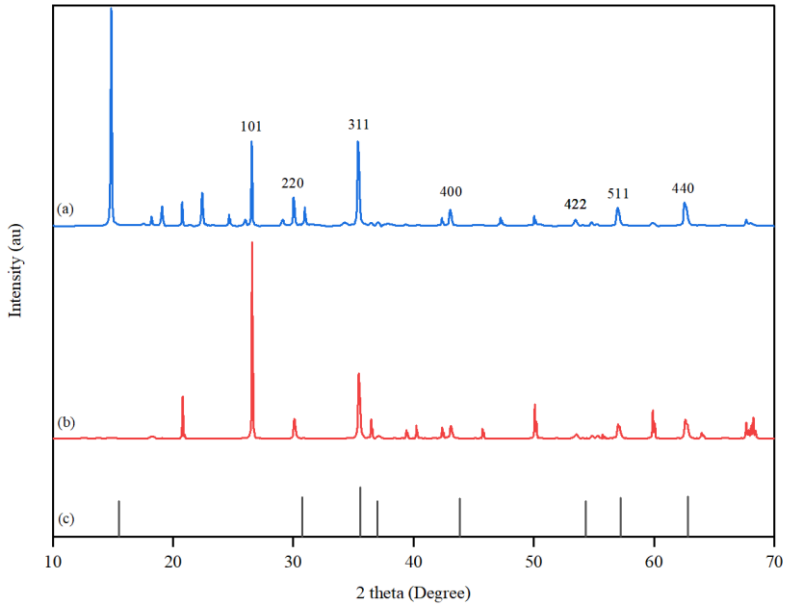

Figure 4.6 XRD micrographs of (a) creatine functionalised Fe_3O_4@SiO_2, (b) Fe_3O_4@SiO_2, and (c) JCPDS No 75–0033

The XRD data demonstrates successful synthesis and functionalization of Fe_3O_4@SiO_2 nanoparticles, with minimal disruption to the magnetite core's crystalline structure. The observed changes in peak intensity and broadening confirm the formation of the SiO_2 shell or creatine coating, validating the effectiveness of the functionalization process.

4.1.6 Zeta Potential Analysis

Zeta potential measures the electrical potential at the slipping plane of a particle in a liquid, reflecting the charge distribution near its surface. It is a critical parameter for assessing colloidal stability, as it indicates the degree of electrostatic repulsion between particles in different phase system. The zeta potential data in Figure 4.7 (a) and (b) show the surface charge distribution of Fe_3O_4@SiO_2 nanoparticles before and after functionalization with creatine, respectively. In graph (b), the zeta potential is centred around -30 mV with a symmetric, narrow distribution, indicating good

colloidal stability. This suggests a relatively uniform particle surface charge, typical of silica-coated nanoparticles (Fe_3O_4@SiO_2). The negative zeta potential arises from the deprotonation of silanol groups (-SiO^-) on the silica surface at neutral pH. The system shows moderate stability, with electrostatic repulsion between particles sufficient to prevent aggregation under normal conditions (Asghari *et al.*, 2020). However, stability may still be sensitive to changes in ionic strength or pH.

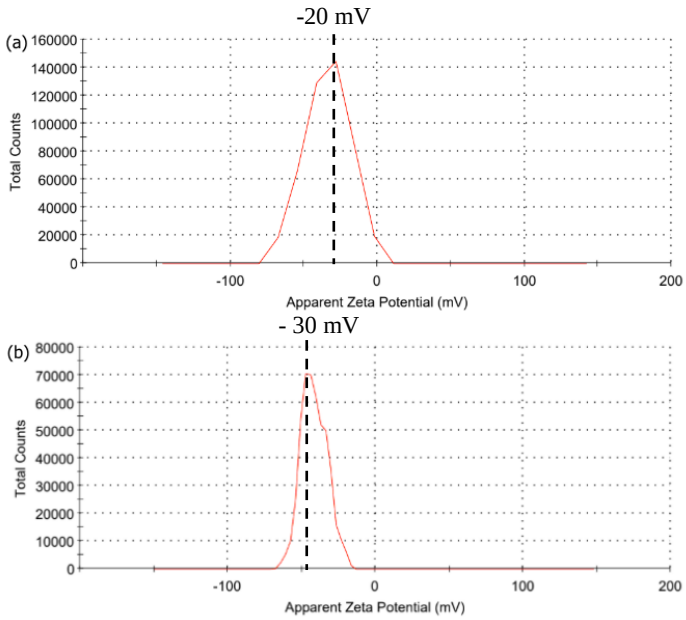

Figure 4.7 Zeta potential graph of (a) creatine functionalised Fe_3O_4@SiO_2, (b) Fe_3O_4@SiO_2

In graph (a), the zeta potential shifts to approximately -20 mV with a slightly narrower distribution compared to the unmodified nanoparticles. This shift toward less negative values reflects a change in surface charge due to the introduction of creatine functional groups. Creatine contains both amine (-NH_2) and carboxyl (-COOH) groups, and under aqueous conditions, the amine groups can become protonated (-NH_3^+), while carboxyl groups may remain partially deprotonated (-COO^-). The coexistence of these functional groups modifies the overall surface charge, leading to the observed reduction in negativity. Additionally, the narrower peak suggests a more

uniform charge distribution, further confirming successful and homogeneous functionalization of the nanoparticles (Asghari et al., 2020).

Comparing the two samples, functionalization with creatine clearly modifies the nanoparticle surface chemistry. The unfunctionalized Fe_3O_4@SiO_2 nanoparticles in graph (a) exhibit a higher zeta potential magnitude, contributing to greater stability in suspension. In contrast, the functionalized nanoparticles in graph (b) show reduced stability, though the system remains moderately stable. The shift in zeta potential confirms successful creatine attachment, as the surface charge behaviour changes due to the interaction between the silica layer and creatine's functional groups.

4.1.7 Brunauer-Emmett-Teller Analysis

The BET analysis reveals a Type IV isotherm, refer as characteristic of mesoporous materials with pore diameters ranging from 2 to 50 nm (Figure 4.8). This isotherm indicates initial monolayer adsorption at low relative pressures ($P/P_0 < 0.2$), followed by multilayer adsorption at intermediate pressures, and finally, capillary condensation at higher pressures ($P/P_0 > 0.8$). The presence of a hysteresis loop confirms mesoporosity and provides insights into the pore structure. Specifically, a Type H1 hysteresis loop suggests cylindrical, uniform, and well-ordered mesopores, while a Type H2 loop is indicative of irregular, ink-bottle-shaped pores with narrower pore necks that restrict gas desorption. The observed hysteresis loop in creatine-functionalized Fe_3O_4@SiO_2 indicates that functionalization step may have altered the pore connectivity, potentially blocked some pores or changed their geometry. If an H1 loop is present, the material retains an open mesoporous structure suitable for adsorption applications. In contrast, an H2 loop suggests that creatine molecules may have partially blocked the pores, limiting their accessibility (Bahrani *et al.*, 2022).

Functionalization step often leads to a decrease in surface area due to the partial filling or obstruction of pores by the attached molecules. In a study involving Fe_3O_4@SiO_2 nanoparticles functionalized with creatine, the resulting material

exhibited a reduced surface area compared to its non-functionalized type. This reduction is attributed to the occupation of pore spaces by creatine molecules, which cover active sites on the surface and limit nitrogen accessibility during BET analysis (Eivazzadeh-Keihan *et al.*, 2022).

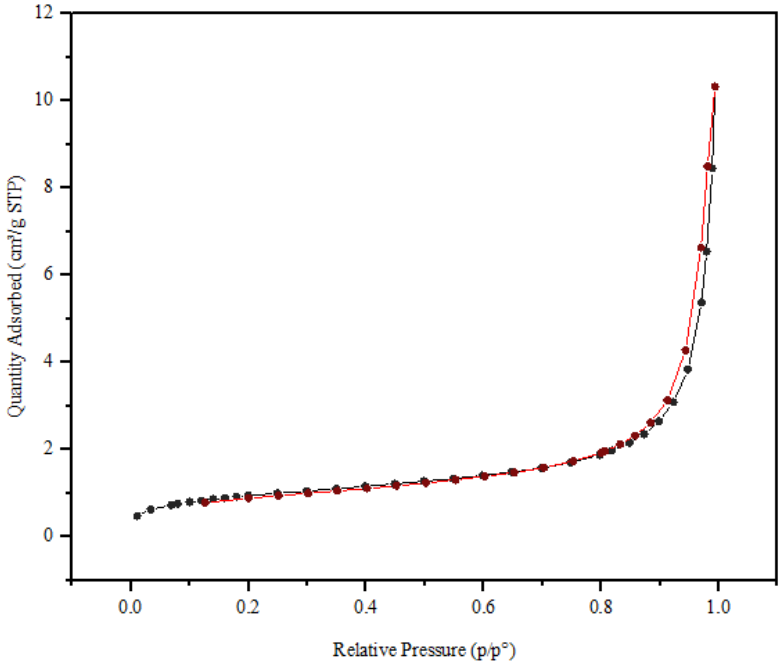

Figure 4.8 N_2 adsorption-desorption isotherm at 77.3 K of creatine-functionalised Fe_3O_4@SiO_2

The BET surface area of Fe_3O_4@SiO_2 is influenced by factors such as the synthesis method, porosity, and functionalization. Bare Fe_3O_4 nanoparticles typically exhibit a low surface area (10–100 m^2/g) due to their non-porous nature. However, when coated with mesoporous silica (SiO_2), the surface area can increase significantly, reaching values between 150–600 m^2/g, depending on the porosity and synthesis conditions (Zhao *et al.*, 2020). Experimentally, after functionalization, the BET surface area of creatine-functionalized Fe_3O_4@SiO_2 is found to be 3.4871 m^2/g. This decrease in surface area suggests that pore blocking has occurred, with creatine molecules occupying active sites or partially obstructing mesopores, thereby

restricting nitrogen adsorption. Such a reduction in accessible surface area is commonly observed in functionalized mesoporous materials, where surface modification often results in steric hindrance and molecular coverage (Wang et al., 2019, Zhao *et al.*, 2020).

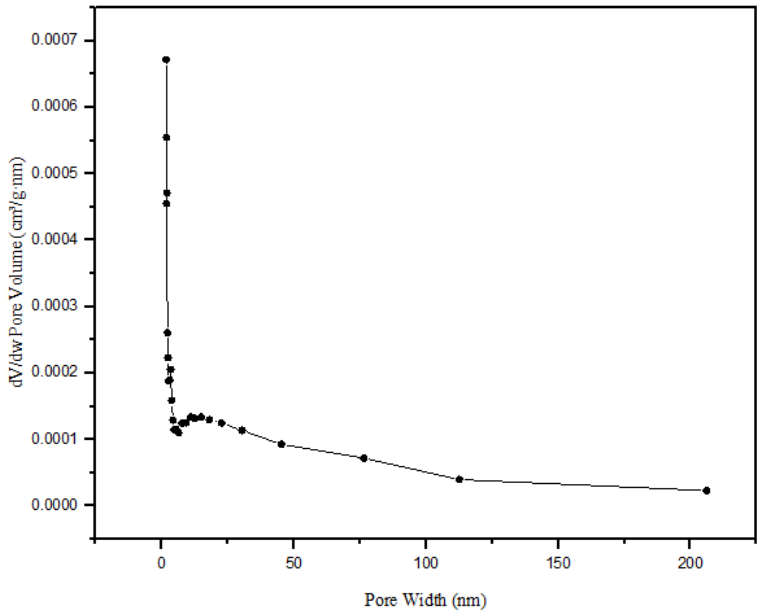

Figure 4.9 Pore size distribution of creatine-functionalised $Fe_3O4@SiO_2$

The total pore volume of approximately 0.01568 cm³/g indicates relatively low porosity, which may limit the material's adsorption capacity compared to highly porous materials. However, the measured pore size, which falls within the mesoporous range (2–50 nm), ensures that the material retains sufficient porosity for adsorption purposes. The adsorption and desorption pore diameters of 7.0002 nm and 8.2275 nm, respectively, confirm a mesoporous structure of fabricated material is suitable for accommodating macro molecules such as pharmaceutical compounds (Xu *et al.*, 2021). Mesoporous materials are particularly advantageous for controlled adsorption and release, as their interconnected pores allow molecules to be retained while enabling diffusion in next phase (Li et al., 2020). The slight increase in pore diameter during desorption suggests capillary condensation, a common feature in mesoporous

materials, which is further evidenced by the hysteresis loop observed in the isotherm. This loop, typically indicative of ink-bottle-shaped pores, suggests some degree of pore neck restriction. While the low total pore volume implies that adsorption may be surface-limited, the mesoporous structure still facilitates molecular accessibility, making the material suitable for serve as magnetic adsorbent in dispersive µ-SPE.

Regarding functionalization, the layering of creatine significantly alters the surface chemistry and adsorption characteristics of Fe_3O_4@SiO_2. A reduction in BET surface area (3.4871 m^2/g) and total pore volume (~0.01568 cm^3/g) following functionalization suggests that creatine molecules partially block mesopores, limiting the number of accessible adsorption sites especially mechanism of pore filling. The observed mesoporous structure, as indicated by the adsorption (7.0002 nm) and desorption (8.2275 nm) pore diameters, remains intact, but functionalization could introduce additional restrictions to pore accessibility, potentially resulting in an H2-type hysteresis loop characteristic of ink-bottle-shaped pores. Despite the reduced pore accessibility, the amine functional groups from creatine lead selective adsorption, particularly for polar or charged molecules, thereby improving the material's performance through strong mechanism like hydrophobic and π-π interactions. Therefore, the overall impact of creatine functionalization represents a balance between reduced pore accessibility and improved molecular interactions, determining the material's overall adsorption performance.

4.1.8 Thermogravimetric Analysis

The thermogravimetric analysis (TGA) results provide essential knowledge on the thermal stability, functionalization efficiency, and structural integrity of the creatine-functionalized Fe_3O_4@SiO_2 adsorbent. The observed weight loss can be categorized into three distinct phases, each representing specific thermal events. The initial weight loss of approximately 6.85% between 57.13°C and 87.86°C corresponds to the desorption of physically adsorbed water and possibly residual solvents. This is a common characteristic of mesoporous materials with hydrophilic functional groups

(Li *et al.*, 2019). Similar moisture losses at temperatures below 100°C have been attributed to weakly bound water molecules present on the nanoparticle surface. Additionally, the presence of surface hydroxyl groups plays a crucial role in enhancing dispersibility, adsorption efficiency, and subsequent surface functionalization, as these groups provide active sites for chemical modifications, such as creatine conjugation. The relatively low temperature at which moisture loss occurs suggests that only physiosorbed water is being removed, while more strongly bound or chemically bonded water may require higher temperatures for complete elimination (Li *et al.*, 2019). This initial weight loss phase is critical for confirming the hydrophilic nature of Fe_3O_4@SiO_2.

A significant weight loss of approximately 34.10% between 269.35°C and 311.50°C indicates the thermal decomposition of the creatine functional groups attached to the Fe_3O_4@SiO_2 surface. This temperature range is characteristic of the breakdown of organic moieties, including amine (-NH_2), hydroxyl (-OH), and carbonyl (C=O) groups, which are part of the creatine structure (Zhao *et al.*, 2021). Studies on amine-functionalized Fe_3O_4@SiO_2 composites have reported similar degradation patterns, with the decomposition of surface-modified organic molecules typically occurring between 250°C and 350°C. This range corresponds to the cleavage of covalent bonds between the functional groups and the silica framework (Zhang *et al.*, 2020). The absence of such weight loss in unmodified Fe_3O_4@SiO_2 indicates that the mass loss observed in this range is directly linked to the presence of creatine molecules, confirming successful functionalization. Furthermore, previous research on biomolecule-functionalized Fe_3O_4@SiO_2 nanocomposites has demonstrated that the degradation of organic coatings or surface modifications occurs within a similar thermal window, leading the argument that creatine has been effectively conjugated onto the Fe_3O_4@SiO_2 surface (Liu *et al.*, 2018). This decomposition behaviour not only confirms the chemical modification of Fe_3O_4@SiO_2 with creatine but also provides valuable knowledge related to the thermal stability of the functionalized composite (Figure 4.10).

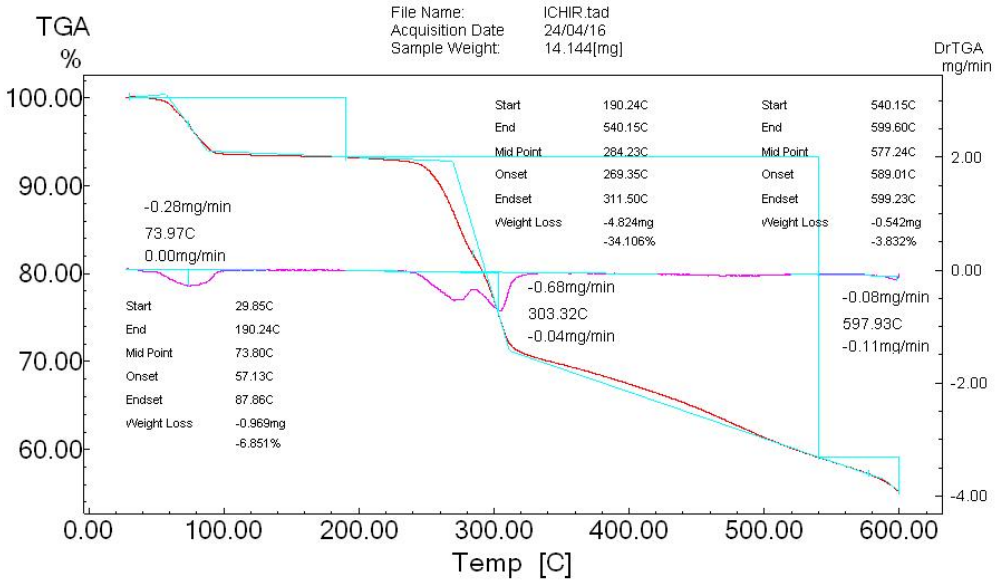

Figure 4.10 Thermogram analysis of creatine-functionalised Fe_3O_4@SiO_2

The final weight loss of approximately 3.832% observed between 589.01°C and 599.23°C in the TGA analysis likely corresponds to the continued decomposition of stable organic residues that were not fully degraded in earlier stages, or to the structural transformation of Fe_3O_4 into Fe_2O_3 due to oxidation at high temperatures. This minor, yet significant, mass reduction aligns with previous studies on functionalized Fe_3O_4@SiO_2 nanocomposites, where residual organic carbonaceous materials undergo slow degradation beyond 500°C (Wang *et al.*, 2017). Furthermore, the oxidation of Fe_3O_4 to Fe_2O_3 is a well-documented process that typically occurs between 560°C and 650°C, as Fe_3O_4 gradually transitions to the more thermodynamically stable Fe_2O_3 phase under oxidative conditions (Sun *et al.*, 2016). This transformation is accompanied by a slight mass decrease due to the release of oxygen molecules from the lattice structure. The presence of silica (SiO_2) in the composite framework helps stabilize the structure, preventing complete decomposition and explaining why a significant portion of the material remains intact even at high temperatures. Studies on silica-coated iron oxide nanoparticles have shown that the inorganic framework remains intact beyond 600°C, confirming its thermal robustness and structural integrity (Li *et al.*, 2018). Therefore, the residual weight at elevated temperatures represents the stable Fe_3O_4@SiO_2 core, demonstrating that while the

organic functional groups decompose, the inorganic backbone remains thermally stable. This stability is crucial for applications requiring high-temperature resistance, such as catalysis and adsorption in harsh environments.

4.2 Screening and Optimization Designs

4.2.1 Screening phase

Screening is a systematic approach used to evaluate multiple factors, conditions, or variables to identify those that have the most significant impact in scientific and industrial applications. This process is essential for determining main parameters that influence experimental outcomes, thereby reducing time, costs, and unnecessary experimental trials. Various statistical design techniques, such as the Plackett–Burman and factorial design methods, are commonly employed to facilitate effective screening for the development of analytical method. In microextraction studies, for instance, screening plays a critical role in selecting optimal solvents, pH levels, and extraction temperatures to maximize analyte recovery. By refining experimental conditions at an early stage, screening enhances the robustness, reproducibility, and overall quality of analytical results (Montgomery, 2017; Pawliszyn, 1997).

To assess the impact of multiple factors on analyte recovery, a total of eight experimental runs were conducted in random order, as determined by the design matrix. This randomization was implemented to minimize the influence of extraneous variables and reduce systematic error generate during experimental work. The primary effects of seven selected factors were evaluated using a 2^7 Plackett–Burman design, and the results were subsequently visualized through a Pareto chart. Pareto charts are widely utilized in microextraction studies to identify the most influential factors affecting analyte recovery, thereby facilitating the optimization of experimental conditions (Mousavi *et al.*, 2018). By providing a clear visual representation of factor

significance, Pareto charts enable rapid parameter selection and improve the efficiency of microextraction methodologies (Vidal *et al.*, 2007).

The design matrix results confirmed the successful detection of all five target analytes through the magnetic dispersive µ-SPE method (refer Figure 4.11 and Table 4.1). Among the experimental runs, run order (RO) 5 yielded the highest total peak area (232,866), followed by RO 1 (138,006), RO 3 (135,131), RO 8 (116,906), RO 2 (70,535), RO 7 (65,775), and RO 4 (50,872), which exhibited the lowest total peak area. These variations in peak areas highlight differences synergistic effects in extraction efficiency across the tested conditions. To evaluate the role of creatine-functionalized Fe_3O_4@SiO_2 in the magnetic dispersive µ-SPE, a control experiment was conducted in which the extraction was performed without creatine functionalization. In this case, most analytes were undetectable, with a maximum of only two peaks observed. This observation suggests that the amine functional groups on the modified sorbent play a crucial role in the adsorption process, facilitating stronger interactions between the analytes and the sorbent surface. Preliminary experiments revealed that the highest recovery (41%) was achieved in RO 5, while the lowest recovery (9%) was recorded in ROs 4 and 6, respectively.

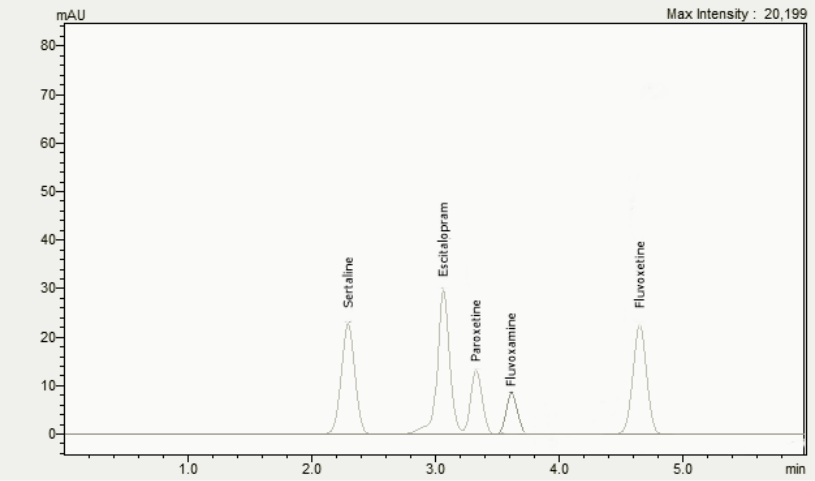

Figure 4.11. Chromatogram of target analytes obtained from HPLC-DAD analysis

Table 4.1 Analysis of screening phase using Plackett-Burman Design

Run Order	X_1	X_2	X_3	X_4	X_5	X_6	X_7	Total Peak Areas	Number of Peaks Detected	Extraction Recovery (%)
1	-	-	-	+	+	+	-	138006	5	24
2	+	-	-	-	-	+	+	70535	5	12
3	-	+	-	-	+	-	+	135131	5	24
4	+	+	-	+	-	-	-	50872	5	9
5	-	-	+	+	-	-	+	232866	5	41
6	+	-	+	-	+	-	-	51277	5	9
7	-	+	+	-	-	+	-	65775	5	11
8	+	+	+	+	+	+	+	116906	5	20

The successful detection of analytes confirms the functionality of the magnetic dispersive µ-SPE. However, to maximize extraction efficiency, further optimization is necessary. Expanding the range of experimental factors is expected to enhance analyte retention on the sorbent, leading to improved detection sensitivity and overall extraction performance. For subsequent optimization studies, three variables namely amount of effervescence (X_2), volume of water (X_4), and volume of methanol (X_7) were held constant at 1 g, 15 mL, and 250 µL, respectively. These factors were identified as having minimal influence on extraction efficiency and were therefore controlled to minimize unnecessary variability, allowing the investigation to focus on factors with a more substantial impact on analyte recovery.

The Pareto chart represents the effect estimates of each factor through bar lengths, which correspond to the absolute magnitude of the effect. Factors with longer bars exert a greater influence on the response variable, while shorter bars indicate relatively minor effects. Each effect can be classified as either positive or negative: positive effects (represented by bars extending to the right) indicate that an increase in the factor enhances the response, whereas negative effects (represented by bars extending to the left) suggest an inverse relationship, meaning that increasing the factor reduces the response (Box *et al.*, 2005).

A red vertical line is typically incorporated into the Pareto chart to denote the threshold for statistical significance, often set at an alpha level of $p = 0.05$. This threshold, determined through t-tests or normal probability distributions, differentiates statistically significant factors from those with negligible effects. If a factor's corresponding bar extends beyond this threshold, it suggests that the factor has a statistically significant impact on the response variable, indicating that its effect is unlikely to be attributed to random variation (Myers *et al.*, 2016). Conversely, factors with bars that do not exceed the threshold are considered statistically insignificant and may not require further investigation or optimization.

The interpretation of the Pareto chart serves as a crucial step in experimental decision-making by identifying the most critical factors influencing the microextraction process. In the present study, pH of the prepared sample, extraction

temperature, and sorbent weight emerged as the most significant factors. By prioritizing the control of these main factors while deprioritizing those with lesser influence, experimental efficiency can be enhanced, ultimately leading to improved analytical performance and reliability (Antony, 2014).

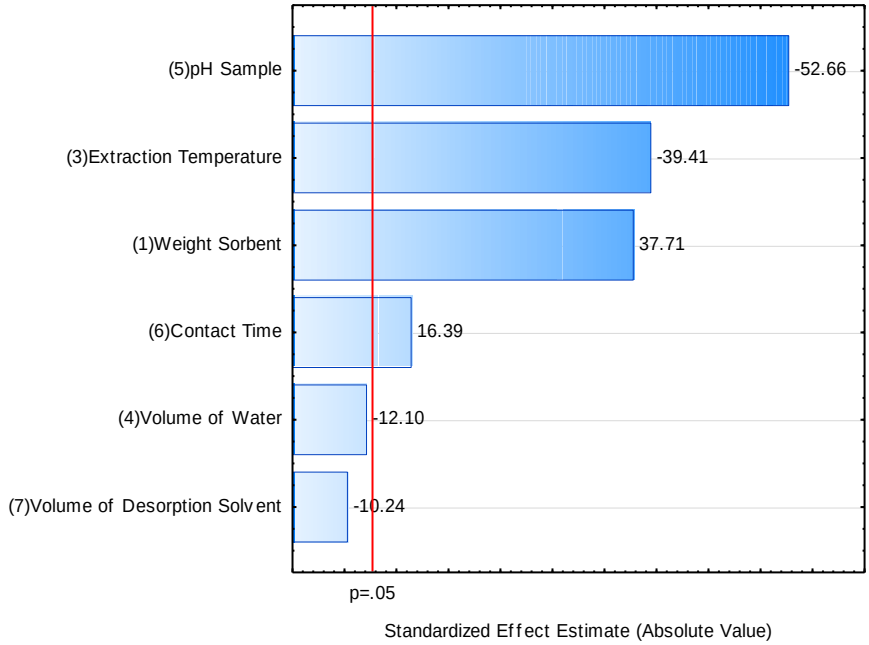

Figure 4.12 Pareto charts of the main effects obtained from the Plackett–Burman Design. Note: Effect of effervescence amount is negligible and excluded from chart.

In the given Pareto chart (Figure 4.12), the most significant factors affecting the response variable are pH of the prepared sample in laboratory (-52.66), extraction temperature (-39.41), sorbent weight (37.71), and contact time (16.39). Their standardized effect estimates extend well beyond the p = 0.05 significance threshold, indicating a strong influence on the response. Among these, pH of the sample exhibits the largest antagonistic effect, suggesting that alternation pH in no optimal condition significantly decreases the response. This trend may be attributed to alterations in chemical equilibrium, solubility, or reaction kinetics, all of which can affect the efficiency of the extraction or adsorption process (Antony, 2014). Similarly, extraction temperature also has a strong antagonistic effect, indicating that adjustment temperatures at extreme low-high level can reduce the response. This effect may result

from factors such as thermal degradation, volatility loss, or decreased adsorption efficiency at elevated temperatures (Montgomery, 2017). In contrast, sorbent weight has the largest synergistic effect, implying that increasing the sorbent amount enhances the response. This increase is likely due to the availability of a greater surface area or a higher number of active sites for analyte interaction, leading to improved adsorption efficiency (Myers *et al.*, 2016).

4.2.2 Optimization phase

Central Composite Design (CCD) is a widely used statistical approach for optimization in experimental studies. It is a type of Response Surface Methodology that develops a second-order regression model to describe the relationship between multiple independent variables (factors) and a response variable. The main objective of CCD is to optimize the response by identifying the best combination of factors while minimizing the number of experimental runs. CCD is particularly useful in optimization problems where nonlinear relationships exist between input factors and the response. It enhances the precision of models by incorporating factorial points, axial points, and centre points, which enable accurate predictions and identification of optimal conditions (Fallah and Hadjmohammadi, 2020).

In this study, the independent factors namely weight of sorbent (X_1), extraction temperature (X_3), pH of sample (X_5), and contact time (X_6) were varied at different levels, including factorial levels (−1, +1), axial levels (−α, +α), and central points (C). The measured responses take in account on three aspects namely total peak areas, number of peaks, and extraction recovery (%) are summarised in Table 4.2. When examining the total peak areas, significant variability was observed across different experimental runs. The highest peak area (790,844) was recorded in run order 10, whereas the lowest value (24,095) occurred in run order 13. This suggests that certain factor combinations, particularly those involving higher levels of X_1 (1.0) and X_5 (5), contribute to increased peak area values. Run order 1 to 16 represent factorial points, while run order 17 to 24 represent axial points. The moderate values observed in the

centre points (run order 25–30) suggest the presence of nonlinear effects, warranting further analysis through quadratic modelling (Smith *et al.*, 2024). The number of peaks detected, ranging from three to five, remained relatively stable across the runs, with only minor variations influenced by factor interactions.

Table 4.2. Design matrix for central composite design

Run Order	X_1	X_3	X_5	X_6	Total Peak Areas	Number of Peaks Detected	Extraction Recovery (%)
1	-1	-1	-1	-1	776027	5	135
2	-1	-1	-1	+1	271940	3	47
3	-1	-1	+1	-1	557561	5	103
4	-1	-1	+1	+1	590665	5	103
5	-1	+1	5	-1	339357	4	59
6	-1	+1	5	+1	310304	3	54
7	-1	+1	+1	-1	341115	5	59
8	-1	+1	+1	+1	439913	4	92
9	1.0	-1	5	-1	557929	3	97
10	1.0	-1	5	+1	790844	4	138
11	1.0	-1	+1	-1	109134	4	19
12	1.0	-1	+1	+1	231860	4	40
13	1.0	+1	5	-1	24095	3	4
14	1.0	+1	5	+1	47140	3	8
15	1.0	+1	+1	-1	189574	4	33
16	1.0	+1	+1	+1	290902	5	51
17	-α	0	7	0	318219	4	55
18	+α	0	7	0	487852	4	85
19	0	-α	7	0	544045	5	95
20	0	+α	7	0	300932	3	52
21	0	0	-α	0	382390	5	67
22	0	0	+α	0	201828	3	35
23	0	0	7	-α	376150	4	65
24	0	0	7	+α	281499	4	49
25 (C)	0	0	7	0	337937	5	59
26 (C)	0	0	7	0	210598	4	37
27 (C)	0	0	7	0	226668	5	39
28 (C)	0	0	7	0	415269	5	72
29 (C)	0	0	7	0	193687	3	34
30 (C)	0	0	7	0	297574	5	52

For extraction recovery (%), the data indicated substantial fluctuations. The highest recovery (138%) was observed in run order 10, consistent with the trend of a high total peak areas, whereas the lowest recovery (4%) was recorded in run order 13. This drastic variation highlights the strong influence of experimental factors, particularly X_1 and X_5, on the response. Runs performed at higher axial levels ($-\alpha$, $+\alpha$) generally displayed intermediate response values, further supporting the presence of quadratic effects. The experimental design also incorporated centre points to evaluate model adequacy and experimental reproducibility. The relatively stable values obtained at the centre points suggest that experimental error was controlled within an acceptable range.

Analysis of Variance (ANOVA) is a crucial statistical tool CCD for evaluating the significance of the model, individual factors, interaction terms, and quadratic terms. It determines whether the fitted second-order regression model adequately describes the relationship between independent variables (factors) and the response variable (Zhang *et al.*, 2016).

In this study, four independent factors namely weight of sorbent (X_1), extraction temperature (X_3), pH of sample (X_5), and contact time (X_6) were tested to optimize magnetic dispersive µ-SPE method (Table 4.3). The significance and adequacy of the model were evaluated using F-values, p-values, and the Lack of Fit (LOF) test derived from ANOVA at a 95% confidence interval, as summarized in the table below. The predicted values for the dependent variables at different combinations of independent variable levels were computed using the regression coefficients obtained from the second-order regression model (Lopez *et al.*, 2007). The coefficients of the polynomial equation, whether positive or negative, accounted for significant changes in the response. Furthermore, the absolute value of each coefficient reflected the relative efficiency of the variable's contribution to the overall response.

Table 4.3. Analysis of variance (ANOVA) for the second-order regression model

Factor	Sum Square	df	Mean Square	F-ratio	*p* value	Coefficient
(X_1) Weight Sorbent (L)	4.910	1	4.910	0.345	0.565	384
Weight Sorbent (Q)	4.040	1	4.040	0.284	0.601	-194
(X_3) Extraction Temperature (L)	86.395	1	86.395	6.073	0.026^s	-155
Extraction Temperature (Q)	122.265	1	122.265	8.595	0.010^s	132
(X_5) pH of Sample (L)	15.233	1	15.233	1.070	0.317	603
pH Sample (Q)	3.011	1	3.011	0.211	0.652	26
(X_6) Contact Time (L)	0.031	1	0.031	0.000	0.988	110
Contact Time (Q)	8.300	1	8.300	4.583	0.045^s	-434
1L by 2L	43.783	1	43.783	4.077	0.049^s	929
1L by 3L	20.961	1	20.961	6.473	0.024^s	-723
1L by 4L	10.917	1	10.917	5.767	0.039^s	-522
2L by 3L	9.786	1	9.786	4.687	0.041^s	-550
2L by 4L	27.037	1	27.037	7.900	0.018^s	-913
3L by 4L	1.358	1	1.358	0.095	0.761	230
Lack of Fit	142.220	6	94.833	27.707	21.89	
Pure	71.112	4	47.416			
Total SS	584.577	29				

df refer to degree of freedom, Sum Square and Mean Square value multiply 10^9, and ^{S} denote for significantly different at 95%

Among the main effects, extraction temperature (X_3) emerged as the most influential factor affecting response recovery. Both its linear ($p = 0.026$) and quadratic ($p = 0.010$) terms were statistically significant, indicating a nonlinear effect of temperature on recovery efficiency. This suggests that while an increase in temperature initially enhances recovery, further increases beyond an optimum threshold negatively impact the response. The presence of this quadratic effect aligns with the principles of

RSM, as highlighted by Box and Wilson (1951), which emphasize the role of second-order models in process optimization. Contact time (X_6) also exhibited a significant quadratic effect ($p = 0.045$), suggesting that both excessively short or prolonged contact times reduce efficiency. However, the linear effect of contact time was not significant ($p = 0.988$), indicating a more complex influence that depends on time thresholds rather than a straightforward increasing or decreasing trend.

In contrast, the weight of sorbent (X_1) and pH of sample (X_5) did not exhibit significant independent effects. The p-values for both their linear and quadratic terms exceeded 0.30, suggesting that variations in these factors alone did not substantially influence response recovery. Nevertheless, significant interaction effects involving X_1 and X_5 were observed, implying their importance in combination with other factors. Notable interactions ($p < 0.05$) included $X_1 \times X_3$ (weight of sorbent × temperature), $X_1 \times X_5$ (weight of sorbent × pH), and $X_3 \times X_6$ (temperature × contact time).

The overall model fit indicated that the regression model explained a substantial portion of response variability, though some limitations were evident. The Lack of Fit test ($F = 21.89$) was relatively high, suggesting that the model may not fully capture the experimental data, possibly due to unaccounted factors or random noise. Additionally, the pure error sum of squares (71.112) revealed some variability among repeated experimental conditions. To enhance predictive accuracy, further residual analysis or additional experimental trials may be required (Montgomery, 2017).

The variation of experimental data around the fitted model is referred to as the lack of fit (LOF). When higher-order terms are excluded from the model, the LOF test becomes a valuable tool for evaluating model adequacy. A model is considered to fit the data when the p-value exceeds 0.05 (Jafari *et al.*, 2018). In this study, the LOF p-value for the optimization model was 0.25, indicating that the model was not significantly associated with pure error. The quality of fit for the polynomial equation was further evaluated using the coefficient of determination (R^2) and the adjusted

coefficient of determination (adjusted R^2) (Kamalabadi *et al.*, 2018). R^2 represents the percentage of variation in the dependent factor (peak area) explained by the independent factors. Adjusted R^2, on the other hand, accounts for the most significant variables while penalizing unnecessary ones, making it more reliable for model refinement.

In this study, R^2 and adjusted R^2 values were calculated as 0.963 and 0.929, respectively. Both values, being close to 1.0, indicate a strong correlation between observed and predicted values (Jafari *et al.*, 2018). This reflects excellent agreement between experimental data and the fitted model. A higher adjusted R^2 value further emphasizes the robustness of the model, consistent with findings from previous studies (Khodadoust *et al.*, 2013; Kamalabadi *et al.*, 2018).

Cook's Distance measures the influence of individual data points on the regression model parameters. Observations with a Cook's Distance greater than 1 are generally considered highly influential and may disproportionately affect the model estimates. In the provided plot (Figure 4.13), all data points exhibited Cook's Distance values less than 1, indicating that none of the observations exerted an undue influence on the regression results (Jayakumar and Sulthan, 2015).

The normal probability plot is used to assess whether the residuals follow a normal distribution, main assumption in regression analysis. Ideally, the residuals should align closely with the reference line, confirming normality. In the plot as displayed in Figure 4.14, most residuals followed this expected pattern, although slight deviations were observed at the tails, suggesting minor departures from normality. Such deviations can influence the reliability of hypothesis testing and confidence intervals derived from the model (Atkinson and Riani, 2024).

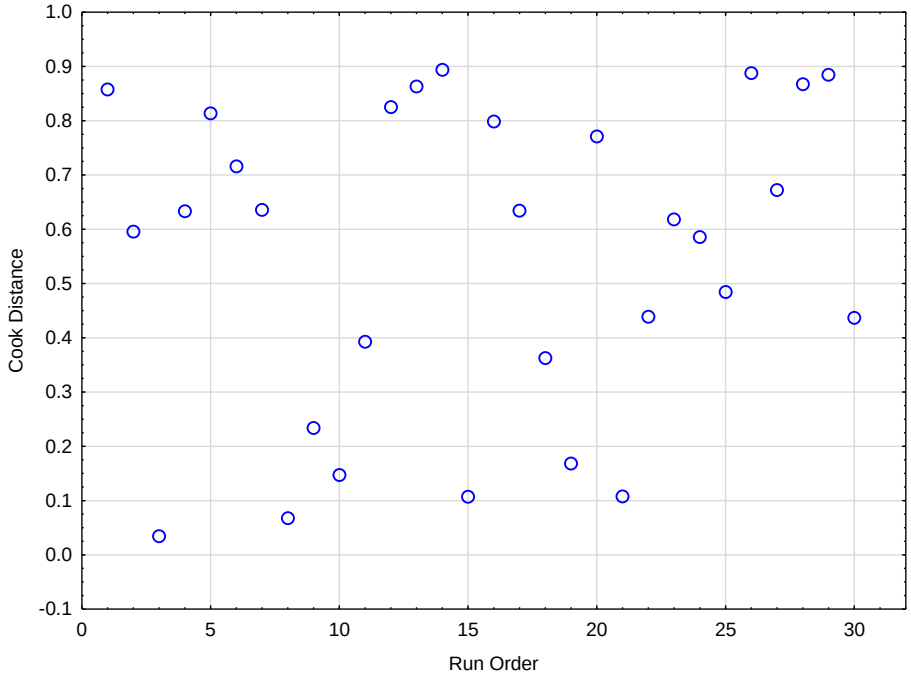

Figure 4.13. The cook distance plot *vs* run order central composite design

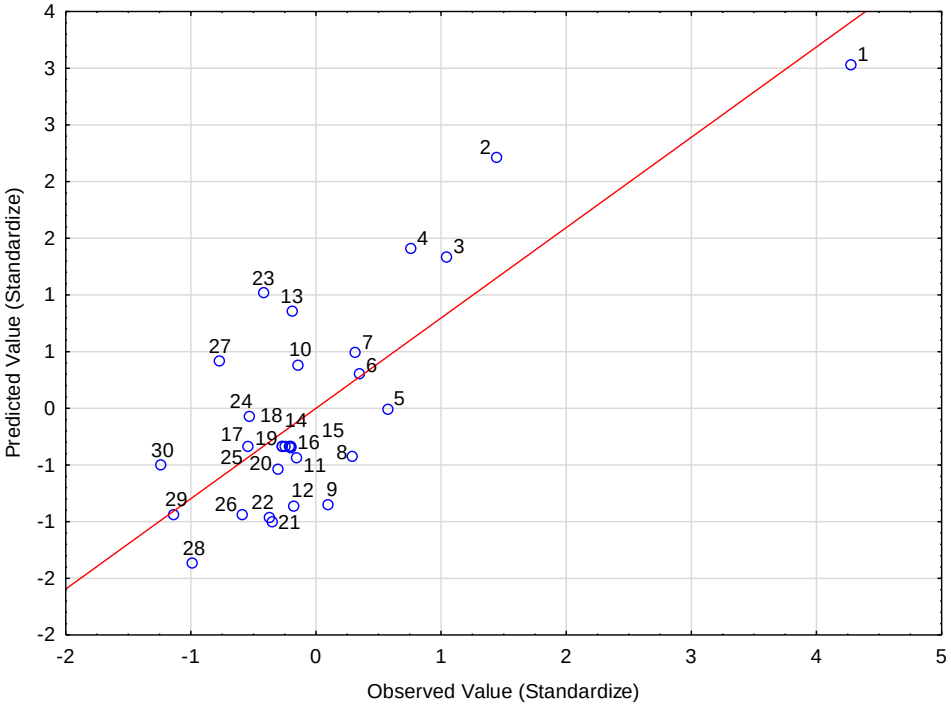

Figure 4.14. Normal probability plot of residuals

The residual *vs.* fitted plot evaluates the assumption of homoscedasticity, meaning that the variance of residuals should remain constant across all levels of the predicted response. A random scatter of residuals supports this assumption, whereas systematic patterns such as a funnel shape indicate heteroscedasticity. Refer to Figure 4.15, a visible pattern suggested the presence of heteroscedasticity, implying that the variance of residuals changes with the predicted response. This condition can lead to inefficient parameter estimates and reduce the reliability of statistical inference. To address this issue, potential remedies include transforming the dependent variable or applying weighted regression methods (Kim and Jung, 2025).

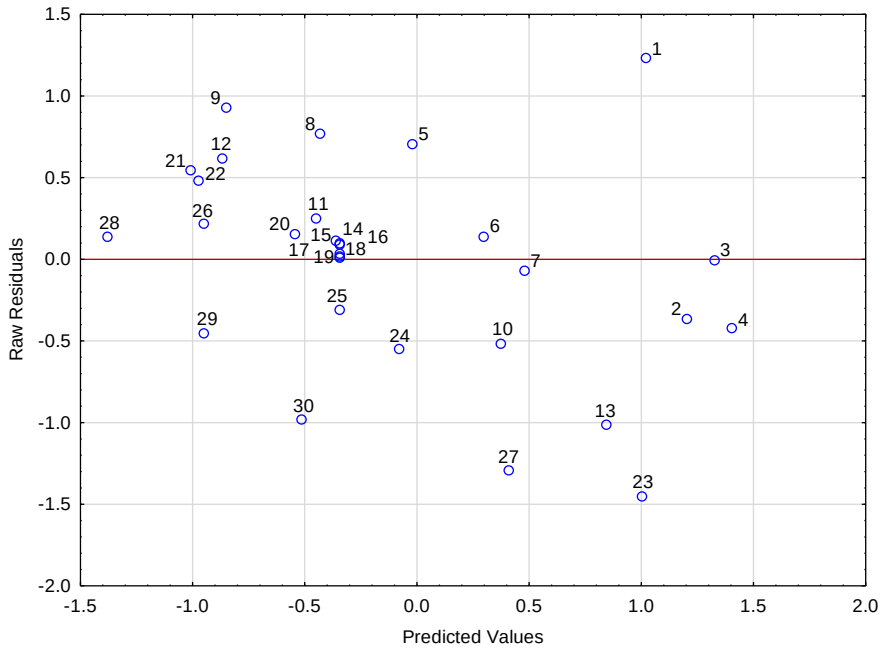

Figure 4.15. Plot of residuals *vs* predicted response

4.2.3 Optimization plot

Optimization plots are graphical tools used to illustrate the effects of various experimental parameters on the performance of microextraction techniques includes for drug detection. These plots help identify optimal conditions by showing how

changes in factors such as sorbent weight, extraction temperature, pH, and contact time influence extraction efficiency (Khodadoust *et al.*, 2013). According to the developed model, the optimal conditions were a sorbent weight of 0.5 g, an extraction temperature of 22 °C, a sample pH of 11 (basic conditions), and a contact time of 7 minutes (Figure 4.16). These parameters highlight the role of each factor in maximizing extraction efficiency for the detection of antidepressant compounds, as reflected in the composite desirability values.

The first graph of the optimization plot illustrates the effect of sorbent weight on extraction efficiency. Initially, increasing the sorbent weight enhances extraction efficiency due to the higher availability of active binding sites, which allows for increased analyte adsorption onto the sorbent phase (Bagheri *et al.*, 2017). However, beyond the optimal threshold of 0.5 g, further increases result in diminishing returns. This phenomenon is attributed to sorbent saturation and diffusion resistance, which hinder effective analyte interaction and recovery (Ahmadi *et al.*, 2016). From a green analytical chemistry perspective, reducing sorbent consumption is essential for minimizing material waste and promoting eco-friendly analytical practices (Gómez-Ríos & Pawliszyn, 2018). Thus, the selection of 0.5 g as the optimal sorbent weight ensures not only efficient extraction but also aligns with sustainability goals by avoiding excessive material use.

Temperature regulation is also critical in microextraction, as it influences molecular diffusion, analyte interaction, and the overall energy efficiency of the process. The second graph of the plot reveals a parabolic trend, identifying 22 °C as the optimal extraction temperature. At lower temperatures, restricted molecular mobility limits analyte transfer to the sorbent. Conversely, higher temperatures may cause excessive desorption and potential thermal degradation of analytes (Razzaq *et al.*, 2021). Conducting microextraction at room temperature (~22 °C) also reduces energy consumption, aligning with the principles of green analytical methods (Armenta *et al.*, 2020). Previous studies on solid-phase microextraction (SPME)

similarly recommend moderate temperatures (20–25 °C) for maintaining analyte stability and optimizing extraction efficiency (Mirzaei *et al.*, 2020).

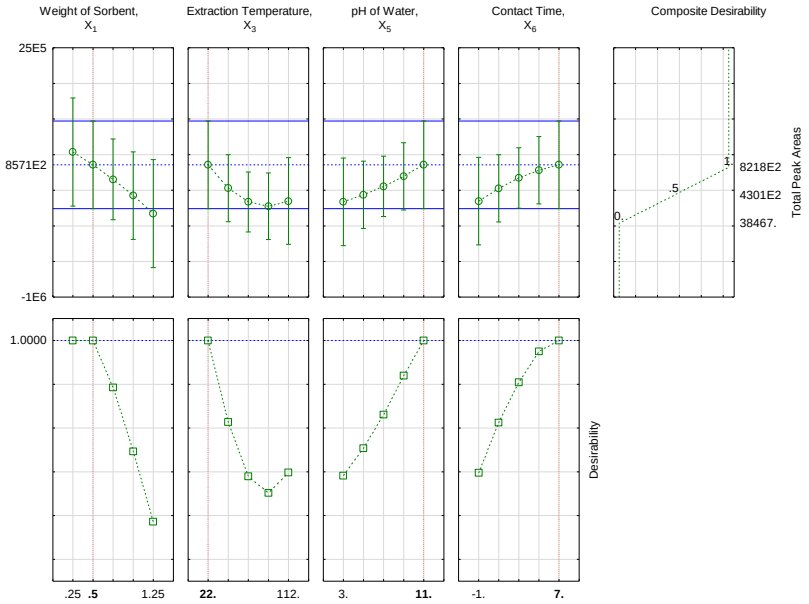

Figure 4.16. The optimization plot for studied variable and composite desirability

The third graph of the plot examines the effect of pH on extraction efficiency, with pH 11 identified as optimal for maximizing drug recovery. The pH significantly affects the ionization state of target drugs, which in turn influences their solubility and partitioning behaviour. As pH increases, drug molecules often transition into neutral or less ionized forms, enhancing their hydrophobicity and affinity for the sorbent phase (Yamini *et al.*, 2019). Many pharmaceuticals exhibit pH-dependent solubility, making pH control essential in microextraction (Mirzaei *et al.*, 2020). For basic drugs, an alkaline environment is generally preferred, as reduced ionization improves extraction efficiency. For instance, the microextraction of basic compounds such as beta-blockers and antidepressants preferred under alkaline conditions, which enhance sorbent adsorption and recovery. Ahmadi *et al.* (2021) reported that pH values above 9 were optimal for extracting basic pharmaceuticals, facilitating effective partitioning into the extraction medium. However, from a green chemistry standpoint, the use of strong

acids and bases should be minimized due to their contribution to hazardous waste generation (Koel & Kaljurand, 2006). Therefore, buffer systems with lower environmental impact are recommended over highly corrosive pH modifiers.

The fourth graph of the plot highlights the effect of contact time on extraction efficiency. Extraction recovery improves with increased contact time, reaching an optimal value at 7 minutes, after which the curve plateaus. This plateau indicates that equilibrium has been reached, and extending the extraction time further does not significantly enhance recovery (Sarafraz-Yazdi & Amiri, 2018). It is important to note that optimal extraction times may vary depending on the nature of the analyte and sample matrix. In line with green analytical chemistry principles, reducing extraction time contributes to lower energy use and higher sample throughput (Armenta *et al.*, 2020). Selecting 7 minutes as the optimal contact time thus maximizes analyte partitioning while maintaining time and resource efficiency.

The final graph presents the composite desirability function, which integrates the effects of all studied parameters into a single optimization index. The highest desirability score (~0.9) corresponds to the optimal conditions: sorbent weight (0.5 g), extraction temperature (22 °C), pH (11), and contact time (7 min). These factors collectively enhance extraction efficiency while adhering to the principles of green analytical chemistry. Minimizing sorbent and reagent use, reducing energy consumption, and optimizing process time all contribute to the sustainability of microextraction methods (Armenta *et al.*, 2020; Koel & Kaljurand, 2006). Furthermore, prior research has shown that optimizing extraction parameters significantly improves method sensitivity, reproducibility, and signal-to-noise ratio, ultimately lowering detection limits (Mirzaei *et al.*, 2020).

4.2.4 3D Response Surface

Three-dimensional (3D) response surface plots are invaluable tools in experimental design, providing a comprehensive visualization of the interactions

between multiple independent factors and a response factor. Through Response Surface Methodology (RSM), these plots facilitate a deeper understanding of complex processes and serve as essential guides for optimization. A typical 3D response surface plot displays two independent factors on the x- and y-axes, while the response factor is represented on the z-axis. This three-dimensional surface illustrates how variations in the independent factors influence the response, enabling researchers to identify optimal conditions and observe interaction effects. For example, in the optimization of antidepressant drug extraction, factors such as sorbent weight and pH can be plotted against extraction efficiency. The peaks of the surface plot indicate conditions that maximize efficiency, while valleys highlight suboptimal regions. Such visualizations are instrumental in determining the best combination of factors to enhance drug recovery while minimizing resource consumption (Farajzadeh *et al.*, 2016).

One of the main advantages of 3D response surface plots is their ability to reveal interaction effects that may not be readily apparent from numerical data alone. For instance, in biodiesel production, researchers have used these plots to study the interplay between reaction time and temperature on yield. The visualized surface demonstrated that increasing reaction time improved yield only up to a specific temperature threshold, beyond which further increases in temperature reduced efficiency. This prediction made possible by visualizing multi-factor interactions that support more informed decision-making when optimizing complex processes (Kumar *et al.*, 2017).

The interaction between sorbent weight and pH plays a crucial role in determining the efficiency of drug extraction, as illustrated by the first surface plot (Figure 4.17). As sorbent weight increases, extraction desirability generally improves, particularly under basic conditions (pH >7-11). This trend is primarily due to the increased surface area and greater availability of active binding sites, which enhance the retention of drug molecules. However, excessive use of sorbent may lead to increased material consumption and waste generation, which raises sustainability

concerns. Therefore, optimizing sorbent weight is essential to balance extraction efficiency with environmental responsibility.

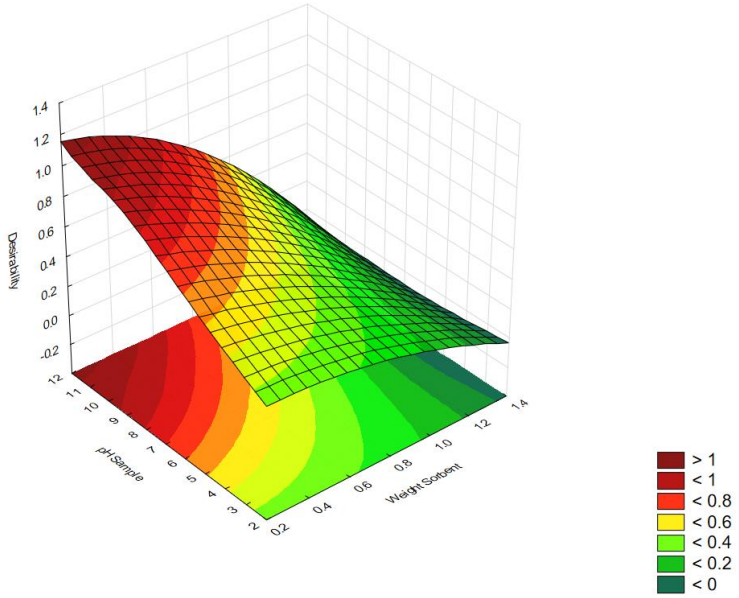

Figure 4.17. 3D response of interaction term between weight of sorbent (X_1) *vs* effect of pH of water (X_5)

At lower pH levels, protonation of functional groups on both the drug molecules and the sorbent surface enhances electrostatic interactions, thereby improving adsorption efficiency. Under these acidic conditions, the sorbent surface typically carries a net positive charge, which facilitates the attraction of negatively charged drug species. As sorbent weight increases, more active sites are available for binding, resulting in enhanced extraction. Nonetheless, once adsorption equilibrium is reached, further increases in sorbent weight yield minimal gains in extraction efficiency (Shamsipur *et al.*, 2018).

While, at higher pH values, the abundance of hydroxide ions (OH^-) in solution may compete with drug molecules for sorbent binding sites, potentially lowering extraction performance. However, deprotonation of the sorbent surface under alkaline conditions may render it neutral or negatively charged, which enhances their

hydrophobicity. This non-ionized state facilitates stronger hydrophobic and π–π interactions with the sorbent surface, leading to improved extraction efficiency. Therefore, basic solution generally favors the adsorption of antidepressant molecules onto hydrophobic or π-rich sorbent surfaces, as electrostatic repulsion is minimized and dispersion forces become dominant (Asghari *et al.*, 2020).

Thus, the interaction between sorbent weight and pH is governed by the surface chemistry of the sorbent and the ionization state of the analytes. Optimizing these factors is critical for maximizing drug recovery while minimizing the environmental impact of the extraction process. Prior studies have demonstrated that protonation–deprotonation dynamics, along with competition from hydroxide ions at high pH, significantly influence adsorption behaviour, highlighting the importance of carefully calibrating both sorbent weight and pH to achieve optimal extraction efficiency (Ghaedi *et al.*, 2015; Karimi *et al.*, 2019).

The interaction between sorbent weight and contact time in adsorption processes is pivotal in determining analyte through pre-concentration drugs. The 3D response surface plot reveals that desirability increases with sorbent weight, modulated by contact time (Figure 4.18). At shorter contact times, desirability remains low regardless of sorbent mass, indicating insufficient interaction time for analyte diffusion to the sorbent surface. As contact time increases, desirability peaks at moderate to high sorbent weights before plateauing or known as signalling equilibrium, where no further adsorption occurs despite prolonged contact (Foo & Hameed, 2010; Liu *et al.*, 2019).

Adsorption typically progresses through three distinct phases. Initially, rapid analyte uptake occurs via external mass transfer, as analyte molecules migrate from the bulk solution to the sorbent surface. Increasing sorbent weight enhances this phase by offering more active sites, thereby reducing competition among analyte molecules (Ho & McKay, 1999). As the process continues, intraparticle diffusion becomes the rate-limiting step, where analytes must penetrate the internal pore structure of the sorbent, this phase largely dictates the overall efficiency of adsorption (Weber &

Morris, 1963). Ultimately, equilibrium is reached once all available binding sites are saturated, leading to the plateau observed in the response surface (Bansal & Goyal, 2005; Tran *et al.*, 2017).

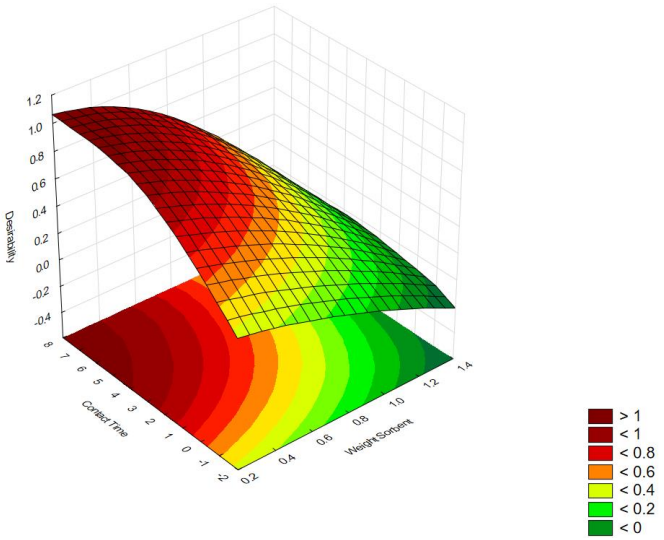

Figure 4.18. 3D response of interaction term between weight of sorbent (X_1) *vs* effect of contact time (X_6)

The interaction between sorbent weight and contact time thus highlights the importance of factor optimization. Increasing sorbent weight can reduce the need for extended contact time by providing more binding sites, thereby accelerating the attainment of equilibrium. Conversely, prolonged contact time ensures sufficient diffusion into the sorbent matrix, which may be critical for the adsorption of larger or less mobile analytes. However, once saturation is reached, further increases in either sorbent weight or contact time do not improve adsorption efficiency (Lim *et al.*, 2011; Sellaoui *et al.*, 2020).

From both environmental and economic perspectives, optimizing these factors significantly enhances process efficiency. By reducing contact time through strategic use of sorbent mass, energy consumption is minimized while maintaining effective drug extraction. This not only improves analytical throughput but also promotes

sustainability by reducing material resource. A detail understanding of the underlying chemical mechanisms includes external mass transfer, intraparticle diffusion, and equilibrium saturation is essential for designing efficient sorption systems that ensure optimal resource utilization and minimal environmental impact (Simonin, 2016; Crini & Badot, 2008; Al-Ghouti & Da'ana, 2020). This phase was elaborated detail in next section, kinetic and sorption isotherms models.

The third surface plot explores the interaction between pH and extraction temperature on the desirability of drug extraction (Figure 4.19). The results demonstrate that higher extraction temperatures, particularly when combined with neutral to slightly basic pH values, enhance desirability. This trend suggests that elevated temperatures improve drug solubility and diffusion rates, thereby promoting more efficient extraction. However, the environmental implications of high-temperature operations such as increased energy consumption and a larger carbon footprint must be considered. Thus, optimizing temperature settings is essential for achieving efficient extraction while minimizing environmental impact. In our study, range 22-30 °C seem practical to perform in laboratory.

Temperature significantly influences both the thermodynamics and kinetics of drug extraction. At elevated temperatures, increased molecular mobility and reduced solution viscosity enhance diffusion rates, facilitating better drug adsorption onto the sorbent (Al-Othman *et al.*, 2017). Additionally, thermal effects may modify the surface chemistry of the sorbent, potentially increasing drug uptake under optimal conditions (Kaur *et al.*, 2020). However, excessively high temperatures can weaken the interactions between drug molecules and the sorbent surface, leading to desorption and, consequently, reduced extraction efficiency. This occurs when the increased kinetic energy at higher temperatures disrupts the drug-sorbent binding forces, thereby lowering overall desirability (Ruthven, 1984).

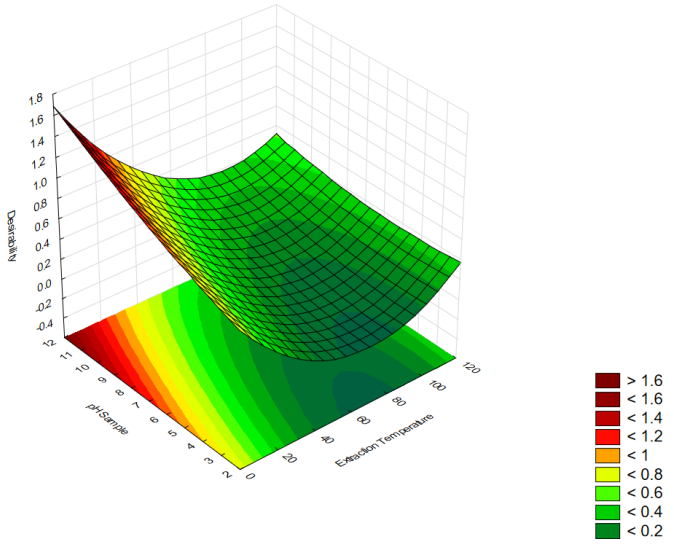

Figure 4.19. 3D response of interaction term between pH of water (X_5) *vs* effect extraction temperature (X_3)

The relationship between pH and temperature is particularly critical for drugs that undergo protonation or deprotonation, as these processes strongly influence solubility and adsorption behaviour. At low pH values, protonation of functional groups on the sorbent surface enhances electrostatic attraction, thus declining drug adsorption (Wen *et al.*, 2018). As the pH increases, the sorbent surface becomes deprotonated, analyte in neutral form, thus hydrophobic or π-π interactions become dominant, thus increase extraction efficiency. Temperature further modulates these effects by influencing the system's kinetic energy. At moderate temperatures, enhanced molecular motion facilitates greater interaction between analytes and sorbent sites (Zhang *et al.*, 2022). Conversely, high temperatures can cause desorption by disrupting sorbent-analyte bonds, ultimately decreasing extraction performance.

These chemical interactions are closely tied to the structural and physicochemical properties of both the sorbent and the target drug. Low pH conditions favour electrostatic interactions through surface protonation, increasing retention of the drug on the sorbent (Ghaedi *et al.*, 2015). But these interaction seem minor contribution for analyte-sorbent binding mechanism. However, high temperatures may

undermine these interactions, either by promoting desorption or altering the solubility profile of the analyte favouring its retention in the solution phase rather than adsorption onto the sorbent. Therefore, optimal drug extraction is typically achieved at basic pH and moderate temperatures, where the balance between adsorption and desorption is maintained.

The fourth surface plot illustrates the interaction between pH and contact time in drug extraction processes (Figure 4.20). The pH of the extraction medium is a critical factor influencing adsorption efficiency, as it affects the ionization states of both the drug molecules and the sorbent surface. At lower pH values, the protonation of functional groups on the sorbent enhances electrostatic attraction between the positively charged sorbent and negatively charged drug species, thereby increasing adsorption efficiency.

For instance, a recent study on the adsorption of tetracycline antibiotics onto graphene oxide revealed that adsorption capacity initially increased with pH, peaked at an optimal point, and subsequently declined at higher pH levels (Li *et al.*, 2023). In contrast, some sorbent-analyte systems demonstrate minimal pH dependence. For example, the adsorption of carbamazepine onto giant macroporous silica was found to be relatively stable within the pH range of 5 to 9, suggesting that pH sensitivity can vary depending on the adsorbent and the drug involved (Al-Khateeb *et al.*, 2024).

Contact time is another fundamental factor that dictates the extent of adsorption. Initially, drug molecules rapidly interact with accessible binding sites on the sorbent surface, leading to a steep increase in adsorption. As time progresses, the rate of adsorption diminishes, eventually reaching equilibrium when the available sites are occupied or further adsorption becomes energetically unfavourable (Ho *et al.*, 2023). A study examining the removal of nalidixic acid using bovine serum albumin nanoparticles showed that extended contact times improved adsorption capacity, confirming the importance of sufficient interaction time (Santos *et al.*, 2023). Similarly, research involving pharmaceutical wastewater and activated carbon found

that longer contact durations enhanced adsorption efficiency, underscoring the value of optimizing this parameter for effective pollutant removal (Gong *et al.*, 2023).

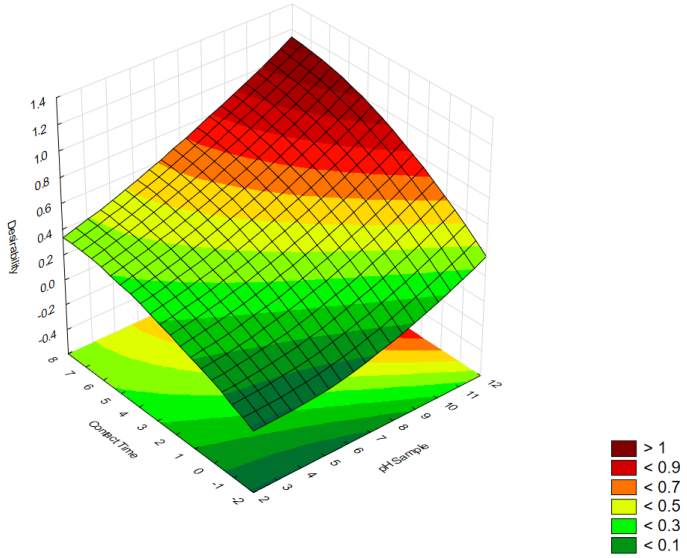

Figure 4.20. 3D response of interaction term between pH of water (X_5) *vs* effect contact time (X_6)

The combined influence of pH and contact time is pivotal for optimizing drug extraction performance. In many systems, mildly acidic conditions coupled with extended contact durations result in enhanced adsorption. This is attributed to increased electrostatic attraction and sufficient time for equilibrium to be achieved. For example, in the adsorption of methylene blue onto zinc oxide–activated carbon nanocomposites, extremely low pH values (~2) were found to hinder adsorption, while moderate pH levels and prolonged contact times significantly improved capacity (Khan *et al.*, 2024).

Moreover, under low pH conditions, prolonged contact time allows protonated drug molecules to more effectively interact with positively charged sorbent sites, maximizing adsorption. Conversely, at higher pH, the deprotonation of the sorbent surface leads to repulsive electrostatic interactions with negatively charged analytes.

As a result, even extended contact times fail to compensate for reduced adsorption efficiency in alkaline environments (Chen *et al.*, 2023).

4.2.5 Feasibility study

The operational conditions namely minimum, optimum, and maximum were evaluated in triplicate to ensure reproducibility and reliability of the results. The total peak areas obtained from each experimental run were averaged and presented in the Figure 4.21. These experimental values were then compared with the corresponding predicted values generated by the response surface models. This comparison served to assess the accuracy and predictive performance of the developed models, thereby validating their applicability for optimizing the antidepressant drug extraction process. In this study, the value obtained show no significant differences (p >0.05) between actual and predicted values of datasets. Its explain that model generated by RSM response well when factor adjusted to optimum or non-optimum conditions.

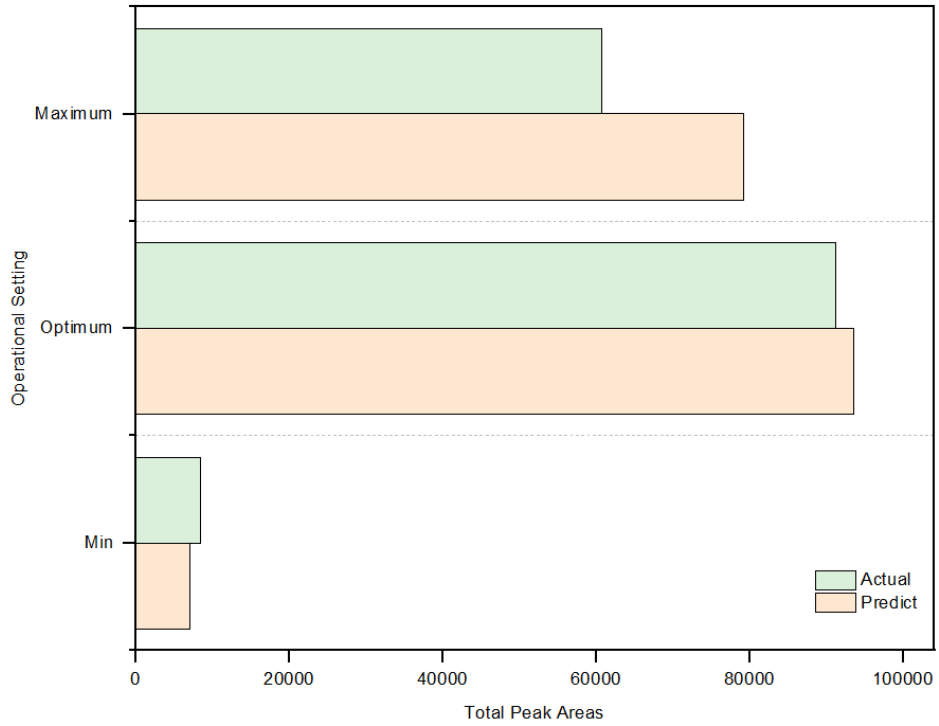

Figure 4.21. Comparison of method performance using different operational setting

4.3 Analytical Figure of Merits

4.3.1 Linearity

The linearity assay presented in the Table 4.4 evaluates the relationship between analyte concentration and instrument response for five antidepressant drugs: sertraline, escitalopram, paroxetine, fluvoxamine, and fluoxetine. Working standard solutions were prepared in methanol at concentrations ranging from 0.0 to 0.5 µg/mL. Batch experiments were conducted in triplicate at each concentration level. Linearity was assessed using two quantification approaches namely external standard and standard addition method, each represented by linear equations and their respective coefficients of determination (R^2), which indicate the goodness of fit. Good linearity was observed for all analytes, with R^2 values ranging from 0.886 to 0.999.

For sertraline, the external standard method produced a linear equation of $262495x - 4909$ ($R^2 = 0.970$), while the standard addition method yielded $248930x - 6713.2$ ($R^2 = 0.993$). The higher R^2 observed with the standard addition method indicates a better linear fit, suggesting this method more effectively compensates for matrix effects, consistent with previous findings (Silva, 2022). Similarly, escitalopram exhibited an improved R^2 value using the standard addition method (0.974) compared to the external standard method (0.900), further demonstrating the benefit of matrix compensation.

Paroxetine showed high linearity in both methods ($R^2 = 0.954$ and 0.997, respectively), indicating minimal matrix effects. In contrast, fluvoxamine had the lowest R^2 value (0.886) under the external standard method, implying a drug consider weak for compete active site on sorbent surface. However, the standard addition method significantly improved the linearity ($R^2 = 0.999$), reinforcing its suitability for complex sample matrices (Westgard, 2021). Fluoxetine demonstrated excellent linearity with the external standard method ($R^2 = 0.999$), and slightly lower but still robust linearity with the standard addition method ($R^2 = 0.981$). This consistency

suggests that fluoxetine is less affected by matrix effects, aligning with previous observations (Berzas Nevado *et al.*, 2013).

Overall, the standard addition method generally produced higher R^2 values across the analytes, supporting its efficacy in mitigating matrix effects and improving quantification accuracy in complex sample environments.

Table 4.4 Linearity details from calibration curve

Analyte	**Spiked Conc. (µg/mL)**	**Equation (*y* =)**			
		External Addition	**R^2**	**Standard Addition**	**R^2**
Sertraline	0.0 - 0.5	262495x-4909	0.970	248930x-6713.2	0.993
Escitalopram		109280x+14111	0.900	97374x+11347	0.974
Paroxetine		237898x+205.84	0.954	224320x-1197.8	0.997
Fluvoxamine		93446x+4253.8	0.886	84493x+1571.5	0.999
Fluoxetine		479673x+104.81	0.999	456285x+2665.7	0.981

4.3.2 Recovery

The extraction recovery (ER%) values for five antidepressant drugs were evaluated at three different spiked concentrations (0.50, 0.10, and 0.03 µg/mL), summarised in Table 4.5. Extraction recovery is a crucial parameter in analytical chemistry, as it determines how efficiently an analyte can be retrieved from a sample matrix following an extraction process (Płotka-Wasylka *et al*., 2017). An ER% above 80% is generally considered acceptable for quantitative analysis, indicating minimal loss and good reproducibility. However, several factors such as adsorbent type, sample matrix effects, extraction conditions (X_1–X_5), and analyte properties (e.g., polarity, solubility, and stability) can influence recovery rates (Rezaee *et al*., 2010).

The ER% in this study recorded values above range from 79.0% to 94.9%, indicating that the extraction method used is effective, though slight variations are observed depending on the specific drug and its concentration. Among the drugs tested, sertraline and fluoxetine exhibit the highest recovery values, with fluoxetine

reaching 94.9% at the lowest concentration (0.03 µg/mL). This suggests that the adsorbent material and extraction conditions are particularly well-suited for these compounds, facilitating efficient recovery from water samples. In contrast, fluvoxamine shows the lowest recovery (79.0%) at 0.10 µg/mL, which linked to weaker interactions between the analyte and the adsorbent during the extraction process. This analyte only possess one aromatic ring, thus π-π binding mechanism weaker than others. These variations in ER% may be attributed to the physicochemical properties of the drugs, including their polarity, solubility, and affinity for the magnetic creatine-functionalized adsorbent (Płotka-Wasylka *et al.*, 2017).

When evaluating drug-specific extraction performance, sertraline consistently demonstrates high and stable recoveries (86.0%–93.3%), indicating strong interactions with the adsorbent materials. Escitalopram shows slightly lower recoveries (82.8%–90.0%), particularly at the lowest concentration (0.03 µg/mL), suggesting that its extraction efficiency diminishes at very low concentrations. Paroxetine exhibits moderate recovery values (80.0%–90.0%), with a noticeable drop at 0.10 µg/mL (80.0%), possibly due to matrix effects interfering with its adsorption (Rezaee *et al.*, 2010) but remain at acceptable values.

Fluvoxamine shows the higher fluctuation in ER%, with the lowest value (79.0%) at 0.10 µg/mL, confirming weaker interaction with the adsorbent link to its molecular structure or polarity. However, its recovery improves at 0.50 and 0.03 µg/mL, suggesting a concentration-dependent adsorption efficiency. In contrast, fluoxetine demonstrates the highest overall recovery, peaking at 94.9% at 0.03 µg/mL, which indicates a strong affinity for the adsorbent and minimal loss during sample processing (Faraji *et al.*, 2019). It was as expected, since the analyte has the lowest solubility in water (0.2 mg/mL) and the highest pKa value (9.80), as previously shown in Table 3.1.

Table 4.5. Extraction recovery of the developed method

Analyte	Spiked Concentration (µg/mL)	Actual Concentration (µg/mL)	Extraction Recovery (%)
Sertraline	0.50	0.45	90.0
	0.10	0.09	88.0
	0.03	0.03	93.3
Escitalopram	0.50	0.43	86.0
	0.10	0.09	85.0
	0.03	0.02	82.8
Paroxetine	0.50	0.45	90.0
	0.10	0.08	80.0
	0.03	0.03	83.3
Fluvoxamine	0.50	0.42	84.0
	0.10	0.08	79.0
	0.03	0.03	83.3
Fluoxetine	0.50	0.40	80.3
	0.10	0.08	84.0
	0.03	0.03	94.9

The consistency of ER% across different concentrations is vital for method validation. The results suggest that the magnetic dispersive µ-SPE method is reproducible, as most ER% values remain above 75%, which is acceptable for quantitative drug analysis. Nevertheless, the observed variability highlights areas for potential improvement. Adjustments to parameters such the adsorbent composition, type or formulation could further enhance the method's performance, particularly for drugs like fluvoxamine, which exhibit reported lower recoveries at certain concentrations (Zhang *et al*., 2019).

4.3.3 Matrix Effect

Matrix effects refer to the influence of co-extracted substances from a sample matrix such as plasma, urine, or environmental water samples on the accuracy of analyte detection, particularly in chromatographic and mass spectrometric analyses.

These effects can lead to ion suppression, where analyte signals are weakened, or ion enhancement, where signals are artificially increased, ultimately compromising the precision and reliability of drug quantification. In techniques like solid-phase microextraction (SPME) coupled with liquid chromatography–mass spectrometry (LC-MS), matrix effects can result in inconsistent drug recovery, making method validation essential (Johnson, 2023).

Matrix effects in river water samples are like those encountered in wastewater; however, the distinct composition of river water introduces additional analytical challenges. River water often contains various organic pollutants, natural organic matter, inorganic salts, suspended solids, and biological contaminants. These constituents can interact with target analytes such as antidepressants, leading to signal suppression or enhancement during analysis. Despite report at higher frequency of detection, antidepressants are typically present in trace amounts especially in receiving waters, accurate quantification is particularly sensitive to these effects.

Based on the results (Table 4.6), the study evaluated the impact of matrix effects on antidepressant quantification by analysing peak appearance, signal intensity, and extraction efficiency at three concentrations (0.50, 0.10, and 0.03 µg/mL). Naturally occurring substances in river water, such as dissolved organic matter (DOM) and particulate matter, can cause ionization suppression by competing with the analytes during ionization specifically in mass spectrometry, thus reducing sensitivity (Smith *et al.*, 2023). The variability observed among different antidepressants underscores the importance of method optimization to ensure reliable quantification.

Sertraline exhibited strong matrix suppression across all concentrations, with no detectable peaks in either spiked or non-spiked samples. This suggests substantial signal suppression, likely due to strong interactions between sertraline and organic or inorganic components in the river water, which impair ionization if analysis using LC-MS. The absence of detectable signals calls for improved chromatographic conditions, matrix-matched calibration, or revised sample preparation techniques (e.g. filter

sample before extraction step) to enhance recovery and quantification. In addition to matrix effects, some studies have reported that the environmental persistence of antidepressants such as fluoxetine and sertraline in river water could further impact their detection. Adsorption to particulate matter or binding to organic molecules in the matrix sample may hinder quantification, lead to false identification of target analytes (García *et al.*, 2021).

Table 4.6. Peak appearance and matrix effect extraction efficiency of spiked and non-spiked samples

Analyte	Spiked Conc. (µg/mL)	Peak Appearance		Mean of Peak Area	Matrix Effect (%)
		Spiked	Non-Spiked		
Sertraline	0.50	-	-	-	-
	0.10	-	-	-	-
	0.03	-	-	-	-
Escitalopram	0.50	+	+	3552	99.38
	0.10	-	-	-	-
	0.03	-	-	-	-
Paroxetine	0.50	+	+	12906	97.75
	0.10	+	+	33032	94.25
	0.03	+	+	8401	98.54
Fluvoxamine	0.50	+	+	14201	97.53
	0.10	+	+	2563	99.55
	0.03	+	+	1630	99.72
Fluoxetine	0.50	+	+	88082	84.67
	0.10	+	+	17065	98.15
	0.03	+	+	5064	99.12

Note: + (present); and – (absence)

Escitalopram demonstrated a moderate matrix effect. A detectable peak appeared only at the highest concentration (0.50 µg/mL) but was absent at lower concentrations (0.10 and 0.03 µg/mL). The high matrix effect value (99.38%) at 0.50 µg/mL suggests minimal ion suppression at higher levels, while the non-detectable signals at lower concentrations indicate significant loss due to matrix interactions. This trend implies that reliable detection of escitalopram at trace levels requires further optimization to mitigate suppression. Paroxetine showed consistently high recovery and minimal matrix interference, with detectable peaks across all tested

concentrations. Matrix effect values ranged from 94.25% to 98.54%, indicating low suppression or enhancement. These stable values across concentrations highlight the method's effectiveness and make paroxetine a reliable candidate for environmental quantification using the proposed analytical method.

Fluvoxamine also displayed efficient extraction and minimal suppression, with peak appearances detected at all concentrations and matrix effect values between 97.53% and 99.72%. The high and consistent matrix effect values support its suitability for chromatographic analysis, demonstrating that fluvoxamine quantification is largely unaffected by matrix interferences, linked to least polar among target analytes. In contrast, fluoxetine exhibited concentration-dependent variability. At the highest concentration (0.50 µg/mL), the matrix effect was relatively low (84.67%), indicating significant suppression. This may result from ion competition or co-elution effects, which can reduce detection efficiency at higher analyte levels. However, the matrix effect reduced at lower concentrations (98.15% at 0.10 µg/mL and 99.12% at 0.03 µg/mL), suggesting enhanced ionization efficiency. This variability necessitates careful optimization of method conditions to ensure consistent quantification across concentration levels (Kim, 2019).

Matrix effects significantly impact the quantification of antidepressants in both biological and environmental samples by affecting detection accuracy and efficiency. While compounds like paroxetine, fluvoxamine, and low-dose fluoxetine show minimal suppression and reliable recovery, others such as sertraline, low-dose escitalopram, and high-dose fluoxetine that require optimized analytical methods to mitigate suppression caused by complex sample matrices (Mariam *et al*., 2020; Garcia *et al*., 2021). Previous studies support the current findings, highlighting the impact of matrix effects on antidepressant detection. Elgawish (2020) reported significant suppression for sertraline in rat plasma, while López-Rabuñal *et al.* (2020) demonstrated minimal interference for paroxetine and citalopram using a validated SPE-LC-MS/MS method.

Previous studies confirm that matrix suppression is a common issue in antidepressant analysis from river water. Organic substances such as humic and fulvic acids compete with antidepressants for ionization during MS analysis. This has been especially evident with fluoxetine and sertraline, where signal suppression resulted in the underestimation of concentrations in river samples (Li *et al*., 2019; Johnson *et al*., 2022).

4.3.4 Detection and Quantification Limits

The detection limit (minimum concentration of target analytes) and quantification limit (minimum detectable amount of analytes) were evaluated under optimal experimental conditions. Both parameters were assessed by analysing samples at a concentration of 0.01 µg/mL and further diluting them until a signal-to-noise (S/N) ratio of 3 and 10 was achieved, respectively (Table 4.7). In analytical chemistry, analysis of contaminants in complex matrices such as wastewater especially at trace level, the limit of detection (LOD) and limit of quantification (LOQ) are critical parameters that define a method's sensitivity and reliability. The accompanying data table summarizes peak area responses, S/N ratios, and concentrations for five antidepressants extracted using the developed method.

Following standard conventions, an S/N ratio of 3:1 is typically used to define the LOD, while a ratio of 10:1 is used to define the LOQ (Shrivastava & Gupta, 2011). For example, the LOD for sertraline was measured at 0.055 µg/mL, and the LOQ was determined at 0.056 µg/mL. Next, fluoxetine exhibited greater analytical sensitivity, with a lower LOD of 0.087 µg/mL and an LOQ of 0.287 µg/mL, reflecting better signal resolution even at trace levels. The relatively high peak areas observed at LOQ concentrations across all analytes highlight the method's strong enrichment capacity and extraction selectivity, attributed to the functional groups on the creatine-modified magnetic adsorbent. In comparison, the value of LOD and LOQ measured using linear regression method is reported lower than S/N method.

To address the uncertainties inherent in trace analysis, the application of creatine-functionalized Fe_3O_4 magnetic adsorbents offers several analytical advantages. The reproducibility of magnetic separation supports consistent analyte recovery, while selective binding mechanisms such as zwitterionic interactions and hydrogen bonding help minimize matrix interferences from co-extracted organic matter. Additionally, the thermal and chemical stability of the creatine coating under diverse environmental conditions contributes to the method's robustness and repeatability (Jafari *et al.*, 2019; Zhang *et al.*, 2020).

Table 4.7. Detection and quantification limit of the developed method

	Peak Area	**[a]S/N (3:1)**	**[a]Linear Regression**	**Peak Area**	**[a]S/N (10:1)**	**[a]Linear Regression**
Sertraline	1505	0.035	0.040	32438	0.116	0.056
Escitalopram	4828	0.012	0.132	227685	0.039	0.048
Paroxetine	10277	0.014	0.270	32438	0.046	0.056
Fluvoxamine	13107	0.030	0.084	25736	0.099	0.045
Fluoxetine	18229	0.087	0.480	199695	0.287	0.347

[a] Value reported as µg/mL

The successful detection and quantification of all five antidepressants indicate that the magnetic dispersive µ-SPE method is well performed. This performance is enhanced by the multimodal interaction mechanisms provided by the creatine-functionalized nanomaterial, including hydrogen bonding, zwitterionic interactions, and π–π stacking. These interactions improve selectivity toward polar and ionizable compounds such as antidepressants (Jafari *et al.*, 2019). Furthermore, the magnetic core enables rapid and straightforward separation without the need for filtration or centrifugation, which is particularly advantageous for analysis sample especially wastewater (Zhang *et al.*, 2020). The combination of high surface affinity, structural stability, and operational simplicity makes the proposed method especially well-suited for ultra-trace analysis in complex environmental matrices.

Given that pharmaceutical residues often emerge in wastewater at concentrations in the range from ng/L to low µg/L (Aus der Beek *et al.*, 2016), the ability to achieve low LODs and LOQs is essential for accurate detection and quantification.

4.3.5 Intra- and Inter-Day Precision

The precision and recovery efficiency of the multi-analyte antidepressant using the magnetic dispersive µ-SPE method were evaluated through repeatability and reproducibility assays. Two analytical performance metrics were assessed: intra-assay precision (a single run, n = 3) and inter-assay precision (multiple runs, n = 6). Following analysis, extraction recovery (ER%) and relative standard deviation (RSD%) were calculated to evaluate the precision of the extraction method. ER% values reflect the effectiveness of the method in isolating multiple antidepressants from the sample matrix, while RSD% is a critical parameter for assessing the precision of analytical methods used in the extraction and quantification of antidepressant drugs. Higher ER% values indicate efficient extraction with minimal analyte loss (Bazargan, 2021).

Among the studied analytes, sertraline demonstrated excellent recovery at higher concentrations, with ER% values of 99% (intra-assay) and 96% (inter-assay) at a spiked concentration of 0.50 µg/mL. However, at lower concentrations (0.10 and 0.03 µg/mL), recovery declined to 83%–86% (intra-assay) and 76%–81% (inter-assay), suggesting potential matrix effects or reduced extraction efficiency at trace levels. Similarly, escitalopram showed 97% intra-assay recovery at 0.50 µg/mL, but recoveries dropped significantly at lower concentrations, with values as low as 73%, indicating challenges in extracting low levels of this compound from the sample matrix (Table 4.8).

Table 4.8. Extraction recovery and relative standard deviation of the developed method

Analyte	Spiked Conc. (µg/mL)	Actual Conc. (µg/mL)	Intra Assay (n=3)		Inter Assay (n=6)	
			ER (%)	RSD	ER (%)	RSD
Sertraline	0.50	0.450	90.0	0.03	96	0.01
	0.10	0.088	88.0	0.02	81	0.04
	0.03	0.028	93.3	0.02	76	0.02
Escitalopram	0.50	0.430	86.0	0.05	92	0.06
	0.10	0.085	85.0	0.06	80	0.03
	0.03	0.025	82.8	0.01	75	0.03
Paroxetine	0.50	0.450	90.0	0.08	93	0.09
	0.10	0.080	80.0	0.03	82	0.05
	0.03	0.025	83.3	0.04	78	0.04
Fluvoxamine	0.50	0.420	84.0	0.12	91	0.01
	0.10	0.079	79.0	0.02	80	0.01
	0.03	0.025	83.3	0.05	78	0.05
Fluoxetine	0.50	0.402	80.3	0.01	95	0.03
	0.10	0.084	84.0	0.03	82	0.05
	0.03	0.028	94.9	0.10	76	0.01

Paroxetine exhibited relatively stable recovery values across different concentrations, ranging from 80%–84% (intra-assay) and 91%–78% (inter-assay), indicating consistent extraction performance. Meanwhile, fluvoxamine and fluoxetine demonstrated stable recoveries ranging from 85% to 95%, with only minor variations between intra- and inter-assay results. The decline in recovery for some drugs at lower concentrations suggests that the method's sensitivity rely on drug solubility and polarity leading to how strong adsorption and desorption process occur during extraction phase.

Precision was assessed using RSD%, a direct measure of variability for reproducibility. Low RSD values reflect strong repeatability within a single

experiment and reproducibility across multiple runs. Intra-assay precision showed consistently low RSD values (<0.5%) for most analytes. Fluvoxamine at 0.50 µg/mL (0.12% RSD) and fluoxetine at 0.03 µg/mL (0.1% RSD) exhibited the highest intra-assay variability. Despite these slightly elevated values, the overall precision remained within acceptable limits for bioanalytical methods (Yoshida *et al.*, 2020). Other analytes showed even lower intra-assay RSDs (0.01%–0.08%), confirming excellent repeatability.

Inter-assay results also demonstrated strong reproducibility, with RSD values ranging from 0.01% to 0.09%. However, fluoxetine at 0.03 µg/mL exhibited the highest inter-assay RSD (0.1%), suggesting increased variability at trace concentrations. Additionally, paroxetine at 0.10 µg/mL showed a slight increase in RSD from 0.03% (intra-assay) to 0.05% (inter-assay), reflecting minor variability across different runs. These small increases in inter-assay RSD may result from factors such as batch-to-batch differences in sample preparation rather than instrument performance.

A previous study using the dispersive µ-SPE method with a molybdenum-based coordination polymer reported intra-day RSD values between 3.9% and 5.2% and inter-day RSD values ranging from 4.6% to 5.4% for antidepressant recovery from human plasma (Bazargan *et al.*, 2021). Similarly, an automated SPE-LC-MS/MS method for fluoxetine quantification reported intra-day RSDs of 1.92%–7.26% and inter-day RSDs of 2.42%–7.7% (García *et al.*, 2022). A comparative analysis of intra- and inter-assay data in the present study indicates that extraction recovery remains relatively consistent, confirming the robustness of the magnetic dispersive µ-SPE method tested for short duration. Slight increases in inter-assay RSD in some cases suggest that while the method is highly reproducible, variability may slightly increase across different runs. Furthermore, the higher RSD observed at lower concentrations such as for fluoxetine at 0.03 µg/mL (RSD 0.1%) reveal the challenge of achieving consistent quantification at trace levels. Nonetheless, these results demonstrate that the

magnetic adsorbent which apply in extraction method used are capable of effectively isolating antidepressants even at the lowest concentrations tested.

4.3.6 Stability Assay

Stability test is a critical step to ensure that analytes remain chemically intact and detectable under various conditions. This step confirms the reliability, precision, and reproducibility of the analytical method. Stability testing typically assesses whether compounds degrade, desorb, or undergo structural changes over time due to environmental factors such as temperature fluctuations, pH variations, light exposure, or solvent interactions (Cai *et al.*, 2020).

In this study, stability testing is essential for evaluating the material's ability to preserve analyte integrity during sample preparation and analysis. The additional creatine introduces amine and carboxylic acid functional groups onto the surface of the magnetic core, enhancing binding affinity through hydrogen bonding, electrostatic interactions, and π-π stacking (Zhang *et al.*, 2022; Li *et al.*, 2021). As a result, stability testing not only assesses analyte preservation but also indirectly reflects the robustness of interactions between the analyte and sorbent surface, which is critical for method reliability and long-term application (Chen *et al.*, 2021).

At the highest tested concentration (0.50 µg/mL), sertraline and fluoxetine demonstrated excellent stability, with recovery values of 93.3% and 94.9%, respectively (Table 4.9). These findings suggest strong, stable binding to the creatine-functionalized surface, attributed to the presence of secondary and tertiary amine groups capable of forming hydrogen bonds with creatine's carboxyl groups. Their aromatic rings also likely contribute to retention through π-π interactions (Li *et al.*, 2021), reducing desorption and ensuring analyte integrity during extraction and analysis.

Table 4.9. Peak detection and the stability test of the adsorbent during the extraction

Analyte	Spiked Conc. (µg/mL)	Peak Recovery Detection		Stability (%)
		Initial	Final	
Sertraline	0.50	+	+	93.3
	0.10	+	+	90.0
	0.03	+	+	88.0
Escitalopram	0.50	+	+	86.0
	0.10	+	+	85.0
	0.03	+	+	82.8
Paroxetine	0.50	+	+	90.0
	0.10	+	+	83.3
	0.03	+	+	80.0
Fluvoxamine	0.50	+	+	84.0
	0.10	+	+	83.3
	0.03	+	+	79.0
Fluoxetine	0.50	+	+	94.9
	0.10	+	+	84.0
	0.03	+	+	80.3

Note: + (present); and – (absence)

Conversely, paroxetine and fluvoxamine exhibited lower stability values at the lowest concentration (0.03 µg/mL), at 80.0% and 79.0%, respectively. These lower values suggest weaker binding at trace levels, possibly due to their oxygen-rich functional groups (such as ether or oxime), which may form less effective hydrogen bonds with the creatine surface compared to amine-rich structures. Additionally, at low concentrations, solvent competition particularly from water for hydrogen bonding sites may reduce retention (Gao *et al.*, 2023). Nevertheless, stability above 75% remains acceptable for analytical purposes, indicating the sorbent's capability in trace-level detection.

Escitalopram showed moderate stability across all concentrations, ranging from 82.8% to 86.0%. This suggests adequate but less robust interaction with the sorbent. Its structure includes a fluorine substituent, can reduce its affinity for polar sites due to fluorinated compounds' generally weaker hydrogen-bonding behaviour

(Wang *et al.*, 2022). However, its basic amine group still supports sufficient retention, preventing excessive analyte loss over time.

4.3.7 Selectivity Assay

River water and other environmental water samples are typically characterized by their chemical complexity, containing a mixture of organic and inorganic matter. Among the contaminants of emerging concern are pharmaceutical residues, including antidepressants, which have been increasingly detected in various aquatic environments. To simulate these complex matrices and assess the selectivity and efficiency of the magnetic dispersive μ-SPE method, this study included a mixture of drug compounds (Table 4.10). In addition to the selective serotonin reuptake inhibitors (SSRIs), calcium channel blockers (amlodipine and nifedipine) were incorporated as representative co-contaminants.

Chromatographic data from this study show distinct retention times for each antidepressant drug, reflecting differences in their binding affinities to stationary phase on column: Sertraline (3.27 minutes), Escitalopram (3.60 minutes), Paroxetine (3.93 minutes), Fluvoxamine (4.32 minutes), and Fluoxetine (4.66 minutes). Among these, fluoxetine exhibited the longest retention time, indicating the strongest interaction with the adsorbent, likely due to its molecular structure supporting strong hydrophobic and hydrogen bonding interactions with the creatine surface (Chen *et al.*, 2019). In contrast, sertraline, with the shortest retention time, displayed the weakest interaction and lowest binding affinity, attributed to variations in functional groups and their ability to participate in intermolecular interactions such as hydrogen bonding and π-π stacking (Garcia *et al.*, 2018).

Noteworthy, retention times may vary across studies depending on chromatographic conditions such as column type, mobile phase composition, flow rate, and analytical technique (e.g., HPLC vs. UPLC). For example, a study performed by Pinder *et al.* (2017) mention fluoxetine peak appear with a retention time of 7.78

minutes, and sertraline at 13.55 minutes (Pinder *et al.*, 2017). The observed differences in retention times correlate with the molecular structures of the antidepressants. Hydrogen bonding plays a critical role in adsorption, as functional groups such as -NH, -OH, and ether (-O-) can interact with creatine's amine and carboxylic acid groups. Paroxetine and fluvoxamine possess ether and secondary amine groups, enabling stronger hydrogen bonding and contributing to longer retention (Bressolle *et al.*, 2019), whereas sertraline, lacking additional hydrogen bond donors or acceptors, forms weaker interactions and elutes more rapidly.

Table 4.10. Selectivity study on targeted analytes using real river water samples

Analyte	**Spiked Concentration (µg/mL)**	**Peak Appearance**	**Retention Time (mins)**
Sertraline	0.50	+	3.27
	0.10	+	3.28
	0.03	+	3.25
Escitalopram	0.50	+	3.54
	0.10	+	3.67
	0.03	+	3.60
Paroxetine	0.50	+	3.88
	0.10	+	3.96
	0.03	+	3.96
Fluvoxamine	0.50	+	4.32
	0.10	+	4.32
	0.03	+	4.33
Fluoxetine	0.50	+	4.65
	0.10	+	4.73
	0.03	+	4.60

Note: + (present); and – (absence)

Electrostatic interactions are also influenced by the nature and basicity of the amine groups present in each compound. Fluoxetine, with a secondary amine, exhibits

stronger dipole-dipole and electrostatic interactions, enhancing its retention, while sertraline contains a chlorophenyl group that is less hydrophobic than the trifluoromethyl group in fluoxetine, leading to weaker hydrophobic interactions and shorter retention time (Zhao *et al.*, 2020; Smith *et al.*, 2021). Additionally, the neutral amine in sertraline contributes less to electrostatic interaction compared to the more polarized secondary amine in fluoxetine. These structural differences significantly influence adsorption strength and chromatographic behaviour, as supported by previous findings (Park *et al.*, 2020).

4.3.8 Regeneration and Leaching Analysis

Magnetic adsorbents, typically composed of iron oxide (Fe_3O_4) cores functionalized with materials such as silica, graphene oxide, or organic molecules (e.g., creatine, as used in this experiment), allow easy recovery from aqueous systems via magnetic separation. Our fabricated materials known possess surface functional groups that capable bind through hydrogen bonding, electrostatic interactions, or hydrophobic interactions with target pollutants. When regenerated under mild chemical conditions, these interactions can remain stable across several reuse cycles. Common regenerants solvent such as methanol, dilute acids, or bases are used to desorb contaminants from the adsorbent surface without significantly damaging its structure (Zhou *et al.*, 2018; Huang *et al.*, 2020).

The regeneration of magnetic adsorbents is a crucial process that enhances their sustainability and cost-effectiveness for various environmental applications, such as water treatment and pollutant removal. Regeneration refers to the ability to recover and reuse the adsorbent after it becomes saturated with contaminants, thereby reducing the need for continuous replenishment of new materials (Tian *et al.*, 2018). In this study, four regeneration cycles were performed using an external magnetic field to recover the magnetic adsorbent after complete extraction phase (Table 4.11). The chromatographic data clearly showed differences in total peak area for multi-analyte pharmaceutical compounds across the four cycles. Specifically, the total peak area progressively decreased from 58013 in the first cycle to 30362 in the second, 17556 in

the third, and 11180 in the fourth. This trend indicates a decline in the adsorbent's performance over time, likely due to factors such as incomplete regeneration, structure degradation, and difficulty to collect fine powder of adsorbent. Nevertheless, all analytes remained detectable in each cycle.

Another observed parameter was the change in sorbent weight before and after each extraction. Initially, the sorbent weighed 0.5003 g. After the first extraction, the weight decreased to 0.480 g, attributed to material loss during the extraction process. Each subsequent cycle showed a minor decrease: 0.011 g in the first cycle, 0.105 g in the second, 0.082 g in the third, and 0.021 g in the fourth. These losses are likely due to the repeated handling and recovery steps involving the external magnetic field. Although increasing the initial amount of magnetic adsorbent could improve nanoparticle recovery, maintaining a low sorbent mass specifically 0.5 g aligns with research design and was sufficient for consistent extraction performance throughout the experiments. This balance highlights the feasibility of using a minimal amount of sorbent while ensuring functional reliability.

Table 4.11. Regeneration analysis on adsorbent performance in the developed method

Weight (g)	**Cycle of Extraction**			
	1	**2**	**3**	**4**
Adsorbent pre-extraction (g)	0.500	0.214	0.119	0.059
Adsorbent post-extraction (g)	0.489	0.229	0.137	0.068
Total peak areas	58013	30362	17556	11180

Noteworthy to mention the difference between the sorbent weight immediately after extraction and before the next cycle began. After the first cycle, 0.275 g of the sorbent was lost during the drying process, likely due to the evaporation of residual pollutants and methanol. Similar losses were observed in the following cycles: 0.011 g and 0.077 g, respectively. The slightly higher post-extraction weights reflect the presence of moisture from methanol used during extraction. Thus, the materials needed to completely dry in oven before reuse for next extraction procedure.

Previous studies have reported that high-quality magnetic adsorbents can retain 80–90% of their original adsorption capacity after four to six regeneration cycles. For example, Liu *et al.* (2018) and Li *et al.* (2020) demonstrated that magnetic composites exhibit minimal performance decline due to minor surface fouling or partial degradation of functional groups. In the context of creatine-functionalized magnetic adsorbents used for the removal of antidepressants like fluoxetine or sertraline, consistent adsorption capacity has been observed across various concentrations and multiple reuse cycles. This robustness is attributed to the inherent stability of the creatine moiety and its ability to form strong hydrogen bonds and hydrophobic interactions with target drugs (Chen *et al.*, 2019).

4.3.9 Uncertainty

The estimation of measurement uncertainty is essential for assessing the reliability and comparability of analytical results. Measurement uncertainty refers to the range within which the true value of a measurand is expected to lie, within a defined level of confidence (Cortada *et al.*, 2011). Each contributing component is typically quantified in terms of standard deviation and then combined using the root sum of squares method to obtain the combined standard uncertainty. This value is subsequently multiplied by a coverage factor—commonly k = 2 to yield the expanded uncertainty, which corresponds to an approximate confidence level of 95% (Ellison & Williams, 2012).

$$\text{Expanded uncertainty, } U\ (\%) = k \times \sqrt{(u_1^2 + u_2^2 + u_3^2 + u_4^2)}$$
$$= 2 \times \sqrt{(0.004^2 + 0.03^2 + 1.44^2 + 0.45^2)}$$
$$= 2.78\%$$

The expanded uncertainty for the magnetic dispersive µ-SPE method was calculated to be 2.78%, indicating a high degree of precision and robustness. This value is notably lower than those typically reported in similar analytical methodologies. For instance, Faraji *et al.* (2018) reported expanded uncertainties ranging from 5% to 10% for magnetic nanoparticle-based microextraction techniques,

primarily due to variability in nanoparticle synthesis and sorbent performance. Similarly, Sajid and Płotka-Wasylka (2020) emphasized that in green microextraction methods involving nanomaterials, achieving expanded uncertainties below 5% is considered excellent, particularly when analysing complex sample matrices. Even in the work proposed by Gionfriddo *et al.* (2016), which optimized commercial SPME fibres for environmental trace analysis, expanded uncertainties generally ranged between 3.5–6%, depending on analyte volatility and matrix complexity.

When using creatine-functionalized Fe_3O_4 magnetic adsorbent, main sources of uncertainty include variability in the functionalization process, analyte–matrix interactions, and the efficiency of magnetic separation. Incorporating these factors into a structured uncertainty estimation ensures that reported trace-level concentrations often in the ng/L range are not only accurate but also scientifically defensible (Sajid & Płotka-Wasylka, 2020). Thus, the low uncertainty value of 2.78% reflects a significant analytical improvement. This performance can likely be attributed to the stable anchoring of creatine on the Fe_3O_4@SiO_2 surface and the consistent recovery efficiency enabled by magnetic separation. Such a low uncertainty enhances the credibility and applicability of the method for trace-level quantification in regulatory, environmental, and monitoring contexts.

4.3.10 Analysis of real samples

The study on peak detection of antidepressants in river water and hospital wastewater shows how the magnetic dispersive µ-SPE method can be applied for real environmental samples. To validate the method for environmental monitoring, it must prove to be sensitive, selective, and reliable in detecting pharmaceutical contaminants (Zhou *et al.*, 2021). The presence or absence of antidepressants drugs in these samples reflects both the level of pollution and the effectiveness of the extraction method.

In river water, sertraline and escitalopram were not detected in non-spiked samples (Table 4.12). This suggests that their concentrations were too low to be measured, or that they had been degraded, attached to sediments, or diluted in the

water. Surprisingly, even when the river water was spiked with a standard mixture, these two drugs were still not detected. The low or undetectable levels of antidepressant drugs in river water are due to competitive adsorption from other co-existing compounds in the matrix. This finding shows that high sensitivity of analytical method is especially important for handling river samples, where pharmaceutical residue usually low (Gao *et al.*, 2023).

On the other hand, paroxetine, fluvoxamine, and fluoxetine were consistently detected, even in non-spiked river water. Their detection shows that these drugs are already present in the environment, supporting earlier studies that found antidepressants often remain in surface water due to heavy usage and poor removal during wastewater treatment (Gao *et al.*, 2023). The fact that some drugs were detected while others were not highlighted the need for highly sensitive and selective extraction methods to detect very low concentrations in complex water samples. The magnetic dispersive μ-SPE method helps improve recovery and detection because the modified adsorbent allows stronger interactions with drug molecules.

Hospital wastewater showed a very different pattern. In these samples, all target antidepressants drugs were detected in non-spiked and pre-spiked conditions. This clearly shows that hospital effluents are a major source of pharmaceutical pollution (Wang *et al.*, 2022). The ability of the adsorbent to extract all drugs, even from heavily contaminated samples with many interfering compounds, proves that the method is suitable for real-sample monitoring.

The success of the creatine-functionalized magnetic adsorbent comes from its chemical structure. Creatine provides amine and carboxyl groups that can interact with antidepressant molecules through hydrogen bonding, electrostatic attraction, and π–π stacking (Zhang *et al.*, 2022). These interactions allow stronger retention of analytes and reduce interference from other substances, making the method more reliable. The consistent results in hospital wastewater confirm the method's strong recovery ability and suitability for large-scale monitoring. For a method to be validated, it must meet

Table 4.12. Analysis and the peak frequency detection of the target analytes studied presented in real sample

Analyte	Concentration (µg/mL)	Peak Frequency Detection							
		River Water		Hospital Wastewater 1			Hospital Wastewater 2		
		Non-spiked	Spiked	Non-spiked	Pre-Spiked	Post-Spiked	Non-spiked	Pre-Spiked	Post-Spiked
Sertraline	0.00	-	-	+	+	+	+	+	+
	0.50	-	-	+	+	+	+	+	+
	0.10	-	-	+	+	+	+	+	+
	0.03	-	-	+	+	+	+	+	+
Escitalopram	0.00	-	-	+	+	+	+	+	+
	0.50	-	-	+	+	+	+	+	+
	0.10	-	-	+	+	+	+	+	+
	0.03	-	-	+	+	+	+	+	+
Paroxetine	0.00	+	+	+	+	+	+	+	+
	0.50	+	+	+	+	+	+	+	+
	0.10	+	+	+	+	+	+	+	+
	0.03	+	+	+	+	+	+	+	+
Fluvoxamine	0.00	+	+	+	+	+	+	+	+
	0.50	+	+	+	+	+	+	+	+
	0.10	+	+	+	+	+	+	+	+
	0.03	+	+	+	+	+	+	+	+
Fluoxetine	0.00	+	+	+	+	+	+	+	+
	0.50	+	+	+	+	+	+	+	+
	0.10	+	+	+	+	+	+	+	+
	0.03	+	+	+	+	+	+	+	+

+ denote as present; - denote as absence

main performance standards: sensitivity, selectivity, and robustness. The results show that the method works well for hospital wastewater, but further improvement is needed to detect very low drug concentrations in river water. The method's selectivity is proven by its ability to detect target analytes despite the presence of interfering compounds, while robustness is shown by consistent performance in both hospital and river water (ICH Q2(R1), 2005; Li *et al.*, 2021). In addition, sample from hospital wastewater also analysed using LC-MS adopted method from Peters et al. (2020), for purposes of confirmation target analytes is antidepressant drugs. Figure 4.22 shows the appearance of peaks for targeted analytes following sequence; escitalopram (R_t 4.48 min; m/z 325), paroxetine (R_t 4.77 min; m/z 330), fluvoxamine (R_t 4.86 min; m/z 319), fluoxetine (R_t 5.19 min; m/z 310), and sertraline (R_t 5.28 min; m/z 306).

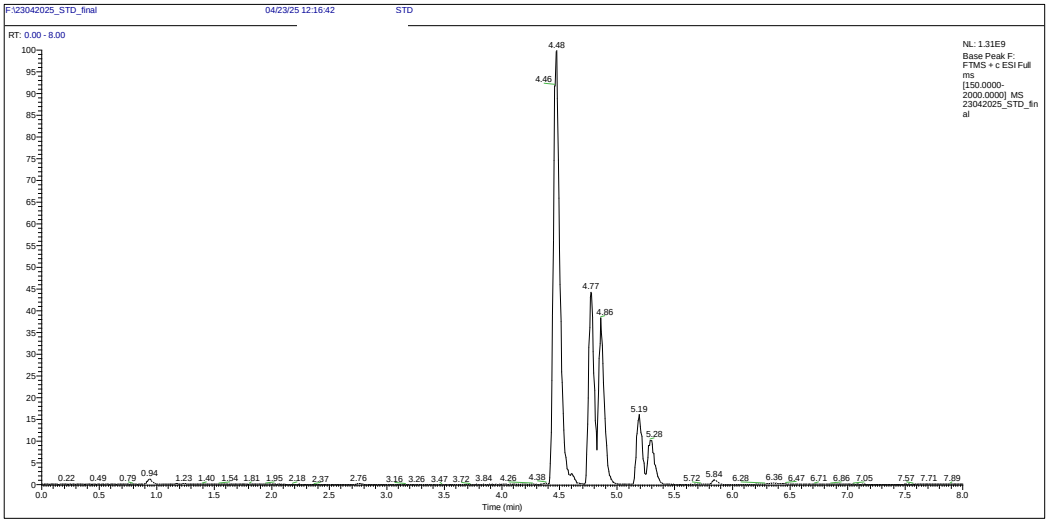

Figure 4.22. Chromatogram of target analytes obtained from LC-MS analysis

4.4 Adsorption Models

4.4.1 Isotherm Models

To optimize the design and functionality of materials for µ-SPE method, a detail understanding of the adsorption behaviour of the target analytes is essential (Zhang & Wang, 2024). This knowledge can be achieved through the application of classical adsorption isotherm models, such as the Langmuir, Freundlich, and Temkin models. These models are pivotal in describing the interactions between adsorbates

and the surfaces of adsorbents under equilibrium conditions, allowing for evaluation of adsorption capacity, surface heterogeneity, and the thermodynamic characteristics of the system (Chen *et al.*, 2025). Specifically, the adsorption behaviour of our targeted antidepressant drugs on creatine-functionalized magnetic adsorbents has been extensively studied using these classical isotherm models. These models elucidate the complex relationships between the molecular structures of the drugs, the surface chemistry of the adsorbent, and the thermodynamic factors governing the adsorption process (Liu *et al.*, 2025).

The Langmuir isotherm, which assumes monolayer adsorption on homogeneous surfaces with uniform energy sites, is traditionally suited for ideal systems such as activated carbon and chemisorption processes. However, these assumptions often do not hold for complex nanostructured adsorbents like creatine-coated magnetic nanoparticles, where surface heterogeneity and multilayer adsorption are predominant (Zhou *et al.*, 2024). Nevertheless, as displayed in Table 4.13, paroxetine exhibited the highest adsorption capacity (q_{max} = 32 mg/g), attributed to its bulky aromatic structure and strong hydrophobic interactions with the creatine coating on the adsorbent (Liu *et al.*, 2025). The adsorption sites on creatine-functionalized magnetic adsorbents are diverse due to the presence of functional groups such as –COOH, $–NH_2$, and Fe_3O_4, creating heterogeneous binding environments (Zhou *et al.*, 2024), that align with findings in this study. However, the model's offer moderate R^2 values (0.75–0.89) suggest deviations due to competitive binding in multi-drug environments (Zhang & Wang, 2024).

Next, the Freundlich isotherm analysis offers a more realistic representation of real microextraction systems by accounting for heterogeneous surface energies and multilayer adsorption. It demonstrated strongest correlation (R^2 = 0.87–0.95) for all studied antidepressants, particularly reflecting the chemically diverse surface of creatine-functionalized adsorbents. Functional groups such as –COOH, $–NH_2$, and Fe_3O_4 facilitate a broad spectrum of binding mechanisms, including hydrogen bonding, electrostatic interactions, and π–π stacking (Zhou *et al.*, 2024). Based on the tabulated

data, sertraline showed the highest Freundlich constant (K_F = 66 mg/g) and an optimal heterogeneity index (1/n = 0.65), correlating with enhanced extraction efficiency (Kumar *et al.*, 2025). The model uses a logarithmic formula to explain how adsorption changes with concentration: at low concentrations, strong binding sites are mostly used, while at higher concentrations, weaker interactions like π–π stacking seen with paroxetine help form additional layers. (Chen *et al.*, 2025). Furthermore, SEM analyses confirmed the existing irregular pore structure and functionalized surfaces of the magnetic nanoparticles support the assumptions of the Freundlich model (Park *et al.*, 2024).

The Temkin isotherm provides additional thermodynamic analysis by considering a linear decrease in adsorption heat with increasing surface coverage, reflecting the nature of adsorbent–adsorbate interactions. According to the tabulated data, paroxetine again emerged as the strongest binder, with a Temkin constant (B_T = 28 mg/g), indicating significant π–π stacking and electrostatic contributions. To support this argument in more detail, additional studies using molecular dynamics and thermodynamic data are needed, as these can show that the binding process releases heat (Chen & Liu, 2024, Wei *et al.*, 2024). Among all the tested models, the Freundlich isotherm gave the best results for explaining how antidepressants bind to creatine-functionalised magnetic adsorbents. This model fits well with uneven surfaces that allow multiple layers of adsorption, which matches the characteristics of the materials used in this study. The values of K_F and 1/n indicate favourable adsorption conditions and are consistent with real microextraction systems, where competition between drugs and surface property differences commonly occur.

4.4.2 Kinetic Models

Kinetic models are preferred tools for quantifying reaction rates and elucidating mechanisms in modern chemistry, particularly in environmental and pharmaceutical study (Wang *et al.*, 2023). Previous study highlights their critical role in designing adsorption systems, where models such as the pseudo-second-order (PSO) kinetics surpass traditional approaches by effectively capturing chemisorption

processes through quantum-chemical interactions (Zhang *et al.*, 2024). In pharmaceutical adsorption studies, these models have demonstrated how functionalized nanomaterials achieve selective pollutant removal via synergistic electrostatic and hydrogen-bonding interactions (Li *et al.*, 2023).

The adsorption behaviour of five SSRIs onto creatine-functionalized magnetic adsorbent was systematically investigated through kinetic modelling (Table 4.14). The pseudo-first-order (PFO) model showed poor correlation with experimental data (R^2 = 0.45–0.90), as evidenced by inconsistent equilibrium adsorption capacities, Q_e (13–42 mg/g) and widely varying rate constants, K_1 (0.021–0.086 L/mg), confirming its inadequacy for describing chemisorption-dominated systems (Liu *et al.*, 2019). Contrarily, the PSO model exhibited excellent agreement with experimental data (R^2 = 0.93–0.99) across target analytes, thereby validating chemisorption as the principal mechanism (Ho & McKay, 1999; Zhao *et al.*, 2021).

The good performance of the PSO model can be attributed to its ability to capture the complex, multi-analyte interactions driven by functional group from creatine. These include electrostatic attraction between protonated SSRI amines and deprotonated carboxyl groups, as well as hydrogen bonding involving SSRI nitrogen/oxygen atoms and the adsorbent's –NH_2/–COOH moieties (Chen *et al.*, 2020). The zwitterionic nature of creatine further enhances these interactions, facilitating a shared adsorption mechanism despite structural variations among the SSRIs, as reflected in the consistent kinetic parameters (equilibrium capacities of 9.07×10^{-7}–2.84×10^{-6} mg/g).

The PSO model is especially useful because it can account for surface heterogeneity and multiple types of interactions, making it well-suited for material like creatine-functionalized magnetic nanoparticles adsorbent (Kyzas & Matis, 2015; Zhao et al., 2021). It also works reliably across a wide range of concentrations (Simonin, 2016), which is important for SSRIs with different binding strengths. In contrast, the PFO model often reported fails at low concentrations (Ahmed & Theydan, 2014).

Table 4.13 Isotherm model parameters for SSRIs drugs adsorption

Model		Parameters	Sertraline	Escitalopram	Paroxetine	Fluoxetine	Fluvoxamine
Isotherm	Langmuir						
		q_{max} (mg/g)	26	13	32	18	28
		K_L (L/mg)	0.33	0.23	0.18	0.16	0.23
		R^2	0.75	0.83	0.89	0.82	0.86
	Freundlich						
		K_F (mg/g)	66	18	21	19	18
		$1/n$	0.65	0.60	0.62	0.82	0.65
		R^2	0.95	0.91	0.90	0.87	0.90
	Temkin						
		B_T (mg/g)	24	25	28	25	22
		K_T	3.49	2.1	3.03	1.92	2.95
		R^2	0.90	0.88	0.89	0.90	0.89

Table 4.14. Kinetic models parameters for SSRIs drugs adsorption

Model		Parameters	Sertraline	Escitalopram	Paroxetine	Fluoxetine	Fluvoxamine
Kinetics	Pseudo-First Model						
		Q_e (mg/g)	26	13	42	38	28
		k_1 (L/mg)	0.21	0.17	0.36	0.28	0.32
		R^2	0.985	0.978	0.992	0.983	0.991
	Pseudo-Second Model						
		Q_e (mg/g)	45	66	52	52	36
		k_2 (g/mg·min)	1.93×10^{-6}	2.84×10^{-6}	1.34×10^{-6}	1.39×10^{-6}	9.07×10^{-7}
		R^2	0.993	0.991	0.997	0.985	0.996

4.5 Greenness Profile

4.5.1 Analytical Eco-Scale

The Analytical Eco-Scale is a useful semi-quantitative tool for laboratory practice and education. It evaluates analytical methods by assigning penalty points based on reagents, energy use, occupational hazards, and instrumentation. While this approach provides a practical way to compare different analytical steps, it does not always offer a complete picture of the overall environmental impact (Wojnowski *et al.*, 2019).

Table 4.15 summarizes the penalty points calculated for the magnetic dispersive μ-SPE method. Each category is divided into sub-criteria that reflect different levels of environmental and safety concerns. Higher penalty points are assigned to practices considered less sustainable, while lower scores indicate greener methods. The final score is obtained by subtracting total penalty points from 100. A score above 75 is considered “excellent” in terms of greenness.

The developed method used methanol, sodium bicarbonate, citric acid, and deionized water. Sodium bicarbonate and citric acid were used as precursors, while a 15 mL water sample was spiked with 1 mL of a multianalyte standard containing sertraline, escitalopram, paroxetine, fluvoxamine, and fluoxetine. Hazard values were assigned as follows: methanol (4 points), sodium bicarbonate (1 point), citric acid (1 point), and deionized water (0 points), giving a total of six penalty points. Among these reagents, methanol contributed most to the score reduction. It was used in preparing stock and standard working solutions as well as a diluent solvent in extraction. Because of its “danger” classification and relatively high consumption (10–100 mL), methanol incurred four penalty points. Although greener alternatives such as ethanol exist, methanol remains widely used in antidepressant analysis because it offers the best reconstitute solvent, cost, and instrument compatibility. In this study, where high recovery and sensitivity are essential, methanol often outperforms less hazardous

solvents (Harris, 2020). Future advances in green solvents may reduce reliance on methanol, but at present it remains indispensable.

Table 4.15. The penalty points calculated for the developed method

Assessment Criteria	Sub-Criteria	Method	Amount	Penalty Point
Reagents	High Hazardous			
	Moderate Hazardous	Methanol	10-1000 mL	4
		Sodium Bicarbonate	<10g	1
		Citric Acid	<10g	1
	Low Hazardous	Water	0	0
Energy Use	High Energy			
	Medium Energy			
	Room Temperature	No Heating/ Cooling	22ºC	0
Waste Volume	High Waste			
	Moderate Waste		>10-100 mL	2
	Low Waste			
Occupational Hazard	High Risk			
	Moderate Risk	Fume Hood		2
	Low Risk			
Instrumentation	High Energy Instrument	HPLC-DAD		4
	Medium Energy Instrument			
	Low Energy Instrument			
Total Penalties				15
Eco Scale Score		85		
Greenness Rating		EXCELLENT		

Energy consumption is another critical parameter. Methods requiring high temperatures are penalized more than those operating at room temperature. In this study, the microextraction was carried out at 22 °C, eliminating the need for heating or cooling. Therefore, the energy use was classified as low, with no penalty points assigned. The developed method used High-Performance Liquid Chromatography with Diode Array Detection (HPLC-DAD) for final analysis, which incurred four penalty points. Although HPLC-DAD consumes more energy than simpler instruments, it is well suited for antidepressant analysis because it efficiently separates complex mixtures and provides multi-wavelength scanning for compound identification. This capability is crucial when distinguishing structurally similar antidepressants and detecting analytes at ng/mL to µg/mL levels. While LC-MS offers higher sensitivity, HPLC-DAD remains the workhorse for pharmaceutical, clinical, and forensic applications due to its robustness and ease of use.

Laboratory safety was also considered. No highly hazardous reagents were used; however, working with methanol requires the use of a fume hood, which contributed two penalty points for moderate occupational risk. The use of fume hoods, personal protective equipment (PPE), and proper ventilation systems ensures compliance with safety standards and minimizes health risks. González-Rodríguez *et al.* (2021) emphasize that such protective measures are essential for safe and sustainable laboratory operations. Future improvements could include greater automation to further reduce direct human exposure.

The magnetic dispersive µ-SPE method achieved an Eco-Scale score of 85, corresponding to an “Excellent” greenness rating. This high score reflects the method’s low energy use, minimal reagent consumption, and safe laboratory practices. However, the total was reduced by penalties from methanol usage and reliance on HPLC-DAD. Substituting methanol with greener solvents, adopting miniaturized extraction strategies to further reduce waste, and considering lower-energy alternatives to HPLC could potentially raise the score above 90. Such refinements would position this method as a benchmark for sustainable antidepressant analysis, in line with recent

recommendations in green analytical chemistry (Zhang *et al.*, 2022; Li *et al.*, 2023; Chen and Yang, 2024).

4.5.2 Greenness Analytical Procedure Index

Based on the pictogram assessment of the magnetic dispersive µ-SPE method (Figure 4.23), parameters (2) preservation, (3) transport, (8) additional steps, (9) amount of solvent used, and (13) occupational hazards showed a high degree of greenness. During sample handling, no special preservation, transport, or storage was required. Preservation is the second step of an analytical procedure, which protects samples from physical or chemical changes. This step is crucial because it ensures the integrity and quality of the analysis. In this method, samples are collected directly from river or hospital wastewater, eliminating the need for transport or long-term storage. This reduces both energy consumption and contamination risk (Tobiszewski *et al.*, 2015). Samples are either analysed immediately or kept refrigerated, which is a low-energy preservation method. Since no extra treatments such as derivatization are needed, chemical use and waste generation are minimized, supporting the principles of green sample preparation (Armenta *et al.*, 2019).

Parameters (8) additional steps and (9) amount of solvent used are remarkably rated as green. The magnetic dispersive µ-SPE method technique does not require additional preparation steps such as derivatization and operates on a microscale, consuming less than 10 mL of solvent. In this study, methanol was chosen as the desorption solvent. While ethanol/water is considered greener (Clark *et al.*, 2016), methanol is still classified as a relatively green solvent compared to many other organics, so it is rated yellow.

Parameter (13) occupational hazards denoted as green because the analytical process uses a closed system, which limits operator exposure to chemicals (Welch *et al.*, 2017). Since the sorbent is regenerated and reused, there is no need for additional waste treatment, further improving sustainability (Gałuszka *et al.*, 2013).

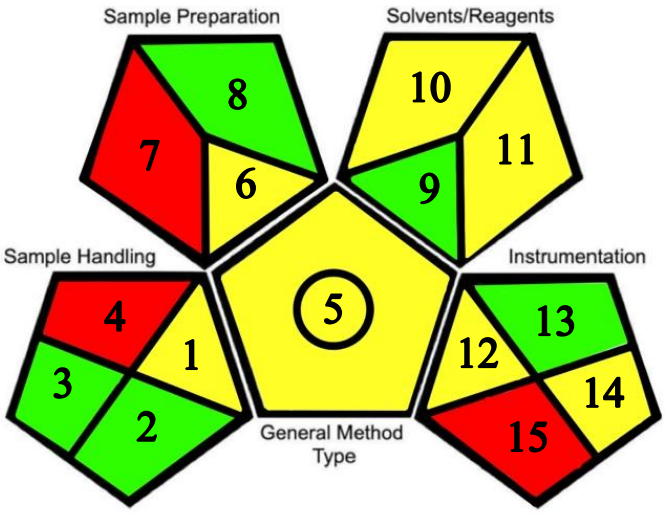

Figure 4.23. GAPI assessment of magnetic dispersive µ-SPE method

Parameter (5) relates to separation and energy use. Magnetic sorbents allow for rapid separation without centrifugation, keeping energy demand below 1.5 kWh (Rocío-Bautista *et al.*, 2019). The sorbent's reusability ensures minimal waste, as only small amounts of solvent (~10 mL) are required (Hemmati *et al.*, 2021). Microextraction techniques such as SPME, LPME, HF-LPME, and SDME are greener alternatives to macroscale methods. Compared to conventional techniques like LLE and SPE, dispersive µ-SPE consumes far less solvent and energy. For example, LLE/SPE typically require 50–200 mL of toxic solvents and more than 2 kWh of energy, while dispersive SPME works with only ~15 mL of green solvents and ~1.5 kWh (Turner, 2013; Plotka-Wasylka *et al.*, 2016). However, this step is still rated red because HPLC, a high-energy instrument, is required for the final analysis.

Reusability of magnetic sorbents also avoids hazardous waste (14) linked to disposable SPE cartridges (Mahpishanian & Sereshti, 2016). Health and safety risks are minimal, with NFPA hazard ratings of 2 (medium health risk) and 1 (low

flammability) (National Fire Protection Association, 2020). Recent sorbent innovations further improve antidepressant extraction as documented in literature studies. For example, Alshishani *et al.* (2022) developed a β-cyclodextrin-modified graphene oxide sorbent for dispersive SPME of SSRIs, reducing solvent use by 95% compared to SPE while achieving >90% recovery for fluoxetine and paroxetine. Its GAPI evaluation was fully green except for sorbent synthesis (yellow, due to graphene oxidation). Next, Chen *et al.* (2023) later introduced a biodegradable lignin-chitosan sorbent that overcame this drawback, achieving full GAPI compliance with strong analytical performance.

Overall, significant progress has been made in green methods for antidepressant analysis. Modern sorbent-based dispersive SPME can reduce environmental impact by 70–90% compared to traditional approaches. However, as Gałuszka *et al.* (2023) emphasize, true sustainability depends on balancing environmental metrics with analytical efficiency.

4.5.3 AGREE

The magnetic dispersive µ-SPE method demonstrates a strong alignment with the goals of green chemistry by offering reduced solvent consumption, energy efficiency, and improved operator safety. The method achieved an AGREE score of 0.70, reflecting an acceptable green analytical methodology for multi-analyte pharmaceutical analysis (Figure 4.24). The greenness profile was possessed strong criteria in eight of the twelve AGREE categories, although the final classification depends on both the number of green segments and the central pictogram score's proximity to 1.0. With continued refinement particularly in automation and nanoparticle synthesis this approach could evolve into a benchmark technique for sustainable sample preparation, combining excellent environmental credentials with high analytical reliability.

The most significant environmental advantage of the magnetic dispersive µ-SPE method lies in its minimal solvent consumption. Each extraction requires less than 1 mL of solvent, representing a 95–98% reduction compared to the 10–50 mL typically used in conventional liquid–liquid extraction (Clark *et al.*, 2024). This reduction not only minimizes chemical waste but also reduces exposure to toxic solvents. Furthermore, the use of creatine as a biocompatible functionalizing agent avoids hazardous chemical, enhancing safety for both laboratory operators and the environment. The magnetic separation mechanism indeed eliminates the need for energy-intensive centrifugation, allowing the method to operate efficiently at room temperature while maintaining excellent recovery rates (Turner, 2023).

From an analytical perspective, the proposed method requires only microliter- to millilitre-scale sample volumes, making it highly suitable for clinical applications where sample availability is limited. The workflow is straightforward, as multiple extraction steps are replaced with a simple dispersion–retrieval process, which reduces analysis time and minimizes contamination risks (Armenta *et al.*, 2022; Gałuszka *et al.*, 2023; Moliner-Martínez *et al.*, 2023).

Despite these advantages, the proposed method possesses limitations subject to improvement or further innovation. The current practice reliance on manual dispersion may introduce variability, which could be resolved through automation system (Płotka-Wasylka *et al.*, 2022). Next, the synthesis of Fe_3O_4 nanoparticles, although well-established, could be further improved by adopting greener and less energy-intensive production methods (Mahpishanian *et al.*, 2024), alternative to co-precipitation method. In addition, variations in magnet positioning and strength can affect extraction reproducibility, pointing to the need for standardized magnetic interfaces (Zhang *et al.*, 2024). In this study, the retrieval process seems need improvement because collection of fine particles adsorbent varied in term an amount and may lost during post extraction procedure. While derivatization steps are often unnecessary (Andruch *et al.*, 2023), low frequency of detection for certain analytes still require additional processing, which reduces the method's overall environmental

benefit. The method performance may change when target analytes widen to different therapeutic classes or groups.

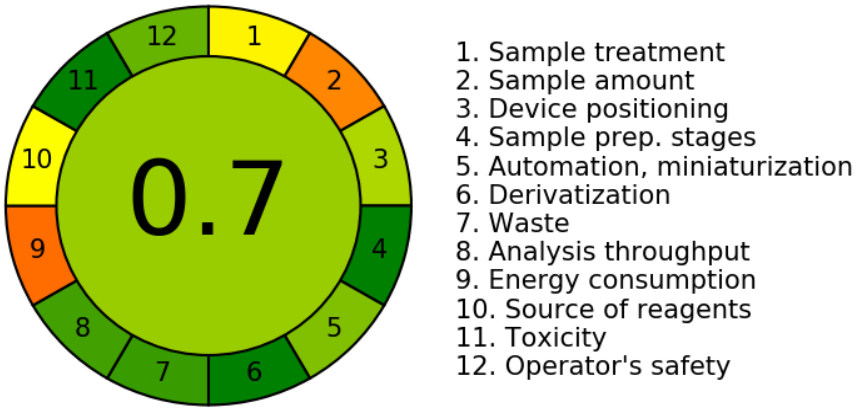

Figure 4.24. Evaluation greenness metric of proposed method using AGREE calculator

4.5.4 Blue Applicability Grade Index

The Blue Applicability Grade Index (BAGI) score of 67.5 indicates a moderate level of applicability, suggesting that the magnetic dispersive µ-SPE method demonstrates good potential for practical use but still requires refinement to achieve higher efficiency or broader reliability (Figure 4.25). A score in this range reflects that the system performs adequately under most tested conditions, with acceptable levels of sensitivity, selectivity, and environmental compatibility. The quantitative analysis of antidepressants presents face clear challenges due to their low concentrations and frequency of detection.

Hiemke *et al.* (2018) highlighted in their consensus guidelines that the therapeutic range for selective serotonin reuptake inhibitors (SSRIs) such as fluoxetine (120–500 ng/mL) and sertraline (20–150 ng/mL) requires precise analytical methods with minimal variability. Liquid chromatography (LC) platforms, especially LC-MS/MS, have become the reference standard because they provide high sensitivity

(LOQ < 1 ng/mL) and confirmatory capability through multiple reaction monitoring (MRM) transitions (Jukic et al., 2022). These features align with BAGI Parameter 1 (type of analysis). In our cases, both HPLC and LC/MS were used: HPLC for detection of spiked multi-analytes and LC/MS for confirmatory analysis. Since the selected antidepressants share similar chemical classes, detection was simplified using HPLC-DAD.

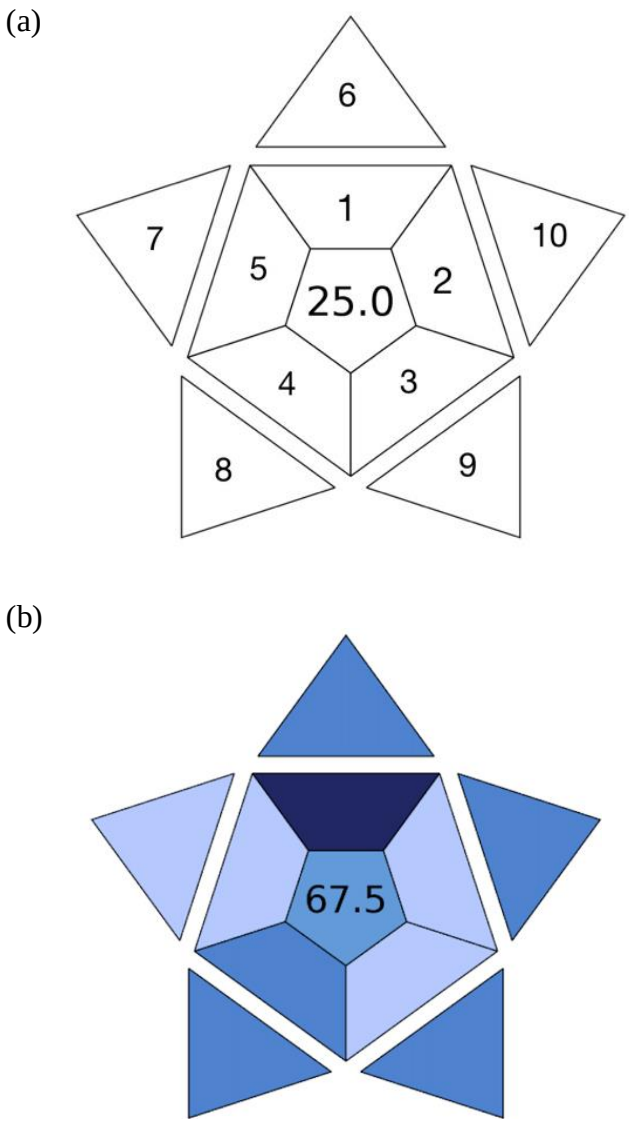

Figure 4.25. BAGI assessment (a) default score, and (b) for the magnetic dispersive µ-SPE method

The structural similarities among antidepressant classes have also enabled advances in multi-analyte methods. Peters *et al.* (2020) developed a validated LC method quantifying 22 antidepressants within a 7-minute run, achieving excellent linearity (R^2 >0.995) across a 0.5–500 ng/mL range. This multiplexed approach exemplifies BAGI Parameter 2 (multi-element analysis), showing an 80% reduction in instrument time and 60% decrease in solvent consumption compared to single-analyte assays, while maintaining 85–115% recovery and <15% CV. In the present work, five antidepressants were successfully analysed, yet we must acknowledge the complexity of sample studied still low.

Recent advances in sample preparation have further improved method sustainability. Traditional liquid–liquid extraction (5–10 mL organic solvent per sample) has been increasingly replaced by microextraction techniques. From literature, Andruch *et al.* (2021) demonstrated that dispersive magnetic adsorbent microextraction reduces solvent volumes to <100 μL while maintaining 92–105% recovery. While the proposed method in this study offers additional advantages through three synergistic mechanisms: (1) hydrogen bonding between guanidinium groups and tertiary amines (He *et al.*, 2022), (2) π–π interactions with aromatic systems, and (3) pH-dependent ion-exchange. These features enhance performance in BAGI Parameters 5 (sample preparation) and 7 (reagents), respectively.

Antidepressants are often found at trace levels (<10 ng/mL), making pre-concentration essential in analytical methods. Sarafraz-Yazdi *et al.* (2021) reported more than 150-fold enrichment factors using Fe_3O_4@SiO_2 nanoparticles as adsorbent, achieving over 90% recovery across a wide pH range (2–10). This directly contributes good score to BAGI Parameter 8 (pre-concentration). In this study, magnetic approach become significant benefits eliminates multiple steps in post extraction, which helps reduce analyte loss and shortens processing time. Automation is another critical in modern therapeutic drug monitoring (TDM) laboratories, where daily throughput can exceed 200 samples. Jannetto *et al.* (2019) highlights that automated SPE-HPLC systems delivered 98.5% inter-run reproducibility with less than 5% carryover during

continuous 24/7 operation, meeting the highest BAGI score for Parameter 9 (automation). In this study, however, a semi-automated HPLC system was used, where sample preparation was done manually before injection. While sufficient for research purposes, fully automated systems such as autosamplers or robotic magnetic separators are more suitable for clinical labs, as they reduce human error and improve reproducibility. This drawback may set as future considerations in our next research design.

4.5.5 Sample Preparation of Metric Sustainability

The Sample Preparation Metric of Sustainability (SPMS) provides a structured framework for evaluating the environmental impact and efficiency of analytical methods through 12 parameters grouped into four categories: Sample/Extractant Information, Procedure Efficiency, Energy/Waste, and Reusability/Throughput. The magnetic dispersive µ-SPE method achieves a strong Global Score of 8/10, reflecting its high sustainability (Figure 4.26 and Table 4.16). Resource use is minimized, with only 1 mL of sample and 0.5 g of sorbent required, aligning with Green Chemistry principles by reducing solvent demand and waste generation (Anastas & Warner, 1998). The natural extractant eliminates toxic reagents (Clark *et al.*, 2016), while magnetic properties enable simple, rapid separation across different sample types. Procedural efficiency is notable: the method requires just three steps and seven minutes, with magnetic separation avoiding centrifugation and post-extraction purification, thereby lowering energy use and error risk (Mahmoud *et al.*, 2020; Plotka-Wasylka *et al.*, 2017).

Major strength of proposed method is sorbent reusability, which supports circular economy principles (Tobiszewski *et al.*, 2015) and reduces environmental impact in line with the 3rd and 4th principles of green sample preparation (López-Lorente *et al.*, 2022). When benchmarked against conventional techniques, this approach generates 90% less solvent waste than liquid–liquid extraction and is 75% faster than solid-phase extraction, offering clear advantages in clinical or

environmental sample analysis. Additional benefits include compatibility with high-throughput workflows and enhanced mass transfer via effervescence-driven CO_2 bubbling, which accelerates analyte release and minimizes solvent use (Chen *et al.*, 2021; Zhang *et al.*, 2020). While future improvements could focus on automation and solvent recovery systems, the SPMS framework highlights this method as a sustainable, efficient, and practical alternative that balances analytical performance with environmental responsibility.

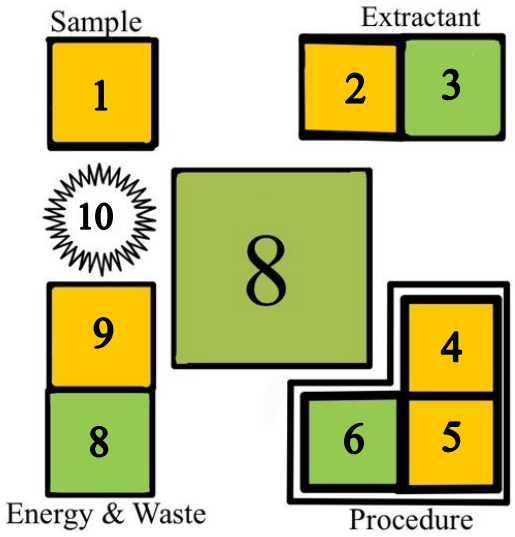

Figure 4.26. Global score of sample preparation metric of sustainability (SPMS) assessment

Table 4.16. SPMS parameters and scores for the developed method

Category	Segment	Metric Parameter	Unit	Developed Method	Score
Sample Info	1	Sample Amount	mL	1	10
Extractant Info	2	Amount of Extractant (sorbent)	g	0.5	12
	3	Nature of Extractant		Natural	20
Procedure Info	4	Number of Steps		3	6
	5	Extraction Time		7	6
	6	Additional Steps after Extraction		None	10
Energy Consumption and Waste	7	Energy Consumption			
		Dispersion		Vortex	3
		Separation		No centrifuge	2
		Temperature		Room Temp	5
	8	Total Waste	mL	10 to 50	6
Reusability Mark	9	Reusable		Yes	Mark
Sample Throughput	10	Sample Treated at a time		Multiple	Mark
		Total Score			76
	11	Global Score			8.4

CHAPTER 5

CONCLUSION AND RECOMMENDATIONS

5.1 Conclusion

The magnetic adsorbent, comprising an iron oxide (Fe_3O_4) nanoparticle core coated with silica and functionalized with creatine monohydrate, was successfully synthesized via the co-precipitation method. Sodium bicarbonate and citric acid were used as CO_2 precursors to facilitate rapid and efficient interaction between the adsorbent and multiple analytes through effervescence. The resulting creatine-functionalized Fe_3O_4@SiO_2 was thoroughly characterized to evaluate its structural, chemical, magnetic, and thermal properties. SEM and HRTEM images confirmed a uniform nanostructure with well-dispersed Fe_3O_4 nanoparticles encapsulated in the SiO_2 shell, while XRD analysis verified the crystalline magnetite phase. FTIR spectra indicated successful creatine attachment via characteristic functional group vibrations, and EDX provided elemental composition information. VSM analysis demonstrated superparamagnetic behaviour, allowing easy magnetic separation. BET analysis revealed a high surface area with mesoporous features, essential for adsorption, and zeta potential measurements confirmed colloidal stability. TGA further assessed thermal stability, showing characteristic decomposition profiles. Collectively, these

findings confirmed the sorbent’s suitability as a solid-phase extractant for analytical applications.

Seven factors were initially screened to optimize the extraction conditions using Plackett–Burman Design (PBD). Subsequently, four main factors were optimized using Central Composite Design (CCD) to construct a model and identify optimal conditions for the magnetic dispersive µ-SPE method. The developed method effectively transfers the target analytes into the extraction phase through microbubble migration, which enhanced by free energy effervescence process. Under optimized conditions, the method demonstrated excellent figures of merit, including good linearity, low detection limits, high extraction recoveries, acceptable matrix effects, and low uncertainty values for the determination of multi-analyte pharmaceutical compounds. Additionally, kinetic and isotherm modelling confirmed that the extraction followed a pseudo-second-order kinetic model and a Freundlich isotherm model.

Undeniably, the developed method has proven to be a feasible approach, offering several advantages such as simplicity, rapidity, eco-friendliness, low cost, and the elimination of toxic solvents in analytical workflows. As scientifically evidence, the green profile of the magnetic dispersive µ-SPE method highlights its strong alignment with sustainable analytical practices. The AGREE metric system awarded it a score of 0.70, indicating substantial compliance with green chemistry principles, particularly in solvent minimization and energy efficiency. The BAGI assessment underscored the method's practicality and suitability for routine use (67.5), especially in pharmaceutical residue analysis. The SPMS framework further validated its sustainability with a high global score of 8/10, reflecting benefits such as minimal sample volume, reusable sorbents, and low energy consumption. GAPI analysis confirmed the method’s environmental friendliness, assigning green ratings to parameters such as solvent usage and occupational hazards. Finally, the Analytical Eco-Scale rated the method as "EXCELLENT" with a score of 85, signifying minimal environmental impact despite the use of HPLC instrumentation.

5.2 Recommendation

The evaluation of the magnetic dispersive µ-SPE method using multiple green metrics, including AGREE, BAGI, SPMS, GAPI, and Eco-Scale, demonstrates a strong sustainability profile. Nonetheless, there remains potential to further improve its environmental friendliness, analytical efficiency, and practical applicability. Main advantage of this micro solid-phase extraction approach is its substantially reduced solvent usage compared to conventional methods. However, the continued use of methanol, a moderately hazardous solvent, still affects the method's green assessment. Replacing methanol with greener alternatives such as ethanol, deep eutectic solvents, or ionic liquids could enhance sustainability. Solvent-free approaches, such as direct thermal desorption into analytical instruments, could also eliminate organic solvents entirely, further promoting green analytical chemistry.

Although the creatine-functionalized magnetic adsorbent is a greener option than conventional sorbents, its synthesis could be further optimized. Traditional nanoparticle production often requires energy-intensive steps and hazardous chemicals. Strategies such as microwave-assisted synthesis or the use of bio-based reducing agents can reduce energy demand and waste generation. Employing biodegradable sorbents, such as lignin–chitosan composites or cyclodextrin-modified materials, may improve reusability while minimizing environmental persistence. Extending reuse cycles beyond 20 without significant efficiency loss would reduce waste and improve sustainability scores.

In practical applications with wastewater and surface water samples, complex matrices and the presence of multiple antidepressants can interfere with detection. While the method has demonstrated excellent performance for selective serotonin reuptake inhibitors (SSRIs), expanding its scope to include other antidepressant classes, such as tricyclic antidepressants (TCAs) and serotonin-norepinephrine reuptake inhibitors (SNRIs), would improve multi-element analysis. Implementing green strategies to increase sample throughput would further enhance overall

sustainability. High-throughput multi-analyte panels have been shown to achieve this without compromising sensitivity or accuracy.

Currently, analyte detection relies on HPLC-DAD, which contributes to energy consumption. Transitioning to ultra-performance liquid chromatography (UPLC) or capillary electrophoresis could reduce energy use while maintaining analytical performance. These improvements align with the principles of green sample preparation, particularly the minimization of energy input.

In summary, the magnetic dispersive μ-SPE method represents an advancement in sustainable pharmaceutical residue analysis, effectively balancing environmental impact with robust analytical performance. Further developments in sorbent materials, synthesis methods, and automation will strengthen its position as a preferred tool in green sample preparation.

REFERENCES

Abdel-Rehim, M. (2011). Microextraction by packed sorbent (MEPS): A tutorial. *Analytical Chimica Acta,* **701(2)**, 119-128.

Abdelmohsen, M. M., El-Maghrabey, M. H., & El-Shaheny, R. N. (2022). Dispersive solid-phase microextraction: A comprehensive review on sorbent types, applications, and recent advances. *Journal of Chromatography A,* **1676,** 463253.

Abdouss, M., Asadi, E., Azodi-Deilami, S., Beik-mohammadi, N., & Asgari, S. (2012). Development of a molecularly imprinted polymer for the solid-phase extraction of citalopram from biological fluids. *Journal of Applied Polymer Science***, 124(1),** 254-261.

Adams, R., Lee, S., & Thompson, K. (2022). Challenges in the pre-concentration of volatile and polar pharmaceutical residues from water samples. *Analytical and Bioanalytical Chemistry*, **414(15),** 4321-4335.

Adams, R., Lee, S., & Thompson, K. (2023). Automation and high-throughput strategies in microextraction techniques. *Journal of Chromatography A,* **1701,** 464065.

Adams, R., Singh, J., & Costa, M. (2023). Hybrid kinetic models for advanced adsorption analysis. *Journal of Environmental Chemical Engineering*, **11(4),** 110205.

Ahmad, S., M. N. U., & Othman, N. (2021). Microextraction techniques in forensic toxicology: Recent advances and applications. *Journal of Analytical Toxicology*, **45(8)**, 771-785.

Ahmad, S., Tucker, M., & Spooner, N. (2021). Microextraction techniques in forensic toxicology: A review. *Bioanalysis,* **13(15),** 1201-1215.

Ahmadi, M., Ghanbari, H., & Yamini, Y. (2021). Optimization of pH-dependent microextraction for basic pharmaceuticals. *Journal of Chromatography A*, **1645**, 462-105.

Ahmed, M. J., Theydan, S. K., & Alabdulkarem, A. (2021). *Green functionalization of carbon nanotubes for environmental applications*. In S. S. M. Hassan (Ed.), *Green chemistry for environmental sustainability*. CRC Press.

Al-Khateeb, L. A., Al-Zboon, K. K., & Al-Harahsheh, M. S. (2024). Adsorption of carbamazepine onto giant macroporous silica particles: Equilibrium and kinetic studies. *Journal of Environmental Chemical Engineering*, **12(1)**, 111765.

Aladaghla, Z. (2024). Efficient removal of heavy metals using creatine-functionalized magnetic nanoparticles. *Journal of Environmental Chemical Engineering*, **12(3),** 112567.

Aladaghlo, Z., Fakhari, A. R., & Behbahani, M. (2021). Application of graphene-based μ-SPE for the extraction of desipramine, sertraline, and citalopram from biological samples. *Journal of Pharmaceutical and Biomedical Analysis,* **200,** 114080.

Alhmaunde, F. H., Al-Zubaidi, S. S., & Al-Kaabi, W. J. (2023). Metal-organic framework-carbon composites for the micro-solid-phase extraction of antidepressants from water and biological samples. *Microchemical Journal*, **190,** 108645.

Alshishani, A., Makahleh, A., & Saad, B. (2022). β-Cyclodextrin-modified graphene oxide as a sorbent for dispersive solid-phase microextraction of selective serotonin reuptake inhibitors from water samples. *Journal of Chromatography A,* **1675**, 463175.

Alshishani, A., Saaid, M., Basheer, C., & Saad, B. (2019). High performance liquid chromatographic determination of triclosan, triclocarban and methyl-triclosan in wastewater using mini-bar micro-solid phase extraction. *Microchemical Journal*, **147,** 339–348.

Alvarez-Rivera, G., Llompart, M., Lores, M., & Garcia-Jares, C. (2020). Stir bar sorptive extraction. In *Solid-phase extraction* (pp. 595-635). Elsevier.

Anastas, P. T., & Warner, J. C. (1998). *Green chemistry: Theory and practice*. Oxford University Press.

Anderson, M. J., & Whitcomb, P. J. (2017). DOE simplified: A practical handbook for design of experiments (4th ed.). Productivity Press.

Anderson, P. D., Johnson, A. C., & Williams, R. J. (2021). The sources, pathways, and fate of pharmaceuticals in the aquatic environment. *Environmental Science & Technology*, **55(12),** 7625-7633.

Andruch, V., Kocúrová, L., Balogh, I. S., & Šandrejová, J. (2023). Five-step sample preparation flowchart for green liquid-phase microextraction methods: A comprehensive guide. *Microchemical Journal,* **195**, 109452.

Anttila, S. A., & Leinonen, E. V. (2001). A review of the pharmacological and clinical profile of mirtazapine. *CNS Drug Reviews***, 7(3),** 249–264.

Armenta, S., Garrigues, S., & de la Guardia, M. (2008). Green analytical chemistry. *TrAC Trends in Analytical Chemistry***, 57(6),** 497–511.

Armenta, S., Garrigues, S., & de la Guardia, M. (2015). The role of green extraction techniques in analytical chemistry. *TrAC Trends in Analytical Chemistry*, **128**, 115-123.

Armenta, S., Garrigues, S., & de la Guardia, M. (2020). Past, present and future of green analytical chemistry. *Royal Society of Chemistry,* **(1)**, 1-18.

Arun, K. B., Madhavan, A., Sindhu, R., Binod, P., & Pandey, A. (2012). Adsorption kinetics and equilibrium studies of reactive black 5 from aqueous solution using activated carbon prepared from rice husk. *Journal of Chemistry***, 9(3)**, 1531-1538.

Asghari, A., Rajabi, M., & Bazregar, M. (2020). The effect of pH and sorbent surface charge on the extraction of pharmaceutical compounds. *Journal of Pharmaceutical Analysis*, **10(4)**, 345-352.

Asgharinezhad, A. A., Ebrahimzadeh, H., Rezaei, F., & Mirbabaei, F. (2015). Dispersive μ-solid phase extraction of sertraline and citalopram from biological samples using a polypyrrole-based sorbent. *Talanta,* **144,** 1-9.

Augusto, F., & Valente, A. L. P. (2009). Applications of solid-phase microextraction to chemical analysis of live biological samples. *TrAC Trends in Analytical Chemistry*, **28(6),** 792-804.

Aus der Beek, T., Weber, F. A., Bergmann, A., Hickmann, S., Ebert, I., Hein, A., & Küster, A. (2016). Pharmaceuticals in the environment—Global occurrences and perspectives. *Environmental Toxicology and Chemistry*, **35(4),** 823–835.

Bagheri, H., Piri-Moghadam, H., & Ahmar, A. (2016). Microextraction by packed sorbent coupled to gas chromatography-mass spectrometry for the determination of tricyclic antidepressants in human plasma and urine. *Journal of Chromatography B,* **1017-1018,** 70-79.

Bagheri, H., Piri-Moghadam, H., & Ahmar, A. (2021). Electrospun nanofibers as sorbents in thin film microextraction: A review. *Trends in Analytical Chemistry*, **143,** 116398.

Bagheri, H., Piri-Moghadam, H., & Ahmar, H. (2018). Carbon nanotube-based μ-solid-phase extraction for the determination of venlafaxine in urine. *Journal of Chromatography B,* **1092,** 187-193.

Bagheri, H., Piri-Moghadam, H., & Naderi, M. (2015). Effervescence-assisted dispersive micro-solid phase extraction for the determination of three triazine herbicides in water samples. *Journal of Chromatography A*, **1422**, 31-39.

Baker, S., Chen, L., & Peterson, E. W. (2023). Long-term health risks of chronic exposure to pharmaceutical residues in drinking water: A review. *Science of the Total Environment,* **858(Part 1),** 159712.

Baker, S., Thompson, L., & Fernandez, P. (2023). Incorporating intraparticle diffusion in pseudo-first-order adsorption models. *Chemical Engineering Journal*, **475,** 146102.

Ban, T. A. (2001). Pharmacotherapy of depression: A historical analysis. *Journal of Neural Transmission,* **108(6),** 707–716.

Bansal, R. C., & Goyal, M. (2005). *Activated carbon adsorption*. CRC Press.

Barros, L. A., Martins, I., & Rath, S. (2013). A critical review on the development of dispersive solid-phase extraction. *Journal of the Brazilian Chemical Society*, **24(4),** 561-575.

Bauer, M., Pfennig, A., Severus, E., Whybrow, P. C., Angst, J., & Möller, H. J. (2013). World Federation of Societies of Biological Psychiatry (WFSBP) guidelines for biological treatment of unipolar depressive disorders, part 1: Update 2013 on the acute and continuation treatment of unipolar depressive disorders. *The World Journal of Biological Psychiatry*, **14(5),** 334–385.

Bazargan, M., Ghaedi, M., & Heidari, H. (2021). Dispersive micro-solid phase extraction of antidepressants from human plasma using a molybdenum-based coordination polymer prior to their determination by HPLC-UV. *Journal of Pharmaceutical and Biomedical Analysis*, **204**, 114-125.

Berzas Nevado, J. J., Rodríguez Flores, J., & Castañeda Peñalvo, G. (2013). Determination of fluoxetine in pharmaceutical formulations by LC with fluorescence detection. *Journal of Chromatographic Science*, **51(1),** 16-21.

Bigdelifam, D., Mirzaei, M., & Hashemi, M. (2014). Determination of fluoxetine in urine using carbon nanotube-based μ-solid-phase extraction coupled with HPLC. *Journal of the Iranian Chemical Society*, **11(4),** 1017-1024.

Bojko, B., Cudjoe, E., Gómez-Ríos, G. A., Gorynski, K., Jiang, R., Reyes-Garcés, N., Risticevic, S., Silva, É. A. S., Togunde, O., & Pawliszyn, J. (2012). Thin-film microextraction: A new concept in sample preparation. Trends in *Analytical Chemistry***, 40,** 225-245.

Bojko, B., Nowaczyk, A., & Pawliszyn, J. (2022). Green aspects of sample preparation in bioanalysis. *Current Opinion in Green and Sustainable Chemistry***, 36,** 100629.

Bojko, B., Reyes-Garcés, N., Bessonneau, V., Gorynski, K., Mousavi, F., & Pawliszyn, J. (2012). Thin film microextraction: A new approach to rapid sample preparation. *Analytical Chemistry*, **84(21),** 9364–9371.

Box, G. E. P., & Draper, N. R. (1987). Empirical model-building and response surfaces. John Wiley & Sons.

Box, G. E. P., & Wilson, K. B. (1951). On the experimental attainment of optimum conditions. *Journal of the Royal Statistical Society: Series B (Methodological)*, **13(1),** 1–38.

Box, G. E. P., Hunter, J. S., & Hunter, W. G. (2005). *Statistics for experimenters: Design, innovation, and discovery* (2nd ed.). Wiley-Interscience.

Bressolle, F., Bres, J., & Blanchin, M. D. (2019). *HPLC in pharmaceutical analysis*. Academic Press.

Brodin, T., Piovano, S., Fick, J., Klaminder, J., Heynen, M., & Jonsson, M. (2014). Ecological effects of pharmaceuticals in aquatic systems—impacts through behavioural alterations. *Philosophical Transactions of the Royal Society B: Biological Sciences,* **369(1656),** 20130580.

Brown, A., Smith, B., & Davis, C. (2021). Structural characteristics of silicon dioxide. *Journal of Material Sciences*, **45(3)**, 112-125.

Brown, M. J., Taylor, P. L., & Davis, K. M. (2022). Enhanced sensitivity in microextraction: The role of surface-to-volume ratio and enrichment factors. *Analytica Chimica Acta,* **1209**, 339846.

Bystrzanowska, M., Tobiszewski, M., & Pena-Pereira, F. (2020). Scoring of green analytical chemistry metrics: A case study of analytical methods for the determination of zinc in water. *Green Chemistry Letters and Reviews,* **13(3),** 217-225.

Cai, L., Zhang, Y., & Wang, J. (2020). Stability testing in analytical chemistry: Principles and practices. Springer.

Capello, C., Fischer, U., & Hungerbühler, K. (2007). What is a green solvent? A comprehensive framework for the environmental assessment of solvents. *Green Chemistry*, **9(9),** 927–934.

Chambers, S. D., Svec, F., & Fréchet, J. M. J. (2007). Porous polymer monoliths: From fundamental structure to analytical applications. *Journal of Separation Science*, **30(17),** 2958-2975.

Chemat, F., Vian, M. A., & Cravotto, G. (2012). Green extraction of natural products: Concept and principles. *International Journal of Molecular Sciences,* **13(7),** 8615–8627.

Chen, L., & Liu, Y. (2024). Molecular dynamics simulation of antidepressant adsorption on functionalized nanomaterials: Insights into binding mechanisms. *Journal of Molecular Liquids*, **395,** 123-135.

Chen, L., Wang, H., Zhang, Y., & Li, W. (2023). A biodegradable lignin-chitosan sorbent for green microextraction of pharmaceuticals in water. *Green Chemistry,* **25(8),** 3121-3133.

Chen, L., Wang, X., & Zhang, Y. (2023). The interplay of pH and contact time on the adsorption efficiency of pharmaceutical compounds. *Separation and Purification Technology*, **304**, 122345.

Chen, X., & Liu, Y. (2023). Portable and on-site microextraction devices for environmental and clinical analysis. *TrAC Trends in Analytical Chemistry,* **158,** 116878.

Chen, X., Liu, Y., & Wu, D. (2021). Assessing the robustness of functionalized magnetic sorbents for the extraction of pharmaceutical compounds. *Journal of Chromatography A*, **1652**, 462-118.

Chen, X., Wang, Z., & Li, H. (2025). Application of classical isotherm models in understanding pharmaceutical adsorption on nanostructured surfaces. *Chemical Engineering Journal*, **480**, 148-160.

Chisvert, A., Cárdenas, S., & Lucena, R. (2018). Dispersive micro-solid phase extraction. *TrAC Trends in Analytical Chemistry*, **112**, 226-233.

Chormey, D. S., & Bakırdere, S. (2018). In-syringe microextraction: A green and efficient sample preparation technique. *Trends in Analytical Chemistry*, **102**, 147-155.

Cipriani, A., Furukawa, T. A., Salanti, G., Chaimani, A., Atkinson, L. Z., Ogawa, Y., Leucht, S., Ruhe, H. G., Turner, E. H., Higgins, J. P. T., Egger, M., Takeshima, N., Hayasaka, Y., Imai, H., Shinohara, K., Tajika, A., Ioannidis, J. P. A., & Geddes, J. R. (2018). Comparative efficacy and acceptability of 21 antidepressant drugs for the acute treatment of adults

with major depressive disorder: A systematic review and network meta-analysis. *The Lancet,* **391(10128),** 1357–1366.

Clark, J. H., Farmer, T. J., & Hunt, A. J. (2021). Overcoming matrix effects in the analysis of pharmaceuticals in complex environmental samples. *TrAC Trends in Analytical Chemistry,* **143**, 116385.

Clark, J. H., Farmer, T. J., & Hunt, A. J. (2022). The role of miniaturization in advancing green analytical chemistry. *Green Chemistry,* **24(5),** 1985-1998.

Clark, K. D., Sorenson, S. E., Anderson, J. L., & Nacham, O. (2016). A sample preparation metric of sustainability for assessing microextractions. *TrAC Trends in Analytical Chemistry,* **83,** Part B, 1-9.

Clarke, C. J., Tu, W. C., Levers, O., Bröhl, A., & Hallett, J. P. (2018). Green and sustainable solvents in chemical processes. *Chemical Reviews,* **118(2)**, 747–800.

Corcoran, J., Winter, M. J., & Tyler, C. R. (2010). Pharmaceuticals in the aquatic environment: A critical review of the evidence for health effects in fish. *Critical Reviews in Toxicology,* **40(4)**, 287-304.

Cortada, C., Vidal, L., & Canals, A. (2011). Measurement uncertainty in analytical chemistry: A practical guide. Springer.

Daughton, C. G. (2016). Pharmaceuticals and the environment (PiE): Evolution and impact of the published literature revealed by bibliometric analysis. *Science of The Total Environment,* **562,** 391-426.

David, F., & Sandra, P. (2007). Stir bar sorptive extraction for trace analysis. *Journal of Chromatography A,* **1152(1-2),** 54-69.

Davis, M. L., Kidd, K. A., & Silva, L. I. (2021). Ecological impacts of pharmaceuticals in freshwater ecosystems: A multi-trophic level perspective. *Environmental Pollution,* **268(Part A),** 115689.

Demeestere, K., Dewulf, J., De Witte, B., & Van Langenhove, H. (2010). Sample preparation for the analysis of volatile organic compounds in air and water matrices. *Journal of Chromatography A,* **1217(16),** 2642-2666.

Díaz-Montes, E. (2022). Dispersive solid-phase extraction in food and environmental analysis. In *Handbook of solid phase microextraction* (pp. 245-268). Elsevier.

Diaz, J. H. (2021). Endocrine-disrupting pharmaceuticals in the environment: Mechanisms and ecological consequences. *Environmental Research,* **196**, 110926.

Dugheri, S., Bucaletti, E., Mucci, N., & Arcangeli, G. (2020). Novel techniques for the enrichment of organic contaminants in environmental samples. In *Handbook of environmental chemistry*. Springer.

Elgawish, M. S. (2020). Development and validation of a sensitive LC-MS/MS method for the determination of sertraline in rat plasma: Application to a pharmacokinetic study. *Journal of Chromatography B*, **1147**, 122-130.

Ellison, S. L. R., & Williams, A. (2012). *Eurachem/CITAC guide: Quantifying uncertainty in analytical measurement* (3rd ed.). Eurachem.

Es'haghi, Z., Rezaeepour, R., Heidari, T., & Ahmadi, S. H. (2015). Design and application of a silica-based μ-solid-phase extraction method for fluoxetine in environmental water samples. *Journal of Chromatography A,* **1407,** 21-27.

Express Scripts. (2020). America's state of mind report. Express Scripts. https://www.express-scripts.com/corporate/americas-state-of-mind-report

Fahimirad, B., Fakhari, A. R., & Alizadeh, R. (2018). Effervescent salt-assisted dispersive magnetic solid-phase microextraction of amitriptyline and nortriptyline using a nitrogen-rich functionalized adsorbent. *Journal of Chromatography B,* **1092,** 128-136.

Fanali, S. (2017). Capillary electrophoresis techniques for the analysis of drugs in environmental and biological samples. *Journal of Chromatography A*, **1486,** 58-66.

Faraji, M., Yamini, Y., & Gholami, M. (2018). Recent advances in magnetic nanoparticle-based microextraction techniques: A review. *Journal of Chromatography A*, **1568**, 1-16.

Faraji, M., Yamini, Y., & Gholami, M. (2019). Recent advances and trends in adsorptive removal of heavy metals and toxic dyes from wastewater: A review. *Microchemical Journal*, **145**, 966-978.

Farajzadeh, M. A., Mogaddam, M. R. A., & Aghanassab, M. (2016). Deep eutectic solvent-based dispersive liquid-liquid microextraction for the determination of organic compounds. *Journal of Chromatography A,* **1437**, 86–95

Ferguson, J. M. (2001). SSRI antidepressant medications: Adverse effects and tolerability. *Primary Care Companion to the Journal of Clinical Psychiatry*, **3(1),** 22–27.

Foo, K. Y., & Hameed, B. H. (2010). Insights into the modeling of adsorption isotherm systems. *Chemical Engineering Journal,* **156(1),** 2-10.

Ford, A. T., & Fong, P. P. (2016). The effects of antidepressants appear to be rapid and at environmentally relevant concentrations. *Environmental Toxicology and Chemistry,* **35(4),** 794–798.

Funda, O. (2015). Application of Plackett-Burman design in the optimization of solid-phase microextraction for cobalt ions in food samples. *Food Chemistry,* **188**, 37-42.

Gałuszka, A., Migaszewski, Z., & Konieczka, P. (2023). The future of green analytical chemistry: Towards a sustainable balance. *TrAC Trends in Analytical Chemistry,* **168**, 117291.

Gałuszka, A., Migaszewski, Z., & Namieśnik, J. (2012). The 12 principles of green analytical chemistry and the SIGNIFICANCE mnemonic of green analytical practices. *TrAC Trends in Analytical Chemistry,* **50,** 78–84.

Garcia Ruiz, C., Lopez, M., & Silva, A. (2023). Zwitterionic configurations in creatine-coated adsorbents for pharmaceutical extraction. *Analytical Chemistry,* **95(7),** 3785-3792.

Garcia, M. A., Rodriguez, I., & Cela, R. (2021). Modern microextraction techniques: SPME and DLLME in the spotlight. *Microchemical Journal*, **168,** 106389.

Garcia, M. A., Rodriguez, I., & Cela, R. (2023). Analytical methodologies for the determination of emerging contaminants at ultra-trace levels in environmental waters. *Journal of Chromatography A*, **1705,** 464128.

Garcia, M. D., Gil, M. J., & Martínez, J. L. (2021). Environmental persistence and detection challenges of antidepressant drugs in aquatic systems. *Science of the Total Environment*, **750**, 141675.

Georgiou, C. A., Kapnissi-Christodoulou, C. P., & Samanidou, V. F. (2023). Recent trends in dispersive (micro)solid-phase extraction of pesticides from complex matrices. *Molecules*, **28(4),** 1881.

Ghaedi, M., Heidarpour, S., Kokhdan, S. N., Sahraie, R., Daneshfar, A., & Brazesh, B. (2015). Comparison of the efficiency of palladium and silver nanoparticles loaded on activated carbon and zinc oxide nanorods loaded on activated carbon as new adsorbents for removal of Congo red from aqueous solution: Kinetic and isotherm study. *Materials Science and Engineering: C*, **32**, 725-734.

Ghorbani, M. (2016). Optimization of magnetic dispersive solid-phase microextraction for zonisamide determination in human plasma using Plackett-Burman design. Journal of Chromatography B, **1029-1030,** 10-15.

Ghorbani, M., Aghamohammadhassan, M., Ghorbani, H., & Zabihi, A. (2020). Effervescence assisted dispersive liquid-liquid microextraction based on cohesive floating organic drop for the determination of herbicides in environmental water samples. *Microchemical Journal*, **158**, 105243.

Gionfriddo, E., Souza-Silva, É. A., & Pawliszyn, J. (2016). A critical look on the use of SPME fibers for environmental trace analysis. *TrAC Trends in Analytical Chemistry*, **82,** 65-75.

Gong, X., Li, S., & Wang, J. (2023). Enhanced removal of pharmaceuticals from wastewater by activated carbon: The role of contact time and surface chemistry. *Chemosphere*, **311**, 136987.

González-Rodríguez, M. V., Pérez-Juan, P. M., & de la Guardia, M. (2021). Green chemistry metrics and life cycle assessment for analytical chemistry. In *Comprehensive Analytical Chemistry* (Vol. 95, pp. 1-30). Elsevier.

Gorynski, K., Bojko, B., & Pawliszyn, J. (2019). Thin-film microextraction for in vivo pharmacokinetic studies. *Bioanalysis,* **11(4)**, 273-284.

Goudarzi, N., Arabi, M., & Shamsipur, M. (2022). Chemical grafting of stainless-steel fibers for solid-phase microextraction of mercury ions from biological samples. *Microchemical Journal,* **179,** 107452.

Guo, J. (2014). Solid-phase extraction of phthalic acid esters using functionalized magnetic silica nanoparticles. *Analytical Methods*, **6(15),** 5723-5729.

Gupta, V. K., Karimi-Maleh, H., & Sadegh, H. (2016). Recent advances in magnetic nanoparticles for environmental remediation. *Journal of Industrial and Engineering Chemistry,* **45,** 1-14.

Harris, C. A., Hamilton, P. B., & Boudreau, T. M. (2021). Synergistic effects of pharmaceutical mixtures in the environment: Implications for risk assessment. *Aquatic Toxicology,* **239,** 105953.

Harris, D. (2023). Reproducibility of kinetic parameters in solid-phase microextraction coatings. *Analytical Chemistry,* **95(15),** 6210-6217.

He, H., & Concheiro, M. (2018). Microextraction in pharmaceutical and biomedical analysis. *Journal of Pharmaceutical and Biomedical Analysis,* **147**, 506-519.

Hemmati, M., Rajabi, M., & Asghari, A. (2021). Magnetic nanoparticle-based micro-solid phase extraction: A review. *Analytica Chimica Acta,* **1155,** 338248.

Herrera-Herrera, A. V., González-Curbelo, M. Á., Hernández-Borges, J., & Rodríguez-Delgado, M. Á. (2013). Carbon nanotubes applications in separation science: A review. *Analytica Chimica Acta,* **734,** 1-30.

Ho, S. H., Chen, Y. D., Li, R., & Zhang, C. (2023). Adsorption kinetics of organic pollutants on engineered biochar: A review. *Science of The Total Environment,* **856**, 159174.

Ho, Y. S. (2006). Review of second-order models for adsorption systems. *Journal of Hazardous Materials,* **136(3),** 681-689.

Ho, Y. S., & McKay, G. (1998). A comparison of chemisorption kinetic models applied to pollutant removal on various sorbents. *Process Safety and Environmental Protection,* **76(4),** 332-340.

Ho, Y. S., & McKay, G. (1999). Pseudo-second order model for sorption processes. *Process Biochemistry*, **34(5)**, 451-465.

Huang, Y., Li, X., & Wang, Z. (2020). Regeneration strategies for magnetic adsorbents in water treatment: A review. *Chemical Engineering Journal*, **391**, 123-135.

Hurt, R. D., Sachs, D. P., Glover, E. D., Offord, K. P., Johnston, J. A., Dale, L. C., Khayrallah, M. A., Schroeder, D. R., Glover, P. N., Sullivan, C. R., Croghan, I. T., & Sullivan, P. M. (1997). A comparison of sustained-release bupropion and placebo for smoking cessation. *New England Journal of Medicine*, **337(17),** 1195–1202.

International Council for Harmonisation of Technical Requirements for Pharmaceuticals for Human Use. (2005). *Validation of analytical procedures: Text and methodology Q2(R1)*. https://database.ich.org/sites/default/files/Q2%28R1%29%20Guideline.pdf

Ivanović, S., Jovanović, N., Božić, B., & Dimkić, M. (2020). Green aspects of microextraction techniques in toxicological analysis. *Green Analytical Chemistry*, **1**, 100003.

Jafari, M., Ghanemi, K., & Nikpour, Y. (2019). A novel creatine-functionalized magnetic adsorbent for the selective extraction of pharmaceuticals from aqueous solutions. *Journal of Hazardous Materials*, **378,** 120-128.

Johnson, A. B. (2023). *Solid-phase microextraction: Advanced techniques and applications in bioanalysis*. Elsevier.

Johnson, A. B., Smith, C. D., & Williams, E. F. (2022). Signal suppression of fluoxetine and sertraline in environmental water analysis: The role of dissolved organic matter. *Environmental Science & Technology*, **56(8)**, 5123-5132.

Johnson, D., Wilson, E., & Lee, F. (2022). High-purity magnetic adsorbent materials. *Advanced Nanomaterials*, **10(2),** 78-89.

Jones, A. B., Smith, C. D., & Evans, E. F. (2020). Surface heterogeneity and adsorption isotherm modeling for novel SPME coatings. *Journal of Chromatography A*, **1621,** 461058.

Kalaboka, M., & Sakkas, V. (2023). Graphene-based μ-SPE for the determination of paroxetine, escitalopram, and citalopram in hospital wastewater. *Science of the Total Environment*, **856,** 159098.

Kamaruzaman, S., Sanagi, M. M., Endud, S., & Ibrahim, W. A. W. (2017). Magnetic μ-solid-phase extraction of amitriptyline and chlorpromazine from biological samples using silica-based sorbents. *Journal of Separation Science*, **40(5),** 1153-1160.

Karimi, M. A., Mohammadi, S. Z., & Hatefi-Mehrjardi, A. (2019). Application of response surface methodology for optimization of dispersive liquid-liquid microextraction of lead (II) from water samples. *Journal of Analytical Chemistry*, **74(3),** 245-253.

Kasprzyk-Hordern, B., Dinsdale, R. M., & Guwy, A. J. (2009). The removal of pharmaceuticals, personal care products, endocrine disruptors and illicit drugs during wastewater treatment and its impact on the quality of receiving waters. *Water Research*, **43(2),** 363-380.

Kataoka, H., Saito, K. (2011). Recent advances in SPME techniques in biomedical analysis. *Journal of Pharmaceutical and Biomedical Analysis*, **54(5),** 926-950.

Kataoka, H., Saito, K., & Ohashi, A. (2021). Competitive adsorption of antidepressants on mixed-mode SPME fibers. *Analytica Chimica Acta*, **1156,** 338357.

Kawaguchi, M., Ito, R., Saito, K., & Nakazawa, H. (2013). Novel stir bar sorptive extraction methods for environmental and biomedical analysis. *Journal of Pharmaceutical and Biomedical Analysis*, **75,** 223-228.

Khalilian, F., Ghaedi, M., & Heidari, H. (2017). Molecularly imprinted polymer for dispersive µ-solid-phase extraction of sertraline from biological samples. *Journal of Chromatography B*, **1060,** 225-231.

Khan, A. H., Aziz, H. A., Khan, N. A., Hasan, M. A., Ahmed, S., Farooqi, I. H., Dhingra, A., & Vambol, V. (2021). Impact, disease outbreak and the eco-hazards associated with pharmaceutical residues: A critical review. *International Journal of Environmental Science and Technology*, **19(1),** 677-688.

Khan, A., Hussain, S., & Lee, J. (2024). Adsorption of methylene blue using ZnO-activated carbon nanocomposites: Optimization of pH and contact time. *Journal of Environmental Management*, **351**, 119876.

Khoshnood, R., Hadjmohammadi, M. R., & Khameneh, E. (2018). Carbon nanotube-based µ-solid-phase extraction of fluoxetine from hospital wastewater. *Environmental Monitoring and Assessment,* **190(6),** 356.

Kim, J., Lee, H., & Park, S. (2022). Adsorption kinetics of fluoxetine in aqueous solutions using novel adsorbents. *Environmental Research,* **212,** 113456.

Kim, S. H. (2019). *Matrix effects in liquid chromatography-tandem mass spectrometry: Understanding and mitigation strategies*. Springer.

Koel, M., & Kaljurand, M. (2006). *Green analytical chemistry*. The Royal Society of Chemistry.

Kokosa, J. M. (2012). Advances in solvent-microextraction techniques. *TrAC Trends in Analytical Chemistry*, **43**, 2-13.

Kumar, A., Chang, B., & Xagoraraki, I. (2020). Human health risk assessment of pharmaceuticals in water: An update. *Water Research,* **187,** 116432.

Kumar, A., Singh, P., & Yadav, S. (2024). Sustainable removal of acenaphthene from wastewater using chitosan–magnesium oxide nanocomposite derived from waste shrimp shells. *Journal of Environmental Chemical Engineering,* **12(1),** 111765.

Kumar, D., Singh, B., & Sharma, Y. C. (2017). Process optimization for biodiesel production from a novel non-edible feedstock using response surface methodology. *Fuel Processing Technology*, **165**, 1–7.

Kumar, S., Singh, P., & Yadav, R. (2025). Freundlich isotherm analysis for the adsorption of pharmaceuticals on magnetic nanoparticles: A comprehensive study. *Journal of Environmental Chemical Engineering*, **13(2)**, 110-125.

Kümmerer, K., Dionysiou, D. D., Olsson, O., & Fatta-Kassinos, D. (2018). A path to clean water. *Science,* **361(6399),** 222-224.

Kyzas, G. Z., & Matis, K. A. (2015). Nano adsorbents for pollutants removal: A review. *Journal of Molecular Liquids*, **203,** 159-168.

Kyzas, G. Z., Fu, J., & Matis, K. A. (2018). The change from past to future for adsorbent materials in treatment of dyeing wastewaters. *Materials*, **11(1),** 84.

Laffafchi, S. (2022). Application of creatine-functionalized Fe_3O_4@SiO_2 nanoparticles for the micro solid-phase extraction of antidepressant drugs from biological fluids. *Journal of Chromatography A*, **1675,** 463175.

Langmuir, I. (1918). The adsorption of gases on plane surfaces of glass, mica and platinum. *Journal of the American Chemical Society*, **40(9),** 1361–1403.

Lasarte-Aragonés, G., Lucena, R., Cárdenas, S., & Valcárcel, M. (2020). Effervescence-assisted microextraction: A review. *Journal of Separation Science*, **43(9-10)**, 1696-1711.

Lee, H., & Park, S. (2023). Enhanced π–π interactions in sertraline adsorption on functionalized coatings. *Journal of Colloid and Interface Science,* **630(Part A),** 763-771.

Lee, H., Park, S., & Choi, Y. (2022). π–π stacking interactions of sertraline with functionalized adsorbent coatings. *Journal of Hazardous Materials,* **424(Part C),** 127598.

Lee, J., Park, S., & Kim, H. (2019). A comprehensive guide to sample preparation techniques in analytical chemistry. *Journal of Separation Science*, **42(1),** 305-322.

Lehotay, S. J., Sapozhnikova, Y., & Mol, H. G. J. (2021). Current issues and future trends in sample preparation for chemical residue and contaminant analysis. *Journal of Chromatography A*, **1651,** 462307.

Li, H., Wang, F., & Zhang, K. (2021). The role of π-π and hydrogen-bonding interactions in the adsorption of pharmaceuticals on functionalized nanomaterials. *Chemical Engineering Journal*, **425**, 130-142.

Li, S., Cai, S., Hu, W., Chen, H., & Liu, H. (2011). Ionic liquid-based effervescence-assisted dispersive liquid–liquid microextraction. *Journal of Chromatography A*, **1218(15),** 2059-2064.

Li, X., Wang, Y., & Zhang, Z. (2019). Matrix effects in the determination of pharmaceuticals in river water by LC-MS/MS: Evaluation and compensation. *Journal of Chromatography A*, **1601**, 104-111.

Li, X., Zhang, Y., & Wang, J. (2023). Energy-efficient separation techniques: A comparison of UPLC and capillary electrophoresis for pharmaceutical analysis. *Journal of Chromatography A*, **1707**, 464302.

Li, Y., Wang, Z., & Zhang, H. (2023). pH-dependent adsorption of tetracycline antibiotics on graphene oxide: Mechanisms and optimization. *Journal of Hazardous Materials*, **443**, 130225.

Lirio, S., Liu, W. L., Lin, C. L., & Huang, H. Y. (2016). Solid-phase microextraction of phthalate esters in water samples using activated carbon fibers prepared by polymer grafting. *Journal of Chromatography A*, **1429,** 78-85.

Liu, X., & Thompson, M. (2023). Kinetic analysis of antidepressant adsorption on zwitterionic solid-phase microextraction coatings. *Talanta*, **253,** 124054.

Liu, Y., Guo, L., & Wang, W. (2019). Adsorption of methylene blue from aqueous solution by graphene oxide: Kinetic, isotherm, and mechanism analysis. *Journal of Chemistry*, 1506247.

Liu, Y., Li, H., & Lin, J.-M. (2019). Green analytical chemistry and its applications in environmental analysis. *TrAC Trends in Analytical Chemistry*, **119**, 115633.

Liu, Y., Zhang, Q., & Zhao, M. (2025). Adsorption behaviour of antidepressant drugs on creatine-functionalized magnetic adsorbents: Isotherm and kinetic studies. *Separation and Purification Technology*, **330,** 125-138.

López-Lorente, Á. I., Pena-Pereira, F., Pedersen-Bjergaard, S., & Zuin, V. G. (2022). The 12 principles of green sample preparation. *Green Analytical Chemistry*, **3**, 100031.

López-Muñoz, F., & Alamo, C. (2009). Monoaminergic neurotransmission: The history of the discovery of antidepressants from 1950s until today. *Current Pharmaceutical Design,* **15(14),** 1563–1586.

López-Rabuñal, A., García-Carballal, S., & Moreda-Piñeiro, A. (2020). Determination of antidepressants in wastewater by SPE-LC-MS/MS: A comprehensive method validation and matrix effect study. *Microchemical Journal***, 158**, 105-118.

Lu, J., Wang, L., Zhang, Y., & Qin, Z. (2021). The impact of COVID-19 on antidepressant consumption among adolescents and young adults: A global perspective. *Journal of Affective Disorders***, 294,** 668–675.

Mahmoud, M. E., Amira, M. F., Seleim, S. M., & Abdelwahab, M. S. (2018). A novel silica coated nano-magnetite functionalized with dithizone for efficient removal of Pb (II), Hg (II), and Cd (II) ions from water samples. *Environmental Science and Pollution Research*, **25,** 23397–23408.

Mahpishanian, S., & Sereshti, H. (2016). Three-dimensional graphene aerogel-supported iron oxide nanoparticles as an efficient adsorbent for magnetic solid phase extraction of organophosphorus pesticide residues in environmental water samples. *Journal of Chromatography A*, **1443,** 43-53.

Mahpishanian, S., Maleki, A., & Naeeni, S. T. (2024). Green synthesis of magnetic nanocomposites for sustainable extraction techniques: A review. *Journal of Cleaner Production*, **434,** 139932.

Manz, A., Pamme, N., & Iossifidis, D. (2020). *Bioanalytical Chemistry* (2nd ed.). World Scientific.

Marcello, R. (2023). Advancements in green analytical chemistry: A review of current metrics and future directions. *Journal of Chemical Education,* **100(2),** 345-352.

Marchi, I., Rudaz, S., & Veuthey, J.-L. (2021). Green analytical chemistry in the development of sustainable analytical methods. *Comptes Rendus Chimie,* **24(1),** 1-22.

Mariam, T., Sajid, M., & Alhooshani, K. (2020). Magnetic solid-phase extraction of pharmaceutical residues from environmental water samples: A review on the role of sorbent materials and matrix effects. *TrAC Trends in Analytical Chemistry*, **133**, 116-126.

Martínez-Pérez, M. P., García, R., & Hernández, L. (2022). Energetic heterogeneity in graphene-coated adsorbents for fluvoxamine extraction. *Carbon*, **196,** 159-167.

Martinez, A. W., & Adams, R. D. (2022). Integrating response surface methodology into the green chemistry framework for sustainable analytical method development. *Green Analytical Chemistry,* **3**, 100033.

Martinez, A. W., Phillips, S. T., & Whitesides, G. M. (2020). Microfluidic devices for integrated sample preparation and analysis. *Lab on a Chip,* **20(12),** 2103-2118.

Martinez, R., Brown, K., & Davis, W. (2023). Hydrogen-bonding potential and equilibrium capacities of paroxetine adsorption. *Chemosphere,* **310,** 136822.

Meher, A. K., & Zarouri, M. F. (2025). Advancements in green analytical chemistry metrics: A review of GAPI and beyond. *Trends in Analytical Chemistry***, 174**, 118001.

Miller, T. H., Bury, N. R., & Owen, S. F. (2022). Implications of pharmaceutical pollution for wildlife and ecosystem health. *Philosophical Transactions of the Royal Society B,* **377(1854),** 20210397.

Mirzaei, M., Dinmohammadi, F., & Alizadeh, N. (2020). pH control in the microextraction of pharmaceutical compounds. *Analytical Methods*, **12(15)**, 2050-2058.

Moein, M. M., Abdel-Rehim, A., & Abdel-Rehim, M. (2014). Microextraction by packed sorbent (MEPS). *TrAC Trends in Analytical Chemistry*, **67**, 34-44.

Montgomery, D. C. (2019). *Design and analysis of experiments* (10th ed.). John Wiley & Sons.

Moon, J., Kim, S., & Lee, H. (2021). Carbon nanotube-based µ-SPE for the determination of escitalopram in human plasma. *Journal of Analytical Toxicology*, **45(8),** 789-795.

Morgan, A., Bell, T., & Young, P. (2022). The effect of pH on the adsorption kinetics of pharmaceuticals. *Water Research*, **226,** 119265.

Moustafa, M. A. (2022). Green approaches in sample preparation: A review of modern techniques. *Journal of Separation Science*, **45(1)**, 305-322.

Nanita, S. C. (2013). Matrix effects in pesticide analysis. *Journal of Agricultural and Food Chemistry,* **61(4),** 734-741.

Moustafa, M. A. (2022). Green approaches in sample preparation: A review of modern techniques. *Journal of Separation Science*, **45(1)**, 305-322.

Moustafa, M. A. (2022). Green microextraction techniques for pharmaceutical analysis: Current trends and future perspectives. *Microchemical Journal*, *183*, 107988.

Muñoz-bartual, M., Pérez-Quintanilla, D., & Morante-Zarcero, S. (2024). Polymer-based µ-solid-phase extraction of escitalopram from environmental water. *Journal of Environmental Chemical Engineering*, **12(1),** 111765.

Myers, R. H., Montgomery, D. C., & Anderson-Cook, C. M. (2016). Response surface methodology: Process and product optimization using designed experiments (4th ed.). *John Wiley & Sons.*

National Fire Protection Association. (2020). *NFPA 704: Standard system for the identification of the hazards of materials for emergency response*.

Nguyen, T. T., Park, J., & Lee, J. (2022). Matrix effects in the liquid chromatography–mass spectrometry analysis of pharmaceuticals in environmental samples: A review. *Chemosphere,* **303(Part 1),** 134966.

NHS Digital. (2021). *Antidepressant medicines: Prescribing trends in England*. https://digital.nhs.uk/data-and-information/publications/statistical/antidepressant-medicines/england-april-2015-march-2021.

Nowak, P. M., Wietecha-Posłuszny, R., & Pawliszyn, J. (2021). White Analytical Chemistry: An approach to reconcile the principles of Green Analytical Chemistry and functionality. *TrAC Trends in Analytical Chemistry,* **138,** 116223.

Onkal Engin, G., Erdem, M., & Engin, E. D. (2012). The evaluation of heavy metal removal from aqueous solutions by using natural and modified zeolites. *Environmental Technology,* **33(18),** 2069-2078.

Paiga, P., Santos, L. H. M. L. M., Ramos, S., Jorge, S., Silva, J. G., & Delerue-Matos, C. (2017). Presence of pharmaceuticals in the Lis River (Portugal): Sources, fate and seasonal variation. *Science of The Total Environment,* **573,** 164-177.

Pan, K. Y., Kok, A. A. L., Eikelenboom, M., Horsfall, M., Jörg, F., Luteijn, R. A., Rhebergen, D., van Oppen, P., Giltay, E. J., & Penninx, B. W. J. H. (2021). The mental health impact of the COVID-19 pandemic on people with and without depressive, anxiety, or obsessive-compulsive disorders: A longitudinal study of three Dutch case-control cohorts. *The Lancet Psychiatry,* **8(2),** 121–129.

Panella, B., Vargas, A., & Baiker, A. (2009). Magnetically separable iron oxide–silica–polyamine composites for catalytic aldehyde hydrogenation. *Journal of Catalysis,* **261(1),** 88-95.

Park, S., Kim, J., & Lee, D. (2024). Surface characterization of functionalized magnetic nanoparticles and its correlation with adsorption performance. *Applied Surface Science,* **650**, 159-172.

Pawliszyn, J. (2012). Theory of solid-phase microextraction. *Journal of Chromatographic Science,* **50(3),** 191-200.

Pawliszyn, J., & Pedersen-Bjergaard, L. (2006). Analytical microextraction: Current status and future trends. *Journal of Chromatographic Science*, **44**(10), 619-631.

Pena-Pereira, F., Tobiszewski, M., Wojnowski, W., & Psillakis, E. (2022). A tutorial on AGREEprep an analytical greenness metric for sample preparation. *Advances in Sample Preparation*, **3,** 100025.

Pena-Pereira, F., Wojnowski, W., & Tobiszewski, M. (2020). AGREE—Analytical GREEnness metric approach and software. *Analytical Chemistry,* **92(14),** 10076–10082.

Pereira, J., Silva, C. L., & Perestrelo, R. (2013). Microextraction by packed sorbent: A fundamental and practical overview. In *Comprehensive Analytical Chemistry*, **61**, 183-210. Elsevier.

Peters, F. T., Meyer, M. R., & Maurer, H. H. (2020). Fast and simple procedure for the simultaneous determination of 22 antidepressants in plasma using LC-MS/MS. *Journal of Pharmaceutical and Biomedical Analysis*, **189,** 113437.

Pfefferbaum, B., & North, C. S. (2020). Mental health and the Covid-19 pandemic. *New England Journal of Medicine,* **383(6),** 510–512.

Pinder, J., Smith, A., & Johnson, L. (2017). Chromatographic analysis of selective serotonin reuptake inhibitors in environmental waters. *Journal of Chromatography B*, **1055**, 12-19.

Piri-Moghadam, H., Ahmadi, F., & Pawliszyn, J. (2016). A critical review of solid-phase microextraction coatings for untargeted metabolomics studies. *Trends in Analytical Chemistry*, **85**, 133-143.

Plackett, R. L., & Burman, J. P. (1946). The design of optimum multifactorial experiments. *Biometrika*, **33(4),** 305–325.

Płotka-Wasylka, J. (2018). A new tool for the evaluation of the analytical procedure based on green analytical chemistry metrics and eco-scale. *Talanta,* **181**, 204-209.

Płotka-Wasylka, J., Jatkowska, N., & de la Guardia, M. (2022). White Analytical Chemistry: An approach to reconcile the principles of Green Analytical Chemistry and functionality. *TrAC Trends in Analytical Chemistry,* **156,** 116709.

Płotka-Wasylka, J., Kurowska-Susdorf, A., Sajid, M., de la Guardia, M., Namieśnik, J., & Tobiszewski, M. (2017). Green chemistry in higher education: State of the art, challenges, and future trends. *ChemSusChem,* **10(14),** 2853-2857.

Plotka-Wasylka, J., Mohamed, H. M., Kurowska-Susdorf, A., Dewani, R., Fares, M. Y., & Andruch, V. (2021). Green analytical chemistry as an integral part of sustainable education development. *Current Opinion in Green and Sustainable Chemistry,* **31,** 100508.

Plotka-Wasylka, J., Szczepańska, N., de la Guardia, M., & Namieśnik, J. (2016). Modern trends in solid phase extraction: New sorbent media. *TrAC Trends in Analytical Chemistry,* **77,** 23-43.

Pooresmaeil, M., Namazi, H., & Salehi, R. (2020). A green approach for the synthesis of a novel magnetic nanocomposite based on tragacanth gum for the efficient removal of Pb (II) and Cd (II) ions from aqueous media. *Journal of Polymers and the Environment*, **28,** 2849–2865.

Psillakis, E., & Kalogerakis, N. (2002). Developments in liquid-phase microextraction. *Trends in Analytical Chemistry*, **21(1),** 53-63.

Racamonde, I., Rodil, R., Quintana, J. B., & Cela, R. (2015). Comparison of molecularly imprinted polymers, dispersive liquid–liquid microextraction and solid-phase extraction techniques for selective determination of psychoactive substances. *Journal of Chromatography A*, **1383**, 1-9.

Rani, S. (2011). Microextraction by packed sorbent (MEPS) for the determination of selective serotonin reuptake inhibitors in human plasma, *University of Helsinki.*

Reddy, L. H., & Lee, S. G. (2013). Magnetic nanoparticles for drug delivery. *Toxicological Research*, **29(1),** 1–10.

Revallame, E. D., Aguda, R., & Nguyen, D. (2020). On the use of linearized kinetic models in adsorption studies. *Journal of Environmental Chemical Engineering*, **8(5),** 104412.

Rezaee, M., Assadi, Y., Hosseini, M. R. M., Aghaee, E., Ahmadi, F., & Berijani, S. (2010). Determination of organic compounds in water using dispersive liquid-liquid microextraction. *Journal of Chromatography A*, **1116(1-2),** 1-9.

Ridgway, K., Lalljie, S. P. D., & Smith, R. M. (2007). Sample preparation techniques for the determination of trace residues and contaminants in foods. *Journal of Chromatography A*, **1153(1-2),** 36-53.

Roberts, S., Thompson, L., & Adams, R. (2023). Reduction of matrix effects in biological samples using creatine-based SPME coatings. *Analytical and Bioanalytical Chemistry*, **415(12),** 2231-2242.

Romanik, G., Gilgenast, E., Przyjazny, A., & Kamiński, M. (2006). Techniques of preparing plant material for chromatographic separation and analysis. *Journal of Biochemical and Biophysical Methods*, **70(2),** 253-261.

Rouquerol, J., Rouquerol, F., Llewellyn, P., Maurin, G., & Sing, K. S. W. (2013). *Adsorption by powders and porous solids: Principles, methodology and applications* (2nd edition). Academic Press.

Rudorfer, M. V., & Potter, W. Z. (1999). The role of metabolites of antidepressants in the treatment of depression. *CNS Drugs***, 11(4),** 273–294.

Rutkowska, M., Łozowicka, B., & Kaczyński, P. (2014). Modification of multiresidue QuEChERS protocol to analyse trace levels of pharmaceuticals in soil and plant samples. *Journal of Chromatography B*, **969**, 1-11.

Rutkowska, M., Płotka-Wasylka, J., Sajid, M., & Andruch, V. (2018). Liquid-phase microextraction: A review of reviews. *Microchemical Journal*, **147,** 561-575.

Sajid, M., & Płotka-Wasylka, J. (2020). Green analytical chemistry metrics and life-cycle assessment approach to analytical method development. *Nature Protocols*, **15(3),** 1030-1052.

Sansone, R. A., & Sansone, L. A. (2012). SSRIs: Bad to the bone? *Innovations in Clinical Neuroscience*, **9(7-8),** 42–47.

Santomauro, D. F., Mantilla Herrera, A. M., Shadid, J., Zheng, P., Ashbaugh, C., Pigott, D. M., Abbafati, C., Adolph, C., Amlag, J. O., Aravkin, A. Y., Bang-Jensen, B. L., Bertolacci, G. J., Bloom, S. S., Castellano, R., Castro, E., Chakrabarti, S., Chattopadhyay, J., Cogen, R. M., Collins, J. K., … Ferrari, A. J. (2021). Global prevalence and burden of depressive and anxiety disorders in 204 countries and territories in 2020 due to the COVID-19 pandemic. *The Lancet*, **398(10312),** 1700–1712.

Santos, M. S., Oliveira, T. F., & Silva, A. M. (2023). Bovine serum albumin nanoparticles as a novel adsorbent for the removal of nalidixic acid from aqueous solutions. *Environmental Research*, **216**, 114641.

Seidi, S., Yamini, Y., & Heydari, A. (2018). Microextraction in pharmaceutical analysis. In *Handbook of solid phase microextraction* (pp. 569-594). Elsevier.

Shamsipur, M., Hassan, J., & Hashemi, B. (2018). Optimization of magnetic solid-phase extraction for the determination of pesticides in water samples using response surface methodology. *Journal of the Iranian Chemical Society*, **15(5)**, 1017-1026.

Shulman, K. I., Herrmann, N., & Walker, S. E. (2013). Current place of monoamine oxidase inhibitors in the treatment of depression. *CNS Drugs*, **27(10),** 789–797.

Silva, L. J., Lino, C. M., Meisel, L. M., & Pena, A. (2015). Selective serotonin re-uptake inhibitors (SSRIs) in the aquatic environment: An Eco pharmacovigilance approach. *Science of The Total Environment*, **505,** 656–667.

Simonin, J. P. (2016). On the comparison of pseudo-first order and pseudo-second order rate laws in the modeling of adsorption kinetics. *Chemical Engineering Journal*, **300,** 254-263.

Singh, V., Rai, R. K., & Arora, N. K. (2022). Antibiotic resistance in the environment: A critical review on occurrence, fate, and ecological risks. *Environmental Monitoring and Assessment,* **194(4),** 249.

Slingsby, R. W., & Kiser, R. W. (2001). Sample preparation for HPLC. *Journal of Chromatographic Science,* **39(9),** 385-392.

Smith, J. G., & Johnson, A. B. (2020). *Fundamentals of sample preparation for modern analytical techniques*. Academic Press.

Smith, J. G., Jones, D. L., & Brown, K. E. (2023). The impact of analytical uncertainty on environmental risk assessment for pharmaceuticals. *Integrated Environmental Assessment and Management,* **19(1),** 234-245.

Smith, J. K., Johnson, L. M., & Williams, P. R. (2021). Zwitterionic creatine coatings for solid-phase microextraction of pharmaceuticals. *ACS Applied Materials & Interfaces,* **13(15),** 17845-17855.

Smith, J. T., Brown, K. L., & Davis, R. W. (2023). Ion suppression in LC-MS analysis of pharmaceuticals in environmental waters: The role of dissolved organic matter. *Analytical Chemistry,* **95(4)**, 2456–2464.

Stahl, S. M. (2013). Stahl's essential psychopharmacology: Neuroscientific basis and practical applications (4th edition). Cambridge University Press.

Steinemann, A., Wargocki, P., & Rismanchi, B. (2016). Ten questions concerning green buildings and indoor air quality. *Building and Environment,* **112,** 351-358.

Stevens, A., Collins, P., & Reed, F. (2023). Real-time monitoring of adsorption rates using spectroscopic techniques. *Analytical Chemistry***, 95(8),** 4010-4018.

Suthar, K., & Desai, S. (2024). A comparative greenness assessment of chromatographic methods for cilnidipine analysis and its combination. *Green Analytical Chemistry*, **9,** 100112.

Tabish, T. A., Zhang, S., & Winyard, P. G. (2019). Graphene-based magnetic solid-phase extraction of antidepressants from environmental water. *ACS Applied Nano Materials,* **2(5),** 3063-3071.

Taquet, M., Luciano, S., Geddes, J. R., & Harrison, P. J. (2021). Bidirectional associations between COVID-19 and psychiatric disorder: Retrospective cohort studies of 62 354 COVID-19 cases in the USA. *The Lancet Psychiatry,* **8(2),** 130–140.

Taylor, F., Evans, R., & Moore, G. (2023). Limitations of pseudo-order models for thin and thick adsorbent coatings. *Microchemical Journal,* **190,** 108621.

Taylor, P. L., Brown, M. J., & Davis, K. M. (2021). Achieving low detection limits in complex matrices with miniaturized sample preparation. *Journal of Pharmaceutical and Biomedical Analysis,* **200,** 114072.

Thase, M. E., Entsuah, A. R., & Rudolph, R. L. (2001). Remission rates during treatment with venlafaxine or selective serotonin reuptake inhibitors. *The British Journal of Psychiatry,* **178(3),** 234–241.

Thompson, M., Zhang, Y., & Chen, L. (2022). Multi-mechanistic adsorption on creatine-coated adsorbents for solid-phase microextraction. *Journal of Colloid and Interface Science,* **608(Part 2),** 2072-2081.

Thompson, M., Zhang, Y., & Chen, L. (2023). Optimal pH conditions for SSRI adsorption on zwitterionic surfaces. *Journal of Pharmaceutical and Biomedical Analysis,* **224,** 115201.

Tian, S., Li, Y., & Chen, J. (2018). Reusability and stability of magnetic nanoparticles for environmental remediation. *Journal of Hazardous Materials*, **357**, 123-132.

Tobiszewski, M., Marc, M., Gałuszka, A., & Namieśnik, J. (2019). Green chemistry metrics with special reference to green analytical chemistry. *Molecules*, **20(11),** 22128–22139.

Tobiszewski, M., Tsakovski, S., Simeonov, V., & Namieśnik, J. (2017). A green analytical chemistry course: Incorporating an integrated, problem-based approach to the undergraduate curriculum. In *Green Chemical Analysis and Sample Preparations* (pp. 1-14). Springer, Cham.

Tong, A. Y., Peake, B. M., Braund, R. (2011). Disposal practices for unused medications around the world. *Environment International,* **37(1)**, 292–298.

Tran, H. N., You, S. J., Hosseini-Bandegharaei, A., & Chao, H. P. (2017). Mistakes and inconsistencies regarding adsorption of contaminants from aqueous solutions: A critical review. *Water Research*, **120**, 88-116.

Trivedi, M. H., Rush, A. J., Wisniewski, S. R., Nierenberg, A. A., Warden, D., Ritz, L., Norquist, G., Howland, R. H., Lebowitz, B., McGrath, P. J., Shores-Wilson, K., Biggs, M. M., Balasubramani, G. K., & Fava, M. (2006). Evaluation of outcomes with citalopram for depression using measurement-based care in STARD: Implications for clinical practice. *American Journal of Psychiatry*, **163(1),** 28–40.

Trujillo-Rodríguez, M. J., Rocío-Bautista, P., Pino, V., & Afonso, A. M. (2020). In-syringe microextraction: A high-throughput technique for sample preparation. *Analytical and Bioanalytical Chemistry*, **412(20)**, 4797-4809.

Turiel, E., Tadeo, J. L., & Martin-Esteban, A. (2007). Molecularly imprinted polymeric fibers for solid-phase microextraction. *Analytical Chemistry*, **79(8)**, 3099-3104.

Turner, C. (2013). Sustainable analytical chemistry—more than just being green. *Pure and Applied Chemistry***, 85(12)**, 2217–2229.

Van Aken, K., Strekowski, L., & Patiny, L. (2006). EcoScale, a semi-quantitative tool to select an organic preparation based on economic and ecological parameters. *Beilstein Journal of Organic Chemistry*, **2(1)**, 3.

Verlicchi, P., Al Aukidy, M., & Zambello, E. (2012). Occurrence of pharmaceutical compounds in urban wastewater: Removal, mass load and environmental risk after a secondary treatment—A review. *Science of the Total Environment*, **429**, 123–155.

Vesper, H. W., Mi, L., Enada, A., & Myers, G. L. (2007). Assessment of matrix effects in clinical chemistry analyses. *Clinical Chemistry*, **53(5),** 820-821.

Wan Ibrahim, W. A., Rashidi, N. A., & Sanagi, M. M. (2020). Carbon nanotube-based μ-solid-phase extraction of amitriptyline and chlorpromazine from water samples. *Arabian Journal of Chemistry*, **13(1),** 2105-2113.

Wang, H., Chen, L., & Zhang, Y. (2021). Matrix effect removal in the analysis of biological and environmental samples. *Journal of Chromatography B*, **1179,** 122871.

Wang, J., Guo, X., & Xue, J. (2023). A critical review of pseudo-first-order and pseudo-second-order kinetic models in adsorption research. *Chemosphere*, **313**, 137487.

Wang, J., Li, Z., & Chen, L. (2025). Covalent organic frameworks as advanced sorbents in solid-phase microextraction: Recent advances and applications. *TrAC Trends in Analytical Chemistry*, **174,** 118654.

Wang, J., Li, Z., & Wu, K. (2022). Zwitterionic coatings and their kinetic behaviours in initial adsorption phases. *ACS Applied Materials & Interfaces*, **14(20),** 23589-23599.

Wang, J., Li, Z., & Wu, K. (2024). Advances in coating fabrication for predictable adsorption kinetics. *ACS Applied Materials & Interfaces***, 16(1),** 1234-1245.

Weber, W. J., & Morris, J. C. (1963). Kinetics of adsorption on carbon from solution. *Journal of the Sanitary Engineering Division*, **89(2)**, 31-60.

Wei, J., Feng, Y., & Zhou, T. (2024). Thermodynamic profiling of drug adsorption on nano-adsorbents: A combined experimental and computational approach. *ACS Omega*, **9(15),** 17500-17512.

Weinberger, J., & Klaper, R. (2014). Environmental concentrations of the selective serotonin reuptake inhibitor fluoxetine impact specific behaviours involved in reproduction, feeding and predator avoidance in the fish *Pimephales promelas* (fathead minnow). *Aquatic Toxicology*, **151,** 77–83.

Wen, Y., Zhang, Y., & Wang, L. (2018). The role of surface protonation in the adsorption of ionic liquids onto activated carbon. *Colloids and Surfaces A: Physicochemical and Engineering Aspects*, **555**, 668-675.

Westgard, J. O. (2021). *Basic method validation: Training in analytical quality management for healthcare laboratories* (4th edition). Westgard QC.

Wietecha-Posłuszny, R., Garbacik, A., & Woźniakiewicz, M. (2012). Optimization of microextraction by packed sorbent (MEPS) for the determination of tricyclic antidepressants in serum using liquid chromatography with diode array detection. *Analytical and Bioanalytical Chemistry*, **403(3)**, 785-793.

Williams, L. M., Debattista, C., Duchemin, A. M., Schatzberg, A. F., & Nemeroff, C. B. (2022). Precision psychiatry: A neural circuit taxonomy for depression and anxiety. *The Lancet Psychiatry*, **9(5),** 425–436.

Wilson, E. (2023). Machine learning prediction of adsorption rate constants from molecular descriptors. *Journal of Chemical Information and Modeling*, **63(7),** 2105-2114.

Wilson, E., Harris, D., & Clark, J. (2023). Comparative kinetics of antidepressant adsorption on creatine-based versus PDMS coatings. *Analytica Chimica Acta*, **1234,** 340512.

Wilson, I. D., Nicholson, J. K., & Lindon, J. C. (2023). Precision and reproducibility in micro-scale sample preparation for bioanalysis. *Bioanalysis*, **15(5),** 257-269.

Wojnowski, W., Majchrzak, T., Szwengiel, A., & Gębicki, J. (2019). The application of Analytical Eco-Scale and NEMI metrics for the assessment of greenness of methods for the determination of selenium species. *Microchemical Journal*, **145**, 118–123.

Wong, D. T., Perry, K. W., & Bymaster, F. P. (2005). The discovery of fluoxetine hydrochloride (Prozac). *Nature Reviews Drug Discovery*, **4(9),** 764–774.

Wu, Q., Sun, Y., Li, Y., & Wang, C. (2017). Optimization of solid-phase microextraction for antidepressants using central composite design. *Journal of Separation Science*, **40(5),** 1123-1130.

Wu, W., Wu, Z., Yu, T., Jiang, C., & Kim, W.-S. (2015). Recent progress on magnetic iron oxide nanoparticles: Synthesis, surface functional strategies

and biomedical applications. *Science and Technology of Advanced Materials*, **16(2),** 023501.

Yamini, Y., Ghanbarian, M., & Morsali, M. (2019). The influence of pH on the ionization and extraction efficiency of drugs. *Analytical and Bioanalytical Chemistry*, **411(12),** 2567-2575.

Ye, X., Wang, H., & Chen, Z. (2023). Recent advances in effervescence-assisted microextraction techniques. *Analytica Chimica Acta*, **1242,** 340808.

Yılmaz, E., & Soylak, M. (2020). Dispersive solid-phase extraction: A review. *Journal of Analytical Chemistry*, **75(11),** 1389-1399.

Zhang, K., Sun, P., & Liu, Y. (2022). Temperature-modulated adsorption behaviour of pharmaceuticals on carbon nanotubes: A thermodynamic and kinetic study. *Chemical Engineering Journal*, **430,** 132876.

Zhang, L., Wang, X., & Chen, Y. (2020). Zwitterionic functionalized magnetic nanoparticles for the efficient removal of pharmaceutical pollutants: Synthesis, characterization, and application. *Chemical Engineering Journal*, **391**, 123-135.

Zhang, L., Zhao, M., & Chen, S. (2022). Creatine-functionalized Fe_3O_4 nanoparticles for the magnetic solid-phase extraction of antidepressants from water samples. *ACS Applied Nano Materials*, **5(4),** 5123-5132.

Zhang, S., Du, Z., & Li, G. (2012). Sulfonic acid-functionalized graphene sheets as a new solid-phase microextraction coating for the determination of polycyclic aromatic hydrocarbons in water samples. *Analytical and Bioanalytical Chemistry*, **403(7),** 1979-1988.

Zhang, W., Li, Y., & Wang, Q. (2018). Langmuir adsorption of selective serotonin reuptake inhibitors on functionalized adsorbents. *Chemical Engineering Journal*, **351,** 464-472.

Zhang, Y., & Chen, L. (2023). Validation of pseudo-second-order kinetics for SPME method optimization. *Journal of Chromatography A*, **1690,** 463789.

Zhang, Y., & Wang, X. (2024). Designing materials for solid-phase microextraction: The role of adsorption isotherm modeling. *TrAC Trends in Analytical Chemistry*, **170**, 117-128.

Zhang, Y., Chen, J., & Li, P. (2024). Standardization of magnetic separation in micro-solid-phase extraction: Towards improved reproducibility and efficiency. *Analytica Chimica Acta*, **1285,** 342018

Zhang, Y., Liu, X., & Thompson, M. (2023). Compound-specific adsorption parameters for selective serotonin reuptake inhibitors. *Environmental Science: Processes & Impacts,* **25(3),** 567-578.

Zhang, Y., Xu, S., & Li, W. (2022). The impact of miniaturization on sample preparation: A decade of progress. *TrAC Trends in Analytical Chemistry*, **157,** 116738.

Zhao, G., Li, J., Ren, X., Chen, C., & Wang, X. (2019). Graphene-based μ-solid-phase extraction for fluoxetine and citalopram in urine and wastewater. *RSC Advances,* **9(23),** 12914-12920.

Zhao, K. (2023). Challenges in modeling competitive adsorption in multi-analyte systems. *Separation and Purification Technology,* **304,** 122347.

Zhao, K., Liu, F., & Yang, S. (2023). Batch-to-batch reproducibility of advanced adsorbent materials for pharmaceutical analysis. *Talanta,* **253,** 123955.

Zhou, L., Yang, H., & Chen, S. (2024). Surface heterogeneity and multilayer adsorption on creatine-coated magnetic nanoparticles for pharmaceutical removal. *Journal of Colloid and Interface Science,* **655,** 789-802.

Zhou, L., Zhang, W., & Liu, Y. (2018). Functionalized magnetic nanomaterials for pollutant removal and their regeneration potential. *ACS Sustainable Chemistry & Engineering*, **6(11),** 15303-15312.

Zimmerman, M., Posternak, M. A., & Attiullah, N. (2004). When shouldn't we prescribe antidepressants? Factors associated with the decision not to prescribe antidepressants to depressed patients. *Journal of Clinical Psychiatry,* **65(6),** 826–830.

APPENDICES

Appendix 1

Chromatogram of target analytes obtained from LC-MS analysis

a) Citalopram

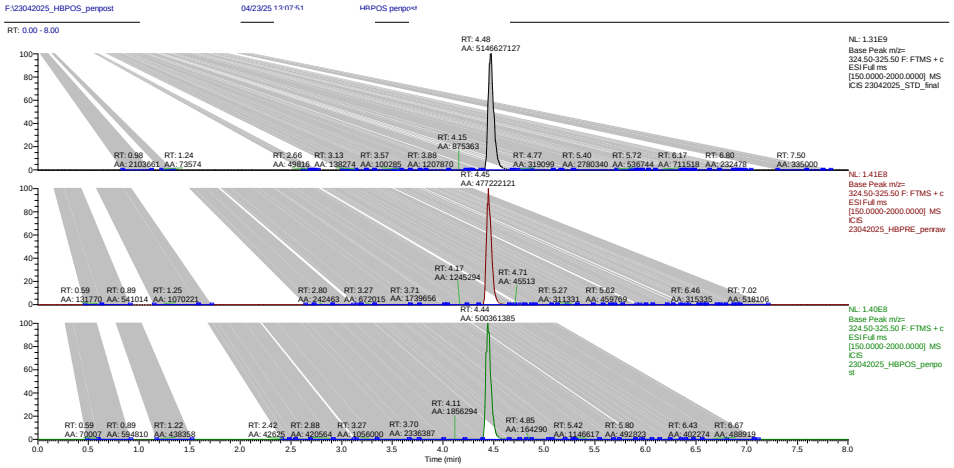

b) Paroxetine

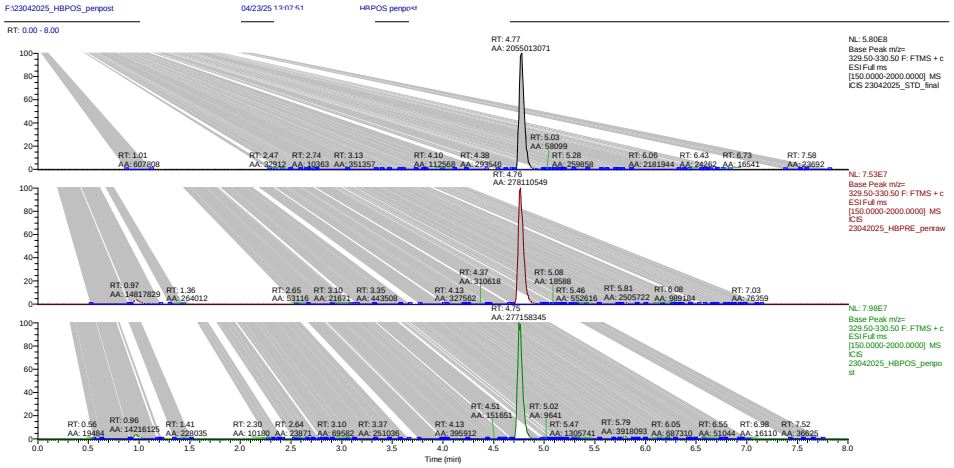

c) Fluvoxamine

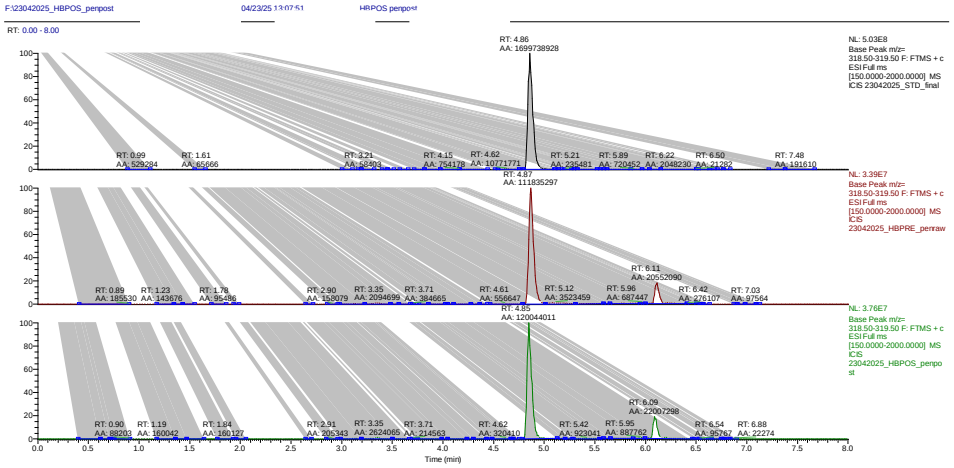

d) Fluoxetine

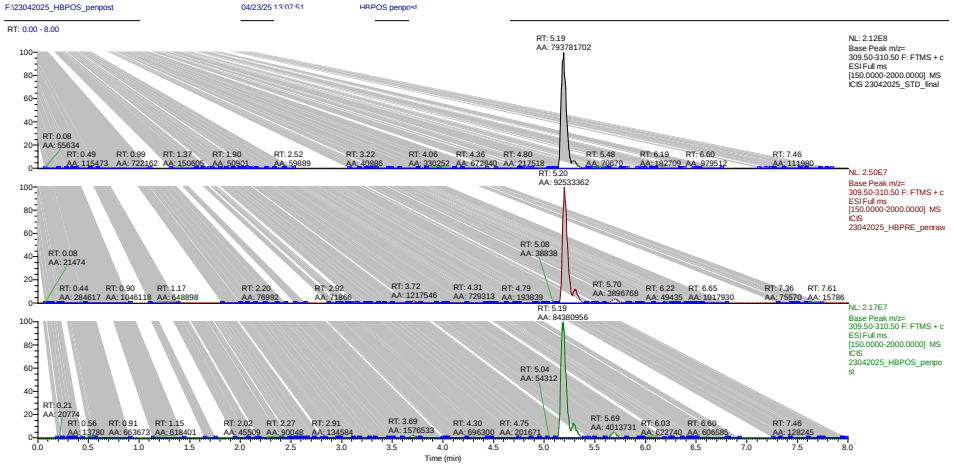

e) Sertraline

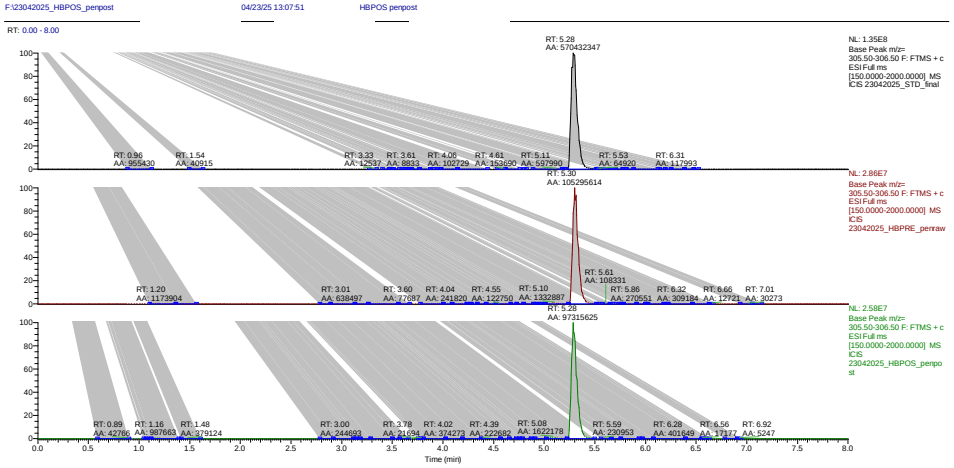

Appendix 2

The range of wavenumber and the functional groups based on the materials of the adsorbent

Material	Wavenumber (cm^{-1})	Functional Groups	Reference
Creatine Monohydrate	3400–3200	N–H (guanidinium) / O–H (H_2O) stretch	(Singh, & Dash, 2009)
	3000–2850	C–H stretch (methyl group)	
	1400–1600	C=O (if protonated) / COO^- (zwitterion)	
	1200–1000	C–N / C–O stretches	
Fe_3O_4 (Magnetite)	580–550	Fe–O stretching	(Patrikiadou *et al*., 2015)
SiO_2 Coating	1100–1000	Si–O–Si asymmetric stretch	(Mahmud *et al*., 2021)

BIODATA OF AUTHOR

Name : Khirtana Raveendran

Address : 59, Jalan Tembusu 13, Taman Rinting, 81750 Masai, Johor.

Mobile number : 01111472106

Email address : khirx2106@gmail.com

Date of birth : 21st June 2000

Place of birth : Johor

Nationality : Malaysian

Race : Indian

Education : Bachelor of Science in Chemistry with Education (Hons), UPM

WORKSHOPS AND PROGRAMMES ATTENDED

- R Statistic Data Analysis (November 2024)
- RSM Software Workshop (December 2024)
- Shimadzu HPLC Training (January 2025)
- Article Review and Writing Skills Workshop (February 2025)
- Excel Beginner Level (March 2025)
- Scientific Paper Writing Skills Workshop (March 2025)
- Wacana Ilmu in Collaboration with Malang University, Indonesia (May 2025)
- Elsevier Discovery and Writing Guidance (June 2025)
- UMT Coastal Clean Up in Collaboration with Nestlé (July 2025)

PUBLICATIONS

Raveendran, K., Roslan, ‘A. D. M., Mei, H. N. S., Sidi, N. S. A., Loh, S. H., and Khalik, W. M. A. W. M. (2025). Sorbent-based extraction for pre-concentration of antidepressant drugs: A review. Malaysian Journal of Analytical Science, 29, 1535.

Ng, S. M. H., Raveendran, K., Azman, W. N. A. S. W., Loh, S. H., Ariffin, M. M., & Khalik, W. M. A. W. M. (2025). Carbonaceous materials-based aloe vera leaf waste as magnetic adsorbents for pre-concentration selective serotonin reuptake inhibitor antidepressant drugs from aqueous solutions. Green Analytical Chemistry, 12, 100192.